IMPROVING THE DEVELOPMENT CHARACTERISTICS OF STEEL REINFORCING BARS

By

Emmanuel K. Idun

David Darwin

A Report on Research Sponsored by

THE CIVIL ENGINEERING RESEARCH FOUNDATION
Contract No. 91-N6002

THE NATIONAL SCIENCE FOUNDATION
Research Grants No. MSS-9021066 and CMS-9402563

THE REINFORCED CONCRETE RESEARCH COUNCIL
Project 56

Structural Engineering and Engineering Materials
SM Report No. 41

UNIVERSITY OF KANSAS CENTER FOR RESEARCH, INC.
LAWRENCE, KANSAS
AUGUST 1995

ABSTRACT

The bond characteristics of deformed reinforcing bars are investigated and design equations for development and splice lengths are obtained with the goal of improving the bond strength of steel reinforcing bars to concrete. The research includes both experimental and analytical studies.

The experimental studies involved evaluating the performance of deformed steel reinforcing bars with different deformation patterns and the effects of epoxy coating on these bars, using friction, beam-end, and splice tests.

The friction tests are used to determine the coefficient of friction between reinforcing steel and mortar, for both epoxy-coated and uncoated steel. The results indicate that the coefficient of friction is about 0.49 between epoxy-coated reinforcing steel and mortar and about 0.56 between uncoated reinforcing steel and mortar.

The beam-end tests are used to study the effects of deformation pattern on bond strength as affected by epoxy coating. Fifty-eight beam-end specimens, containing No. 8 bars with different deformation patterns (relative rib area and rib face angle) were tested. Epoxy coating appears to have a less detrimental effect on bond strength for high relative rib area bars than for previously tested conventional bars. Bars with high rib face angles also appear to be affected less by epoxy coating.

The splice tests are used to study the effects of deformation pattern on splice strength as affected by epoxy coating and confinement by transverse reinforcement. Fifty-four splice specimens containing No. 8 bars with different deformation patterns were tested. Concretes containing two different coarse aggregates were used to evaluate the effect of aggregate properties on bond strength. Epoxy coating appears to be less detrimental on splice strength for high relative rib area bars than for conventional bars. The splice strength of uncoated reinforcement confined by transverse reinforcement increases with an increase in the relative rib area. The

increase in splice strength provided by transverse reinforcement increases as the strength of the coarse aggregate increases. The results indicate that current development/splice lengths can be reduced by an average of 9 to 16% if high relative rib area bars are used with confinement provided by transverse reinforcement.

The analytical study focused on obtaining splice and development length expressions for bars with and without transverse reinforcement. The analyses demonstrate that the relationship between bond force and development or splice length is linear but not proportional. $f_c'^{1/2}$ does not provide an accurate representation of the effect of concrete strength on bond strength. Development/splice strengths are underestimated for low strength concretes and overestimated for high strength concretes. $f_c'^{1/4}$ provides an accurate representation of the effect of concrete strength on bond strength. The yield strength of transverse reinforcement does not play a role in the effectiveness of the transverse reinforcement in improving development/splice strength. The effectiveness of the transverse reinforcement depends on the total area of stirrups crossing the potential plane of splitting. LRFD concepts and Monte Carlo techniques are applied to the bond strength expressions to obtain a strength reduction (ϕ) factor of 0.85 which, together with the bond strength expressions, are used to obtain prototype design equations for splice and development length. For high relative rib area bars confined by transverse reinforcement, development/splice lengths average 9 to 16% lower than obtained for conventional bars. For high relative rib area bars confined by transverse reinforcement, development lengths average 9 to 17% lower and splice lengths average 30 to 36% lower than those obtained with ACI 318-95. depending on the value of R_r for the high relative rib area bar.

Keywords: bond (concrete to reinforcement); deformed reinforcement; relative rib area; reliability; structural engineering.

ACKNOWLEDGEMENTS

The report is based on a thesis prepared by Emmanuel K. Idun in partial fulfillment of the requirements of the Ph.D. degree. Support for the research was provided by the Civil Engineering Research Foundation under CERF Contract No. 91-N6002, the National Science Foundation under NSF Grants No. MSS-9021066 and CMS-9402563, the Reinforced Concrete Research Council under RCRC Project 56, ABC Coating, Inc., Birmingham Steel Corporation, Chaparral Steel Company, Fletcher Coating Company, Florida Steel Corporation, Morton Powder Coatings, Inc., North Star Steel Company, O'Brien Powder Products, Inc., and 3M Corporation. Support was also provided by Geiger Ready-Mix, Iron Mountain Trap Rock Company, and Richmond Screw Anchor Company.

TABLE OF CONTENTS

LIST OF SYMBOLS

A_b	Bar area.
A_I	Influence area.
A_T	Tributary area.
A_{tr}	Area of each stirrup or tie crossing the potential plane of splitting adjacent to the reinforcement being developed or spliced.
A_v	Stirrup area.
B	Basalt coarse aggregate.
b	Beam width.
$\tilde{b}$	Beam width, b, random variable.
C_b	Concrete bottom cover.
$\tilde{C}_b$	Concrete bottom cover, C_b, random variable.
C_M	Maximum of C_b and C_s.
$\tilde{C}_M$	Maximum of $\tilde{C}_b$ and $\tilde{C}_s$.
C_m	Minimum of C_b and C_s.
$\tilde{C}_m$	Minimum of $\tilde{C}_b$ and $\tilde{C}_s$.
COF	Coefficient of friction.
COV	Coefficient of variation.
C_s	Minimum of C_{so} and C_{si} + 0.25 in. or C_{so} and C_{si}.
$\tilde{C}_s$	Minimum of $\tilde{C}_{so}$ and $\tilde{C}_{si}$ + 0.25 in.
C_{si}	One-half clear bar spacing.
$\tilde{C}_{si}$	One-half clear bar spacing, C_{si}, random variable.
C_{so}	Concrete side cover.
$\tilde{C}_{so}$	Concrete side cover, C_{so}, random variable.
C/U	Relative bond strength of epoxy-coated bar to uncoated bar.

c	Smaller of either the distance from the center of the bar to the nearest concrete surface or one-half the center-to-center spacing of the bars being developed or spliced.
d_b	Nominal bar diameter.
d_s	Nominal stirrup diameter.
F	Fraction.
f_c'	Concrete compressive strength.
$\tilde{f}_c'$	Concrete compressive strength, f_c', random variable.
$f_c'^p$	Concrete compressive strength raised to the power p.
f_{cr}'	Required average compressive strength of concrete.
$\bar{f}_{cstr35}$	Mean in-situ concrete compressive strength at 35 psi/sec loading rate.
$\bar{f}_{cstr\dot{R}}$	Mean in-situ concrete compressive strength at $\dot{R}$ psi/sec loading rate.
f_s	Bar stress at failure.
f_y	Bar yield strength.
f_{yt}	Stirrup yield strength.
h	Beam depth.
I	Integer.
K_1, K_3, K_5	Constants representing slopes.
K_2, K_4, K_6	Constants representing intercepts.
K_{tr}	Represents the expression $A_{tr}f_{yt}/(1500sn)$.
L	Limestone coarse aggregate.
L_o	Basic (unreduced) live load.
l	Beam length.
l_c	Span of constant moment region.
l_d	Development length.
$\tilde{l}_d$	Development or splice length, l_d, random variable.
l_s	Splice length.

M_u	Ultimate beam moment.
n	Number of developed or spliced bars along the plane of splitting
n_b	Number of developed or spliced bars.
N_l	Number of stirrups legs per section.
N	Number of stirrups along splice length.
P	Ultimate beam load.
p	Power for which concrete compressive strength is raised to.
Q	random variable for total load.
Q_D	Random variable representing dead load effects.
Q_{D_n}	Nominal dead load.
Q_L	Random variable representing live load effects.
Q_{L_n}	Nominal live load.
$(Q_L/Q_D)_n$	Nominal dead load.
q	Random loading.
R	Random variable for resistance or ratio of predicted to nominal bond strength for a beam obtained from Monte Carlo simulation.
$\dot{R}$	Loading rate for concrete compression.
R_n	Nominal resistance.
R_p	Predicted capacity random variable.
R_r	Relative rib area.
$\overline{R}$	Mean test/prediction ratio of bond strength obtained from Monte Carlo simulations.
r	Ratio of random variable for resistance to nominal resistance, R/R_n.
$\bar{r}$	Cumulative mean test/prediction ratio of bond obtained strength from Monte Carlo simulations.
r^2	Coefficient of determination.
s	Stirrup spacing.

s/c	Sand-cement ratio.
T_b	Total bond force in a bar at splice failure.
T_c	Concrete contribution to total bond force in a bar at splice failure.
T_s	Confining steel contribution to total bond force in a bar at splice failure.
T/P	Mean test/prediction ratio of bond strength based on the results of test beams.
$\tilde{T/P}$	Mean test/prediction ratio of bond strength based on the results of test beams, T/P, random variable.
U	Average bond force per unit length.
u	Bond stress.
V_{ccyl}	COV for concrete cylinder compressive strength.
$V_{cstr\dot{R}}$	COV for in-situ concrete compressive strength at $\dot{R}$ psi/sec loading rate.
V_m	Variability of bond strength model equation.
V_Q	COV for random variable for total load.
V_{Q_D}	COV of random variable representing dead load effects.
V_{Q_L}	COV of random variable representing live load effects.
V_R	COV for random variable for resistance.
$V_{\tilde{R}}$	COV for mean test/prediction ratio bond strength obtained from Monte Carlo simulations.
V_r	COV of resistance random variable or Cumulative COV for mean test/prediction ratio bond strength obtained from Monte Carlo simulations.
V_{spec}	Variability representing the errors introduced due to variations in specimen strength and dimensions.
$V_{T/P}$	COV for test/prediction ratio of bond strength.
V_{test}	Variability representing the uncertainties in the measured loads.
$V_{\phi q}$	COV of loading random variable q.
w/c	Water-cement ratio.
wr	Water reducer.

z_i	Randomly generated number.
β	Reliability index.
ϕ	Resistance factor.
ϕ_b	Nominal resistance factor for bond strength.
ϕ_d	Effective resistance factor for bond strength.
γ	Rib face angle.
γ_D	Dead load factor.
γ_L	Live load factor.
μ_c	Coefficient of friction between epoxy-coated bar and concrete.
μ_u	Coefficient of friction between uncoated bar and concrete.
σ_b	Standard deviation for beam width.
σ_{C_b}	Standard deviation for concrete bottom cover.
$\sigma_{C_{sd}}$	Standard deviation for concrete side cover.
σ_{cstrR}	Standard deviation for mean in-situ compressive strength of concrete.
σ_{l_d}	Standard deviation for development or splice length.

LIST OF TABLES

LIST OF FIGURES

CHAPTER 1: INTRODUCTION

1.1 Background

In designing reinforced concrete structures, the embedded steel reinforcing bars and the surrounding concrete must be bonded together to transfer forces between the two materials. Bond between deformed reinforced steel bars and concrete is the result of chemical adhesion, friction, and bearing. Chemical adhesion comes from the attraction of cement paste to steel. Friction is due to the contact between the concrete and the steel bar, arising from the movement of the bar. Bearing is provided by the deformations on the steel bar bearing against the surrounding concrete. Bond loss between reinforcing steel and concrete may cause a reinforced concrete structure to fail.

When reinforcing bars are spliced, or terminated in reinforced concrete, adequate length must be provided to develop the strength of the steel. This splice or development length is a function of the bond characteristics of the reinforcing bar and the surrounding concrete. These bond characteristics depend upon the geometry of both the bar and the concrete.

Epoxy coating reduces bond strength and therefore requires longer splice and development lengths. Longer splice and development lengths mean more steel and money, and sometimes construction difficulties, making reinforced concrete construction less competitive. It is, therefore, desirable to substantially improve the bond characteristics of reinforcing bars so that shorter splice and development lengths will be required.

To evaluate the improvement in bond strength provided by any new reinforcing bar requires an accurate characterization of the splice and development strength of current bars to serve as a baseline. Such a characterization must accurately account for the effects of concrete cover, bar size, bar spacing, concrete

strength, and confining reinforcement.

This project focuses on improving the bond characteristics of steel reinforcing bars by developing new deformation patterns and comparing the properties of the new bars with those of conventional reinforcing bars. To establish a baseline for comparison, accurate bond strength expressions are developed for both unconfined and confined conventional reinforcing bars. Using these expressions and probability techniques, resistance (ϕ) factors are calculated and used in prototype design equations for splice and development length. The effects of epoxy coating on the bond characteristics of the new bars are also evaluated.

1.2 Previous Work

1.2.1 Deformed Reinforcing Bar Development

The earliest recorded work on the bond strength of deformed or smooth bars was done by Abrams (1913), who reported higher bond stresses for deformed bars than for smooth bars. Abrams' work also indicated that the higher the bearing area of the deformations per unit length of the bar (the area of a deformation projected on a plane perpendicular to the bar axis divided by the deformation spacing), the higher the slip resistance of the bar.

Work by Clark (1946, 1949) on 17 different deformation patterns serves as the basis for current deformed bars used in the United States. Clark evaluated bond characteristics by comparing the bond forces developed at preselected values of bar slip using pullout and beam specimens. Based on his work, Tentative Specification ASTM A 305-47T was developed and later modified (ASTM A 305-49) to include a maximum average spacing of deformations, or ribs, equal to 70% of the nominal diameter of the bar and a minimum height of deformations equal to 4% for bars with a nominal diameter of 1/2 in. or smaller, 4.5% for bars with a nominal diameter of 5/8

in., and 5% for larger bars.

In addition to the rib spacing and height criteria, Clark recommended that the ratio of the shearing area between ribs (bar perimeter times distance between ribs) to the rib bearing area (projected rib area normal to the bar axis) be limited to a maximum of 10, and if possible 5 or 6. Today this criterion is usually described in terms of the inverse ratio, that is, the ratio of the bearing area to the shearing area, known as "relative rib area", R_r, and his recommendations then become a minimum relative rib area, R_r, of 0.10 with preferable values of 0.20 or 0.17.

Clark's recommendations on relative rib area were not included in ASTM A 305-49, and typical values of R_r for bars currently manufactured in the U.S. range from 0.057 to 0.084 (Choi, Hadje-Ghaffari, Darwin, and McCabe 1990). The major impact of Clark's work was to remove the weakest deformation patterns, rather than to establish the best possible deformation patterns. Clark observed that bottom-cast bars develop higher bond strengths than top-cast bars and that the more gradual the inclination to the rib face, the greater the slip for a given force.

Rehm (1957, 1961) found that if the ratio of rib spacing to rib height is less than 7 and if the rib face angle is greater than 40°, the concrete in front of the ribs crushes gradually, followed by a pullout failure. If the ribs have a spacing to height ratio greater than 10, for a rib face angle greater than 40°, the concrete in front of the ribs crushes first, forming wedges that induce tensile stress, causing transverse cracking and longitudinal splitting of the concrete. Most structural applications are such that splitting failure dominates (Clark 1949, Menzel 1952, Chinn, Ferguson, and Thompson 1955, Ferguson and Thompson 1962, Losberg and Olsson 1979, Soretz and Holzenbein 1979, Johnston and Zia 1982, Treece and Jirsa 1989, Choi, Hadje-Ghaffari, Darwin, and McCabe 1991, and Darwin and Graham 1993a).

Lutz, Gergely, and Winter (1966) and Lutz and Gergely (1967) showed that

the rib face angle determines whether or not the concrete in front of the ribs crushes when there is slip of the reinforcing bar with respect to the concrete. Crushing occurs when the rib face angle is greater than 40° to 45°, but no crushing occurs if the rib face angle is less than about 30°. Skorobogatov and Edwards (1979) tested bars with rib face angles of 48.5° and 57.8° and obtained results that supported the earlier work by Lutz et al. Skorobogatov and Edwards concluded that the two rib face angles did not affect the maximum bond strength since the high rib face angle is flattened by the crushed concrete wedge in front of the ribs, reducing the effective face angle to a smaller value.

Losberg and Olsson (1979) tested three deformation patterns commonly used in Sweden and concluded that traditional pullout tests, of the type used by Clark (1946, 1949), are not accurate for predicting the response of reinforcing bars in actual structures, because the state of stress around the bars in pullout specimens is considerably different from that in actual structures: In actual structures, the bar and the concrete surrounding it are simultaneously placed in tension, while in a pullout test, the bar is placed in tension while the concrete surrounding it is placed in compression. Losberg and Olsson also tested specially machined bars, with different rib spacings and rib heights, and found that when splitting failure governs, bond strength is not sensitive to rib spacing or rib height. Their tests indicated that, when confinement is provided and splitting failure does not govern, bond strength decreases once ribs become closer than about two-thirds of the bar diameter (d_b).

Soretz and Holzenbein (1979) studied a number of bar parameters, including the height and spacing of ribs, the inclination of ribs with respect to the bar axis, and the cross-sectional shape of ribs along the longitudinal direction of the bar. They concluded, in conflict with the observations of Losberg and Olsson, that the optimum geometry would be a rib spacing of $0.3d_b$ and a rib height of $0.03d_b$ to give the best

combination of increased bond strength and limited splitting.

Recently, Darwin and Graham (1993a, 1993b), using beam-end specimens to provide a more realistic measure of bond performance, studied the effect of rib height, rib spacing, and relative rib area on bond strength, including the conditions under which changes in deformation pattern play a role. Beam-end specimens have the advantage of placing both the steel bar and the surrounding concrete simultaneously in tension. Darwin and Graham conducted 156 tests on bars with different deformation patterns. The tests included both conventional reinforcing bars and specially machined bars. The machined bars included nine deformation patterns, with three rib heights, 0.05 in., 0.075 in., and 0.10 in. and rib spacings ranging from 0.263 in. to 2.20 in. to produce relative rib areas of 0.20, 0.10, and 0.05 for each rib height. They observed that an increase in relative rib area results in an increase in the stiffness of the initial portion of the load-slip curve, matching observations by Clark (1946, 1949). Their test results also showed that the effect of relative rib area on bond strength depends on the degree of confinement provided to the reinforcing bar by transverse reinforcement or increased concrete cover. The bond strength of bars with low cover and not confined by transverse reinforcement was independent of relative rib area, while the bond strength of bars confined by transverse reinforcement or higher concrete cover increased significantly with an increase in relative rib area. Darwin and Graham observed splitting failures in all test specimens, with the nature being brittle or ductile, depending on the absence or presence of transverse reinforcement.

1.2.2 Epoxy-Coating

Mathey and Clifton (1976) were the first to study the bond of epoxy-coated bars to concrete. Using pullout specimens, they observed unsatisfactory bond

performance for bars with thick epoxy coatings (about 25 mils), but observed satisfactory bond performance for bars with epoxy coatings between 1 and 11 mils. The average bond strength of their 19 pullout specimens for bars with epoxy coatings between 1 and 11 mils was just 6% less than that for specimens with uncoated bars. Because pullout specimens place the concrete in compression and the bar in tension, the applicability of these test results to actual structures is limited.

To obtain a more realistic measure of bond strength, Johnston and Zia (1982) used 6 slab and 40 beam-end specimens to study the effect of epoxy coating on bond strength. The epoxy-coated bars had coating thicknesses between 6.7 and 11.1 mils, with the majority between 8 and 9 mils. All of the specimens were confined with No. 3 transverse reinforcement, spaced at 6 and 3 inches for No. 6 and 11 bars, respectively. They observed that the slab specimens with epoxy-coated bars had slightly higher deflection, wider cracks, and about 4% lower strength than those with uncoated bars. The beam-end specimens with epoxy-coated bars developed about 85% of the bond strength of specimens with uncoated bars. As a result of their findings, Johnston and Zia recommended that the development length of uncoated bars should be increased by 15% for epoxy-coated bars.

Treece and Jirsa (1987, 1989), investigating the bond strength of epoxy-coated bars using splices without transverse reinforcement, reported a strength reduction of about 34%. They tested 21 specimens in all, four with bottom-cast bars and the rest with top-cast bars. There were 10 No. 6 and 11 No. 11 bar specimens, with epoxy coating thicknesses ranging from 4.5 to 14 mils. Concrete strengths ranged from 3860 to 12600 psi and concrete cover was less than $1.5d_b$ for 16 specimens and greater than $2.5d_b$ for 3 specimens. Four of the No. 6 bar specimens had covers less than or equal to the maximum size of the aggregate, which can be expected to reduce bond strength (Donahey and Darwin 1985). The main conclusion of the study by

Treece and Jirsa was that the amount of the bond strength reduction due to epoxy coating depends on the mode of failure, pullout or splitting. They assumed that the specimens tested by Mathey and Clifton (1976) and Johnston and Zia (1982) failed in a pullout mode because the steel was confined by large concrete cover or transverse reinforcement, preventing a splitting failure (in fact, Johnston and Zia observed splitting failure in their test specimens). Treece and Jirsa concluded that, if a pullout mode of failure occurs, the reduction in bond strength is about 15%, but if a splitting failure occurs, as it did in their tests, the reduction in bond strength is about 35%. Based on these conclusions, they recommended that the basic development length of uncoated bars be multiplied by a factor of 1.5 for epoxy-coated bars with a cover of less than $3d_b$ or a clear spacing between bars of less than $6d_b$. For all other epoxy-coated bars, a factor of 1.15 should be used. They also recommended that the product of the epoxy-coating factor and top-bar factor be limited to a maximum of 1.7. These recommendations were adopted in full by AASHTO (1989), while ACI Committee 318 (1989) adopted the 1.5 factor and the 1.7 maximum, but increased the 1.15 factor to 1.20.

Choi, Hadje-Ghaffari, Darwin, and McCabe (1990, 1991) studied the effects of coating thickness, deformation pattern, and bar size on the reduction in bond strength caused by epoxy coating, using both beam-end and splice test specimens. The study included No. 5, No. 6, No. 8, and No. 11 bars, with three deformation patterns and average coating thicknesses ranging from 3 to 17 mils. All bars were bottom-cast. Choi et al. observed significant reductions in bond strength, but found that coating thickness has little effect on the amount of bond strength reduction for No. 6 bars and larger. However, they found that a thicker coating results in a greater reduction in bond strength for No. 5 bars. They observed that, in general, the reduction in bond strength caused by epoxy coating increases with bar size and

depends on the deformation pattern. Bars with larger relative rib areas were affected less by the epoxy coating than bars with smaller relative rib areas.

Hadje-Ghaffari, Darwin, and McCabe (1991, 1992) and Hadje-Ghaffari, Choi, Darwin, and McCabe (1994) extended the work of Choi, Hadje-Ghaffari, Darwin, and McCabe (1990, 1991) to include the effects of concrete cover, casting position, concrete slump, consolidation, concrete strength, and transverse reinforcement on the reduction in bond strength caused by epoxy coating. Hadje-Ghaffari et al. found that, as with uncoated bars, the bond strength of epoxy-coated bars increases as concrete cover increases, and that, while the bottom to top-cast bar strength ratio increases for uncoated bars, it decreases for epoxy-coated bars as concrete slump increases. They also observed that the presence of transverse reinforcement increases the bond strength of epoxy-coated reinforcement. Using beam-end specimens, they found that consolidation improved the bond strength of both epoxy-coated and uncoated bottom and top-cast bars, even when superplasticized concrete was used. Hadje-Ghaffari et al. concluded that, although epoxy coating reduces the bond strength of reinforcing bars to concrete, the extent of the reduction is less than that used to establish the development length modification factors in the 1989 ACI Building Code and the 1989 AASHTO Bridge Specifications. Among their recommendations was that the development length modification factor of 1.5 for epoxy-coated bars with cover less than $3d_b$ or clear spacing less than $6d_b$ be reduced to 1.35. For epoxy-coated bars with cover greater than $3d_b$ and clear spacing greater than $6d_b$, they recommended retaining the ACI development length modification factor of 1.2, if the current 0.8 factor for widely spaced bars is used (ACI 318-89), and using a factor of 1.0, if the 0.8 factor for widely spaced bars is not used. They further recommended a reduction in the development length modification factor for coated top bars from 1.3 to 1.15 and a reduction in the upper limit on the product of the epoxy-coating factor and top-bar

factor from 1.7 to 1.5.

Using nonlinear finite element analysis, Choi, Darwin, and McCabe (1991) and Hadje-Ghaffari, Darwin, and McCabe (1992) also studied the role played by epoxy coatings on the failure of test specimens. Their finite element model included representations for the deformed steel bar, the concrete, and the interfacial material. They observed close agreement between the laboratory behavior and the finite element results. Choi et al. found that the interfacial properties, mainly friction, govern the bond performance, and also that epoxy coatings reduce bond strength. They also observed that the bond strengths of coated and uncoated bars increase nearly linearly with additional cover and lead length, but that the relative bond strength of coated bars is independent of cover and lead length, matching experimental observations (Choi, Hadje-Ghaffari, Darwin, and McCabe 1990, 1991). Hadje-Ghaffari et al. observed that increasing the cover, lead length, or bar size, will result in an increase in the lateral force provided by the concrete, thus increasing the bond strength.

Hamid and Jirsa (1990, 1993) studied the effects of epoxy coating on the bond characteristics of reinforcing bars. In one portion of their study, using 72 pullout specimens, Hamid and Jirsa observed that the reduction in bond strength of epoxy-coated bars was between 10 to 25% of that of uncoated bars and that this reduction was independent of bar size, coating thickness, bar deformation pattern, concrete strength, and level of confinement provided to the reinforcing bar. In another portion of the study, with 12 beam splice specimens containing top-cast No. 6 or No. 11 bars, they found that the splice strength of the epoxy-coated No. 11 bars relative to uncoated bars improved from 74% in the absence of transverse reinforcement to 80% to 85% when transverse reinforcement was provided. For the No. 6 bars, the improvement was from 67% to 74%. Hamid and Jirsa concluded that the ACI

Building Code (1989) bond provisions are quite conservative for both uncoated and epoxy-coated bars.

DeVries, Moehle, and Hester (1991) studied the effects of concrete strength and casting position on the reduction in splice strength caused by epoxy coating using 36 beam specimens. Their results show that casting position and epoxy coating affect bond strength, although the effects do not appear to be cumulative. They also found that the design equations in ACI 318-89 are conservative and recommended the use of development length modification factors of 1.3 for uncoated top-cast bars and 1.5 for epoxy-coated bars, regardless of casting position.

Hester, Salamizavaregh, Darwin, and McCabe (1991, 1993) studied the effects of epoxy coating and transverse reinforcement on the splice strength of reinforcing bars in concrete. They tested 65 beam and slab splice specimens containing No. 6 or No. 8 bars and three deformation patterns with average coating thicknesses ranging from 6 to 11 mils. They observed that epoxy coating reduces the splice strength of deformed reinforcing bars in concrete, but that the extent of the reduction is less than used to select the development length modification factors in the 1989 AASHTO Bridge Specifications and the 1989 ACI Building Code. The percentage decrease in splice strength caused by epoxy coating was found to be independent of the amount of transverse reinforcement. Hester et al. further found that the percentage increase in splice strength due to the presence of transverse reinforcement is approximately the same for both coated and uncoated bars, for equal amounts of transverse reinforcement. They recommended development length modification factors of 1.35 for epoxy-coated bars without transverse reinforcement and 1.20 if minimum transverse reinforcement is provided.

Cairns and Abdullah (1994) studied the effects of epoxy coating on bond strength using both friction and pullout test specimens. They compared the friction

characteristics of flat steel specimens with mill scale in contact with concrete to the friction characteristics of similar specimens coated with fusion-bonded epoxy. The friction test specimens consisted of 50 mm by 100 mm by 100 mm (1.97 in. by 3.94 in. by 3.94 in.) concrete prisms cast between a pair of steel plates, 50 mm (1.97 in.) wide by 20 mm (0.79 in.) thick, giving two contact surfaces between steel plate and concrete, each 50 mm by 100 mm (1.97 in. by 3.94 in.). They observed shear failure along the steel-concrete interface for all specimens. Slip usually began between 40% and 55% of the ultimate load, and increased slowly over the period of loading. Slip at failure ranged between 0.12 and 0.18 mm (4.7 and 7.1 mils). Although not specifically stated in the paper, results presented by Cairns and Abdullah show that the adhesion for coated and uncoated steel plates is 1.7 N/mm^2 (246.5 psi) and 3.4 N/mm^2 (493 psi), respectively, and the coefficients of friction for coated and uncoated steel are 0.487 and 0.527, respectively. These results indicate a 50% reduction in adhesion, and an 18% reduction in the coefficient of friction for epoxy-coated steel compared with uncoated steel. Based on the results of the pullout tests, Cairns and Abdullah concluded that epoxy coating reduces bond between reinforcement and concrete, and that this bond reduction depends on the bar-concrete slip at which the comparison is made (the reduction being greatest at a small slip) and on the inclination of the face of the bar ribs. They observed that if splitting-type failures are resisted by thick concrete cover or heavy confining reinforcement, the bond strength of coated reinforcement with a high rib face angle of 66° may equal or exceed that of uncoated reinforcement with a low rib face angle of 30°.

1.2.3 Design Equations

Experimental results from studies of bond strength have been used to derive relationships describing bond capacity. The 1963 ACI Building Code subsection on

ultimate bond stress was based on studies by Mathey and Watstein (1961) and Ferguson and Thompson (1962). From these studies, the ultimate average bond force per unit length of the bar, U, (in pounds per inch) was expressed as

$$U = 35\sqrt{f'_c} \tag{1.1}$$

in which f'_c = the compressive strength of the concrete in psi.

Orangun, Jirsa, and Breen (1975, 1977) used dimensional and nonlinear regression analyses on test results of 62 beams to arrive at an expression for splices without transverse reinforcement:

$$\frac{u}{\sqrt{f'_c}} = 1.22 + \frac{3.23C_m}{d_b} + \frac{53d_b}{l_s} \tag{1.2}$$

and recommended the use of a smoothed version of the equation

$$\frac{u}{\sqrt{f'_c}} = 1.2 + \frac{3C_m}{d_b} + \frac{50d_b}{l_s} \tag{1.3}$$

in which u = bond stress in psi; C_m is the least of concrete bottom cover, side cover or one-half the clear spacing between bars, in in.; d_b = the bar diameter in in.; l_s = the splice length in in. Of the 62 beams, 4 contained side-cast bars and 1 contained top-cast bars. Using Eq. 1.3 and test results for beams with transverse reinforcement, they formulated the following expression:

$$u = \left(1.2 + \frac{3C_m}{d_b} + \frac{50d_b}{l_s} + \frac{A_{tr}f_{yt}}{500sd_b}\right)\sqrt{f'_c} \tag{1.4}$$

with the limit

$$\frac{A_{tr}f_{yt}}{500sd_b} \leq 3 \tag{1.5}$$

in which A_{tr} = the area of the transverse reinforcement normal to the plane of splitting through the anchored bars in in.^{2}; f_{yt} = the yield strength of transverse reinforcement in psi; and s = the spacing of the transverse reinforcement in in.

Zsutty (1985) developed an empirical equation for predicting the strength of lapped splices with or without transverse reinforcement as

$$f_s = 560(f'_c)^{1/3}\left(\frac{l_s}{d_b}\right)^{1/2}\left(\frac{C_m}{d_b}+\frac{200A_{tr}}{bs}\right)^{1/2} \tag{1.6}$$

in which f_s = the bar stress of tension lapped splice in psi; l_s is the splice length in in.; C_m is the least of concrete bottom cover, side cover or one-half the clear spacing between bars, in in.; d_b = the bar diameter in in.; b = the beam width in in.; A_{tr} = the area of the transverse reinforcement normal to the plane of splitting through the anchored bars in in.^{2}; and s = the spacing of the transverse reinforcement in in.

In a recent study, Darwin, McCabe, Idun, and Schoenekase (1992a, 1992b) used linear regression techniques on the results of 147 development and splice tests to obtain an expression for beams without transverse reinforcement.

$$\frac{A_b f_s}{\sqrt{f'_c}} = 6.67\, l_s(C_m + 0.5d_b)\left(0.92 + 0.08\frac{C_M}{C_m}\right) + 300A_b \tag{1.7}$$

in which A_b = the area of the developed or spliced bar in in.^{2}; f_s = the bar stress in psi;

and C_M and C_m are, respectively, the maximum and minimum of the concrete bottom cover or, the lesser of one-half the clear spacing between bars or the concrete side cover, in in. Of the 147 tests, 20 contained side-cast bars and 33 contained top-cast bars.

Harajli (1994) analytically evaluated the bond strength and anchorage characteristics of reinforcing bars embedded in plain and fiber reinforced concrete. His analysis was based on a numerical solution scheme of the bond problem and incorporates an experimentally derived local bond stress-slip relationship applicable to pullout and splitting-type bond failure. Based on his work, he concluded that development/splice strength design expressions derived from test data in which the steel stresses were below yield at bond failure are unsafe when extended linearly to the post-yield range of reinforcing bars.

1.2.4 Probability Based Design

The use of load factors (factors used to increase predicted structural loads) and ϕ-factors (factors used to reduce the predicted strength of structural members), now referred to as Load and Resistance Factor Design (LRFD), was pioneered by the American Concrete Institute in the 1956 and 1963 Building Codes (ACI Committee 318 1956, 1963).

The principal reasons why load and ϕ-factors are used in structural design in place of safety factors are 1) variability in strength (the actual strength of structural members is almost always different from predicted values), 2) variability in loads (actual loads can vary significantly from those used in design), and 3) the consequences of failure (potential loss of life and property). The variability of the applied load may lead to conditions of overload, while the variability of the strength may lead to conditions of understrength. Load and resistance factors result in a

structure that is designed for higher than predicted loadings using lower than the predicted strength, making the structure stronger than it would be otherwise and reducing the probability of failure to an acceptable value. Over the past 30 years, major advances have occurred in all aspects of safety, and sophisticated procedures have evolved for estimating load and resistance factors. A technique that is widely used in structural reliability and probability-based studies is Monte Carlo analysis. This technique is a powerful engineering tool that enables one to perform a statistical analysis that reflects the uncertainty in structural engineering problems, being particularly useful for complex problems where numerous random variables are related in a nonlinear fashion.

Allen (1970) used probability techniques to study the ultimate moment and ductility ratio of reinforced concrete beams in bending and concluded, among other things, that the variability of the ultimate moment expected in practice increases when either the member is thin or the percentage of steel is high. This increase in variability, however, is reduced considerably by good workmanship.

MacGregor (1976) studied the concepts of safety and limit states design for reinforced concrete. In the study, he reviewed a number of techniques for establishing safety provisions for structures and found that procedures based on attaining a specific probability of failure were most satisfactory.

Grant, Mirza, and MacGregor (1978) used the Monte Carlo analysis to study the effects of variations in the strength of the concrete and steel, the cross sectional dimensions of the concrete and steel, and the location of steel reinforcement on the variability of the strength of rectangular short reinforced concrete tied columns. Based on previous studies by Drysdale (1975) and Grant (1976), Grant et al. assumed a beta distribution for the mill test yield strength of reinforcing bars and normal distributions for all other parameters, and found that the specified concrete strength

and the ratio of reinforcement area to gross concrete area of a column have significant influences on the distribution properties of the ratio of theoretical strength to strength predicted by ACI 318-71.

Ellingwood, Galambos, MacGregor, and Cornell (1980), Ellingwood, MacGregor, Galambos, and Cornell (1982), and Galambos, Ellingwood, MacGregor, and Cornell (1982) worked on probability based load criteria. They proposed a set of recommended load factors and load combinations for use with loads in the then proposed 1980 version of American National Standard A58 and proposed the use of reliability index, β (defines the relative reliability or safety of a structure) to select ϕ-factors. The choice of β depends on material, member type and failure mode, and load combinations. They further recommended reliability indices to be used with different structural members and also presented charts for determining ϕ-factors for given values of β.

Mirza and MacGregor (1986) also used the Monte Carlo method to study the effects of variations in the material (concrete and steel) strengths and steel placement on the variability of bond strength between concrete and bottom tension reinforcing bars in cast-in-place beams. Like Grant et al. (1978), Mirza and MacGregor assumed a beta distribution for the mill test yield strength of reinforcing bars and normal distributions for all other parameters, and found that the concrete cover, the transverse reinforcement, the bar size, and the quality of construction influence bond strength ratios (theoretical bond strength divided by bond strength computed from expressions in ACI 318-83 and proposed by ACI Committee 408). However, they found that the effects of concrete strength, steel grade, and seismic loading on the variability of bond strength ratios may be neglected.

Mirza (1992) used Monte Carlo analysis to analyze the strength of slender composite beam-columns and found that the strength ratio (ratio of theoretical

strength to nominal strength) was influenced most significantly by the slenderness ratio, the ratio of the area of structural steel section to the gross area of the cross section, and the end eccentricity ratio. He observed that the variability in column strength was caused by the variations in the strengths of concrete and steel, the cross-sectional dimensions of concrete and steel sections, the placement of steel sections and reinforcing bars, and the strength model itself.

Lundberg (1993) used the Monte Carlo method to determine β for composite columns and beam-columns and obtained a β of 2.7 for concrete encased steel shapes and 2.5 for concrete filled steel tubes.

Ruiz (1993) used the Monte Carlo method to study the reliability of short and slender concrete columns. She calculated β for compression and bending of unconfined short columns, and for flexure, shear, and torsion limit states complying with the Mexico City Technical Regulations for Reinforced Concrete Structures (NTC-87) and ACI 318-89. The results indicated that β is higher for NTC-87 than for ACI 318-89. In a similar study, Ruiz and Aguilar (1994) calculated β complying with the Mexico City concrete design regulations RCDF-87 and ACI 318-89 and found the values of β to be higher for RCDF-87 than for ACI 318-89.

1.3 Discussion

In spite of the numerous research studies on the bond strength of deformed reinforcing bars, little attention has been given to improving bond characteristics by developing new deformation patterns. The majority of the studies to date have focused on evaluating the effects of a number of parameters, such as member geometry, transverse reinforcement, concrete strength, casting position, and epoxy coating, on existing deformed bars, instead of investigating the performance of entirely new deformation patterns. Clark's work (1946, 1949) is a clear example of

work focused on the existing deformation patterns. Studies of new deformation patterns to improve the bond performance of steel reinforcing bars are therefore very appropriate. Darwin and Graham's (1993a, 1993b) work, using machined bars with different deformation patterns, serves as the first phase of this study. The results obtained by Darwin and Graham are used as guidelines in the design of bars with new deformation patterns that are rolled in steel mills for further study. Since epoxy coating affects bond performance, the effects of epoxy coating on the bond strength of the new bars are also evaluated.

The performance of the new bars must be compared with the performance of conventional bars. To do this effectively requires an accurate and unbiased characterization of the bond strength of current bars. It is also important that effects like casting position be eliminated from the data used to arrive at any such characterization. The work on development length criteria by Darwin et al. (1992a, 1992b) provides an expression for bars without transverse reinforcement. However, the data used in that analysis, like that used by Orangun et al. (1975, 1977), contained test specimens with different casting positions. In this study, the work by Darwin et al. is extended, using only bottom-cast bars, to arrive at bond strength expressions for bars both without and with transverse reinforcement. These expressions are then used as the basis for evaluating the performance of the new bars and for formulating design equations for splice and development length.

1.4 Objective and Scope

The objective of this study is to extend the work by Darwin et al. (1992a, 1992b) and Darwin and Graham (1993a, 1993b) to improve the bond characteristics of deformed reinforcing bars and to obtain accurate design equations for splice and development length.

The bond strength between reinforcing steel and concrete is evaluated based on flexural bond strength. The key parameters are deformation pattern and bonded length. In addition, the effects of concrete cover, bar spacing, transverse reinforcement, concrete strength, and epoxy coating are investigated.

The experimental program, which involves evaluating the performance of deformed steel reinforcing bars and the effects of epoxy coating, determines 1) the coefficient of friction of both epoxy-coated and uncoated steel and 2) the bond strength of new and conventional reinforcement using beam-end and splice test specimens.

The analytical part of this study focuses on obtaining splice and development length expressions for bars with and without transverse reinforcement. First, linear regression techniques are employed to arrive at expressions for the bond strength of conventional reinforcing bars. The parameters considered include splice and development length, concrete strength and cover, bar size and spacing, and transverse reinforcement. Then, applying LRFD concepts and Monte Carlo techniques to the bond strength expressions, ϕ-factors are determined, which together with the bond strength expressions, are used to arrive at prototype design equations for splice and development length.

The test results and splice and development length expressions are used to develop rational design recommendations for the reinforcing bars, both with or without epoxy coating.

CHAPTER 2: COEFFICIENT OF FRICTION BETWEEN REINFORCING STEEL AND MORTAR

2.1 General

This chapter presents the experimental program, results, and evaluation of tests to determine the coefficient of friction, COF, between reinforcing steel and concrete. Mortar with water-cement ratios, w/c, and sand-cement ratios, s/c, representative of the mortar constituent of concrete were used in place of concrete because of the small size of the test specimens. The tests were carried out in three series: 229 specimens in series 1; 317 specimens in series 2; and 132 specimens in series 3.

2.2 Test Specimens

Test specimens consisted of pieces of reinforcing steel cut from No. 11 steel reinforcing bars (Fig. 2.1) in contact with small mortar blocks (Fig. 2.2).

Steel specimens (0.25 in thick, 0.5 in. wide, and 0.25 in. high) were cut from two No. 11 steel reinforcing bars, one epoxy coated and one uncoated, from between the ribs on the bar. The barrel of the bar provided the testing surface. For the tests, the steel specimens were placed in a slot in a reusable steel yoke (Fig. 2.3).

Mortar specimens measured about 0.5 in. by 0.625 in. by 0.75 in. and were cast in a specially designed formwork, using 0.75 in. plywood pieces tightly held together with C-clamps. The 0.75 in. plywood form was manufactured with a polymeric resin coating that did not require the use of a release agent.

2.3 Test Parameters

The mortar specimens for each test series were cast in groups of five or more. The parameters studied in each series were as follows:

Series 1: The principal test parameters were mortar age (7 and 28 days) and the nature of the mortar surface (formed and hand finished). The two mortar surfaces (formed and hand finished) were selected to determine which might better represent the actual contact interface between a reinforcing bar and concrete. A w/c of 0.5 and a s/c of 1.5 were used for all specimens. Steel specimens in this series were reused several times (more than 10 times), raising the concern of possible damage to the original surface of the steel. Steel specimens were also placed such that their entire surfaces were in contact with mortar prior to testing. This created a condition where the front edge of the steel specimens sometimes dug into the mortar during the test, chipping off portions of the mortar.

Series 2: In addition to the parameters investigated in series 1, the following parameters were evaluated in series 2: w/c (0.4, 0.5 and 0.6), s/c (1.5, 2.0 and 2.5), and mortar strength (from 2500 to 5960 psi). Like series 1, the steel specimens in this series were reused several times (more than 10 times) and were also placed such that their entire surfaces were in contact with mortar prior to testing.

Series 3: In this series, the effect of epoxy coating on the COF between reinforcing bar and mortar was measured. The effect of mortar strength on the COF was also evaluated in this series using mortar strengths ranging from 5610 to 6860 psi. A w/c of 0.5 and s/c of 1.5 were used for all specimens. All mortar surfaces were formed, and tests were carried out at 7 days. Unlike the steel specimens in series 1 and 2, the steel specimens in series 3 were used only once to avoid the possibility of damaging the original surface of the steel. To prevent steel specimens from digging into mortar, the steel specimens in this series were placed so that small portions of the front end extended beyond the front edges of mortar specimens. The test results from series 3 are therefore more useful than those from series 1 and 2.

2.4 Materials

2.4.1 Reinforcing Steel

Epoxy-coated and uncoated conventional ASTM A 615 Grade 60 No. 11 deformed steel reinforcing bars with a bamboo pattern (ribs perpendicular to the axis of the bar) were used. The bamboo pattern was used because it offered enough room between the ribs to cut specimens. The fusion bonded epoxy coating on the coated bar was commercially applied and was about 10 mils thick.

2.4.2 Mortar

Mortar was hand-mixed in the laboratory using Type I portland cement and Kansas river sand (bulk specific gravity ssd = 2.62, absorption = 0.5%) that had been passed through a No. 16 sieve. Five different mortar mixes were used, with w/c of 0.4, 0.5 and 0.6, and s/c of 1.5, 2.0 and 2.5, producing mortar strengths ranging from 2500 to 6970 psi at 7 or 28 days. Mortar mix proportions are summarized in Table 2.1. Series 1 and 3 mortar specimens were made using mix 2 (w/c = 0.5, s/c = 1.5).

2.5 Placement and Curing

The mortar was hand-mixed and placed in two lifts using a spoon. Each lift was consolidated on a vibration table. After placement, the forms were covered with plastic sheeting to prevent excessive loss of moisture from the mortar. 1 in. square by 5 in. high prismatic test specimens were cast in steel molds and cured the same manner as the friction specimens. The prismatic test specimens were cast vertically and stored horizontally.

Specimens were removed from the forms on the following day and stored in lime-saturated water until the time of test.

2.6 Test Procedure

Tests were carried out at either 7 or 28 days. Mortar strengths ranged from 2500 to 5960 psi at 7 days, and from 3570 to 6970 psi at 28 days.

Specimens were tested using a specially designed test apparatus (Figs. 2.4a and 2.4b) mounted on a 110,000 pound capacity closed-loop, servo-hydraulic Instron testing machine (Model No. 1334). The test apparatus is assembled as follows: The mortar specimen is placed on the base of the specimen guide against a steel stopper. The steel stopper, which is about 0.125 in. lower than the mortar specimen, prevents the mortar specimen from moving during the test when the yoke is been pulled by the jack. The steel specimen is then mounted in the slot in the steel yoke so that the original surface of the reinforcing bar is exposed. The yoke, with the mounted steel specimen, is placed so that the original surface of the reinforcing bar makes contact with the mortar surface. The yoke is connected to a load cell, which connects to a 0.75 in. threaded rod running through a 5-ton hollow-core hydraulic jack. Two steel plates, separated by rollers, are placed on top of the yoke. This allows the yoke, with the steel specimen, to move when pulled by the hydraulic jack, while a vertical load is applied to the top plate.

With series 1 and 2, the entire surface of a steel specimen was placed in contact with the mortar surface prior to testing. As described earlier, this created a condition where the front edge of the steel specimen sometimes dug into the mortar, while been pulled, chipping off a portion of the mortar. This situation was corrected in series 3 by placing the mounted steel specimen such that a small portion of the front end extended beyond the edge of the mortar specimen.

Two types of load were applied, one vertical and the other horizontal. The vertical load was applied by means of the Instron testing machine and was kept constant throughout a test. Different vertical loads, ranging from 51 to 272 lb, were

applied for different tests. The horizontal load was applied at a rate of about 10 lb per second by the 5-ton hollow-core hydraulic jack, which was powered by an Amsler hydraulic testing machine. The hydraulic jack exerted a pulling force on the yoke through the 0.75 in. threaded rod and load cell. Friction between the steel and mortar specimens, due to the constant vertical load, prevented the steel specimen from moving relative to the mortar specimen until the horizontal load was greater than the frictional force opposing it.

Horizontal displacement (slip) between the steel and mortar was monitored using a spring-loaded linear variable differential transformer (LVDT) mounted at the non loaded end of the yoke. Vertical displacement was monitored for one group of specimens in series 3 using two LVDT's mounted between the Instron testing machine's top head and the base of the test apparatus.

The load cell and LVDT(s) were connected to a Hewlett-Packard data acquisition system, which was, in turn, connected to a computer so that the information could be stored. The constant vertical load applied by the Instron was also recorded. Tests lasted 1 to 2 minutes, and each group of specimens was tested within the same day. Apart from the steel specimens in series 3, where each steel specimen was used only once, steel specimens for series 1 and 2 were each used more than once.

The 1 $in.^2$ by 5 in. prismatic mortar test specimens were tested in compression following testing to determine the mortar strength. Prior to testing, the prismatic specimens were shortened to 3 in. by removing equal portions from each end using a high speed masonry saw.

2.7 Test Results and Observations

2.7.1 General

Apart from a few concrete specimens that crushed due to excessive vertical loads (the results of these test specimens were discarded), as the vertical load was maintained and the horizontal load applied and increased steadily, the steel specimens slipped relative to the mortar specimens. This continued until a peak horizontal load was reached, after which the horizontal load dropped steadily with increasing slip, with the steel specimens leaving indentations on the surface of the mortar specimens. These indentations were generally more pronounced as the applied vertical load increased. Some mortar powder (due to grinding of the mortar surface) was also found on the surface of the mortar specimens, especially for the hand finished mortar specimens. The amount of powder increased as the vertical load increased. Some mortar specimens in series 1 and 2 had a small piece chipped off in front of the steel specimen due to the front edge of the steel specimen digging into the mortar.

The coefficients of friction, COF, are evaluated in two ways. The first is based on the evaluation of the individual COF, which is obtained by dividing the maximum shear force (peak horizontal load) by the normal force (constant vertical load) for each test, from which mean COF and weighted mean COF values are calculated for groups of tests. The second is based on linear regression analysis (best fit lines) of maximum shear force versus normal force to obtain a single COF (representing the slope of the best fit line) for groups of tests.

2.7.2 Series 1

The key parameters are mortar age (7 and 28 days) and nature of mortar surface (formed and hand finished). Detailed test results and the COF (ratio of maximum shear force to normal force) for series 1 (mix 2: w/c = 0.5, s/c = 1.5) are

presented in Tables 2.2a through 2.2d. The mean COF for each group of tests is also presented in the tables. A summary of the tests in series 1 is presented in Table 2.3.

As shown in Table 2.3, the COF varied as follows: Between 0.573 and 0.684 for the 7 day formed-surface tests, with an average of 0.643; between 0.436 and 0.581 for the 7 day hand finished-surface tests, with an average of 0.539; between 0.517 and 0.730 for the 28 day formed-surface tests, with an average of 0.659; and between 0.447 and 0.638 for the 28 day hand finished-surface tests, with an average of 0.547. The results indicate a consistently higher mean COF for the formed-surface mortar specimens than for the hand finished-surface mortar specimens at both the 7 and 28 days. The coefficient of variation, COV, is lower for the formed-surface mortar specimens than for the hand finished-surface mortar specimens at the same test age. The lower COF and higher COV for the hand finished-surface mortar specimens are due to the rough nature of the hand finished-surface which accelerates the grinding of the mortar surface during the test, producing more mortar powder, reducing the COF, and increasing the inconsistency of the results. The weighted mean COF at 7 and 28 days for formed-surface mortar of 0.643 and 0.659, respectively, compare closely, as do the weighted mean COF at 7 and 28 days for hand finished-surface mortar of 0.539 and 0.547, respectively.

The best-fit line plots of maximum shear force versus normal force are presented in Figs. 2.5a through 2.6b for each group of tests in series 1. From these plots, the intercepts, slopes (COF), and coefficients of determination, r^2, are, respectively, 1.9 lb, 0.629 and 0.96 for 7 day formed-surface specimens, 3.3 lb, 0.521 and 0.94 for 7 day hand finished-surface specimens, 14.8 lb, 0.583 and 0.90 for 28 day formed-surface specimens, and 19.6 lb, 0.446 and 0.78 for 28 day hand finished-surface specimens. These results again indicate that the COF between reinforcing steel and mortar is higher and more consistent on a formed surface than on a hand

finished surface. Comparing the 7 and the 28 day tests, it is observed that the 28 day tests have higher intercepts but lower slopes.

Comparing the two ways of evaluating the COF, it is observed that the weighted mean COF (Table 2.3) are higher than the COF obtained using best-fit lines (Figs. 2.5a to 2.6b).

2.7.3 Series 2

The key parameters are mortar age (7 and 28 days), nature of mortar surface (formed and hand finished), w/c (0.4, 0.5 and 0.6) and c/s (1.5, 2.0 and 2.5). Detailed results for each test in series 2 are presented in Tables 2.4a through 2.4d. A summary of the results is presented in Table 2.5. The best-fit line plots of maximum shear force versus normal force for the different mortar mixes, surface conditions, and test ages, are shown in Figs. 2.7a through 2.15b. The slopes (COF) and r^2 values obtained from Figs. 2.7a through 2.15b are summarized in Table 2.6. From the results in Tables 2.5 and 2.6, a comparison of the formed-surface tests with the hand finished-surface tests generally indicates higher COF values for a formed-surface. This observation is consistent with the observation made in series 1.

The effect of w/c on COF was studied using the test results for formed-surface mortar specimens at 7 and 28 days. The plots of mean COF versus w/c are shown in Figs. 2.16a and 2.16b, respectively, for 7 and 28 days, with their best fit lines. The intercepts, slopes, and values of r^2 are, respectively, 0.26, 0.91 and 0.86 for the 7 day tests, and, respectively, 0.17, 1.12 and 0.91 for the 28 day tests. The strong r^2 values indicate that there is a strong correlation between w/c and mean COF. As shown in Figs. 2.16a and 2.16b, the mean COF increases as the w/c ratio increases at ages of both 7 and 28 days. The reason for this increase is most likely due to the decrease in mortar strength with increasing w/c, which allows the front edge of the steel specimen

to dig into the mortar and increase the slip resistance.

The effect of s/c on COF was studied using the test results for formed-surface mortar specimens tested at 7 and 28 days. The plots of mean COF versus s/c are shown in Figs. 2.17a and 2.17b, respectively, for 7 and 28 days. Based on these plots (Figs. 2.17a and 2.17b), there is no discernible relationship between the mean COF and the s/c.

The effect of mortar strength on COF was studied using the test results for formed-surface mortar specimens tested at 7 days. Two mortar mixes (mixes 2 and 4) were used for this study. The plots of mean COF versus mortar strength are shown in Figs. 2.18a and 2.18b, respectively, for mixes 2 and 4. These plots show no relationship between the mean COF and mortar strength, although it would be expected that the COF would decrease as mortar strength increases. This is because mortar strength decreases as w/c increases, and since the COF increases with increasing w/c, the COF should decrease with increasing mortar strength. The limited number of tests may be the reason why such a relationship is not apparent.

2.7.4 Series 3

The key parameters for this series are the effects of epoxy coating and mortar strength on the COF between reinforcing steel and mortar. Tests with uncoated and epoxy-coated reinforcing steel specimens, using mix 2 formed-surface mortar at 7 days were used in the studies. Formed-surface mortar specimens were used because they give more consistent results compared with hand finished-surface mortar specimens. The 7 day tests were used, instead of the 28 day tests, because mortar age has no significant effect on COF, as determined from series 1 and 2.

The testing procedure for series 3 was different from that used in series 1 and 2 in that the steel specimens in series 3 were placed on the mortar specimens with a

small portion of the front end of the steel extending beyond the front edge of the mortar. This prevented the front edge of the steel from digging into the mortar during the test. In addition, the steel specimens in series 3 were used only once, as opposed to steel specimens in series 1 and 2 which were used more than once. Series 3 therefore provide a better evaluation of the frictional properties between reinforcing steel and mortar.

Typical horizontal load versus horizontal displacement (slip) curves are presented in Figs. 2.19a and 2.19b for uncoated and epoxy-coated specimens, respectively. A remarkable difference between these curves is that the horizontal loads for the uncoated specimens remain approximately constant after reaching the peak horizontal load, while the horizontal load for the epoxy-coated specimens decreases steadily after reaching the peak horizontal load, as slip increases.

Fig. 2.20 is a typical plot of horizontal load versus both horizontal and vertical displacements. Positive vertical displacements indicate downward movement and negative vertical displacements indicate upward movement of the steel specimen. The curve for horizontal load versus vertical displacement indicates an initial slight upward movement (up to about one-half the peak horizontal load), followed by downward movement (up to the peak horizontal load). The initial upward movement is caused by the steel specimen trying to rise as it is been pulled. However, as the horizontal load and displacement increase, the surface of the mortar specimen begins to grind off, reducing the thickness of the mortar. The grinding process continues (tending to cause the steel specimen to move downward) until the resulting reduction in mortar thickness exceeds the initial upward movement.

Detailed results for each specimen in series 3 are presented in Table 2.7. A summary of the results is presented in Table 2.8. The results indicate that the mean COF varies from 0.503 to 0.627 for uncoated specimens, and from 0.379 to 0.591 for

epoxy-coated specimens, with a weighted mean COF of 0.561 for uncoated specimens and 0.491 for epoxy-coated specimens. Apart from the results in group T1, where the mean COF was higher for epoxy-coated specimens than for uncoated specimens, the mean COF is lower for epoxy-coated specimens than for uncoated specimens.

Figs. 2.21a and 2.21b are the best-fit line plots of maximum shear force versus normal force, for uncoated and epoxy-coated specimens, respectively. From these plots, the intercepts, slopes (COF), and values of r^2 are, respectively, -0.43 lb, 0.57 and 0.89 for uncoated specimens and 2.41 lb, 0.48 and 0.86 for epoxy-coated specimens. The ratio of the COF of epoxy-coated to uncoated specimens is obtained as 0.850. This indicates a 15% reduction in COF due to epoxy coating.

Figs. 2.22a and 2.22b are the plots of mean COF versus mortar strength, for uncoated and epoxy-coated specimens, respectively. Again, these plots indicate no clear relationship between COF and mortar strength, although Fig. 2.22b appears to indicate that the COF increases as the mortar strength increases. The small range of mortar strengths used for this series of tests prevents a full analysis of the relationship between COF and mortar strength.

2.8 Evaluation of Test Results and Summary

Because the steel specimens in series 1 and 2 were used more than once, and because the testing procedure was such that the front edge of some of the steel specimens dug into the mortar, the results from the first two series are used only to compare the effects of test parameters and as pilot tests for series 3. The evaluation and summary are therefore based on the test results for series 3 only.

From series 3, the COF at the steel-mortar interface averaged 0.56 for uncoated steel surface and 0.49 for epoxy-coated steel surface. These values compare with average COF values at the steel-concrete interface of 0.527 for a mill-scale steel

surface and 0.487 for an epoxy-coated steel surface obtained by Cairns and Abdullah (1994). The COF for an epoxy-coated steel surface obtained in this study is nearly identical with that obtained from the study by Cairns and Abdullah (see section 1.2.2). However, the COF for uncoated steel surface from this study is higher than that obtained by Cairns and Abdullah. This difference is likely due to the different steel surfaces used in the two studies. Cairns and Abdullah used a steel plate covered with mill-scale rather than an uncoated reinforcing steel bar, as used in this study. Considering the scatter in the data (standard deviation = 0.088), the results are quite close.

When a deformed reinforcing steel bar embedded in concrete is placed in tension, normal and tangential forces are introduced at the faces the ribs. These forces increase simultaneously as the tension increases, creating a condition different from the constant normal force and increasing tangential force used in this study. It is therefore suggested that future friction tests be modified to better model the simultaneous increase in the two forces. Further tests are also recommended using better test methods, to reinvestigate the effects of epoxy-coating, w/c, s/c, age, and mortar or concrete strength on the COF between reinforcing steel and mortar or concrete.

In summary, it is concluded that the COF at the steel-mortar interface is about 0.56 for an uncoated steel surface and 0.49 for an epoxy-coated steel surface. These values of COF will be used in Chapter 4 to address the effect of rib face angle on the relative bond strength of epoxy-coated reinforcing steel to uncoated reinforcing steel in concrete.

CHAPTER 3: BEAM-END AND SPLICE TESTS

3.1 General

This chapter describes the experimental procedures and test results for beam-end and splice test specimens used to study the effects of deformation pattern on bond strength as affected by epoxy coating and confinement by transverse reinforcement. The variables and configurations of the beam-end and splice specimens are described, together with the material properties, techniques for specimen fabrication, test procedures, observations during and after the tests, and the modes of failure for each type of specimen. A total of 58 beam-end specimens and 54 splice specimens, containing bars with 13 different deformation patterns were tested.

3.2 Test Parameters

Specimens were cast in groups to study the effects of specific parameters, using No. 8 (1 in. nominal diameter) steel reinforcing bars. The beam-end tests consisted of six groups (0-3, 5, and 8), some with up to six replications, for epoxy-coated and uncoated bars. The splice tests consisted of twelve groups (1-11 and 14). The key test parameters are described next:

Deformation pattern: Determining the effects of deformation pattern on bond strength as affected by epoxy-coating and confinement by transverse reinforcement was the main objective of this study. Reinforcement with a total of 13 different deformation patterns, comprising both rolled reinforcing steel and machined bars, was tested.

Splice/bonded length: Splice lengths ranged from 16 in. to 28 in. The splice length for each specimen was chosen to ensure that the splices failed before either the concrete crushed or the bars yielded. Bonded lengths for the beam-end specimens were set at 12 in.

Concrete cover and bar spacing: Nominal bottom cover, side cover, and

clear spacing used for the splice specimens ranged from 1 1/4 in. to 3 in., 1 in. to 3 in., and 1 in. to 6 in., respectively. A nominal concrete cover of 2 in. was used for the beam-end specimens.

Concrete strength: Concrete strengths ranged from 4,090 to 5,440 psi.

Transverse reinforcement: Uncoated No. 3 or No. 4 closed stirrups were used to evaluate the effects of confinement on the splice strength of uncoated reinforcement. The number and the size of the stirrups were selected to ensure that a bond failure resulted. The confinement provided by the stirrups was characterized by the total effective stirrup area in the splice region crossing the potential plane of splitting per splice, NA_{tr}/n, in which N is the number of stirrups in the development or splice region; A_{tr} is the total cross-sectional area of the stirrups crossing the potential plane of splitting at one point along the length of the development or splice; and n is the number of developed or spliced bars along the plane of splitting. The value of n is determined by the smaller of C_b or C_s. If C_b is smaller (controls), the plane of splitting passes through the cover and n = 1. If C_s controls, the plane of splitting intersects all of the bars and n = the total number of bars developed or spliced at one location.

Epoxy coating: Beam-end and splice specimens with epoxy-coated and uncoated bars were used to evaluate the effect of epoxy coating on bond strength. For the epoxy-coated bars, average coating thicknesses ranged from 8.5 to 16.8 mils.

3.3 Test Specimens

Beam-end test specimens similar to those developed by Darwin and Graham (1993a. 1993b) were used in this study (Fig. 3.1). Each specimen contained a 1 in. nominal diameter bottom-cast test bar with a 2 in. cover and 15 in. of concrete above the bar, for a total depth of 18 in. The specimens were 9 in. wide and 24 in. long.

Test bars extended 22 in. out from the face of the specimens. Bonded lengths

(lengths of test bars in contact with the concrete) and lead lengths (lengths of test bars at the loaded end not in contact with the concrete) for the beam-end specimens were set at 12 in. and 0.5 in., respectively. Two polyvinyl chloride (PVC) pipes, with an inside diameter matching that of the bar, located at the loaded end and 12.5 in. from the loaded end, were used to control the lead and bonded lengths of the test bar, respectively. The lead length is used to avoid a localized cone-type failure of the concrete at the loaded end of the specimen. A 1 in. diameter steel pipe adjacent to the unloaded end of the test bar and extending to the end of the specimen provided access for measuring unloaded end slip using an LVDT touching the end of the test bar. Joints between the PVC, the steel pipe, and the reinforcing bar were sealed with modeling clay to prevent mortar leakage.

Two No. 6 auxiliary bars were placed parallel to the test bar to prevent the specimens from failing in flexure. These auxiliary bars, one on either side of the test bar, had bottom and side covers of 1.5 in. Each specimen was provided with four No. 3 closed stirrups, two on each side of the test bar, oriented parallel to the sides of the test specimen and resting on the auxiliary bars, as shear reinforcement.

A single No. 5 transverse bar, placed approximately 2 in. beyond the end of the bonded length, was used to support the test bar. Two No. 5 lifting bars, located as shown in Fig. 3.1, were used to help move the beam-end specimens.

The splice specimens consisted of simply supported beams (Figs. 3.2a - 3.2e). Beams of length 13 ft or 16 ft contained two or three adjacent splices located within constant moment regions, with lengths of 4 ft or 6 ft. respectively. Splice lengths ranged from 16 in. to 36 in. The distance between the ends of a splice and the supports was, in all cases, greater than the beam depth. No. 3 or No. 4 closed stirrups were equally spaced within the splice region to evaluate the effect of stirrups on splice strength. No. 3 stirrups spaced at 6 in. were provided outside of the constant moment region to prevent a shear failure. Typical arrangements of splices with and without

stirrups are shown in Figs. 3.3a and 3.3b, respectively. One test beam, specimen 1.2 (see Fig. 3.2e), had two adjacent splices and two continuous bars to study the behavior of a member for which splice strength did not lead to immediate collapse.

Two No. 8 lifting bars, one at each of the quarter points, were provided to help move the specimens. Two No. 5 top bars were provided to support the stirrups. Reinforcing steel cages were fabricated inside the forms using wire ties. All spliced bars were bottom-cast. Bars within the splice region were cleaned with acetone just prior to placing concrete.

Forms for the beam-end and splice specimens were constructed using 3/4 in. plywood forms, 2 x 4 studs, and all-thread rods. The majority of the plywood was manufactured with a polymeric resin coating (DriForm 90 No-Oil panels, manufactured by Champion International Corp.) that did not require the use of a release agent. Plywood without the polymeric resin were coated with polyurethane and a release agent. Joints in the forms were sealed with flexible caulk to prevent leakage.

3.4 Materials

3.4.1 Reinforcing Steel

Two kinds of reinforcing steel were used in this project: machined bars fabricated from 1 1/4 in. diameter 110 ksi yield strength ASTM A 311 cold-rolled steel and No. 8 mill rolled deformed bars satisfying ASTM A 615.

Five bamboo deformation patterns (designated M1, M45.3, M45.4, M60.3 and M60.4) were used for the machined test bars (Fig. 3.4). Table 3.1a presents the properties and designations of the machined test bars. All bars had a 0.55 in. rib spacing and a 1.0 in. nominal diameter. The M1 bars had ribs with a rib face angle (the acute angle between the rib face and the bar axis) of 90° and a height of 0.1 in., providing a relative rib area, R_r, of 0.2, and a rib radius (the radius of curvature

between the rib face and the rib top surface and the bottom fillet) of 0.02 in. The other bars had ribs with a face angle of 45° or 60°, a height of 0.075 in., providing R_r of 0.15, and rib radii of 0.03 in. or 0.04 in.

The ASTM A 615 No. 8 rolled bars, with eight deformation patterns, are shown in Fig. 3.5. Four of the deformation patterns were conventional, with relative rib areas ranging from 0.065 to 0.085, while the other four were new patterns. Of the four, one had a relative rib area of 0.073, while the other three ranged from 0.101 to 0.140. The four conventional patterns were rolled by Chaparral Steel Company (designation C0), North Star Steel Company (designation N0), Sheffield Steel Company (designation SH0), and Structural Metals Inc. (designation S0). The new patterns were rolled by Chaparral Steel Company (designation C1), Florida Steel Corporation (designations F1 and F2), and North Star Steel Company (designation N3). All bars with the same designation were produced from the same steel heat. Table 3.1b lists the properties and designations of the rolled reinforcing test bars. The yield strengths reported for No. 8 bars were obtained from mill test reports. For No. 3 and No. 4 bars used as transverse reinforcement, the yield strength reported is the average of three samples tested.

3.4.2 Epoxy Coating

Epoxy coating was commercially applied. The machined bars were epoxy coated by Fletcher Coating Company. The coatings used on the machined bars were 3M Scotchkote 213 for the 0M1 bars, 3M Scotchkote 413 for the 1M1 bars, and 3M Scotchkote 206N for the other machined bars. The rolled bars were coated by the following coating companies: Florida Steel Corporation coated the Florida bars using Corvel Green 10-6071 from Morton Powder Coatings, Inc.; ABC Coating Company coated the Chaparral bars using Nap-Gard 7-2709 from O'Brien Powder Products, Inc.; and Simcote, Inc. coated the North Star bars using Scotchkote 413 from 3M

Corporation. Readings of coating thickness were taken at 20 points along a test bar within the bonded or splice length using a magnetic pull-off gage (Mikrotest III Thickness Gage). The average coating thicknesses ranged from 8.5 mils to 16.8 mils and are listed in Tables 3.1a and 3.1b for machined and rolled bars, respectively.

3.4.3 Concrete

Air-entrained concrete was supplied by a local ready mix plant. Type I portland cement and Kansas river sand were used. Two types of coarse aggregate (crushed limestone and basalt) were used, each with a 3/4 in. maximum nominal size. Water-cement ratios, w/c, of 0.41, 0.42, 0.44, and 0.45 were used for concrete mixes without water reducers. A w/c of 0.36 for concrete mixes with 3 oz. of water reducer per 100 lb. cement was used. Concrete strengths ranged from 4,340 psi to 5,440 psi at testing ages of 7 to 18 days for the beam-end specimens, and from 3,810 psi to 5,250 psi at testing ages of 5 to 16 days for the splice specimens. Concrete strengths reported are the average of three 6 × 12 in. cylinders. Air contents and slumps ranged from 2.1 to 4.7% and from 1 to 5.25 in., respectively. Mix proportions and concrete properties are summarized in Tables 3.2a and 3.2b for beam-end and splice specimens, respectively.

3.5 Placement, Curing and Handling

The casting procedure was planned to ensure that the concrete was as uniform in quality as possible from specimen to specimen. All specimens in a group were cast from one batch of concrete. The concrete was placed in two lifts, using shovels for the beam-end specimens and a bucket and overhead crane for the splice specimens. The first lift was placed in all specimens in a group before any specimen received a second lift. Each lift was vibrated at regular intervals.

Concrete was placed in the beam-end specimens as follows: The specimens in

a group were numbered, starting from 1, and arranged according to the numbering. For each lift, the concrete was placed, in order, starting with the first specimen.

Concrete was placed in the splice specimens as follows: The specimens in a group were numbered and arranged in the order of placement. For the first lift, concrete was placed at the two ends (about one-third the specimen length) of each specimen first, followed by the middle third. For the second (last) lift, concrete was placed in the middle third of each specimen first, followed by the two ends. Each lift of concrete was placed, in order, starting with the first specimen.

Standard 6 × 12 in. test cylinders were cast in steel molds and cured in the same manner as the test specimens. Forms were stripped after the concrete had reached a strength of at least 3,000 psi and then left to dry until the time of test.

Cover and bar spacing for the splice specimens were measured prior to concrete placement. Cover on the beam-end specimens and other dimensions on the splice specimens were measured just before testing.

3.6 Test Procedures

3.6.1 Beam-End Specimens

Beam-end tests were carried out at concrete strengths of 4,340 to 5,440 psi, 7 to 18 days after casting. The specimens were inverted and then tested using an apparatus developed by Donahey and Darwin (1983, 1985), and later modified by Brettmann et al. (1984, 1986) and Darwin and Graham (1993a, 1993b) (Fig. 3.6).

The specimens and the testing apparatus were tied down to the structural floor by two wide flange sections and four tie-down rods. Load was applied at a rate of about 6 kips per minute by two 60-ton hollow-core hydraulic jacks. The jacks were powered by an Amsler hydraulic testing machine through two 1 in. diameter load rods instrumented as load cells using two longitudinal and two transverse 350 ohm Micro-Measurements strain gages. The hydraulic jacks exerted a pulling force on the yokes

which loaded the test bar in tension through a wedge-grip assembly. The tensile force on the bar was counteracted by a compressive force imposed on the concrete specimen through a bearing pad by the frame of the testing assembly. The center of the pad was located 13.75 in. below the center of the test bars.

Slip was monitored at the loaded and unloaded ends of the test bars using spring-loaded linear variable differential transformers (LVDTs). Two LVDTs were attached with an aluminum yoke to the test bar, 4 in. from the concrete surface, to measure the loaded end slip. A spring-loaded LVDT was placed in contact with the back end of the test bar through the steel conduit to measure unloaded end slip. With the exception of the specimens in group 0, the width of the crack on the top surface of the specimen parallel to the test bar was measured with an LVDT during testing. This LVDT was positioned across the top surface of the specimen half-way along the 12 in. bonded length of the test bar.

3.6.2 Splice Tests

Splice specimens were inverted and tested as shown in Fig. 3.7, at ages ranging from 5 to 16 days and concrete strengths ranging from 3,810 to 5,250 psi. The beams were supported at two points, 4.5 ft or 5 ft from the ends of the 13 ft or 16 ft long specimens, respectively, by pin and roller supports mounted on concrete pedestals. A steel plate was attached to the bottom of the specimen at each support location, using a layer of high strength gypsum cement (Hydrostone) to distribute the reaction into the concrete. Downward loads were applied 6.0 in. from each end of the beam, providing a constant moment in the splice region between the two supports. The loads were applied to two spreader beams (one at each end of the specimen) by four hydraulic jacks through four 1.5 in. diameter load rods instrumented as load cells, similar to those used in the beam-end test. The load rods were attached to the steel beams with semi-cylindrical rollers so that the applied load remained vertical as

the ends of the test specimen rotated. The beams were loaded continuously to failure at a rate of about 3 kips per minute at each end.

The deflections at each load point and the middle of the beam were measured with spring-loaded LVDTs placed underneath the beam. The LVDTs were mounted on stands, using clamps, and placed underneath the beam so that the springs held the ends of the LVDTs against the bottom of the beam.

3.6.3 Instrumentation and Test Duration

The load cells and LVDTs were connected through a Hewlett-Packard data acquisition system to a computer, allowing the data to be saved on a computer disk. Load-loaded end slip curves were plotted for beam-end specimens, and load-deflection curves were plotted for splice specimens, as the tests progressed. A typical test lasted about 10 minutes for beam-end specimens and 15 minutes for splice specimens. Each group of specimens was tested within a 12 hour period. The standard 6 × 12 in. concrete cylinders were tested in compression soon after completing the tests.

Following the tests, the test bars were exposed by removing the top concrete cover to observe the test bar and the concrete-steel interface. In the case of the specimens with machined bars, the test bars were removed for reuse.

3.7 Test Results

3.7.1 Beam-End Specimens

Load, loaded end slip, and unloaded end slip were recorded throughout each test. The crack width was also recorded, except for the specimens in group 0. Test results for beam-end specimens are presented in Table 3.3.

Load-Slip Response: Average load-loaded end slip and load-unloaded end slip curves for all eight deformation patterns are presented in Figs. 3.8a through 3.8h

and Figs. 3.9a through 3.9h, respectively. Each figure shows the curves for both the epoxy-coated and uncoated bars with the same deformation pattern, allowing for direct comparison. These curves are obtained by averaging the modified loads at the same slip for all test specimens for each deformation pattern. Modified loads are obtained by multiplying loads by $(5000/f'_c)^{1/4}$ to account for the variations in concrete strength. [Note: The use of the 1/4 power rather than the more traditional 1/2 power is based on analyses described in Chapter 5.]

Loaded end slip is highly dependent upon local effects at the loaded face of the beam-end specimen. In contrast, unloaded end slip depends on the bond over the entire bonded length and, therefore, generally varies more smoothly with load than loaded end slip. This is evident by comparing the load-loaded end slip curves in Figs 3.8a - 3.8h with the corresponding load-unloaded end slip curves in Figs. 3.9a - 3.9h. The load-unloaded end slip curves are used to evaluate the bond performance of beam-end specimens.

In general, the load-unloaded end slip curves do not show much difference between the epoxy-coated and uncoated test bars with the same deformation pattern. The slopes of the load-unloaded end slip curves are very much the same for most of the deformation patterns, except for those of F1, F2, and M45.4 (Figs. 3.9c, 3.9d and 3.9f), where the load-unloaded end slip curves for the uncoated test bars had slightly steeper slopes than their epoxy-coated counterparts. At ultimate load, the unloaded end slip is nearly identical for specimens with the same deformation pattern, regardless of whether the bars were coated or not.

Crack Width: Crack widths (actually change in width of the specimen) due to longitudinal splitting were recorded as the tests progressed using an LVDT positioned across the width of the specimen 6.5 in. from the loaded end, on the top surface. Average load-crack width curves for epoxy-coated and uncoated bars for each deformation pattern are presented in Figs. 3.10a through 3.10h. Cracking in all

cases started at loads above 15 kips. The cracks developed rapidly, once initiated.

The crack widths just before the peak load are more consistent than the crack widths at peak load. This is because at the peak load the specimen is highly unstable and the crack width depends on whether the splitting failure of the specimen is very brittle or not. Crack widths just before the peak load for both uncoated and epoxy-coated test bars are shown in Fig. 3.11. Out of the eight deformation patterns tested, only two (C1 and M45.3) had average crack widths just before peak load that were wider for specimens with epoxy-coated bars than for those with uncoated bars. The fact that clamping force is greater for uncoated bars than epoxy-coated bars may be the reason why the average crack widths just before peak load are generally wider for specimens with uncoated bars than for those with epoxy-coated bars. For the uncoated bars with the same relative rib area (M45.3, M45.4, M60.3, and M60.4), the results (Fig. 3.11) indicate that crack width increases with increase in the rib face angle and also with an increase in the rib radius. However, for the epoxy-coated bars, the results indicate an opposite trend for both rib face angle and rib radius.

3.7.2 Splice Tests

The force in each load rod and the deflections at the middle and the ends of a beam were recorded throughout each test. Detailed dimensions and test results for splice specimens are presented in Table 3.4. Total beam deflection is taken as the sum of the average of the end deflections and the deflection at the middle of the beam. Load-deflection curves for the specimens are plotted by test group in Figs. 3.12a through 3.12l. Except for the specimens in group 1 (Fig. 3.12a), the load-deflection curves for beams within a test group having the same number of splices are virtually identical up to the point of failure. Within a test group, beams with three splices exhibit steeper load-deflection curves than those with two splices (Figs. 3.12c, 3.12e, 3.12f, 3.12g, 3.12h, and 3.12k). Specimens without stirrups generally failed in a

brittle manner, with the load dropping immediately after the specimen attained the peak load (e.g., specimens 2.4, 2.5 and 2.6 in Fig. 3.12b). In contrast, specimens with stirrups were more ductile in behavior, with the load dropping slowly as additional deflection was applied (e.g., specimens 2.1, 2.2 and 2.3 in Fig. 3.12b). Specimens with stirrups also exhibited higher strengths than similar specimens without stirrups.

Comparisons of the load-deflection curves for splice specimens with epoxy-coated and uncoated bars (Figs. 3.13a - 3.13e) indicate that the beams exhibit similar behavior up to point of failure. As a rule, specimens containing epoxy-coated bars failed at a lower load than those containing uncoated bars.

3.8 Observations

3.8.1 Beam-End Specimens

A splitting type of bond failure was observed in all tests. The nature of the failure was brittle, as there were no transverse stirrups present.

Except for specimen 5M60.4-8CN (Fig. 3.14a), failure was preceded by the initiation of a main crack above the bar, running parallel to the bar, vertically through the cover along the top surface of the specimen (Fig. 3.14b). Bond failure in specimen 5M60.4-8CN (Fig. 3.14a) was preceded by the initiation of horizontal cracks on each side of the test bar. The cracks intersected the No. 6 auxiliary bars and ran to the sides of the specimen. Since no crack occurred above the test bar, no crack width was recorded for this specimen. Minor cracks were also observed on the sides of a few of the specimens. Specimens with epoxy-coated and uncoated test bars exhibited similar crack patterns.

The test bars and both sides of the concrete-steel interface were examined after the tests by removing the top concrete cover over the bonded region. Uncoated test bars showed evidence of good adhesion to the concrete, in the form of concrete particles left on the shafts of the test bars and on the sides of the deformations, while

epoxy-coated test bars showed virtually no evidence of adhesion to the concrete. These observations match those of Zia and Johnston (1982); Treece and Jirsa (1987, 1989); Choi et al. (1990, 1991); Darwin et al. (1990); and Hadje-Ghaffari et al. (1991, 1992, 1994).

For uncoated test bars, the concrete surrounding the loaded side of the ribs closer to the loaded end of test bars was crushed as the bar slipped under load. This was evident by the presence of concrete powder found lodged against the loaded face of some of the ribs. Crushing of the concrete was generally limited to a 3 in. region on test bar closest to the loaded end. Further away from the loaded end (closer to the unloaded end) some concrete particles (not powder) were found lodged between the ribs. These concrete particles were not crushed and, where they could be removed, came off intact, indicating that they have not been crushed.

Unlike the uncoated test bars, concrete was not lodged against the face of the ribs or between the ribs of epoxy-coated test bars. Both sides of the concrete-steel interface were smooth and glossy, with very little or no damage to the epoxy coating on the bars, indicating that the epoxy-coated bars did not crush the surrounding concrete when slip occurred under load.

3.8.2 Splice Specimens

Splice failure was either ductile or brittle, depending on whether stirrups were present or not. Failure was preceded by extensive longitudinal and transverse cracking in the splice region (Figs. 3.15a - 3.15c). Longitudinal cracks began first on the tension face of the specimens, forming later on the sides at the level of the splices, and terminating at the ends of the splice region. At each end of the splice region, transverse cracks, normal to the longitudinal cracks on the tension surface, ran across the full width of the beam, extending over to the sides. Generally, the cracks were more extensive for splices confined by stirrups (Fig. 3.15c) than for splices without

confinement (Figs. 3.15a and 3.15b).

A study of the bars following the tests indicated good adhesion of concrete to the uncoated bars compared with the epoxy-coated bars. The concrete-steel interface of specimens with epoxy-coated splices had very little or no concrete shear, with smooth, glossy surfaces, exhibiting prominent and undisturbed markings from the ribs.

For specimens with uncoated bar splices without stirrups, the concrete between the ribs at the concrete-steel interface showed signs of crushing. Crushing was generally more pronounced at the concrete-steel interface on the side of the bar further away from the tension face of the specimen than on the side of the bar closer to the tension face. For beams with more than two splices, the concrete at the concrete-steel interfaces of the interior splices exhibited more crushing than those on the outside.

The concrete cover on specimens with splices confined by stirrups was very difficult to remove. As a result, the bottom concrete cover was destroyed in the process of exposing the splices. After exposure, the concrete failure looked like shear failure along some sections and like crushing failure along other sections of the concrete-steel interface. The shear failure was more predominant, with sections of concrete remaining intact between the ribs. Generally, the concrete between the ribs near the discontinuous ends of the splice showed progressively more damage than the concrete between the ribs elsewhere.

CHAPTER 4: EVALUATION OF BEAM-END AND SPLICE TEST RESULTS

4.1 General

In this chapter, the results of the beam-end and splice tests described in Chapter 3 are evaluated to examine the effects of the test parameters on the bond strength of reinforcing steel bars to concrete using beam-end and splice test specimens. The principal parameters are deformation pattern and the presence or absence of epoxy-coating.

The study of epoxy-coating is focused on how it affects the bond strength of reinforcing bars to concrete. The effect of epoxy-coating on bond strength is evaluated based on the ratio of the bond strength of coated bars to the bond strength of uncoated bars, C/U. The results obtained are compared to other test results and to the modification factors for epoxy-coating in the ACI Building Code (1989) and AASHTO Bridge Specifications (1989).

The study of deformation pattern is principally aimed at selecting characteristics that improve the bond strength of both uncoated and epoxy-coated bars. The two deformation characteristics studied are the rib face angle, γ, and the relative rib area, R_r. The γ study is limited to how it affects the C/U ratio for beam-end and splice specimens. The R_r study focuses on both how it affects the C/U ratio and how it affects the bond strength of splices that are confined by transverse reinforcement.

4.2 Effect of Epoxy-Coating on Bond Strength

To study the effect of epoxy-coating on the bond strength of steel reinforcing bars to concrete, 29 pairs of beam-end specimens and 5 pairs of splice specimens containing epoxy-coated and uncoated bars were tested. For the beam-end tests, the

C/U ratios are calculated using both individual and average modified bond strengths for uncoated bars of each bar type. For the splice specimens, the C/U ratio is based on the bar stress at bond failure in individual specimens. The calculated C/U ratios for the beam-end and splice specimens are presented in Tables 4.1a and 4.1b, respectively. The average calculated C/U ratio for each of the bar types is also presented in the tables. For the beam-end tests (Table 4.1a), the C/U ratios range from 0.74 to 1.02 with an average value of 0.92, while for the splice tests (Table 4.1b) the C/U ratios range from 0.82 to 0.94 with an average value of 0.88.

The results of previous work performed at the University of Kansas by Choi, Hadje-Ghaffari, Darwin, and McCabe (1990, 1991) and Hester, Salamizavaregh, Darwin, and McCabe (1991, 1993) are presented in Tables 4.2a through 4.2c. For the beam-end tests by Choi et al. (Table 4.2a), the C/U ratios range from 0.71 to 0.99 with an average of 0.86; for the splice tests (Table 4.2b), the C/U ratios range from 0.72 to 0.94 with an average of 0.82. For the splice tests by Hester et al. (Table 4.2c), the C/U ratios range from 0.65 to 0.86 with an average of 0.74.

The C/U ratios obtained from the current beam-end and splice tests are higher than those obtained by Choi et al. and Hester et al. From Table 4.1a, it is noted that the F2 bar, the bar with the lowest relative rib area ($R_r = 0.073$), also has the lowest C/U ratio. Also from Tables 4.1a to 4.2c, it is noted that R_r for the bars used in the current tests is generally higher than those used by Choi et al. and Hester et al. Could this explain why the current tests produce higher C/U ratios? The answer to this question calls for an evaluation of the effect of R_r, and, for that matter, all aspects of the deformation pattern on the C/U ratio. This evaluation must therefore be addressed first before any comparison of the current results can be made with other test results.

4.3 Effect of Deformation Pattern on C/U Ratio

The study of the effects of deformation pattern on C/U in this chapter is primarily aimed at learning what can be done to reduce the effect of epoxy-coating on the bond strength of steel reinforcing bars to concrete. The rib face angle and the relative rib area are the characteristics that will be studied.

4.3.1 Effect of Rib Face Angle on C/U Ratio

The effect of the rib face angle, γ, on the C/U ratio is studied using the results of the 29 pairs of beam-end specimens and the 5 pairs of splice specimens presented in Tables 4.1a and 4.1b, respectively. C/U is compared with γ in Figs. 4.1a and 4.1b, respectively, for the beam-end and splice specimens. From the plots it is observed that, generally, the C/U ratio increases as γ increases.

Choi, Darwin, and McCabe (1990) derived the theoretical statical relationship between C/U and γ as

$$C/U = \frac{(\tan\gamma + \mu_c)(1 - \mu_u \tan\gamma)}{(\tan\gamma + \mu_u)(1 - \mu_c \tan\gamma)} \qquad (4.1)$$

in which γ = rib face angle; and μ_c and μ_u are the coefficients of friction, COF, for epoxy-coated and uncoated bars, respectively. In deriving this relation, Choi et al. assumed that the cohesion between a reinforcing steel bar and concrete drops to zero once any relative movement occurs. In follow on work, Hadje-Ghaffari, Darwin, and McCabe (1991) limited the maximum value of γ for uncoated bars to values between 30° and 40°, based on studies by Rehm (1961) and Lutz and Gergely (1967), who observed that, for uncoated bars with γ greater than 40°, the concrete in front of the ribs is crushed, producing ribs with an effective value of γ between 30° and 40°. In

this chapter, therefore, γ is limited to a maximum value of 40° for uncoated bars. As reported in Chapter 2, the values of μ_c and μ_u obtained experimentally in this study are 0.491 and 0.561, respectively. The theoretical C/U ratio is limited to 1.0. The theoretical relation in Eq. 4.1, using $\mu_c = 0.491$, $\mu_u = 0.561$, $\gamma \leq 40^{\circ}$ for uncoated bars, and C/U $\leq$ 1.0, is plotted along with the beam-end and splice test results in Figs. 4.1a and 4.1b, respectively. It is interesting to note the close agreement between the test results and the theoretical relation, suggesting that Eq. 4.1 can serve as a useful tool in the study of the effect of γ on C/U.

As shown in Figs. 4.1a and 4.1b, the theoretical relation has three distinct parts. The first part, which is non-linear, represents γ less than 40°. For this part of the plot, the theoretical C/U ratio increases very slightly as γ increases from 0° to about 20°, then reduces very slightly as γ increases up to 40°. The range in C/U of this first part of the plot is so small that it can be said that, practically, from 0° to 40°, γ has no effect on C/U. The second part, which is linear, represents γ between 40° and 43°. For this range, C/U increases nearly linearly with γ. The third part of the theoretical plot corresponds to C/U = 1.0. The significance of this third part is that, theoretically epoxy-coating will not affect the bond strength of bars with γ greater than about 43°. This observation is supported by the beam-end specimen test results for the M45.4 bars ($\gamma = 45^{\circ}$) with an average C/U ratio of 0.98, the M60.3 and M60.4 bars ($\gamma = 60^{\circ}$) with average C/U ratios of 1.03 and 0.96, respectively, and the M1 bars ($\gamma = 90^{\circ}$) with an average C/U ratio of 0.98. The only deviation is provided by the two M45.3 tests with individual C/U ratios 0.91 and 0.74, of which only the last data point represents a significant deviation. It should be noted that each portion of the theoretical relationship depends upon both μ_c and μ_u.

4.3.2 Effect of Relative Rib Area on C/U Ratio

To study the effect of R_r on the C/U ratio, the current test results are combined with the earlier test results of Choi et al. (Tables 4.2a and 4.2b) and Hester et al. (Table 4.2c). These results are plotted in Figs 4.2a and 4.2b for beam-end and splice specimens, respectively, along with the best fit lines, which indicate that C/U increases as R_r increases, although the correlation is poor. The values of the coefficients of determination, r^2, for these best fit lines are 0.299 and 0.142 for the beam-end (Fig. 4.2a) and splice specimens (Fig. 4.2b), respectively. The poor correlation may be due to the effects of another parameter(s), in this case γ. The zero intercepts and slopes are, respectively, 0.758 and 1.257 for the beam-end specimens, and 0.700 and 1.308 for the splice specimens. These zero intercepts and slopes compare closely with each other. Overall, it appears that the effect of epoxy-coating on bond strength of reinforcing bars can be reduced by using bars with higher values of R_r.

4.4 Deformation Pattern and Bond Strength

The principal goal of this research is to improve the bond characteristics of steel reinforcing bars. In an earlier study using machined bars with different deformation patterns in beam-end specimens, Darwin and Graham (1993a, 1993b) found that the higher the relative rib area, the higher the bond strength of bars confined by transverse reinforcement. They also found, however, that the bond strength of bars with low cover and not confined by transverse reinforcement was independent of R_r.

Based on the results of the work by Darwin and Graham, 39 splice specimens, containing 2 or 3 splices confined by No. 3 or No. 4 transverse reinforcement (stirrups) were tested to determine the increase in bond strength provided by

transverse reinforcement as a function of R_r. Both conventional bars (R_r between 0.064 and 0.085) and high R_r bars (C1, N3 and F1 with R_r of 0.101, 0.119 and 0.140, respectively) were used. The results of these tests are combined with 10 earlier splice tests by Hester, Salamizavaregh, Darwin, and McCabe (1991, 1993) using conventional bars.

Table 4.3 provides direct comparisons of bar stresses for 15 of the current splice tests from 7 test groups. For this comparison, the bar stresses at splice failure for specimens in the same group having identical nominal test parameters, except for bar types (R_r), are compared. The comparisons clearly show that, for splices confined by stirrups, the higher the value of R_r, the higher the bond strength.

To study the effect of R_r on splice strength, the effect of confining stirrups on bond strength must be accurately characterized. This characterization must consider the effects of splice length, side and bottom cover, bar spacing, concrete strength, and the number and size of the confining stirrups. In this study, the characterization is based on the increase in bond force, T_s, above that expected for the same member geometry without confining stirrups, T_c, that is, $T_s = T_b - T_c$, in which $T_b = A_b f_s$ at failure, and

$$\begin{aligned} T_c &= A_b f_s \text{ (without stirrups)} \\ &= \left[63\, l_d (C_m + 0.5 d_b) + 2280 A_b\right]\left(0.082 \frac{C_M}{C_m} + 0.918\right) f_c'^{1/4} \end{aligned} \tag{4.2}$$

in which A_b = the area of the development/splice bar in in.^{2}; f_s is the bar stress in psi; f_c' is concrete compressive strength in psi; $f_c'^{1/4}$ in psi; l_d is development/splice length in in.; d_b is bar diameter in in.; C_M and C_m are, respectively, the maximum and minimum of C_s and C_b in in.; C_s = minimum of C_{si} + 0.25 in. and C_{so}, in in.; C_{si} =

one-half of the clear spacing between bars in in.; and C_{so} and C_b are concrete side cover and bottom cover, respectively, in in.

Modified bond forces are obtained by multiplying bond forces by $(5000/f_c')^{1/4}$ to account for the variations in concrete strength. As explained in Chapter 5, the effect of stirrups is based on the parameter, NA_{tr}/n, in which N is the number of stirrups in the development or splice region; A_{tr} is the total cross-sectional area of the stirrups crossing the potential plane of splitting at one point along the length of the development or splice; and n is the number of developed or spliced bars along the plane of splitting. The value of n is determined by the smaller of C_b or C_s. If C_b is smaller (controls), the plane of splitting passes through the cover and n = 1. If C_s controls, the plane of splitting intersects all of the bars and n = the total number of bars developed or spliced at one location. The development of expressions for T_c and T_s is described in Chapter 5. The results of the splice tests, including the values of T_s and NA_{tr}/n, are presented in Tables 4.4a and 4.4b, respectively, for the current test results and those of Hester et al. (1991, 1993).

In Chapter 3 (Table 3.2b), it was noted that two different types of coarse aggregate (basalt and limestone) were used in the concrete for the current splice specimens. To investigate the effect of coarse aggregate on bond strength, plots of T_s versus NA_{tr}/n for identical bar types (F1 and conventional) are presented in Fig. 4.3 for the two coarse aggregates. A comparison of the best-fit lines shows that the increase in bond strength due to transverse reinforcement is higher for bars cast in concrete with basalt coarse aggregate than for bars cast in concrete with limestone coarse aggregate, indicating that T_s is dependent on concrete properties, as well as the degree of confinement provided by transverse reinforcement and the relative rib area of the bars. Therefore, in an evaluation of the effect of R_r on bond strength, it would

appear best not to combine the results for the two coarse aggregates, but rather to consider the test results for the two types of concrete separately.

The results in Fig. 4.3 suggest that much of the scatter observed in test results from different studies for splices confined by transverse reinforcement can be assigned to the effects of concrete properties other than compressive strength.

Data and best fit lines for T_s versus NA_{tr}/n are presented for F1, C1 and conventional bars in Fig. 4.4a and for F1, N3 and conventional bars in Fig. 4.4b for bars cast in concrete with limestone coarse aggregate and basalt coarse aggregate, respectively. In both figures, the best-fit lines for bars with higher R_r are above those with lower R_r, supporting the observations of Darwin and Graham (1993a, 1993b) that T_s is dependent on R_r.

4.5 Discussion of Test Results

In this section the results and observations obtained from the beam-end and splice tests are discussed. A comparison of the current test results with earlier test results is also presented.

4.5.1 General Observations

The M1 bars used in this study had a ratio of rib spacing to rib height of 5.5 and γ of 90°. Despite the low ratio of rib spacing to rib height (lower than 7) and high γ (higher than 40°), all 12 beam-end specimens containing M1 bars exhibited a splitting mode of failure. This observation conflicts with the observation made by Rehm (1957, 1961) that a pullout failure will occur when the ratio of rib spacing to rib height is less than 7 and γ is greater than 40°, but matches the observations of Darwin and Graham (1993a, 1993b).

4.5.2 Deformation Pattern and Epoxy-Coating

The effects of two characteristics of deformation pattern (γ and R_r) on the C/U ratio were evaluated. Plots of C/U versus γ were compared to the plot of a theoretical relation between C/U and γ derived by Hadje-Ghaffari et al. (1991). The comparison indicates a close agreement between the test results and the theoretical relation, suggesting that the theoretical relation can be used to predict the effect of γ on C/U. According to the theoretical relation for the values of μ_u and μ_c obtained in this study, when γ is greater than about 43°, epoxy-coating will not reduce the bond strength of steel reinforcing bars to concrete. Test results for the beam-end specimens (Fig. 4.1a), generally agree with this prediction.

The effect of R_r on the C/U ratio was evaluated using best-fit line plots. From the evaluation, C/U is found to generally increase as R_r increases, but the data is highly scattered. As shown in Tables 4.1a to 4.2c, all of the bars used for the current tests, except the F2 bars, had higher R_r values than those used by Choi et al. (1990, 1991) and Hester et al. (1991, 1993). The C/U ratios from the current tests are higher, on average, than those obtained by Choi et al. and Hester et al.

Combining the results of the effects of γ and R_r on C/U, it is conclusive that deformation pattern plays an important role in the effect of epoxy coating on bond strength. Bars with higher γ and R_r give higher C/U ratios.

All of the splice specimens tested exhibited a splitting failure mode. However, the maximum reduction in bond strength due to epoxy-coating was only 18%. Treece and Jirsa (1987, 1989) concluded that, if a splitting failure occurs in splice specimens, the reduction in bond strength is about 35%. Treece and Jirsa (1987, 1989) did not report R_r for the bars they tested, although they likely fell within the range for conventional bars, which have values of R_r that are much lower than the values of R_r for the bars tested in this study. The big difference between the C/U ratio

obtained by Treece and Jirsa to that obtained here could be due to differences in R_r and γ. The reduction in bond strength for bars with higher γ and/or R_r would be expected to be lower than 35%, even when failure is caused by splitting of the concrete. The 35% reduction reported by Treece and Jirsa may represent the maximum reduction in bond strength due to epoxy-coating for bars with poor deformation patterns, especially patterns with low γ and R_r.

4.5.3 Relative Rib Area and Bond Strength

Using the combined splice test results of the current study and those reported by Hester et al. (1991, 1993), the bond strength of splices confined by stirrups has been found to increase as R_r increases. This observation matches the earlier observations made by Darwin and Graham (1993a, 1993b) for machined bars. Based on the evaluation of the test results, it is clear that splice lengths of reinforcing bars confined by stirrups can be significantly reduced, if bars with higher R_r are used.

CHAPTER 5: DEVELOPMENT LENGTH CRITERIA

5.1 General

Darwin et al. (1992a, 1992b) used linear regression techniques on the results of 147 development and splice tests to obtain an equation for the bond strength (maximum bond force, $A_b f_s$) of reinforcing bars in beams without transverse reinforcement:

$$\frac{A_b f_s}{\sqrt{f'_c}} = 6.67\, l_d \left(C_m + 0.5 d_b\right)\left(0.92 + 0.08\frac{C_M}{C_m}\right) + 300 A_b \qquad (5.1)$$

in which A_b = the area of the development or splice bar in in.^{2}; f_s = the bar stress in psi; $\sqrt{f'_c}$ = square root of concrete compressive strength in psi; l_d = development or splice length in in.; d_b = bar diameter in in.; and C_M and C_m are, respectively, the maximum and minimum of the concrete bottom cover or the lesser of one-half of the clear spacing between bars or the side cover, in in. They compared the test/prediction ratios obtained with their equation to the test/prediction ratios obtained using the equation developed by Orangun et al. (1975, 1977) for 257 test specimens from 14 different test series. The comparisons showed that Eq. 5.1 generally produces lower coefficients of variation, COV, as well as smaller ranges in the test/prediction ratio. However, of the 147 test specimens used by Darwin et al., 53 were side or top-cast bars, and of the 62 test specimens used by Orangun et al., 5 were side or top cast-bars. Since casting position affects bond strength, it is important that specimens with different casting positions not be combined in such an analysis.

In this chapter, the results of 115 development and splice specimens containing only bottom-cast bars without transverse reinforcement (stirrups) are statistically analyzed to obtain an equation for the bond strength of bottom-cast bars

not confined by stirrups. Using this equation and test results for 102 specimens with conventional bars and 25 specimens with high R_r bars in which the bars are confined by stirrups, equations are obtained for the added bond strength provided by transverse reinforcement.

The 115 development and splice tests containing bottom-cast bars not confined by stirrups represent tests by Chinn, Ferguson and Thompson (1955), Chamberlin (1956, 1958), Ferguson and Breen (1965), Thompson, Jirsa, Breen and Meinheit (1975), Zekany, Neumann and Jirsa (1981), Choi, Hadje-Ghaffari, Darwin and McCabe (1990, 1991), Hester, Salamizaregh, Darwin and McCabe (1991, 1993), Rezansoff, Akanni and Sparling (1993), and the current study, using No. 3, No. 4, No. 5, No. 6, No. 8, No. 9, No. 11, and No. 14 bars. The 102 splice tests containing bottom-cast conventional bars confined by stirrups represent tests by Ferguson and Breen (1965), Thompson, Jirsa, Breen and Meinheit (1975), Zekany, Neumann and Jirsa (1981), DeVries, Moehle and Hester (1991), Rezansoff, Konkankar and Fu (1991), Hester, Salamizaregh, Darwin and McCabe (1991, 1993), Rezansoff, Akanni and Sparling (1993), and the current study, using No. 6, No. 8, No. 9, and No. 11 bars. The 25 splice tests containing bottom-cast high R_r bars confined by stirrups represent tests from the current study, using No. 8 bars with 3 different values of R_r (F1, N3, and C1, having R_r of 0.140, 0.119, and 0.101, respectively).

5.2 Bars Not Confined by Transverse Reinforcement

5.2.1 Variables

The technique and steps used in the analysis to arrive at the bond strength equation for bars not confined by stirrups is similar to that used by Darwin et al. (1992a, 1992b). The key variables that are considered are concrete strength, development and splice length, concrete cover and bar spacing, and bar size.

Concrete Strength: Traditionally, the effect of concrete strength on bond strength has been represented using the 1/2 power of the concrete compressive strength, f_c' (Orangun et al. 1975, 1977, ACI 318-89, Darwin et al. 1992a, 1992b). Although this model works well with normal concrete strengths, it does not seem to work well with higher concrete strengths. To investigate the performance of other powers to use with the f_c' term, Eq. 5.1 is rewritten in the form

$$\frac{A_b f_s}{f_c'^{p}} = 6.67\, l_d (C_m + 0.5 d_b)\left(0.92 + 0.08\frac{C_M}{C_m}\right) + 300 A_b \qquad (5.2)$$

in which $f_c'^{p}$ = concrete compressive strength raised to the power p in psi.

Using the left side of Eq. 5.2 as the test strength and the right side as the predicted strength, a series of dummy variables analyses (Draper and Smith 1981) of test versus prediction based on f_c' were carried out to determine the power, p, that would minimize the spread in the data. These dummy variables analyses were carried out at the beginning of the study using 154 development and splice test results of bars not confined by stirrups which are different from the final 115 test results reported in this study. The change in the test data from 154 to 115 resulted from the removal of all non-bottom-cast bars and also the addition of new test data. Based on the initial dummy variables analyses, the 0.24 power was found to provide the best match (minimum spread). However for convenience, the 1/4 power was selected for use in the balance of the study.

A comparison of the dummy variables analyses of test versus prediction results based on f_c', using the 115 tests for bars not confined by stirrups, is presented in Table 5.1. The comparison shows that the 1/4 power provides a higher (better) coefficient of determination, r^2, of 0.9789 and a lower ratio of the weighted standard

deviation of the intercepts to the range (difference between the maximum and minimum predicted bond strengths) of 0.0033 than the 1/2 power. The corresponding values for the 1/2 power are, respectively, 0.9771 and 0.0137. The dummy variables plots for the 1/4 power and 1/2 power are shown, respectively, in Figs. 5.1a and 5.1b. For each plot, the right side of Eq. 5.2 is multiplied by the slope obtained from the results of the respective dummy variables analysis (Table 5.1), so that the slope of the plots is 1.0. This allows for easy comparison. Figs. 5.1a and 5.1b show that the best-fit lines for the 1/4 power are much closer together than the lines for the 1/2 power. The dummy variables plots for the 1/4 power do not also show any trend with respect to f_c' as the plots for the 1/2 power do (the lower the value of f_c', the higher the intercept and therefore the higher the relative bond strength).

In this analysis, both the 1/4 power and the 1/2 power will be used to obtain new equations for the bond strength of bars not confined by stirrups. The two bond strength equations will then be compared to see which better represents the bond strength of development and splice specimens containing bottom-cast bars not confined by stirrups.

Development and Splice Length: Bond strengths are found to increase with development and splice length in a linear fashion. Although this increase is linear, bond strength is not proportional to development or splice length.

Concrete Cover and Bar Spacing: Figs. 5.2a and 5.2b show two ways that spliced concrete beams fail in the splitting mode. It is expected that the splitting mode failure depicted in Fig. 5.2b will occur when the bottom cover, C_b, is greater than the smaller of one-half the clear spacing between spliced bars, C_{si}, and the side cover, C_{so}. In the study by Darwin et al. (1992a, 1992b), these variables were represented using C_M and C_m, where C_M and C_m were, respectively, defined as the larger and smaller of C_b and C_s; and C_s defined as the smaller of C_{si} and C_{so}.

However, as shown in Fig. 5.2b, when $C_m = C_{si}$, the two cracks propagating towards each other from adjacent developed or spliced bars do not exactly coincide. This suggests that the effective value of C_{si} that should be used to derive bond strength equations should be larger than the actual C_{si} value. Therefore, at the beginning of this study, it was decided to determine the best effective value of C_{si} that would be used in the model

$$\frac{A_b f_s}{f_c'^p} = K_1 l_d (C_m + 0.5 d_b) + K_2 \qquad (5.3)$$

in which K_1 and K_2 are constants representing the slope and the intercept, respectively, for the cases when p = 1/4 and 1/2. The values of K_1 and K_2 were then determined for different definitions of effective C_{si} from dummy variables analyses of $A_b f_s / f_c'^p$ versus $l_d (C_m + 0.5 d_b)$, based on bar size, using the 154 initial development and splice test results, for p = 1/4 and 1/2. Then, using the 32 tests for which C_{si} controlled, and $A_b f_s / f_c'^p$ and $K_1 l_d (C_m + 0.5 d_b) + K_2$ as test and prediction strengths, respectively, the test/prediction ratio for each of the 32 tests was evaluated for each set of K_1 and K_2. The COV was then calculated for the 32 test/prediction ratios for each set of K_1 and K_2 values and the two values were compared.

Two approaches to obtaining the effective value of C_{si} were investigated: one involved multiplying C_{si} by a factor and the other involved increasing C_{si} by a constant. Different factors and constants were evaluated, and adding the constant 0.25 in. to C_{si} was found to give the best match (minimum COV). This was adopted and the definition of C_s was revised to be the smaller of the sum of C_{si} + 0.25 in. or C_{so}. Comparisons of test/prediction ratios for C_{si} and C_{si} + 0.25 in. are presented in Table 5.2 for the 1/4 and 1/2 powers of f_c', using the 34 (out of the final 115) test results for which C_{si} controls. The results of the comparisons show that using C_{si} +

0.25 in. produces lower (better) COV values for both the 1/4 and 1/2 powers of f'_c than using C_{si}.

5.2.2 Bond Strength Equations

Eq. 5.3 is used as a model for the bond strength for bottom-cast bars not confined by stirrups. To determine K_1 and K_2 for the 1/4 and 1/2 powers of f'_c, dummy variables analyses of best-fit equations of $A_b f_s / f'^{p}_c$ (test) versus $l_d(C_m + 0.5d_b)$ based on bar size are carried out, using the 115 test results. For p = 1/4, K_1 = 66.3 and K_2 = 412 for No. 3 bars, 517 for No. 4 bars, 1229 for No. 5 bars, 995 for No. 6 bars, 1648 for No. 8 bars, 3068 for No. 9 bars, 4264 for No. 11 bars, and 4102 for No. 14 bars. For p = 1/2; K_1 = 9.31 and K_2 = 44 for No. 3 bars, 52 for No. 4 bars, 119 for No. 5 bars, 98 for No. 6 bars, 146 for No. 8 bars, 309 for No. 8 bars, 461 for No. 11 bars, and 486 for No. 14 bars. The results are presented in Table 5.3 and plotted in Figs. 5.3a and 5.3b, respectively, for p = 1/4 and p = 1/2. The results show that the values of K_2 are roughly proportional to the bar area, A_b. Based on this observation, the intercept for each bar size is divided by the nominal bar area and then the weighted mean intercepts are obtained, 2412 and 238 for p = 1/4 and p = 1/2, respectively. Based on the results of the dummy variables analyses Eq. 5.3 can be rewritten as

$$\frac{A_b f_s}{f'^{1/4}_c} = 66.3\, l_d(C_m + 0.5d_b) + 2412A_b \qquad (5.4a)$$

$$\frac{A_b f_s}{f'^{1/2}_c} = 9.31\, l_d(C_m + 0.5d_b) + 237A_b \qquad (5.4b)$$

Using the right sides of Eqs. 5.4a and 5.4b, each as the "predicted bond

strength," the effect of C_M/C_m is determined. To do this, the ratio of test strength (left side of Eqs. 5.4a and 5.4b) to predicted strength (test/prediction) is compared to the C_M/C_m ratio as a function of bar size using dummy variables analysis for each of the two predictive equations. The dummy variables plots are shown in Figs. 5.4a and 5.4b, respectively, for the 1/4 and 1/2 powers of f_c', and the results of the analyses are presented in Table 5.4. The equations obtained from these analyses for the 1/4 and 1/2 powers are, respectively,

$$\frac{A_b f_s / f_c'^{1/4}}{66.3\, l_d (C_m + 0.5 d_b) + 2412 A_b} = 0.077 \frac{C_M}{C_m} + K_3 \qquad (5.5a)$$

$$\frac{A_b f_s / f_c'^{1/2}}{9.31\, l_d (C_m + 0.5 d_b) + 238 A_b} = 0.087 \frac{C_M}{C_m} + K_4 \qquad (5.5b)$$

with K_3 = 1.077 for No. 3 bars, 0.912 for No. 4 bars, 1.114 for No. 5 bars, 0.836 for No. 6 bars, 0.847 for No. 8 bars, 0.981 for No. 9 bars, 0.862 for No. 11 bars, and 0.839 for No. 14 bars; and K_4 = 1.060 for No. 3 bars, 0.906 for No. 4 bars, 1.032 for No. 5 bars, 0.827 for No. 6 bars, 0.817 for No. 8 bars, 0.956 for No. 8 bars, 0.859 for No. 11 bars, and 0.885 for No. 14 bars. The weighted mean intercepts are 0.868 and 0.853 for the 1/4 and 1/2 powers of f_c' (Eqs. 5.5a and 5.5b), respectively. Using these weighted mean intercepts, the bond strength equations can be written as

$$\frac{A_b f_s}{f_c'^{1/4}} = \left[66.3\, l_d (C_m + 0.5 d_b) + 2412 A_b\right]\left(0.077 \frac{C_M}{C_m} + 0.868\right) \qquad (5.6a)$$

$$\frac{A_b f_s}{f_c'^{1/2}} = \left[9.31\, l_d (C_m + 0.5 d_b) + 237 A_b\right]\left(0.087 \frac{C_M}{C_m} + 0.853\right) \qquad (5.6b)$$

If the coefficients obtained in the dummy variables analyses for the C_M/C_m effect are modified so that the term containing the ratio C_M/C_m equals 1.0 when $C_M/C_m = 1.0$ and the coefficients of the terms within the brackets in Eqs. 5.6a and 5.6b are adjusted accordingly, the final bond strength equations, after simplification and rounding, become

$$\frac{A_b f_s}{f_c'^{1/4}} = \left[63\, l_d\left(C_m + 0.5d_b\right) + 2280A_b\right]\left(0.082\frac{C_M}{C_m} + 0.918\right) \qquad (5.7a)$$

$$\frac{A_b f_s}{f_c'^{1/2}} = \left[8.8\, l_d\left(C_m + 0.5d_b\right) + 220A_b\right]\left(0.093\frac{C_M}{C_m} + 0.907\right) \qquad (5.7b)$$

5.2.3 Comparison with Experimental Results

The results predicted by the right sides of Eqs. 5.7a and 5.7b are compared with the 115 test results used to obtain the equations in Tables 5.5a through 5.5j. The results are summarized in Table 5.6. A comparison of the COV values for the 10 test series used in the analysis shows that Eq. 5.7a produces the lower COV for 5 series and Eq. 5.7b produces the lower COV for the other 5. Eq. 5.7a, however, produces a lower range and lower COV for all 115 tests. This demonstrates that the equation based on the 1/4 power of f_c' (Eq. 5.7a) does a better job than the equation based on the 1/2 power of f_c' (Eq. 5.7b) of representing the bond strength of bottom-cast bars not confined by stirrups.

Comparisons of dummy variables analysis plots of test strength (left sides of Eqs. 5.7a and 5.7b) versus predicted strength based on f_c' are presented for the bond strength equations obtained with the 1/4 power (Eq. 5.7a) and 1/2 power (Eq. 5.7b) of f_c', respectively, in Figs. 5.5a and 5.5b and the results summarized in Table 5.7. A comparison of the two figures shows that the plots using the expression based on the

1/4 power of f_c' (Fig. 5.5a) are less scattered than those using the expression based on the 1/2 power (Fig. 5.5b). In addition, the intercepts obtained from the analysis with the 1/2 power of f_c' (Fig 5.5b) exhibit a trend (the higher f_c', the lower the intercept). There is, however, no trend for the intercepts obtained with the 1/4 power (Fig. 5.5a). r^2 obtained from the analysis with the 1/4 power (0.9808) is also higher than r^2 obtained from the analysis with the 1/2 power (0.9757).

Based on the comparison of the results of the dummy variables analyses based on f_c', it is clear that the 1/4 power better reflects the effect of f_c' on the bond strength of bottom-cast bars not confined by stirrups than the 1/2 power. The bond strength equation obtained with the 1/4 power (Eq. 5.7a) is therefore selected to represent the bond strength equation for bottom-cast bars not confined by stirrups.

5.3 Bars Confined by Transverse Reinforcement

In Chapter 4, it was demonstrated that coarse aggregate properties and the relative rib area, R_r, affect the bond strength of bars confined by transverse reinforcement (stirrups). In the development of the bond strength equation for bars confined by stirrups therefore, bars with different values of R_r will be treated separately: The conventional bars (R_r between 0.064 and 0.085) are treated as one group and the high R_r bars (F1, N3 and C1 with R_r = 0.101, 0.119 and 0.140, respectively) are treated as 3 separate groups.

In developing the equations for bars confined by stirrups, the bond strength in a developed or spliced bar confined by stirrups, T_h, is represented as the sum of a "concrete contribution," T_c, and a "steel contribution," T_s. T_c is assumed to be the bond strength of an identical bar not confined by stirrups, calculated using Eq. 5.7a, while T_s is assumed to be the increase in the bond strength due to the presence of the stirrups. This relationship can be represented as

$$T_b = T_c + T_s \tag{5.8}$$

The effect of stirrups has historically been modeled to include the yield strength of the stirrup, f_{yt} (Orangun et al. 1975, 1977). The presence of f_{yt} is based on the assumption that the stirrups yield at the time of splice or development failure. However, work by Maeda et al. (1991), Sakurada et al. (1993), and Azizinamini et al. (1995) demonstrates that stirrups remain elastic at the time of bond failure, strongly suggesting that there is no justification for including f_{yt} in the analysis.

To specifically evaluate whether to include f_{yt} in a term modeling the effect of stirrups on T_s, the term is initially represented as $NA_{tr}f_{yt}/n$; in which N is the number of stirrups in the development or splice region; A_{tr} is the total cross-sectional area of the stirrups crossing the potential plane of splitting at one point along the length of the development or splice; and n is the number of developed or spliced bars along the plane of splitting. The value of n is determined by the smaller of C_b or C_s. If C_b is smaller (controls), the plane of splitting passes through the cover and n = 1. If C_s controls, the plane of splitting intersects all of the bars and n = the total number of bars developed or spliced at one location. Next, dummy variables analyses of $T_s/f_c'^{1/4}$ versus $NA_{tr}f_{yt}/n$ are performed with different limits on f_{yt} values, and the results are compared. The analyses include cases with no limits on f_{yt} and cases where f_{yt} is limited to 75 ksi, 60 ksi or 40 ksi for the 102 conventional bar splice tests. The results are presented in Table 5.9.

A comparison of the results shows that the correlation between $T_s/f_c'^{1/4}$ and $NA_{tr}f_{yt}/n$ improves as the limit on f_{yt} is reduced. The best result is obtained when f_{yt} is limited to 40 ksi. However, since all of the studies used stirrups with f_{yt} greater than 40 ksi, f_{yt} can be considered as a constant, which can therefore be dropped from the analysis to obtain a new term, NA_{tr}/n. This new term which represents the total area

of stirrups crossing the potential plane of splitting will be referred to as "the total effective stirrup area" as it has the units of area (in.^{2}) and will be used throughout the remainder of this report to model the effect of stirrups on bond strength.

5.3.1 Conventional Bars

The 102 tests for specimens with conventional bars confined by stirrups include the results from the current study plus seven others. Since concrete properties affect the bond strength of bars confined by stirrups, the data from each study is treated separately. The test results from the current study with crushed limestone coarse aggregate are treated separately from those with basalt coarse aggregate but are combined with the results reported by Hester at al. (1991, 1993), since both used the same concrete materials and test setup. These tests are identified as "KU limestone", while the tests with basalt coarse aggregate are identified as "KU basalt". The other tests are identified by the authors. The total number of test groups (series) making up the 102 conventional bars confined by stirrups therefore becomes eight (KU basalt, KU limestone, Rezansoff et al. 1993, Rezansoff et al. 1991, Zekany et al. 1981, Thompson et al. 1975, Ferguson and Breen 1965).

To obtain an equation for the bond force of bars confined by stirrups, a linear relation between $T_s/f_c'^{1/4}$ and NA_{tr}/n is represented as

$$\frac{T_s}{f_c'^{1/4}} = K_5\left(\frac{NA_{tr}}{n}\right) + K_6 \qquad (5.9)$$

where K_5 and K_6 are constants representing the slope and the intercept, respectively.

To obtain the values of K_5 and K_6, a dummy variables analysis of $T_s/f_c'^{1/4}$ versus NA_{tr}/n based on test series is performed. The plots of the dummy variables

analysis are shown in Fig. 5.6, and the results presented in Table 5.10. The results show a wide difference in the intercepts for different test series. The two test series from the University of Kansas (KU basalt and KU limestone) have the lowest intercepts, while the two test series by Rezansoff et al. (1991, 1993) have the highest intercepts. The reason for this trend in the results can be attributed to differences in concrete properties and possibly testing procedures. To account for these differences and obtain a representative equation for all tests using conventional, the weighted mean intercept is used. Using the slope and the weighted intercept, Eq. 5.9 becomes

$$\frac{T_s}{f_c'^{1/4}} = 2187\frac{NA_{tr}}{n} + 202 \tag{5.10}$$

with $r^2 = 0.7152$. The final bond strength equation for conventional bars confined by stirrups is, therefore,

$$\frac{A_b f_s}{f_c'^{1/4}} = \left[63\, l_d\left(C_m + 0.5d_b\right) + 2280A_b\right]\left(0.082\frac{C_M}{C_m} + 0.918\right) + 2187\frac{NA_{tr}}{n} + 202 \tag{5.11}$$

5.3.2 High Relative Rib Area Bars

In the previous section it was noted that concrete properties and testing procedures can affect the bond strength of bars confined by stirrups. It was also noted that tests from the University of Kansas generally produce results that are lower than the overall average. Therefore, since all of the high R_r tests come from the University of Kansas, it is logical to expect that equations obtained using these tests will predict lower bond strengths than would be expected if the splice tests were carried out with other concretes at other test sites. Therefore, to obtain an expression for T_s that is

representative of a broad range of concrete properties and test sites using only test results from the University of Kansas, the same adjustment needed to make the best-fit line equation for conventional bars tested at the University of Kansas coincide with that of the overall average will be made to the best-fit equations for the high R_r bars.

Figs. 5.7a and 5.7b show the best-fit lines for $T_s/f_c'^{1/4}$ versus NA_{tr}/n for spliced bars tested at the University of Kansas cast in concrete containing basalt and limestone coarse aggregate, respectively. Evaluation of the high R_r bars will be based on the combined results for the two types of concrete. The results of the linear regression analyses are presented in Table 5.11.

For the F1 bars, with R_r = 0.140, splice tests were carried out using both concretes. However, for the N3 bars, with R_r = 0.119, splice tests were carried out only in concrete with basalt coarse aggregate. Therefore, the slope and intercept for R_r = 0.119 in concrete with limestone coarse aggregate must be estimated. The values of the slope and intercept for R_r = 0.119 in concrete containing limestone are taken as the average of the values for R_r = 0.101 and R_r = 0.140. Similarly, since C1 bars, with R_r = 0.101, were tested only in concrete containing limestone coarse aggregate, the slope and intercept for R_r = 0.101 bars in concrete containing basalt coarse aggregate are estimated to be equal to the average of the KU conventional bars (R_r = 0.064 - 0.085) and bars with R_r = 0.119 cast in concrete with basalt. Using the individual slopes and intercepts obtained (or estimated) for splice tests using basalt and limestone coarse aggregates, an average slope and intercept is calculated for each bar type.

As expected, the average slope and intercept for the KU conventional bars (2122 and -416) are lower than the slope and intercept obtained for all conventional bars (2187 and 202). To adjust the KU conventional bar average slope and intercept to match the slope and intercept for all conventional bars requires adding the

difference between the slopes (2187 - 2122 = 65) and intercepts (202 + 416 = 618), respectively, to the values for the KU conventional bars. Using the same differences in slope and intercept, the average slopes and intercepts for the high R_r bars are adjusted to obtain representative equations. Table 5.12 summarizes the results of the calculations for obtaining the estimated slopes and intercepts for high R_r bars.

Using the estimated slopes and intercepts, the bond strength equations for the high R_r bars can best be represented as follows:

For $R_r = 0.140$ (F1) bars

$$\frac{A_b f_s}{f_c'^{1/4}} = \left[63\, l_d\left(C_m + 0.5d_b\right) + 2280A_b\right]\left(0.082\frac{C_M}{C_m} + 0.918\right) + 3399\frac{NA_{tr}}{n} + 533 \qquad (5.12)$$

For $R_r = 0.119$ (N3) bars

$$\frac{A_b f_s}{f_c'^{1/4}} = \left[63\, l_d\left(C_m + 0.5d_b\right) + 2280A_b\right]\left(0.082\frac{C_M}{C_m} + 0.918\right) + 2791\frac{NA_{tr}}{n} + 531 \qquad (5.13)$$

For $R_r = 0.101$ (C1) bars

$$\frac{A_b f_s}{f_c'^{1/4}} = \left[63\, l_d\left(C_m + 0.5d_b\right) + 2280A_b\right]\left(0.082\frac{C_M}{C_m} + 0.918\right) + 2413\frac{NA_{tr}}{n} + 471 \qquad (5.14)$$

Like Figs. 5.7a and 5.7b, Eqs. 5.12 to 5.14 reflect the increase in the

contribution of stirrups to bond strength as R_r increases.

5.3.3 Comparison of Test and Predicted Bond Strength Equations

The test results are compared to the predicted bond strengths (from Eqs. 5.11 through 5.14) for all of the test results used to obtain the bond strength equations. Comparisons for the 102 conventional bar tests are presented in Tables 5.13a through 5.13i and those for the 25 high R_r bar tests presented in Tables 5.13j through 5.13m.

For the conventional bars, the test/prediction ratios for the tests from the University of Kansas (Tables 5.13a through 5.13c) produce ratios lower than 1.0, as expected. Of the 24 tests with conventional bars at the University of Kansas, only 2 produce test/prediction ratios higher than 1.0. The mean test/prediction ratios for the current tests with basalt coarse aggregate, the current tests with limestone coarse aggregate, and the tests by Hester et al. (1991, 1993) (0.922, 0.849, and 0.901, respectively) are less than 1.0. These three test series provide the lowest mean test/prediction ratios, while the 2 test series reported by Rezansoff et al. (1991, 1993) provide the highest mean ratios (1.124 and 1.062). For all 102 conventional bar tests, the minimum, maximum, mean, and COV values for the test/prediction ratio are, respectively, 0.711, 1.313, 0.999, and 0.135.

For the high R_r bars, the test/prediction ratios are all low. Of the 25 tests, only 1 produces a test/prediction ratio higher than 1.0. The mean test/prediction ratios, 0.944, 0.856, 0.931, and 0.880 for Rr = 0.140 (basalt), 0.140 (limestone), 0.119, and 0.101, respectively, are all less than 1.0.

A plot of test versus predicted strength for all 102 conventional and 25 high R_r bar tests in which the splices were confined by stirrups (using the appropriate predicted bond strength equation based on bar type) is presented in Fig. 5.8.

5.4 Comparisons of Test/Prediction Ratios for Bars based on Bar Stress

In this section, test/prediction ratios are compared based on the bar stress at failure, f_s. Specimens are grouped first based on the absolute bar stress at bond failure and next based on the ratio of the bar stress at bond failure to the yield strength of the bar. Comparisons are made for bars not confined by stirrups and for conventional bars confined by stirrups.

5.4.1 Comparison based on the Bar Stress at Bond Failure

For this comparison, the test/prediction ratios of the 115 tests in which the bars were not confined by stirrups and the 102 conventional tests in which the bars were confined by stirrups are grouped based on the bar stress at bond failure, f_s.

For bars not confined by stirrups, 4 groups ($f_s \leq 40$ ksi, 40 ksi $< f_s \leq 50$ ksi, 50 ksi $< f_s \leq 60$ ksi, and $f_s > 60$ ksi) of test/prediction ratios are obtained. The test/prediction ratio for each test and the minimum, maximum, mean, standard deviation and COV for each group are presented in Tables 5.14a through 5.14d. The tables show that the mean test/prediction ratios, 0.937, 1.015, 1.028, and 0.992 for the 4 groups, respectively, increase for each f_s range up to $f_s = 60$ ksi and then decrease for $f_s > 60$ ksi.

For conventional bars confined by stirrups, 3 groups ($f_s \leq 50$ ksi, 50 ksi $< f_s \leq$ 60 ksi, and $f_s > 60$ ksi) of test/prediction ratios are obtained. The test/prediction ratio for each test and the minimum, maximum, mean, standard deviation and COV for each group are presented in Tables 5.15a through 5.15c. The tables show that the mean test/prediction ratios, 0.915, 0.974, and 1.076 for the 3 groups, respectively, increase as f_s increases.

Based on the comparisons of test/prediction ratios for bars with and without confining reinforcement, it is observed that the lowest f_s range produces the lowest

mean test/prediction ratio. The test/prediction ratio generally increases as f_s increases. The significance of these observations is that the bond strength equations derived in this chapter appear to be unconservative for $f_s < 50$ ksi, but provide a reasonable estimate of f_s for higher values of stress.

5.4.2 Comparison based on the Ratio of Bar Stress at Bond Failure to the Yield Strength of the Bar

For this comparison, only tests in which the yield strengths of the bars are known are studied. The test/prediction ratios are grouped based on the ratio of the bar stress at bond failure to the yield strength of the bar, f_s/f_y.

For the bars not confined by stirrups, 4 groups ($f_s/f_y \leq 1/2$, $1/2 < f_s/f_y \leq 3/4$, $3/4 < f_s/f_y \leq 1$, and $f_s/f_y > 1$) of test/prediction ratios are obtained. The test/prediction ratio for each test and the minimum, maximum, mean, standard deviation and COV for each group are presented in Tables 5.16a through 5.16d. The tables show that the mean test/prediction ratio increases as f_s/f_y increases up to $f_s/f_y = 1$. There is, however, a slight decrease in the mean test/prediction ratio as f_s/f_y increases beyond 1. The mean test/prediction ratios are 0.818, 0.991, 1.016, and 0.994 for the 4 groups, respectively.

For the conventional bars confined by stirrups, 3 groups ($1/2 < f_s/f_y \leq 3/4$, $3/4 < f_s/f_y \leq 1$, and $f_s/f_y > 1$) of test/prediction ratios are obtained. The test/prediction ratio for each test and the minimum, maximum, mean, standard deviation and COV for each group are presented in Tables 5.17a through 5.17c. The tables show that the mean test/prediction ratio increases as the f_s/f_y range increases. The mean test/prediction ratios are 0.926, 1.016, and 1.149 for the 3 groups, respectively.

Based on the comparisons of test/prediction ratios for bars with and without confining reinforcement, it is observed that the lowest f_s/f_y range in each case

produces the minimum mean test/prediction ratio, and that the test/prediction ratio generally increases as f_s/f_y increases. The significance of these observations is that the bond strength equations derived in this chapter appear to be unconservative for $f_s <$ 3/4 f_y and conservative for high values of stress. This increase in relative bond strength with increasing bar stress may be due to higher slip that occurs with increased f_s. The higher slip would have the effect of producing a more uniform clamping force and, thus, a more uniform bond force along the developed/spliced length of the bar.

CHAPTER 6: PROBABILITY-BASED DESIGN EQUATIONS

6.1 Introduction

For any structural member, the applied load and the strength (resistance) are variable quantities. Variability in the applied load may lead to conditions of overload, while variability in the strength may lead to conditions of understrength. To reduce the probability of failure in reinforced concrete members to an acceptable level, the American Concrete Institute (ACI) specifies the use of load and resistance (ϕ) factors for design. The current ACI Building Code (ACI 318-89) has ϕ factors for designing reinforced concrete members to resist flexural, axial, shear and torsion, and bearing.

Since the bond strength of reinforcing bars in concrete depends on parameters such as the concrete strength, development/splice length, concrete cover and bar spacing, the variability associated with these parameters also causes variability in bond strength. This variability may lead to lower bond strengths and, therefore, increase the probability of failure in bond.

The purpose of this chapter is to use probability-based techniques to obtain a resistance factor, ϕ_d, for use with the bond strength equations for conventional bars with and without stirrups presented in the previous chapter. The techniques include the use of Monte Carlo simulation to represent the effects of variability on member strength. ϕ_d obtained from the analysis is incorporated into the bond strength equations to arrive at prototype design equations for development and splice length of both conventional and high R_r bars, with or without stirrups. Finally, development and splice lengths calculated using the prototype design equations are compared with development and splice lengths calculated using the design equations proposed for ACI 318-95.

6.2 Variability of Bond Strength

The actual bond strength of a reinforcing bar in concrete is a statistical variable that is controlled by a number of factors that are themselves statistical variables. The major statistical variables considered in this study are the concrete strength, the member dimensions, and the predicted bond strength equations.

6.2.1 Predicted Bond Strength Equations

The predicted (model) bond strength equations are the expressions presented in the previous chapter for bars without stirrups (Eq. 5.7a)

$$A_b f_s = \left[63\, l_d (C_m + 0.5 d_b) + 2280 A_b\right]\left(0.082 \frac{C_M}{C_m} + 0.918\right) f_c'^{1/4} \qquad (6.1)$$

and for conventional bars with stirrups (Eq. 5.11)

$$A_b f_s = \left\{\left[63\, l_d (C_m + 0.5 d_b) + 2280 A_b\right]\left(0.082 \frac{C_M}{C_m} + 0.918\right) + 2187 \frac{N A_{tr}}{n} + 202\right\} f_c'^{1/4} \qquad (6.2a)$$

in which A_b = the area of the developed or spliced bar in in.^{2}; f_s is the bar stress in psi; f_c' is concrete compressive strength in psi; $f_c'^{1/4}$ is in psi; l_d is development/splice length in in.; d_b is bar diameter in in.; C_M and C_m are, respectively, the maximum and minimum of C_s and C_b in in.; C_s = minimum of C_{si} + 0.25 in. and C_{so}, in in.; C_{si} = one-half of the clear spacing between bars in in.; and C_{so} and C_b are concrete side cover and bottom cover, respectively, in in.; N is the number of stirrups in the development/splice region; A_{tr} is the total cross-sectional area of the stirrups crossing

the potential plane of splitting at one point along the length of the development/splice; and n is the number of developed or spliced bars along the plane of splitting. The value of n is determined by the smaller of C_b or C_s. If C_b is smaller (controls), the plane of splitting passes through the cover and n = 1. If C_s is controls, the plane of splitting intersects all of the bars and n = the total number of bars developed or spliced at one location.

Since, in typical beam detailing, the spacing of the stirrups, s, is specified instead of the number of stirrups in the splice region, N, N in Eq. 6.2a is replaced by l_d/s to obtain the equation

$$A_b f_s = \left\{\left[63\, l_d\left(C_m + 0.5d_b\right) + 2280A_b\right]\left(0.082\frac{C_M}{C_m} + 0.918\right) + 2187\frac{l_d A_{tr}}{sn} + 202\right\} f_c'^{1/4} \qquad (6.2b)$$

For a developed or spliced bar, the development/splice length, l_d, the values of C_b and C_s, and the concrete compressive strength, f_c', can all vary. Following the work by Mirza and MacGregor (1979, 1986) and Mirza, Hatzinikolas, and MacGregor (1979), all of the parameters associated with the bond strength equations are considered to be normally distributed.

6.2.2 Development or Splice Length, l_d

In the Monte Carlo simulation, the development or splice length will be represented by a random variable with a mean equal to the specified value of l_d. For the range of bar sizes used for the analyses in this chapter, ACI 117 specifies a tolerance of -1.0 in. for l_d. If it is assumed that 95% of all bars will meet this criterion, then the standard deviation of l_d, σ_{l_d}, is defined by

$$1.645\sigma_{l_d} = 1.0 \tag{6.3}$$

from which $\sigma_{l_d} = 0.6079$ in.

6.2.3 Concrete Bottom Cover, C_b

The bottom cover will be represented as random variable with a mean equal to the specified value of C_b. ACI 117 specifies a tolerance for C_b as –0.375 in. for beam depth ≤ 12.0 in. and –0.500 in. for beam depth > 12.0 in. Again, assuming that 95% of all members will meet this criterion, the standard deviation of C_b, σ_{C_b}, is defined by

$$1.645\sigma_{C_b} = 0.375 \tag{6.4a}$$

for beam depth ≤ 12.0 in. to give a value of 0.228 in. for σ_{C_b}, and

$$1.645\sigma_{C_b} = 0.500 \tag{6.4b}$$

for beam depth > 12.0 in. to give a value of 0.304 in. for σ_{C_b}.

6.2.4 Concrete Side Cover, C_{so}

The side cover will be represented as a random variable with a mean equal to the specified value of C_{so}. For the range of beam widths used in this chapter, ACI 117 specifies a tolerance for C_{so} as ±0.375 in. for 4.0 in. < beam width ≤ 12.0 in. and ±0.500 in. for beam width > 12.0 in. Assuming that 95% of all members will meet this criterion, the standard deviation, $\sigma_{C_{so}}$, for C_{so} is defined by

$$1.96\sigma_{C_{so}} = 0.375 \tag{6.5a}$$

for 4.0 in. < beam width ≤ 12.0 in. to give a value of 0.1913 in. for σ_{C_w}, and

$$1.96\sigma_{C_w} = 0.500 \tag{6.5b}$$

for beam width > 12.0 in. to give a value of 0.2551 in. for σ_{C_w}, respectively.

6.2.5 One-half Clear Bar Spacing, C_{si}

ACI 117 has no tolerance specified directly for C_{si}. However ACI 117 specifies a tolerance for beam width. Since the sum of the side covers, clear spacings, and bar diameters must always equal the beam width, C_{si} is obtained from the relation

$$C_{si} = \frac{b - 2n_b d_b - 2C_{so}}{2(n_b - 1)} \tag{6.6}$$

in which b = beam width in in.; n_b = number of bars spliced; d_b = diameter of spliced bars in in.; and C_{so} = side cover in in. The variability associated with C_{si} will therefore depend on the variability associated with b and C_{so}. The variability associated with C_{so} has been addressed in the previous section and the variability associated with b is addressed in the next section.

6.2.6 Beam Width, b

For the range of beam widths used in the analysis in this chapter, ACI 117 specifies a tolerance for b as +0.375 in. and –0.250 in. for beam width ≤ 12.0 in., and +0.500 in. and –0.375 in. for 12.0 in. < beam width ≤ 36.0 in. If the mean value of b is taken as the nominal beam width plus the average of the tolerances (b + 0.0625 in.) and assuming that 95% of all members have dimensions between the tolerances, the standard deviation, σ_b, for b is defined by

$$1.96\sigma_b = 0.375 - 0.0625 = 0.3125 \tag{6.7a}$$

for beam width ≤ 12.0 in. to give a value of 0.1594 in. for σ_b, and

$$1.96\sigma_b = 0.500 - 0.0625 = 0.4375 \tag{6.7b}$$

for 12.0 in. < beam width ≤ 36.0 in. to give a value of 0.2232 in. for σ_b, respectively.

6.2.7 Concrete Compressive Strength, f'_c

One area of concern has been how to represent the strength of actual structures based on the properties of standard test specimens. Based on equations and data from Allen (1970), Petersons (1964) and Bloem (1968), MacGregor (1976) proposed representing the mean 28 day in-situ strength of concrete in a structure cured with minimum acceptable curing and tested at an average loading rate of 35 psi/sec (ASTM C 39) as follows

$$\bar{f}_{cstr35} = \left[0.675f'_c + 1{,}100\right] \text{psi} \tag{6.8}$$

but not more than $1.15\,f'_c$.

Using a relationship between the compressive strength of concrete and the rate of loading proposed by Jones and Richart (1936), Mirza, Hatzinikolas, and MacGregor (1979) obtained the mean value for the in-situ compressive strength of concrete at a given rate of loading $\dot{R}$ psi/sec to be

$$\bar{f}_{cstr\dot{R}} = \left[0.89\bar{f}_{cstr35}\left(1 + 0.08\log\dot{R}\right)\right] \text{psi} \tag{6.9}$$

in which $\bar{f}_{cstr35}$ is given by Eq. 6.8.

The selection of the value of $\bar{f}_{cstr35}$, representing the concrete strength in the field, is affected by two considerations: 1) Splice tests are calibrated against the compressive strength of standard cylinders that are cured in the same manner as the splice test specimens, not on the actual strength of the concrete in the splice specimen. The closest thing in concrete construction is the use of field-cured specimens. 2) In practice, concrete must be proportioned to produce a higher strength than used to design the structure to insure that the strength of most of the concrete will exceed the specified value of f_c'.

The two considerations have opposite effects on the value of $\bar{f}_{cstr35}$ used in the analysis, since field-cured cylinders usually produce a lower strength than standard laboratory-cured specimens (the basis upon which f_c' is measured), while the average strength of concrete produced in the field, as measured using standard specimens, exceeds f_c' by a considerable amount. Since these opposing effects largely cancel each other out, and also since the model equations for bond strength in this report were obtained using the compressive strength of concrete cylinders, f_c', instead of $\bar{f}_{cstr35}$, it is justified to use the same f_c' in Eq. 6.9 to obtain

$$\bar{f}_{cstr\dot{R}} = \left[0.89f_c'\left(1 + 0.08\log\dot{R}\right)\right] \text{psi} \qquad (6.10)$$

Assuming that the loading rate in practice will be such that failure will occur in one hour, the rate of loading, $\dot{R}$, in psi/sec can represented as

$$\dot{R} = \frac{\bar{f}_{cstr\dot{R}}}{3600} \qquad (6.11)$$

Combining Eqs. 6.10 and 6.11, $\bar{f}_{cstr\dot{R}}$ can be obtained for any f_c', using any non-linear solution technique.

Using data from work by Davis (1976), Mirza et al. also obtained the coefficient of variation, COV, of the in-situ compressive strength of concrete at a given rate of loading, $V_{cstr\dot{R}}$, to be

$$V_{cstr\dot{R}}^2 = V_{ccyl}^2 + 0.0084 \tag{6.12}$$

in which V_{ccyl} = COV of compressive strength of concrete cylinder.

Ellingwood, Galambos, MacGregor, and Cornell (1980) report a COV of 0.18, 0.18 and 0.15, respectively, for f_c' = 3000 psi, 4000 psi and 5000 psi, with means 2760 psi, 3390 psi and 4028 psi. The corresponding standard deviations obtained for the values reported by Ellingwood et al. (1980) are 497 psi, 610 psi and 604 psi, respectively, for f_c' of 3000 psi, 4000 psi and 5000 psi. In this study, an assumed standard deviation of 550 psi for all values of f_c' will be used.

Using a standard deviation of 550 psi for f_c' and Eq. 5-2 from ACI 318-89 [$f_{cr}' = f_c' + 2.33s - 500$], the COV for the compressive strength of concrete cylinder, V_{ccyl}, can be represented as

$$V_{ccyl} = \frac{550}{f_c' + 781.5} \tag{6.13}$$

from which $V_{cstr\dot{R}}$ can be obtained, using Eq. 6.12. Using $\bar{f}_{cstr\dot{R}}$ and $V_{cstr\dot{R}}$, the standard deviation, $\sigma_{cstr\dot{R}}$, for the mean in-situ compressive strength of concrete at $\dot{R}$ psi/sec loading rate, in psi, is obtained from the relationship

$$\sigma_{cstr\dot{R}} = V_{cstr\dot{R}} \bar{f}_{cstr\dot{R}} \tag{6.14}$$

6.2.8 Model Equation Variability

The variability associated with the model equation itself must also be considered. Based on work by Grant, Mirza, and MacGregor (1978), the variability associated with a model equation for bond strength, V_m, can be represented as

$$V_m = \sqrt{V_{T/P}^2 - V_{test}^2 - V_{spec}^2} \tag{6.15}$$

in which $V_{T/P}$ = COV obtained directly from the comparison of the measured and calculated bond strengths; V_{test} = COV representing uncertainties in the measured loads due to such things as the accuracy of the gages, errors in readings, and definitions of failure; and V_{spec} = COV representing errors introduced by such things as differences between the strengths in the test specimen and control cylinders, and variations in actual specimen dimensions from those measured.

The value of $V_{T/P}$, obtained in the previous chapter, is 0.108 for bars without stirrups and 0.135 for conventional bars with stirrups. Based on the work by Grant et al. (1978), the combined effect of V_{test} and V_{spec} is taken as $V_{test}^2 + V_{spec}^2 = 0.07^2$. Using Eq. 6.15, V_m is calculated to be 0.076 for bars without stirrups and 0.115 for conventional bars with stirrups.

To include V_m in the Monte Carlo simulations, a random variable representing the test/prediction ratio, having a mean of T/P and a COV of V_m, is introduced. From the previous chapter, T/P is 1.001 for bars without stirrups and 0.999 for conventional bars with stirrups.

6.3 Monte Carlo Simulations

The Monte Carlo simulation technique used in this study is adopted from the work by Mirza and MacGregor (1986). The technique generates the variability

associated with the bond strength between concrete and reinforcing steel bars. To do this, a large number of bond strengths are calculated for a selected number of members. Each value is calculated using a deterministic bond strength relation and a randomly generated set of values for the variables. For this study, 70 beams are each simulated 1000 times. Thirty five of the beams contain confining reinforcement and 35 do not. The computer programs used to accomplish the Monte Carlo simulations are listed in Appendix A.

6.3.1 Bars without Confining Reinforcement

For bars without confining reinforcement, the deterministic bond strength relation is obtained from Eq. 6.1 to be

$$A_b f_s = \tilde{T/P}\left[63\,\tilde{l}_d\left(\tilde{C}_m + 0.5d_b\right) + 2280A_b\right]\left(0.082\frac{\tilde{C}_M}{\tilde{C}_m} + 0.918\right)\tilde{f}_c'^{1/4} \quad (6.16)$$

where $\tilde{l}_d = l_s + z_1\sigma_{l_d}$ in in.;

$\tilde{C}_m$ and $\tilde{C}_M$ = minimum and maximum of $\tilde{C}_s$ and $\tilde{C}_b$, respectively, in.;

$\tilde{C}_s$ = minimum of $\tilde{C}_{so}$ and $\tilde{C}_{si} + 0.25$, in.;

$\tilde{C}_{so} = C_{so} + z_2\sigma_{C_{so}}$, in.;

$\tilde{C}_{si} = \dfrac{\tilde{b} - 2n_b d_b - 2\tilde{C}_{so}}{2(n_b - 1)}$, in.;

$\tilde{b} = b + 0.0625 + z_3\sigma_b$, in.;

$\tilde{C}_b = C_b + z_4\sigma_{C_b}$, in.;

$\tilde{f}_c' = \bar{f}_{cstrR} + z_5\sigma_{cstrR}$, in.;

$\tilde{T/P} = T/P(1 + z_6 V_m)$;

and z_i = randomly calculated standard normal variable.

The properties of the 35 beams used for the Monte Carlo simulations are

presented in Table 6.1. The nominal properties and dimensions for the 35 beams were selected to represent those used in practice. The value of l_s for each beam is calculated using Eq. 6.1, with the right side multiplied by an assumed initial value of 0.90 for ϕ_d, and f_s = 60 ksi.

Using Eq. 6.16, the predicted bond strength of each of the 35 beams is calculated a 1000 times, using a differently calculated set of z_i for each of the 1000 runs. Each z_i is calculated by first randomly generating a number between 0 and 1, representing the cumulative probability, and then solving for the corresponding z_i numerically. For each beam, the ratio, R, of the predicted bond strength for each run to the nominal bond strength, calculated using Eq. 6.1 and the nominal beam data (Table 6.1), is calculated. The mean ratio, $\overline{R}$, and the COV, V_R, for each beam is obtained from the ratios of the 1000 runs. The cumulative mean, $\bar{r}$, and cumulative COV, V_r, are also obtained at the end of the 1000 runs of each beam. The results of the Monte Carlo simulations for the 35 beams are summarized in Table 6.2. The beam properties and dimensions presented in Table 6.2 are the average values for the 1000 runs of each beam. The values of $\bar{r}$ and V_r for the 35 beams (that is after 35000 simulations) are 0.951 and 0.103, respectively.

6.3.2 Bars with Confining Reinforcement

For bars confined by transverse reinforcement, the deterministic bond strength relation is obtained from Eq. 6.2b to be

$$A_b f_s = \tilde{T}/P\left\{\left[63\,\tilde{l}_d\left(\tilde{C}_m + 0.5d_b\right) + 2280A_b\right]\left(0.082\frac{\tilde{C}_M}{\tilde{C}_m} + 0.918\right) + 2187\frac{\tilde{l}_d A_{tr}}{sn} + 202\right\}\tilde{f}_c'^{1/4} \qquad (6.17)$$

The properties of the 35 beams used for the Monte Carlo simulations are presented in Table 6.3. With the exception of stirrups, these beams have the same nominal properties and dimensions as the 35 beams used in the Monte Carlo simulations for the beams without stirrups. The value of l_s for each beam is calculated using Eq. 6.2b, with the right side multiplied by an assumed initial value of 0.90 for ϕ_d, and $f_s = 60$ ksi.

Using Eq. 6.17, the predicted bond strength of each of the 35 beams is calculated a 1000 times, using a separate set of z_i for each of the 1000 runs. For each beam, the ratio of the predicted bond strength for each run to the nominal bond strength, calculated using Eq. 6.2b and the nominal beam data (Table 6.3), is calculated.

The number of stirrups in the splice region, N, is always an integer, but the terms l_d/s and $\tilde{l}_d/s$ in Eqs. 6.2b and 6.17, respectively, are likely not to be integers. The terms l_d/s and $\tilde{l}_d/s$ can be represented as the sum of two terms, I and F, such the I is an integer and F is a fraction. It is therefore expected that the actual number of stirrups in the splice region will equal I or I + 1, depending on where in the splice region the first stirrup starts. The closer F is to 1.0 the higher the probability that there are I + 1 stirrups, and the closer F is to 0.0 the higher the probability that there are I stirrups. The probability of having I + 1 stirrups is therefore F and the probability of having I stirrups is 1.0 – F.

In the calculation of the predicted bond strength for each run using Eq. 6.17, two bond strengths (one with $\tilde{l}_d/s = I$ and the other with $\tilde{l}_d/s = I + 1$) are obtained. Each of the two predicted bond strengths is considered to occur in proportion to its probability and treated as separate runs in subsequent calculations. In the calculation of the nominal bond strength for each beam using Eq. 6.2b, the term l_d/s is used.

The mean, $\overline{R}$, and the COV, V_R, for each beam is obtained from the ratios of

the runs. The cumulative mean, $\bar{r}$, and cumulative COV, V_r, are also obtained at the end of the run for each beam. The results of the Monte Carlo simulations for the 35 beams are summarized in Table 6.4. The beam properties and dimensions presented in Table 6.4 are the average values from the runs for each beam. The values of $\bar{r}$ and V_r after all simulations are 0.957 and 0.134, respectively.

6.4 Calculation of Resistance Factor for Bond Strength

The procedure for the calculation of a resistance factor for bond strength in this study is based on the alternative formulation approach presented by Ellingwood, Galambos, MacGregor, and Cornell (1980). From their report, the reliability index, β, for a resistance, R, and a loading, Q, is

$$\beta = \frac{\overline{\ln(R/Q)}}{\sigma_{\ln(R/Q)}} \tag{6.18}$$

in which the bar signifies the mean value. Using the small-variance approximations (Ellingwood et al. 1980),

$$\overline{\ln(R/Q)} \approx \ln(\overline{R}/\overline{Q}) \tag{6.19a}$$

$$\sigma_{\ln(R/Q)} \approx \sqrt{(V_R^2 + V_Q^R)} \tag{6.19a}$$

Eq. 6.18 can be rewritten as

$$\beta \approx \frac{\ln(\overline{R}/\overline{Q})}{\sqrt{(V_R^2 + V_Q^2)}} \tag{6.20}$$

If R, = random variable for resistance, is represented as

$$R = (\tilde{T}/P)R_p \tag{6.21}$$

in which R_p = predicted capacity random variable, depending on the material and geometric properties of the member, which are also random variables.

$$Q = \sum \text{loads} \tag{6.22}$$

For dead load and live load,

$$\begin{aligned} Q &= Q_D + Q_L \\ &= (Q_D/Q_{Dn} + Q_L/Q_{Dn})Q_{Dn} \\ &= [Q_D/Q_{Dn} + (Q_L/Q_{Dn})(Q_{Ln}/Q_{Dn})]Q_{Dn} \\ &= [Q_D/Q_{Dn} + (Q_L/Q_{Dn})(Q_L/Q_D)_n]Q_{Dn} \end{aligned} \tag{6.23}$$

in which Q_D and Q_L = random variables representing dead and live load effects; Q_{Dn} and Q_{Ln} = nominal dead load and live load; and $(Q_L/Q_D)_n$ = nominal ratio of live load to dead load.

In design,

$$\begin{aligned} \phi_b R_n &= \gamma_D Q_{Dn} + \gamma_L Q_{Ln} \\ &= [\gamma_D + \gamma_L (Q_{Ln}/Q_{Dn})]Q_{Dn} \\ &= [\gamma_D + \gamma_L (Q_L/Q_D)_n]Q_{Dn} \end{aligned} \tag{6.24}$$

in which ϕ_b = "composite" strength reduction factor for bond (explained later in this section); R_n = nominal resistance; and γ_D and γ_L = load factors for dead and live loads.

Solving Eq. 6.24 for Q_{Dn} gives

$$Q_{Dn} = \frac{\phi_b R_n}{\gamma_D + \gamma_L (Q_L/Q_D)_n} \tag{6.25}$$

Substituting Eq. 6.25 into Eq. 6.23, the total load, Q, is obtained as

$$Q = \frac{\left[Q_D/Q_{Dn} + (Q_L/Q_{Ln})(Q_L/Q_D)_n\right]\phi_b R_n}{\gamma_D + \gamma_L (Q_L/Q_D)_n} \tag{6.26}$$

Letting

$$q = \frac{\left[Q_D/Q_{Dn} + (Q_L/Q_{Ln})(Q_L/Q_D)_n\right]}{\gamma_D + \gamma_L (Q_L/Q_D)_n} \tag{6.27}$$

Eq. 6.26 can be rewritten as

$$Q = \phi_b q R_n \tag{6.28}$$

Defining

$$r = \frac{R}{R_n} = \frac{\tilde{(T/P)} R_p}{R_n} \tag{6.29a}$$

$$R = \tilde{(T/P)} R_p = r R_n \tag{6.29b}$$

Substituting Eqs. 6.28, 6.29a and 6.29b into Eq. 6.18, and applying the small-variance

approximations (Eqs. 6.19a and 6.19b)

$$\begin{aligned}\beta &= \frac{\overline{\ln\left(rR_n/\phi_b qR_n\right)}}{\sigma_{\ln(rR_n/\phi_b qR_n)}} \\ &= \frac{\overline{\ln\left(r/\phi_b q\right)}}{\sigma_{\ln(r/\phi_b q)}} \\ &= \frac{\ln\left(\bar{r}/\overline{\phi_b q}\right)}{\sigma_{\ln(r/\phi_b q)}} \\ &= \frac{\ln\left(\bar{r}/\phi_b \bar{q}\right)}{\sqrt{\left(V_r^2 + V_{\phi q}^2\right)}}\end{aligned} \tag{6.30}$$

where $\bar{r} = \left[\overline{\frac{(T/P)R_p}{R_n}}\right]$

$$V_r = \frac{\sigma_r}{\bar{r}}$$

$$\bar{q} = \left\{\frac{\overline{\left[Q_D/Q_{Dn} + (Q_L/Q_{Ln})(Q_L/Q_D)_n\right]}}{\gamma_D + \gamma_L(Q_L/Q_D)_n}\right\}$$

$$V_{\phi q} = \frac{\phi_b \sigma_q}{\phi_b \bar{q}} = \frac{\sigma_q}{\bar{q}} = \frac{\left\{\left[\overline{(Q_D/Q_{Dn})}V_{Q_D}\right]^2 + \left[\overline{(Q_L/Q_{Ln})}(Q_L/Q_D)_n V_{Q_L}\right]^2\right\}^{1/2}}{\overline{(Q_D/Q_{Dn})} + \overline{(Q_L/Q_{Ln})}(Q_L/Q_D)_n}$$

From Eq. 6.30,

$$\beta\sqrt{\left(V_r^2 + V_{\phi q}^2\right)} = \ln\left(\bar{r}/\phi_b \bar{q}\right) \tag{6.31}$$

$$e^{\beta\sqrt{\left(V_r^2 + V_{\phi q}^2\right)}} = \frac{\bar{r}}{\phi_b \bar{q}} \tag{6.32}$$

$$\phi_b = \frac{\bar{r}}{\bar{q}} e^{-\beta\sqrt{\left(V_r^2 + V_{\phi q}^2\right)}} \tag{6.33}$$

Based on the Monte Carlo simulations, $\bar{r}$ and V_r are 0.951 and 0.103, respectively, for bars without stirrups, and 0.957 and 0.134, respectively, for bars with stirrups. The ACI factors for dead and live load (γ_D and γ_L), 1.4 and 1.7, respectively, are used in this study. For reinforced concrete beams and columns, $\beta \approx 3.0$ for typical loading conditions (Ellingwood et al. 1980). To ensure that the probability of bond failure is lower, $\beta = 3.5$ is used in this study (producing a probability of failure equal to approximately 1/5 of that obtained with $\beta = 3.0$). For reinforced concrete structures, $\overline{Q_D/Q_{Dn}} = 1.03$ and $V_{Q_D} = 0.093$ (Ellingwood et al. 1980).

The live load, $\overline{Q}_L$, is taken to be equal to the 50-year mean value, which is given in the report by Ellingwood et al. (1980) to be

$$\overline{Q}_L = \left(0.25 + 15/\sqrt{A_I}\right)L_o \tag{6.34}$$

in which A_I and L_o are the influence area in ft^2 and basic live load, respectively, and the nominal live load, Q_{Ln}, is represented according to ASCE 7-93 as

$$Q_{Ln} = \left\{1 - \text{Min}\left[0.0008\left(A_T - 150\right),\ 0.6,\ 0.23\left(1 + \left(Q_D/Q_L\right)_n\right)\right]\right\}L_o \tag{6.35}$$

in which A_T = tributary area in ft^2; In this study, A_T and A_I are taken as 400 ft^2 and 800 ft^2, respectively, and therefore Eqs. 6.34 and 6.35 give $\overline{Q}_L = 0.7803L_o$ and $Q_{Ln} = 0.8L_o$, from which $\overline{Q_L/Q_{Ln}} = 0.9754$.

Using Eq. 6.33 and live/dead load ratios $\left(Q_L/Q_D\right)_n$ of 0.5, 1.0 and 1.5, nominal resistance factors for bond strength, ϕ_b, are calculated. It is noted that the bar force, $A_b f_s$, that appears on the left side of Eqs. 6.1 and 6.2b has already been increased by a factor of $1/\phi$, in which ϕ = strength reduction factor for the main loading, before development/splice design is undertaken. In order not to double-count

ϕ-factors, the resistance to which ϕ_b is applied corresponds to $\phi A_b f_s$. That is,

$$\phi A_b f_s \geq \phi_b[\text{Right side of Eqs. 6.1 or 6.2b}] \tag{6.36}$$

from which

$$A_b f_s \geq \phi_d[\text{Right side of Eqs. 6.1 or 6.2b}] \tag{6.37}$$

where $\phi_d = \phi_b/\phi$ is the effective ϕ-factor for use in calculating development/splice lengths. For reinforced concrete members in bending, with or without axial tension, ϕ = 0.9 (ACI) and $\phi_d = \phi_b/0.9$. The results of the calculations for resistance factors for bond strength are summarized in Table 6.5 for bars with and without stirrups.

From the results, for $(Q_L/Q_D)_n$ = 0.5, 1.0 and 1.5, ϕ_d = 0.943, 0.912 and 0.881, respectively, for bars without confining reinforcement and ϕ_d = 0.874, 0.854 and 0.830, respectively, for bars with confining reinforcement. It is therefore observed that ϕ_d depends on the $(Q_L/Q_D)_n$ ratio. The higher $(Q_L/Q_D)_n$, the lower ϕ_d. It is also observed that ϕ_d is higher for bars not confined by stirrups than for bars confined by stirrups at the same $(Q_L/Q_D)_n$ ratio. This is expected since V_r is higher for bars with stirrups (0.134) than for bars without stirrups (0.103). In this study, ϕ_d is taken conservatively as 0.85, which is close to ϕ_d for bars with stirrups and $(Q_L/Q_D)_n$ = 1.0, since $(Q_L/Q_D)_n$ = 1.0 provides a realistic representation for reinforced concrete beams and columns (Ellingwood et al. 1980).

6.5 Prototype Design Equations

Using Eqs. 6.1 and 6.2b, incorporating the resistance factor for bond strength, ϕ_d, and replacing the stress in the bar, f_s, with the yield stress, f_y, the nominal bond

strength for bars without stirrups can be represented as

$$A_b f_y = \phi_d\left[63\, l_d\left(C_m + 0.5d_b\right) + 2280A_b\right]\left(0.082\frac{C_M}{C_m} + 0.918\right)f_c'^{1/4} \qquad (6.38)$$

and for conventional bars with stirrups as

$$A_b f_y = \phi_d\left\{\left[63\, l_d\left(C_m + 0.5d_b\right) + 2280A_b\right]\left(0.082\frac{C_M}{C_m} + 0.918\right) + 2187\frac{NA_{tr}}{n} + 202\right\}f_c'^{1/4} \qquad (6.39)$$

From Eqs. 6.38 and 6.39, expressions for the development/splice lengths for bars without stirrups and with stirrups are obtained, respectively.

$$l_d = \frac{A_b\left[\frac{f_y}{\phi_d f_c'^{1/4}} - 2280\left(0.082\frac{C_M}{C_m} + 0.918\right)\right]}{63\left(C_m + 0.5d_b\right)\left(0.082\frac{C_M}{C_m} + 0.918\right)} \qquad (6.40)$$

$$l_d = \frac{A_b\left[\frac{f_y}{\phi_d f_c'^{1/4}} - 2280\left(0.082\frac{C_M}{C_m} + 0.918\right)\right] - 202}{63\left(C_m + 0.5d_b\right)\left(0.082\frac{C_M}{C_m} + 0.918\right) + 2187\frac{A_{tr}}{sn}} \qquad (6.41)$$

Similarly, using the bond strength equations for high R_r bars (Eqs. 5.12 to 5.14), the development/splice lengths for high R_r bars can be represented as:

For $R_r = 0.140$ (F1) bars,

$$l_d = \frac{A_b\left[\frac{f_y}{\phi_d f_c'^{1/4}} - 2280\left(0.082\frac{C_M}{C_m} + 0.918\right)\right] - 533}{63\left(C_m + 0.5d_b\right)\left(0.082\frac{C_M}{C_m} + 0.918\right) + 3399\frac{A_{tr}}{sn}} \quad (6.42)$$

For $R_r = 0.119$ (N3) bars,

$$l_d = \frac{A_b\left[\frac{f_y}{\phi_d f_c'^{1/4}} - 2280\left(0.082\frac{C_M}{C_m} + 0.918\right)\right] - 531}{63\left(C_m + 0.5d_b\right)\left(0.082\frac{C_M}{C_m} + 0.918\right) + 2791\frac{A_{tr}}{sn}} \quad (6.43)$$

For $R_r = 0.101$ (C1) bars,

$$l_d = \frac{A_b\left[\frac{f_y}{\phi_d f_c'^{1/4}} - 2280\left(0.082\frac{C_M}{C_m} + 0.918\right)\right] - 471}{63\left(C_m + 0.5d_b\right)\left(0.082\frac{C_M}{C_m} + 0.918\right) + 2413\frac{A_{tr}}{sn}} \quad (6.44)$$

6.6 Comparisons with Proposed ACI 318-95 Design Equations

Apart from the 11 development tests without confining reinforcement from the report by Chamberlin (1956), all of the data used to obtain the bond strength equations in this study were obtained from splice tests. The prototype design equations are therefore directly applicable to splices without any modifications. Lengths calculated using any of the prototype design equations (Eqs. 6.40 to 6.44) are considered to be both development and splice lengths. In this section, comparisons with the proposed ACI 318-95 design equations are made for both development and splice lengths of bottom-cast uncoated reinforcement.

For the equations proposed for ACI 318-95, the more detailed expression of

Section 12.2.3 is used in the comparisons. According to the provisions proposed for ACI 318-95, the development lengths, l_d, for bottom-cast uncoated reinforcement are as follows:

For No. 6 and smaller bars,

$$\frac{l_d}{d_b} = \frac{2.4}{40}\frac{f_y}{\sqrt{f'_c}\left(\frac{c + K_{tr}}{d_b}\right)} \qquad (6.45a)$$

For No. 7 and larger bars,

$$\frac{l_d}{d_b} = \frac{3}{40}\frac{f_y}{\sqrt{f'_c}\left(\frac{c + K_{tr}}{d_b}\right)} \qquad (6.46b)$$

in which $K_{tr} = A_{tr}f_{yt}/(1500sn)$; c = smaller of either the distance from the center of the bar to the nearest concrete surface or one-half the center-to-center spacing of the bars being developed; and $(c + K_{tr})/d_b \leq 2.5$. To obtain splice lengths, l_s, for Class B splices (area of reinforcement provided is not more than twice that required by analysis over the entire splice length or more than one-half the total reinforcement is spliced within the required lap length), under the ACI provisions. l_d is multiplied by a factor of 1.3.

The same 35 beams used in the Monte Carlo simulations to obtain ϕ_d are used for the comparisons.

6.6.1 Bars Not Confined by Transverse Reinforcement

For bars not confined by transverse reinforcement, the prototype design

equation (Eq. 6.40) is compared with the ACI 318-95 provisions, with ϕ_d = 0.85. Development/splice lengths calculated using Eq. 6.40 are compared with l_d and l_s calculated using the ACI provisions. The results of the comparison are presented in Table 6.6.

For l_d, Eq. 6.40 generally produces greater lengths than ACI 318-95. Of the 35 beams compared, only 10 have shorter development lengths with Eq. 6.40 than with ACI 318-95. The average ratio of l_d calculated using Eq. 6.40 to l_d calculated using the ACI provisions is 1.074.

For the l_s comparisons, Eq. 6.40 always produces shorter lengths than ACI 318-95. The average ratio of l_s calculated using Eq. 6.40 to l_s calculated using the ACI 318-95 is 0.826.

6.6.2 Bars Confined by Transverse Reinforcement

For bars confined by transverse reinforcement, prototype design equations Eqs. 6.41, 6.42, 6.43 and 6.44 for conventional, R_r = 0.140 (F1), R_r = 0.119 (N3), and R_r = 0.101 (C1) bars, respectively, are compared with the proposed ACI provisions. ϕ_d = 0.85. Development/splice lengths calculated for each of the 35 beams for each bar type, are compared with l_d and l_s calculated using ACI 318-95. The results of the calculations and comparisons are presented in Table 6.7.

Comparison of prototype design equation for conventional bars with ACI provisions for l_d and l_s - l_d and l_s for conventional bars with stirrups calculated using Eq. 6.41 are compared with l_d and l_s calculated using ACI 318-95. The average ratio of l_d calculated using Eq. 6.41 to l_d calculated using ACI 318-95 is 0.980. The individual ratios, however, vary significantly (from 0.792 to 1.165). For l_s, Eq. 6.41 always produces a shorter l_s than the ACI provisions. The average ratio of l_s calculated using Eq. 6.41 to l_s calculated using the ACI provisions is 0.754,

representing a significant savings of material and reduction in reinforcing bar congestion.

Comparison of prototype design equations for high R_r bars with prototype design equation for conventional bars - l_d and l_s for high R_r bars (R_r = 0.140, 0.119 and 0.101, respectively, for F1, N3 and C1) confined by stirrups calculated using the appropriate equation (Eqs. 6.42 to 6.44) are compared with l_d and l_s for conventional bars with stirrups calculated using Eq. 6.41. For each of the comparison, the high R_r bars always produce shorter lengths than the conventional bars. The average ratios of l_d or l_s for high R_r bars to conventional bars are 0.844, 0.884, and 0.924, respectively, for the R_r = 0.140 (F1), R_r = 0.119 (N3), and R_r = 0.101 (C1) bars. The higher the value of R_r, the lower the average ratio.

Comparison of prototype design equations for high R_r bars with ACI provisions for l_d - The values of l_d for high R_r bars (R_r = 0.140, 0.119 and 0.101, respectively, for F1, N3 and C1) confined by stirrups calculated using the appropriate equation (Eqs. 6.42 to 6.44) are compared with the values of l_d calculated using ACI 318-95. For each comparison, the high R_r bars produce shorter lengths than the ACI provisions. The average ratios of l_d for high R_r bars to l_d for ACI 318-95 are 0.829, 0.868, and 0.906, respectively, for the R_r = 0.140 (F1), R_r = 0.119 (N3), and R_r = 0.101 (C1) bars. The higher the R_r of the bars, the lower the average ratio. The lower development lengths are a function of both the design expression and the effect of R_r on the contribution of transverse reinforcement to bond strength.

Comparison of prototype design equations for high R_r bars with ACI provisions for l_s - The values of l_s for high R_r bars (R_r = 0.140, 0.119 and 0.101, respectively, for F1, N3 and C1) confined by stirrups calculated using the appropriate equation (Eqs. 6.42 to 6.44) are compared with the values of l_s calculated using ACI 318-95. For each comparison, the high R_r bars again produce shorter lengths than the

ACI provisions. The average ratios of l_s for high R_r bars to l_s for ACI 318-95 are 0.637, 0.668, and 0.697, respectively, for the R_r = 0.140 (F1), R_r = 0.119 (N3), and R_r = 0.101 (C1) bars. The lower values of l_s are due to the effect of R_r on the contribution of transverse reinforcement to bond strength and the fact that a development strength modification factor need not be applied when using Eqs. 6.42 to 6.44 for splices.

6.6.3 Practical Advantage of Prototype Design Equations

Over 90% of the tests without confining reinforcement and all the tests with confining reinforcement used to derive the prototype design equations are Class B splice tests. Therefore, the values of l_d calculated using these equations apply to both developed and spliced bars, removing the requirement to multiply l_d by 1.3 to obtain Class B splices. This is important because it simplifies the determination of splice lengths and makes separate splice classifications unnecessary.

On the average, using the prototype design equation for bars without confining reinforcement produces 7.4% longer development lengths and 17.6% shorter splice lengths than obtained using ACI 318-95. Although the development lengths increase, the increase is more than matched by the reductions in splice length.

When compared with the prototype design equations for conventional bars with confining reinforcement, development/splice lengths for high R_r bars confined by stirrups are, on the average, 8.6% to 15.6% shorter. When compared with the ACI 318-95, development and splice lengths are, on the average, 9.4% to 17.1% and 30.3% to 36.3% shorter, respectively, for high R_r bars with stirrups. Using high R_r bars with stirrups will, therefore, significantly reduce both development and splice lengths.

CHAPTER 7: SUMMARY, CONCLUSIONS AND RECOMMENDATIONS

7.1 Summary

The bond characteristics of deformed reinforcing bars are investigated and design equations for development and splice lengths are obtained with the goal of improving the bond strength of steel reinforcing bars to concrete. The research includes both experimental and analytical studies.

The experimental study involved evaluating the performance of deformed steel reinforcing bars with different deformation patterns and the effects of epoxy coating on these bars, using friction, beam-end, and splice tests. The friction tests are used to determine the coefficient of friction between reinforcing steel and mortar, for both epoxy-coated and uncoated steel. A total of 678 specimens were tested. The beam-end tests are used to study the effects of deformation pattern on bond strength as affected by epoxy coating. A total of 58 beam-end specimens, containing No. 8 bars with different deformation patterns (relative rib area and rib face angle) were tested. The splice tests are used to study the effects of deformation pattern on splice strength as affected by epoxy coating and confinement by transverse reinforcement. 54 splice specimens containing No. 8 bars were tested. Concretes containing two different coarse aggregates were used to evaluate the effect of aggregate properties on bond strength.

The analytical part of this study focuses on obtaining splice and development length expressions for bars with and without transverse reinforcement, as well as evaluating a theoretical relation between the relative bond strength of epoxy-coated bars to uncoated bars (C/U) and rib face angle. Linear regression techniques are employed to arrive at expressions for the bond strength of conventional and high relative rib area reinforcing bars. Parameters include splice and development length, concrete strength and cover, bar size and spacing, and transverse reinforcement.

LRFD concepts and Monte Carlo techniques are applied to the bond strength expressions to determine ϕ-factors which, together with the bond strength expressions, are used to obtain prototype design equations for splice and development length.

The development and splice lengths calculated using the prototype design equations are compared with development and splice lengths calculated using the design equations proposed for ACI 318-95.

7.2 Observations and Conclusions

The following observations and conclusions are based on the results and analyses of the experimental and analytical studies presented in this report.

7.2.1 Coefficient of Friction Tests

1. Epoxy coating reduces the coefficient of friction between reinforcing steel and mortar. The coefficient of friction at the steel-mortar interface is about 0.56 for an uncoated steel surface and 0.49 for an epoxy-coated steel surface.
2. The surface conditions of mortar affect the coefficient of friction between steel and mortar. The coefficient of friction is higher and coefficient of variation is lower for formed mortar surfaces than for hand finished mortar surfaces.
3. For the two ages used in the tests (7 and 28 days), mortar age does not appear to affect the coefficient of friction between steel and mortar.
4. The coefficient of friction between steel and mortar appears to increase as the water-cement ratio increases. However, additional tests are needed to verify this observation.

5. In the range of sand-cement ratios used, the coefficient of friction between steel and mortar has no relationship to the sand-cement ratio.
6. In the limited range of mortar strengths tested, the coefficient of friction between steel and mortar appears to have no relationship to mortar strength.

7.2.2 Beam-End Tests

1. Epoxy coating appears to have a less detrimental effect on bond strength for high relative rib area bars than for previously tested conventional bars.
2. Based on the values of μ_u and μ_c obtained from this study and a theoretical relation between C/U and rib face angle, when the rib face angle is greater than about 43°, epoxy-coating will not reduce the bond strength of steel reinforcing bars to concrete. The test results for the beam-end specimens generally support this finding.
3. The load-slip curves for epoxy-coated and uncoated bars with the same deformation pattern are nearly identical.
4. Just before the peak load, the transverse crack widths of specimens with uncoated bar specimens are generally wider than the transverse crack widths of specimens with epoxy-coated bar specimens.

7.2.3 Splice Tests

1. Epoxy coating appears to have a less detrimental effect on splice strength for high relative rib area bars than for previously tested conventional bars.
2. For the bars tested, the splice strength of uncoated bars not confined by stirrups does not appear to be affected by relative rib area.

3. The splice strength of uncoated reinforcement confined by stirrups increases with an increase in the relative rib area of the spliced bars.
4. The increase in splice strength provided by transverse reinforcement is influenced by the properties of the coarse aggregate used in the concrete. For a given concrete compressive strength, higher strength coarse aggregates provide higher bond strengths.

7.2.3 Design Equations

1. The relationship between bond force and development or splice length, l_d, is linear but not proportional. Thus, to increase the bond force (or bar stress) by a given percentage requires more than that percentage increase in l_d.
2. $f_c'^{1/2}$ does not provide an accurate representation of the effect of concrete strength on bond strength. For low strength concretes, development/splice strengths are underestimated, and for high strength concretes, they are overestimated.
3. $f_c'^{1/4}$ provides an accurate representation of the effect of concrete strength on bond strength.
4. The most accurate representation of the effect of transverse reinforcement on bond strength obtained in this study includes parameters that account for the number of transverse reinforcing bars that cross the developed/spliced bar, the area of the transverse reinforcement, and the number of bars developed or spliced at one location.
5. The yield strength of transverse reinforcement does not play a role in the effectiveness of the transverse reinforcement in improving the bond strength of developed/spliced bars.

6. A strength reduction (ϕ) factor of 0.85 is obtained for the bond strength of developed/spliced bars using LRFD concepts and Monte Carlo techniques.
7. With the incorporation of a reliability-based strength reduction (ϕ) factor, the design expressions for development and splice length are identical. This simplifies the determination of splice lengths and makes separate splice classifications unnecessary.
8. The splice lengths obtained with the expressions presented in this report are uniformly lower than those obtained under the provisions of ACI 318-95 for both conventional and high relative rib area reinforcement.
9. For bars that are not confined by transverse reinforcement, development lengths average 7% higher and splice lengths average 18% lower than those obtained with ACI 318-95.
10. For conventional bars confined by transverse reinforcement, development lengths average 12% lower and splice lengths average 25% lower than those obtained with ACI 318-95.
11. For high relative rib area bars confined by transverse reinforcement, development lengths average 9 to 17% lower and splice lengths average 30 to 36% lower than those obtained with ACI 318-95, depending on the value of R_r for the high relative rib area bar. When confined by transverse reinforcement, the development/splice lengths of high relative rib area bars average 9 to 16% lower than those obtained with conventional bars, depending on the value of R_r for the high relative rib area bar.

7.3 Recommendations for Future Study

Research on the effects of deformation pattern on the bond strength of deformed reinforcing bars is continuing at the University of Kansas. This report has

tried to answer some of the questions related to bond strength and deformation pattern. However, there are some questions that have not been addressed or need further research. These include studies:

1. in which the coefficient of friction between reinforcing steel and mortar or concrete is measured under a condition of simultaneous increase in normal and tangential force.
2. of the effects of water-cement ratio, sand-cement ratio, and compressive strength on the coefficient of friction between reinforcing steel and mortar or concrete.
3. of the effect of epoxy-coating on the bond strength of high relative rib area bars confined by transverse reinforcement.
4. of the bond performance of epoxy-coated bars in high strength concrete.
5. of the bond performance of high relative rib area bars in high strength concrete.
6. of the bond performance of high relative rib area bars when used as top-cast bars.
7. of the bond performance of high relative rib area bars when subjected to cyclic loading.
8. to obtain design equations that incorporate the effects of relative rib area, R_r, for developed and spliced bars confined by transverse bars.

REFERENCES

AASHTO (1989). *Standard Specifications for Highway Bridges*, 14th Edition, American Association of State Highway and Transportation Officials, Washington, DC.

Abrams, D. A. (1913). "Tests of Bond between Concrete and Steel," *Bulletin* No. 71, Engineering Experiment Station, University of Illinois, Urbana, IL, 105 pp.

ACI Committee 117. (1990). *Standard Specifications for Tolerances for Concrete Construction (ACI 117-90)*, American Concrete Institute, Detroit, MI, 12 pp.

ACI Committee 318. (1956). *Building Code Requirements for Reinforced Concrete (ACI 318-56)*, Proceedings American Concrete Institute, Detroit, MI, 52 pp.

ACI Committee 318. (1963). *Building Code Requirements for Reinforced Concrete (ACI 318-63)*, American Concrete Institute, Detroit, MI, 144 pp.

ACI Committee 318. (1989). *Building Code Requirements for Reinforced Concrete (ACI 318-89) and Commentary - ACI 318R-89*, American Concrete Institute, Detroit, MI, 353 pp.

ACI Committee 318. (1989) (Revised 1992). *Building Code Requirements for Reinforced Concrete (ACI 318-89) (Revised 1992) and Commentary - ACI 318R-89* (Revised 1992), American Concrete Institute, Detroit, MI, 347 pp.

ACI Committee 318. (1994). "Proposed Revisions to Building Code Requirements for Reinforced Concrete (ACI 318-89) (Revised 1992) and Commentary - ACI 318R-89 (Revised)," *Concrete International*, Vol. 16, No. 12, Dec., pp. 76-128. Cited as ACI 318-95.

ACI Committee 408. (1990). *Suggested Development, Splice, and Standard Hook Provisions for Deformed Bars in Tension (ACI 408.1R-90)*, American Concrete Institute, Detroit, MI, 3 pp.

Allen, D. E. (1970). "Probabilistic Study of Concrete in Bending," ACI Journal, *Proceedings* Vol. 67, No. 12, Dec., pp. 989-993.

ASCE (1993). *Minimum Design Loads for Buildings and Other Structures, ASCE 7-93*, American Society of Civil Engineers, New York.

ASTM A 305-47T. (1947). "Tentative Specifications for Minimum Requirements for Deformations of Deformed Steel Bars for Concrete Reinforcement," American Society for Testing and Materials, Philadelphia, PA.

ASTM A 305-49. (1949). "Specifications for Minimum Requirements for Deformations of Deformed Steel Bars for Concrete Reinforcement," American Society for Testing and Materials, Philadelphia, PA.

ASTM A 311/A 311M-90b. (1995). "Standard Specification for Steel Bars, Carbon, Stress-Relieved Cold-Drawn Subject to Mechanical Property Requirements," *1995 Annual Book of ASTM Standards*, Vol. 1.05, American Society for Testing and Materials, Philadelphia, PA, pp. 125-127.

ASTM A 615/A 615M-94. (1995). "Standard Specification for Deformed and Plain Billet-Steel Bars for Concrete Reinforcement," *1995 Annual Book of ASTM Standards*, Vol. 1.04, American Society for Testing and Materials, Philadelphia, PA, pp. 300-304.

ASTM C 39-93a. (1994). "Standard Test Method for Compressive Strength of Cylindrical Concrete Specimens," *1994 Annual Book of ASTM Standards*, Vol. 4.02, American Society for Testing and Materials, Philadelphia, PA, pp. 17-21.

Azizinamini, A.; Chisala, M.; and Ghosh, S. K. (1995). "Tension Development Length of Reinforcing Bars Embedded in High-Strength Concrete," *Engineering Structures*, accepted for publication.

Brettmann, Barrie B.; Darwin, David; and Donahey, Rex C. (1984). "Effects of Superplasticizers on Concrete - Steel Bond Strength," *SL Report* 84-1, University of Kansas Center for Research, Lawrence, Kansas, Apr., 32 pp.

Brettmann, Barrie B.; Darwin, David; and Donahey, Rex C. (1986). "Bond of Reinforcement to Superplasticized Concrete," ACI Journal, *Proceedings* Vol. 83, No. 1, Jan.-Feb., pp. 98-107.

Bloem, D. L. (1968). "Concrete Strength in Structures," ACI Journal, *Proceedings*, Vol. 65, No. 14, Mar., pp. 176-187.

Cairns, John, and Abdullah, Ramli. (1994). "Fundamental Tests on the Effect of an Epoxy Coating on Bond Strength," *ACI Materials Journal*, Vol. 91, No. 4, July-Aug., pp. 331-338.

Chamberlin, S. J. (1956). "Spacing of Spliced Bars in Beams," ACI Journal, *Proceedings* Vol. 53, No. 1, July, pp. 113-134.

Chamberlin, S. J. (1958). "Spacing of Reinforcement in Beams," ACI Journal, *Proceedings* Vol. 54, No. 8, Feb., pp. 689-698.

Chinn, James; Ferguson, Phil M.; and Thompson, J. Neils. (1955). "Lapped Splices in Reinforced Concrete Beams," ACI Journal, *Proceedings* Vol. 52, No. 2, Oct., pp. 201-214.

Choi, Oan Chul; Darwin, David; and McCabe, Steven L. (1990). "Bond Strength of Epoxy-Coated Reinforcement to Concrete," *SM Report* No. 25, University of Kansas Center for Research, Lawrence, Kansas, July, 217 pp.

Choi, Oan Chul; Hadje-Ghaffari, Hossain; Darwin, David; and McCabe, Steven L. (1990). "Bond of Epoxy-Coated Reinforcement to Concrete: Bar Parameters," *SL Report* 90-1, University of Kansas Center for Research, Lawrence, Kansas, Jan., 43 pp.

Choi, Oan Chul: Hadje-Ghaffari, Hossain; Darwin, David; and McCabe, Steven L. (1991). "Bond of Epoxy-Coated Reinforcement: Bar Parameters," *ACI Materials Journal*, Vol. 88. No. 2, Mar.-Apr., pp. 207-217.

Clark, A. P. (1946). "Comparative Bond Efficiency of Deformed Concrete Reinforcing Bars," ACI Journal, *Proceedings* Vol. 43, No. 4, Dec., pp. 381-400.

Clark, A. P. (1949). "Bond of Concrete Reinforcing Bars," ACI Journal, *Proceedings* Vol. 46, No. 3, Nov., pp. 161-184.

Darwin, David; McCabe, Steven L.; Idun, Emmanuel K.; and Schoenekase, Steven P. (1992a). "Development Length Criteria: Bars Without Transverse Reinforcement," *SL Report* 92-1, University of Kansas Center for Research, Lawrence, Kansas, Apr., 61 pp.

Darwin, David; McCabe, Steven L.; Idun, Emmanuel K.; and Schoenekase, Steven P. (1992b). "Development Length Criteria: Bars Without Transverse Reinforcement," *ACI Structural Journal*, Vol. 89, No. 6, Nov.-Dec., pp. 709-720.

Darwin, David, and Graham, Ebenezer K. (1993a). "Effect of Deformation Height and Spacing on Bond Strength of Reinforcement," *SL Report* 93-1, University of Kansas Center for Research, Lawrence, Kansas, Jan., 68 pp.

Darwin, David, and Graham, Ebenezer K. (1993b). "Effect of Deformation Height and Spacing on Bond Strength of Reinforcing Bars," *ACI Structural Journal*, Vol. 90, No. 6, Nov.-Dec., pp. 646-657.

Davis, S. G. (1976). "Further Investigation into the Strength of Concrete in Structures," *Technical Report*, Cement and Concrete Association, London, England, Apr.

DeVries, R. A.: Moehle, J. P.; and Hester, W. (1991). "Lap Splice of Plain and Epoxy-Coated Reinforcements: An Experimental Study Considering Concrete Strength, Casting Position, and Anti-Bleeding Additives," *Report* No. UCB/SEMM-91/02 Structural Engineering Mechanics and Materials, University of California, Berkeley, California, Jan., 86 pp.

Donahey, Rex C. and Darwin, David. (1983). "Effects of Construction Procedures on Bond in Bridge Decks," *SM Report* No. 7, University of Kansas Center for Research, Lawrence, Kansas. 129 pp.

Donahey, Rex C. and Darwin, David. (1985). "Bond of Top-Cast Bars in Bridge Decks," ACI Journal, *Proceedings* Vol. 82, No. 1, Jan.-Feb., pp. 57-66.

Draper, N. R. and Smith, H. (1981). *Applied Regression Analysis*, Second Edition, John Wiley & Sons, Inc., pp. 241-249.

Drysdale, Robert G. (1975). "Placement Errors for Reinforcing in Concrete Columns," ACI Journal, *Proceedings* Vol. 72, No. 1, Jan., pp. 9-15.

Ellingwood, B; Galambos, T. V.; MacGregor, J. G.; and Cornell, C. A. (1980). "Development of a Probability Based Load Criteria for American National Standard Committee A58," *National Bureau of Standards Special Publication SP-577*, National Bureau of Standards, Washington, D.C., JH June, 222 pp.

Ellingwood, B; MacGregor, J. G.; Galambos, T. V.; and Cornell, C. A. (1982). "Probability Based Load Criteria: Load Factors and Load Combinations," *Journal of the Structural Division*, ASCE, Vol. 108, No. ST5, May., pp. 978-997.

Ferguson, Phil M., and Breen, John E. (1965). "Lapped Splices for High Strength Reinforcing Bars," ACI Journal, *Proceedings* Vol. 62, No. 9, Sept., pp. 1063-1078.

Ferguson, Phil M., and Thompson, J. Neils. (1962). "Development Length of High Strength Reinforcing Bars in Bond," ACI Journal, *Proceedings* Vol. 59, No. 7, July, pp. 887-922.

Galambos, T. V.; Ellingwood, B; MacGregor, J. G., and Cornell, C. A. (1982). "Probability Based Load Criteria: Assessment of Current Design Practice," *Journal of the Structural Division*, ASCE, Vol. 108, No. ST5, May., pp. 959-977.

Grant, Leon H. (1976). "A Monte Carlo Study of the Strength Variability of Rectangular Tied Reinforced Concrete Columns," *MSc Thesis*, Department of Civil Engineering, University of Alberta, Edmonton, 208 pp.

Grant, Leon H.; Mirza, Sher Ali, and MacGregor, James G. (1978). "Monte Carlo Study of Strength of Concrete Columns," ACI Journal, *Proceedings* Vol. 75, No. 8, Aug., pp. 348-358.

Hadje-Ghaffari, Hossain; Darwin, David; and McCabe, Steven L. (1991). "Effects of Epoxy Coating on Bond of Reinforcing Steel to Concrete," *SM Report* No. 28, University of Kansas Center for Research, Inc., Lawrence, Kansas, July, 288 pp.

Hadje-Ghaffari, Hossain; Darwin, David; and McCabe, Steven L. (1992). "Bond of Epoxy-Coated Reinforcement to Concrete: Cover, Casting Position, Slump, and Consolidation," *SL Report* 92-3, University of Kansas Center for Research, Inc., Lawrence, Kansas, July, 42 pp.

Hadje-Ghaffari, Hossain; Choi, Oan Chul; Darwin, David; and McCabe, Steven L. (1994). "Bond of Epoxy-Coated Reinforcement: Cover, Casting Position, Slump, and Consolidation," *ACI Structural Journal*, Vol. 91, No. 1, Jan.-Feb., pp. 59-68.

Hamad, Bilal S. and Jirsa, James O. (1990). "Influence of Epoxy Coating on Stress Transfer from Steel to Concrete," *Proceedings*, First Materials Engineering Congress, ASCE, New York, Vol. 2, pp. 125-134.

Hamad, Bilal S. and Jirsa, James O. (1993). "Strength of Epoxy-Coated Reinforcing Bar Splices Confined with Transverse Reinforcement," *ACI Structural Journal*, Vol. 90, No. 1, Jan.-Feb., pp. 77-88.

Harajli, M. H. (1994). "Development/Splice Strength of Reinforcing Bars Embedded in Plain and Fiber Reinforced Concrete," *ACI Structural Journal*, Vol. 91, No. 5, Sept.-Oct., pp. 511-520.

Hester, Cynthia J,; Salamizavaregh, Shahin; Darwin, David; and McCabe, Steven L. (1991). "Bond of Epoxy-Coated Reinforcement to Concrete: Splices," *SL Report* 91-1, University of Kansas Center for Research, Lawrence, Kansas, May, 66 pp.

Hester, Cynthia J,; Salamizavaregh, Shahin; Darwin, David; and McCabe, Steven L. (1993). "Bond of Epoxy-Coated Reinforcement: Splices," *ACI Structural Journal*. Vol. 90, No. 1, Jan.-Feb., pp. 89-102.

Johnston, David W., and Zia, Paul. (1982). "Bond Characteristics of Epoxy Coated Reinforcing Bars," *Report* No. FHWA-NC-82-002, Federal Highway Administration, Washington, DC, 163 pp.

Jones, P. G., and Richart, F. E. (1936). "The Effects of Testing Speed on Strength and Elastic Properties of Concrete," *Proceedings*, American Society for Testing and Materials, Vol. 36, Part II, pp. 380-391.

Losberg, Anders and Olsson, Per-Ake. (1979). "Bond Failure of Deformed Reinforcing Bars Based on the Longitudinal Splitting Effect of the Bars," ACI Journal, *Proceedings* Vol. 76, No. 1, Jan., pp. 5-18.

Lundberg, Jane (1993). "The Reliability of Composite Columns and Beam-Columns," *Structural Engineering Report* No. 93-2, University of Minnesota, Minneapolis, Minnesota, June, 233 pp.

Lutz, L. A.; Gergely, P.; and Winter, G. (1966). "The Mechanics of Bond and Slip of Deformed Reinforcing Bars in Concrete," *Report* No. 324, Department of Structural Engineering, Cornell University, Aug., 306 pp.

Lutz, L. A., and Gergely, P. (1967). "Mechanics of Bond and Slip of Deformed Bars in Concrete," ACI Journal, *Proceedings* Vol. 64, No. 11, Nov., pp. 711-721.

MacGregor, James G. (1976). "Safety and Limit States Design for Reinforced Concrete," *Canadian Journal of Civil Engineering*, Vol. 3, No. 4, Dec., pp. 484-513.

Maeda, M.; Otani, S.; and Aoyama, H. (1991). "Bond Splitting Strength in Reinforced Concrete Members," *Transactions of the Japan Concrete Inst.*, Vol. 13, pp. 581-588.

Mathey, Robert, and Watstein, David. (1961). "Investigation of Bond in Beam and Pull-Out Specimens with High-Yield-Strength Deformed Bars," ACI Journal, *Proceedings* Vol. 32, No. 9, Mar., pp. 1071-1090.

Mathey, Robert G., and Clifton, James R.. (1976). "Bond of Coated Reinforcing Bars in Concrete," *Journal of the Structural Division*, ASCE, Vol. 102, No. ST1, Jan., pp. 215-229.

Menzel, Carl A. (1952). "Effect of Settlement of Concrete on Results of Pullout Tests," *Research Department Bulletin* 41, Research and Development Laboratories of the Portland Cement Association, Nov., 49 pp.

Mirza, Sher Ali; Hatzinikolas, Michael; and MacGregor, James G. (1979). "Statistical Descriptions of Strength of Concrete," *Journal of the Structural Division*, ASCE, Vol. 105, No. ST6, June, pp. 1021-1037.

Mirza, Sher Ali, and MacGregor, James G. (1979). "Variations in Dimensions of Reinforced Concrete Members," *Journal of the Structural Division*, ASCE, Vol. 105, No. ST4, Apr., pp. 751-766.

Mirza, Sher Ali, and MacGregor, James G. (1986). "Strength Variability of Bond of Reinforcing Bars in Concrete Beams," *Civil Engineering Report Series* No. CE-86-1, Lahehead University, Thunder Bay, Ontario, Canada, Jan., 35 pp.

Mirza, Sher Ali (1992). "Statistical Analysis of Slender Composite Beam-Column Strength," *Journal of Structural Engineering*, Vol. 118, No. 5, May, pp. 1312-1332.

NTC-87 (1987) "Normas Ténicas Complementarias para Diseño y Construcción de Estructuras de Concreto," *Official Bulletin of the Federal District Department*, No. 44, Mexico City, Nov., (in Spanish).

Orangun, C. O.; Jirsa, J. O.; and Breen, J. E. (1975). "The Strength of Anchored Bars: A Reevaluation of Test Data on Development Length and Splices," *Research Report* No. 154-3F, Center for Highway Research, The University of Texas at Austin, Jan., 78 pp.

Orangun, C. O.; Jirsa, J. O.; and Breen, J. E. (1977). "Reevaluation of Test Data on Development Length and Splices," ACI Journal, *Proceedings* Vol. 74, No. 3, Mar., pp. 114-122.

Petersons, N. (1964). "Strength of Concrete in Finished Structures and its Effect on Safety," *Preliminary Publication*, 7th Congress, IABSE, Rio de Janeiro, Brazil, 257 pp.

RCDF-87 (1987) "Reglamento de construcciones para el Distrito Federal," *Official Bulletin of the Federal District Department*, No. 9, Mexico D. F., (in Spanish).

Rehm, G. (1957). "The Fundamental Law of Bond," *Proceedings*, Symposium on Bond and Crack Formation in Reinforced Concrete, Stockholm, RILEM, Paris, (published by Tekniska Hogskolans Rotaprinttrychkeri, Stockholm, 1958).

Rehm, G. (1961). "Uber die Grunlagen des Verbundes Zwischen Stahl und Beton." *Deutscher Ausschuss für Stahlbeton*. No. 1381, pp. 59, (C & CA Library Translation No. 134, 1968. "The Basic Principle of the Bond between Steel and Concrete.").

Rezansoff, T.; Konkankar, U. S.; and Fu, Y. C. (1991). "Confinement Limits for Tension Lap Splices in Reinforced Concrete," *Report* No. S7N 0W0, University of Saskatchewan, Aug., 32 pp.

Rezansoff, T.; Akanni, A; and Sparling, B. (1993). "Tensile Lap Splices under Static Loading: A Review of The Proposed ACI 318 Code Provisions," *ACI Structural Journal*, Vol. 90, No. 4, July-Aug., pp. 374-384.

Ruiz, S. E. (1993). "Reliability Associated with Safety Factors of ACI 318-89 and the Mexico City Concrete Design Regulations," *ACI Structural Journal*, Vol. 90, No. 3, May-June, pp. 262-268.

Ruiz, S. E. and Aquilar, J. C. (1994). "Reliability of Short and Slender Reinforced-Concrete Columns," *Journal of Structural Engineering*, Vol. 120, No. 6, June, pp. 1850-1864.

Sakurada, T.; Morohashi, N; and Tanaka, R. (1993). "Effect of Transverse Reinforcement on Bond Splitting Strength of Lap Splices," *Transactions of The Japan Concrete Inst.*, Vol. 15, pp. 573-580.

Skorbogatov, S. M., and Edwards, A. D. (1979). "The Influence of the Geometry of Deformed Steel Bars on Their Bond Strength in Concrete," *The Institute of Civil Engineers*, Proceedings Vol. 67, Part 2, June, pp. 327-339.

Soretz, S., and Holzenbein, H. (1979). "Influence of Rib Dimensions of Reinforcing Bars on Bond and Bendability," ACI Journal, *Proceedings* Vol. 76, No. 1, Jan., pp. 111-127.

Thompson, M.; Jirsa, J. O.; Breen, J. E.; and Meinheit, D. F. (1975). "The Behavior of Multiple Lap Splices in Wide Sections," *Research Report* No. 154-1, Center for Highway Research, The University of Texas at Austin, Feb., 75 pp.

Treece, Robert A. and Jirsa, James O. (1987). "Bond Strength of Epoxy-Coated Reinforcing Bars," *PMFSEL Report* No. 87-1, Phil M. Ferguson Structural Engineering Laboratory, The University of Texas at Austin, Jan., 85 pp.

Treece, Robert A. and Jirsa, James O. (1989). "Bond Strength of Epoxy-Coated Reinforcing Bars," *ACI Materials Journal*, Vol. 86, No. 2, Mar.-Apr., pp. 167-174.

Zekany, A. J.; Neumann, S.; and Jirsa, J. O. (1981). "The Influence of Shear on Lapped Splices in Reinforced Concrete," *Report* No. 242-2, Center for Transportation Research, Bureau of Engineering Research, University of Texas at Austin, July, 88 pp.

Zsutty, T. (1985). "Empirical Study of Bar Development Behavior," *Journal of Structural Engineering*, ASCE, Vol. 111, No. 1, Jan., pp. 205-219.

Table 2.1: Mortar Mix Proportions

Mix Number	Water-Cement Ratio, w/c	Sand-Cement Ratio, s/c
1	0.4	1.5
2	0.5	1.5
3	0.6	1.5
4	0.5	2.0
5	0.5	2.5

Table 2.2a: Friction Test Results for Formed-Surface Mortar* at 7 days - Series 1

Test No.	Normal Force (lb)	Max. Shear Force (lb)	COF	Mean COF	Test No.	Normal Force (lb)	Max. Shear Force (lb)	COF	Mean COF
1U1-1	166	104	0.625		11U1-1	40	26	0.650	
1U1-2	289	167	0.577		11U1-2	98	63	0.644	
1U1-3	402	230	0.571		11U1-3	144	75	0.519	
1U1-4	518	340	0.657		11U1-4	191	97	0.509	
1U1-5	644	487	0.757	0.637	11U1-5	243	134	0.552	
					11U1-6	278	164	0.592	
2U1-1	152	143	0.939		11U1-7	338	194	0.575	
2U1-2	275	177	0.644		11U1-9	424	231	0.545	0.573
2U1-3	398	280	0.704						
2U1-4	510	343	0.673		12U1-1	49	37	0.748	
2U1-5	605	382	0.631		12U1-2	85	60	0.711	
2U1-6	626	384	0.613		12U1-3	152	85	0.562	
2U1-7	506	328	0.649		12U1-4	200	116	0.578	
2U1-8	404	226	0.561		12U1-5	250	153	0.613	
2U1-9	306	200	0.653		12U1-6	290	175	0.605	
2U1-10	209	162	0.776	0.684	12U1-7	336	216	0.643	
					12U1-8	387	260	0.671	
8U1-1	97	60	0.613		12U1-10	469	312	0.666	0.644
8U1-2	140	67	0.483						
8U1-3	171	83	0.482		13U1-1	63	48	0.763	
8U1-4	187	114	0.612		13U1-2	109	82	0.757	
8U1-5	234	179	0.766		13U1-3	157	102	0.648	
8U1-9	386	239	0.618		13U1-4	210	131	0.622	
8U1-10	458	284	0.621	0.599	13U1-5	249	137	0.552	
					13U1-6	291	164	0.565	
9U1-1	61	31	0.512		13U1-7	338	217	0.643	
9U1-2	110	92	0.843		13U1-8	399	222	0.558	
9U1-3	162	109	0.672		13U1-9	436	228	0.523	
9U1-4	194	116	0.599		13U1-10	499	286	0.572	0.621
9U1-5	229	161	0.700						
9U1-6	298	192	0.643		15U1-1	48	34	0.700	
9U1-7	334	234	0.699		15U1-2	93	67	0.725	
9U1-8	389	249	0.640		15U1-3	150	108	0.719	
9U1-9	444	298	0.672	0.664	15U1-4	193	141	0.729	
					15U1-5	238	168	0.707	
10U1-1	52	36	0.682		15U1-6	293	188	0.640	
10U1-2	103	70	0.686		15U1-7	350	228	0.652	
10U1-3	155	104	0.670		15U1-8	384	249	0.648	
10U1-4	210	150	0.715		15U1-9	430	291	0.677	
10U1-5	249	159	0.640		15U1-10	483	305	0.632	0.683
10U1-6	297	213	0.719						
10U1-7	358	199	0.555		17U1-1	57	36	0.631	
10U1-8	420	244	0.582		17U1-2	94	60	0.636	
10U1-9	448	270	0.601		17U1-3	144	102	0.707	
10U1-10	500	318	0.637	0.649	17U1-4	199	127	0.639	
					17U1-5	239	162	0.677	
					17U1-6	303	210	0.693	
					17U1-7	335	204	0.609	
					17U1-8	399	241	0.603	0.649

* Mortar Mix 2 was used throughout.

Table 2.2b: Friction Test Results for Hand Finished-Surface Mortar* at 7 days - Series 1

Test No.	Normal Force (lb)	Max. Shear Force (lb)	COF	Mean COF	Test No.	Normal Force (lb)	Max. Shear Force (lb)	COF	Mean COF
2U1-11	106	59	0.556		12U1-11	91	49	0.540	
2U1-12	206	128	0.621		12U1-12	191	110	0.577	
2U1-13	317	172	0.544		12U1-13	285	138	0.484	
2U1-14	419	244	0.582		12U1-14	395	220	0.558	
2U1-15	508	305	0.601	0.581	12U1-15	483	284	0.588	0.550
8U1-11	83	34	0.408		13U1-11	91	48	0.535	
8U1-12	170	76	0.447		13U1-12	199	126	0.631	
8U1-13	276	124	0.451		13U1-13	300	163	0.544	
8U1-14	346	145	0.419		13U1-14	404	200	0.496	
8U1-15	459	208	0.452	0.436	13U1-15	502	229	0.457	0.533
9U1-11	124	63	0.510		15U1-11	96	48	0.503	
9U1-12	198	91	0.462		15U1-12	208	126	0.605	
9U1-13	319	169	0.530		15U1-13	290	154	0.530	
9U1-15	503	283	0.564	0.516	15U1-14	417	263	0.630	0.567
10U1-11	108	55	0.507		17U1-11	89	72	0.809	
10U1-12	193	97	0.501		17U1-12	194	120	0.618	
10U1-13	296	170	0.573		17U1-13	280	146	0.519	
10U1-14	400	197	0.494		17U1-14	383	196	0.513	
10U1-15	503	250	0.496	0.514	17U1-15	477	247	0.518	0.596
11U1-11	76	50	0.654						
11U1-12	176	100	0.567						
11U1-13	272	144	0.532						
11U1-14	377	194	0.515	0.567					

* Mortar Mix 2 was used throughout.

Table 2.2c: Friction Test Results for Formed-Surface Mortar* at 28 days - Series 1

Test No.	Normal Force (lb)	Max. Shear Force (lb)	COF	Mean COF	Test No.	Normal Force (lb)	Max. Shear Force (lb)	COF	Mean COF
1U28-1	47	19	0.418		4U28-1	49	32	0.643	
1U28-2	108	61	0.568		4U28-2	102	63	0.612	
1U28-3	140	72	0.512		4U28-3	149	113	0.759	
1U28-4	207	126	0.608		4U28-5	244	159	0.653	
1U28-5	240	102	0.427		4U28-6	306	212	0.693	
1U28-6	294	164	0.560		4U28-7	340	247	0.726	
1U28-7	338	160	0.473		4U28-8	385	247	0.643	
1U28-8	390	166	0.425		4U28-9	431	287	0.667	
1U28-9	452	268	0.593		4U28-10	486	276	0.568	
1U28-10	485	271	0.558		4U28-11	52	29	0.555	
1U28-11	238	129	0.545	0.517	4U28-12	95	87	0.911	
					4U28-13	140	113	0.805	
3U28-1	77	62	0.812		4U28-14	197	144	0.734	
3U28-2	156	89	0.575		4U28-15	234	180	0.770	
3U28-3	187	128	0.681		4U28-16	302	227	0.753	
3U28-4	275	187	0.680		4U28-17	330	231	0.701	
3U28-5	300	160	0.535		4U28-19	446	279	0.627	
3U28-6	346	232	0.671		4U28-21	69	68	0.979	0.711
3U28-7	405	223	0.552						
3U28-8	444	246	0.554		15U28-1	57	50	0.870	
3U28-9	476	267	0.562		15U28-2	98	60	0.609	
3U28-10	46	36	0.780		15U28-3	158	109	0.688	
3U28-11	95	56	0.585		15U28-4	204	148	0.727	
3U28-12	161	103	0.641		15U28-5	260	166	0.639	
3U28-13	204	144	0.704		15U28-6	301	195	0.647	
3U28-14	241	154	0.640		15U28-7	349	228	0.652	0.690
3U28-15	307	197	0.640						
3U28-16	347	198	0.570		16U28-1	57	29	0.511	
3U28-17	405	235	0.580		16U28-4	158	97	0.615	
3U28-18	486	335	0.689		16U28-5	205	166	0.810	
3U28-19	431	253	0.587		16U28-6	251	247	0.981	
3U28-20	81	61	0.758	0.640	16U28-7	307	201	0.654	
					16U28-8	358	194	0.542	
					16U28-9	396	296	0.747	0.695
					17U28-1	56	39	0.698	
					17U28-2	108	91	0.839	
					17U28-3	148	116	0.787	
					17U28-4	194	127	0.655	
					17U28-5	251	182	0.726	
					17U28-6	303	213	0.704	
					17U28-7	329	242	0.735	
					17U28-8	369	258	0.699	0.730

* Mortar Mix 2 was used throughout.

Table 2.2d: Friction Test Results for Hand Finished-Surface Mortar* at 28 days - Series 1

Test No.	Normal Force (lb)	Max. Shear Force (lb)	COF	Mean COF	Test No.	Normal Force (lb)	Max. Shear Force (lb)	COF	Mean COF
1U28-12	94	45	0.486		4U28-22	47	39	0.831	
1U28-13	188	103	0.550		4U28-23	97	77	0.793	
1U28-14	294	142	0.482		4U28-24	147	96	0.658	
1U28-15	393	157	0.400		4U28-25	196	113	0.580	
1U28-16	482	227	0.471	0.478	4U28-26	251	173	0.690	
					4U28-27	298	154	0.517	
3U28-21	63	23	0.361		4U28-28	334	220	0.660	
3U28-22	140	51	0.364		4U28-30	447	191	0.427	0.644
3U28-23	196	108	0.551						
3U28-24	229	121	0.529		16U28-11	150	76	0.506	
3U28-25	294	120	0.409		16U28-12	203	116	0.574	
3U28-26	356	131	0.369		16U28-13	253	211	0.835	0.638
3U28-27	396	166	0.418						
3U28-28	450	259	0.577	0.447	17U28-10	92	52	0.561	
					17U28-11	198	107	0.539	
					17U28-12	302	193	0.639	0.579

* Mortar Mix 2 was used throughout.

Table 2.3: Friction Test Results Summary - Series 1

Test Group No.	7 Day Test				28 Day Test			
	Formed-Surface		Hand Finished-Surface		Formed-Surface		Hand Finished-Surface	
	No. of Tests	Mean COF	No. of Tests	Mean COF	No. of Tests	Mean COF	No. of Tests	Mean COF
1U	5	0.637			11	0.517	5	0.478
2U	10	0.684	5	0.581				
3U					20	0.640	8	0.447
4U					21	0.711	8	0.644
8U	7	0.599	5	0.436				
9U	9	0.664	4	0.516				
10U	10	0.649	5	0.514				
11U	8	0.573	4	0.567				
12U	9	0.644	5	0.550				
13U	10	0.621	5	0.533				
15U	10	0.683	4	0.567	7	0.690		
16U					7	0.695	3	0.638
17U	8	0.649	5	0.596	8	0.730	3	0.579
Wt. Mean		0.643		0.539		0.659		0.547
Std. Dev.		0.077		0.073		0.116		0.134
COV		0.120		0.135		0.176		0.245

Table 2.4a: Friction Test Results for Formed-Surface Mortar at 7 days - Series 2

Test No.	Mortar Strength (psi)	Normal Force (lb)	Max. Shear Force (lb)	COF	Mean COF
1C7-1	5960	86	*	*	
1C7-2	5960	111	79	0.709	
1C7-3	5960	154	110	0.712	
1C7-4	5960	237	163	0.689	
1C7-5	5960	288	157	0.545	
1C7-6	5960	346	200	0.577	
1C7-7	5960	393	255	0.648	
1C7-8	5960	430	281	0.654	
1C7-9	5960	495	289	0.583	
1C7-10	5960	83	50	0.604	
1C7-11	5960	147	84	0.571	
1C7-12	5960	189	150	0.793	
1C7-13	5960	244	170	0.695	
1C7-14	5960	300	201	0.669	
1C7-15	5960	342	205	0.602	0.647
1F7-1	5800	91	45	0.490	
1F7-2	5800	134	62	0.465	
1F7-3	5800	191	109	0.571	
1F7-4	5800	243	160	0.658	
1F7-5	5800	285	175	0.616	
1F7-6	5800	331	190	0.572	
1F7-7	5800	383	260	0.679	0.579
2B7-1	5060	61	44	0.729	
2B7-2	5060	112	89	0.799	
2B7-3	5060	150	109	0.729	
2B7-4	5060	214	141	0.659	
2B7-5	5060	255	204	0.801	
2B7-6	5060	301	184	0.611	
2B7-7	5060	343	228	0.663	0.713
2C7-1	4070	90	71	0.784	
2C7-2	4070	138	80	0.578	
2C7-3	4070	191	140	0.733	
2C7-4	4070	242	178	0.737	
2C7-5	4070	292	198	0.678	
2C7-6	4070	342	194	*	
2C7-7	4070	406	262	0.645	
2C7-8	4070	417	298	0.714	
2C7-9	4070	346	217	0.628	
2C7-10	4070	430	293	0.680	
2C7-11	4070	114	100	0.880	
2C7-12	4070	191	124	0.648	
2C7-13	4070	258	249	0.964	
2C7-14	4070	294	239	0.814	
2C7-15	4070	400	319	0.799	0.734

Test No.	Mortar Strength (psi)	Normal Force (lb)	Max. Shear Force (lb)	COF	Mean COF
2E7-1	3530	99	60	0.603	
2E7-2	3530	145	120	0.828	
2E7-3	3530	135	104	0.770	
2E7-4	3530	179	150	0.835	
2E7-5	3530	238	207	0.870	
2E7-6	3530	290	219	0.757	
2E7-7	3530	327	229	0.701	
2E7-8	3530	381	295	0.774	
2E7-9	3530	401	294	0.733	
2E7-10	3530	447	289	0.647	0.752
2H7-1	4070	43	27	0.622	
2H7-2	4070	137	83	0.608	
2H7-3	4070	236	198	0.841	
2H7-4	4070	341	230	0.677	
2H7-5	4070	435	351	*	0.687
3B7-1	2500	54	63	1.170	
3B7-2	2500	108	86	0.795	
3B7-3	2500	149	97	0.652	
3B7-4	2500	217	174	0.802	
3B7-5	2500	253	182	0.718	
3B7-6	2500	303	147	*	
3B7-7	2500	327	225	0.689	
3B7-8	2500	226	184	0.815	
3B7-9	2500	182	136	0.745	
3B7-10	2500	131	107	0.815	0.800
3C7-1	3100	69	60	0.869	
3C7-2	3100	92	88	0.964	
3C7-3	3100	125	107	0.858	
3C7-4	3100	141	117	0.836	
3C7-5	3100	165	117	0.711	
3C7-6	3100	186	159	0.856	
3C7-7	3100	212	155	0.731	
3C7-8	3100	235	145	0.616	
3C7-9	3100	265	204	0.773	
3C7-10	3100	290	232	0.802	
3C7-19	3100	112	70	0.622	
3C7-20	3100	147	108	0.739	
3C7-21	3100	183	170	0.928	
3C7-22	3100	233	167	*	
3C7-23	3100	242	144	*	
3C7-24	3100	296	214	0.725	0.788

Table 2.4a: Friction Test Results for Formed-Surface Mortar at 7 days - Series 2 (Continued)

Test No.	Mortar Strength (psi)	Normal Force (lb)	Max. Shear Force (lb)	COF	Mean COF	Test No.	Mortar Strength (psi)	Normal Force (lb)	Max. Shear Force (lb)	COF	Mean COF
4B7-1	4530	57	50	0.880		4F7-1	4150	79	40	0.507	
4B7-2	4530	104	91	0.882		4F7-2	4150	130	60	0.462	
4B7-3	4530	155	121	*		4F7-3	4150	180	100	0.556	
4B7-4	4530	150	116	0.779		4F7-4	4150	239	115	0.480	
4B7-5	4530	192	168	*		4F7-5	4150	273	140	0.512	
4B7-6	4530	205	169	0.824		4F7-6	4150	327	175	0.535	
4B7-7	4530	250	194	*		4F7-7	4150	351	177	0.504	
4B7-8	4530	255	184	0.722		4F7-8	4150	383	210	0.548	
4B7-9	4530	295	211	*		4F7-9	4150	234	103	0.441	
4B7-10	4530	292	203	0.697	0.797	4F7-10	4150	329	164	0.499	0.504
4C7-1	4600	83	60	0.726		5B7-1	4830	52	39	0.755	
4C7-2	4600	138	85	0.614		5B7-2	4830	100	87	0.875	
4C7-3	4600	180	124	0.688		5B7-3	4830	148	116	0.784	
4C7-4	4600	225	150	0.666		5B7-4	4830	201	164	0.815	
4C7-5	4600	285	179	0.629		5B7-5	4830	251	163	0.650	
4C7-6	4600	334	195	0.583		5B7-6	4830	297	204	0.687	
4C7-7	4600	395	274	0.694		5B7-7	4830	346	213	0.617	
4C7-9	4600	61	34	0.557		5B7-8	4830	404	232	0.575	
4C7-10	4600	91	60	0.657		5B7-9	4830	452	302	0.668	
4C7-11	4600	108	80	0.739		5B7-10	4830	495	262	*	0.714
4C7-12	4600	115	93	0.807							
4C7-13	4600	162	90	0.556		5E7-1	4190	82	40	0.488	
4C7-14	4600	184	129	0.700		5E7-2	4190	120	80	0.664	
4C7-15	4600	221	130	0.586		5E7-3	4190	183	130	0.710	
4C7-16	4600	217	152	0.701		5E7-4	4190	220	160	0.725	
4C7-17	4600	264	174	0.661		5E7-5	4190	279	249	0.894	
4C7-18	4600	283	184	0.651		5E7-6	4190	333	202	0.608	
4C7-19	4600	310	203	0.655		5E7-7	4190	375	230	0.612	
4C7-20	4600	338	220	0.649		5E7-8	4190	274	169	0.618	
4C7-21	4600	367	254	0.693	0.661	5E7-9	4190	419	261	0.623	
						5E7-10	4190	118	90	*	0.660
4E7-1	4220	102	65	0.639							
4E7-2	4220	124	81	0.654							
4E7-3	4220	183	142	0.777							
4E7-4	4220	234	146	0.625							
4E7-5	4220	287	194	0.677							
4E7-6	4220	336	233	0.694							
4E7-7	4220	383	240	0.625							
4E7-8	4220	406	299	0.735							
4E7-9	4220	441	308	0.698							
4E7-10	4220	482	286	*	0.680						

* Mortar specimen crushed.

Table 2.4b: Friction Test Results for Hand Finished-Surface Mortar at 7 days - Series 2

Test No.	Mortar Strength (psi)	Normal Force (lb)	Max. Shear Force (lb)	COF	Mean COF
1C7-16	5960	126	92	0.729	
1C7-17	5960	239	160	0.669	
1C7-18	5960	336	244	0.726	
1C7-19	5960	433	322	0.743	
1C7-20	5960	480	269	0.561	0.686
2B7-8	5060	63	29	0.459	
2B7-9	5060	103	69	0.673	
2B7-10	5060	149	107	0.717	
2B7-11	5060	196	193	0.984	0.708
2C7-16	4070	98	45	0.459	
2C7-17	4070	134	79	0.588	
2C7-18	4070	196	146	0.745	
2C7-19	4070	236	161	0.684	
2C7-20	4070	310	176	0.566	
2C7-21	4070	344	228	0.663	
2C7-22	4070	387	278	0.718	
2C7-23	4070	441	308	0.698	0.640
2E7-11	3530	83	60	0.725	
2E7-12	3530	176	90	0.510	
2E7-13	3530	276	155	0.562	
2E7-14	3530	363	208	0.574	
2E7-15	3530	436	265	0.607	0.595
2H7-6	4070	48	21	0.437	
2H7-7	4070	149	83	0.556	
2H7-8	4070	251	161	0.641	0.545
3B7-11	2500	107	62	0.576	
3B7-12	2500	205	126	0.615	
3B7-13	2500	307	201	0.656	
3B7-14	2500	368	214	0.580	
3B7-15	2500	242	106	0.438	0.573
3C7-11	3100	88	45	0.516	
3C7-12	3100	141	120	0.851	
3C7-13	3100	193	130	0.672	
3C7-14	3100	246	180	0.729	
3C7-15	3100	289	185	0.640	
3C7-16	3100	343	241	0.704	
3C7-17	3100	434	291	0.670	
3C7-18	3100	473	232	0.491	0.659
4B7-11	4530	53	39	0.736	
4B7-12	4530	109	31	0.279	
4B7-13	4530	163	116	0.715	
4B7-14	4530	200	113	0.565	
4B7-15	4530	250	151	0.606	0.580
4C7-22	4600	76	33	0.438	
4C7-23	4600	118	70	0.591	
4C7-24	4600	166	73	0.439	
4C7-25	4600	224	88	0.394	
4C7-26	4600	270	185	0.687	
4C7-27	4600	283	154	0.544	
4C7-28	4600	335	182	0.543	
4C7-29	4600	332	106	0.318	
4C7-30	4600	342	195	0.570	0.503
4E7-11	4220	89	60	0.676	
4E7-12	4220	175	92	0.525	
4E7-13	4220	278	105	0.377	
4E7-14	4220	386	204	0.528	
4E7-15	4220	339	198	0.584	0.538
4F7-11	4150	86	30	0.350	
4F7-12	4150	146	59	0.404	
4F7-13	4150	188	110	0.583	
4F7-14	4150	249	78	0.312	
4F7-15	4150	296	126	0.427	0.415
5B7-11	4830	107	41	0.380	
5B7-12	4830	207	87	0.420	
5B7-13	4830	306	181	0.592	
5B7-14	4830	400	265	0.664	
5B7-15	4830	463	226	0.487	0.509
5E7-11	4190	79	30	0.376	
5E7-12	4190	140	65	0.463	
5E7-13	4190	228	95	0.416	
5E7-14	4190	292	145	0.495	
5E7-15	4190	373	198	0.531	0.456

* Mortar specimen crushed.

Table 2.4c: Friction Test Results for Formed-Surface Mortar at 28 days - Series 2

Test No.	Mortar Strength (psi)	Normal Force (lb)	Max. Shear Force (lb)	COF	Mean COF	Test No.	Mortar Strength (psi)	Normal Force (lb)	Max. Shear Force (lb)	COF	Mean COF
1B28-1	6970	109	75	0.684		2E28-1	5040	45	36	0.787	
1B28-2	6970	127	100	0.789		2E28-2	5040	97	73	0.754	
1B28-3	6970	153	100	0.655		2E28-3	5040	149	94	0.628	
1B28-4	6970	200	149	0.744		2E28-4	5040	191	133	0.696	
1B28-5	6970	208	134	0.646		2E28-5	5040	243	146	0.600	
1B28-6	6970	224	106	0.475		2E28-6	5040	298	208	0.698	
1B28-7	6970	287	170	0.591		2E28-7	5040	341	266	0.780	
1B28-8	6970	324	192	0.593		2E28-8	5040	397	308	0.777	
1B28-9	6970	376	246	0.655		2E28-9	5040	439	302	0.688	
1B28-10	6970	452	274	0.605	0.644	2E28-10	5040	489	332	0.678	0.709
1D28-1	6640	105	65	0.619		3B28-1	3570	79	70	0.887	
1D28-2	6640	136	95	0.697		3B28-2	3570	133	120	0.900	
1D28-3	6640	184	160	0.866		3B28-3	3570	158	140	0.885	
1D28-4	6640	227	128	0.562		3B28-4	3570	195	153	0.787	
1D28-5	6640	238	146	0.612		3B28-5	3570	218	179	0.822	
1D28-6	6640	344	202	0.587		3B28-6	3570	251	207	0.825	
1D28-7	6640	388	268	0.692		3B28-7	3570	305	225	0.737	
1D28-8	6640	435	274	0.631		3B28-8	3570	310	257	0.827	
1D28-9	6640	485	290	0.599		3B28-9	3570	342	299	0.875	
1D28-10	6640	523	325	0.622		3B28-10	3570	411	246	*	0.838
1D28-11	6640	94	61	0.648							
1D28-12	6640	142	100	0.701		4B28-1	5500	100	69	0.687	
1D28-13	6640	190	99	0.523		4B28-2	5500	168	80	0.477	
1D28-14	6640	231	103	0.448		4B28-3	5500	192	141	0.734	
1D28-15	6640	297	181	0.609	0.628	4B28-4	5500	236	173	0.736	
						4B28-5	5500	296	160	0.539	
1E28-1	6580	41	21	0.502		4B28-6	5500	332	244	0.736	
1E28-2	6580	97	73	0.755		4B28-7	5500	371	270	0.728	
1E28-3	6580	136	62	0.461		4B28-8	5500	439	239	0.546	
1E28-4	6580	190	117	0.615		4B28-9	5500	452	354	0.782	
1E28-5	6580	246	135	0.549		4B28-10	5500	508	327	0.643	0.661
1E28-6	6580	303	139	0.459							
1E28-7	6580	339	203	0.599		4D28-1	4830	77	20	0.258	
1E28-8	6580	386	250	0.647		4D28-2	4830	131	43	0.332	
1E28-9	6580	452	308	0.683		4D28-3	4830	187	70	0.374	
1E28-10	6580	479	267	0.558	0.583	4D28-4	4830	225	100	0.443	
						4D28-5	4830	276	120	0.435	
2B28-1	6520	91	77	0.843		4D28-6	4830	328	160	0.486	
2B28-2	6520	138	93	0.675		4D28-7	4830	377	192	0.511	
2B28-3	6520	185	131	0.708		4D28-8	4830	433	230	0.532	
2B28-4	6520	235	190	0.808		4D28-9	4830	161	95	0.588	
2B28-5	6520	287	222	0.776		4D28-10	4830	276	160	0.578	0.454
2B28-6	6520	340	274	0.807							
2B28-7	6520	385	326	0.846							
2B28-8	6520	426	305	0.718	0.773						

* Mortar specimen crushed.

Table 2.4d: Friction Test Results for Hand Finished-Surface Mortar at 28 days - Series 2

Test No.	Mortar Strength (psi)	Normal Force (lb)	Max. Shear Force (lb)	COF	Mean COF	Test No.	Mortar Strength (psi)	Normal Force (lb)	Max. Shear Force (lb)	COF	Mean COF
1B28-11	6970	88	45	0.508		4B28-11	5500	93	60	0.649	
1B28-12	6970	135	59	0.439		4B28-12	5500	205	120	0.584	
1B28-13	6970	189	70	0.370		4B28-13	5500	330	154	0.468	
1B28-14	6970	300	120	0.400		4B28-14	5500	431	271	0.631	0.583
1B28-15	6970	389	60	*	0.429						
						4D28-11	4830	88	30	0.339	
2B28-9	6520	127	59	0.465		4D28-12	4830	131	40	0.305	
2B28-10	6520	222	130	0.585		4D28-13	4830	177	100	0.564	
2B28-11	6520	311	129	0.415		4D28-14	4830	249	86	0.346	
2B28-12	6520	407	164	0.403		4D28-15	4830	256	147	0.572	0.425
2B28-13	6520	504	335	0.666	0.507						
3B28-11	3570	92	58	0.628							
3B28-12	3570	191	115	0.600							
3B28-13	3570	283	206	0.728							
3B28-14	3570	388	276	0.713	0.667						

* Mortar specimen crushed.

Table 2.5: Friction Test Results Summary - Series 2

Test* Group No.	7 Day Test					28 Day Test				
	Mortar Strength (psi)	Formed		Hand Finished		Mortar Strength (psi)	Formed		Hand Finished	
		No. of Tests	Mean COF	No. of Tests	Mean COF		No. of Tests	Mean COF	No. of Tests	Mean COF
1B						6970	10	0.644	4	0.429
1C	5960	14	0.647	5	0.686					
1D						6640	15	0.628		
1E						6580	10	0.583		
1F	5800	7	0.579							
Wt. Mean			0.624		0.686			0.620		0.429
2B	5060	7	0.713	4	0.708	6520	8	0.772	5	0.507
2C	4070	14	0.734	8	0.640					
2E	3530	10	0.752	5	0.595	5040	10	0.709		
2H	4070	4	0.687	3	0.545					
Wt. Mean			0.730		0.628			0.737		0.507
3B	2500	9	0.800	5	0.573	3570	9	0.838	4	0.667
3C	3100	14	0.788	8	0.659					
Wt. Mean			0.793		0.626			0.838		0.667
4B	4530	7	0.797	5	0.580	5500	10	0.661	4	0.583
4C	4600	21	0.661	9	0.503					
4D						4830	10	0.454	5	0.425
4E	4220	9	0.680	5	0.538					
4F	4150	10	0.504	5	0.415					
Wt. Mean			0.651		0.508			0.558		0.495
5B	4830	9	0.714	5	0.509					
5E	4190	9	0.660	5	0.456					
Wt. Mean			0.687		0.483					

* Number represents mortar mix number (see Table 2.1)

Table 2.6: Linear Regression Analyses Results Summary - Series 2

Mortar Mix No.	7 Day Test				28 Day Test			
	Formed		Hand Finished		Formed		Hand Finished	
	COF	r^2	COF	r^2	COF	r^2	COF	r^2
1	0.619	0.95342	0.598	0.88724	0.605	0.94241	0.354	0.97578
2	0.688	0.93330	0.660	0.92899	0.736	0.96293	0.628	0.81485
3	0.678	0.92633	0.565	0.86142	0.792	0.97046	0.759	0.99055
4	0.622	0.89838	0.503	0.77498	0.687	0.86191	0.615	0.88420
5	0.594	0.91988	0.608	0.93002				

Table 2.7: Friction Test Results for Coated and Uncoated Reinforcing Bar Specimens with Formed-Surface Mortar at 7 days - Series 3

	Uncoated Specimens					Coated Specimens				
Mortar Strength (psi)	Test No.	Normal Force (lb)	Max. Shear Force (lb)	COF	Mean COF	Test No.	Normal Force (lb)	Max. Shear Force (lb)	COF	Mean COF
6420	T1U1	82	40	0.487		T1C1	79	50	0.633	
	T1U2	123	65	0.528		T1C2	124	70	0.561	
	T1U3	177	120	0.675		T1C3	161	90	0.557	
	T1U4	224	130	0.580		T1C4	217	120	0.552	
	T1U5	272	170	0.624		T1C5	264	120	0.454	
	T1U6	66	30	0.456		T1C6	51	40	0.776	
	T1U7	113	65	0.575		T1C7	106	60	0.564	
	T1U8	160	110	0.685		T1C8	166	110	0.662	
	T1U9	215	110	0.511		T1C9	210	105	0.499	
	T1U10	260	160	0.612	0.573	T1C10	260	169	0.652	0.591
5770	T2U1	57	39	0.687		T2C1	58	30	0.520	
	T2U2	98	57	0.581		T2C2	155	88	0.568	
	T2U3	153	94	0.618		T2C3	308	110	0.358	
	T2U4	202	121	0.600		T2C4	57	27	0.476	
	T2U5	258	151	0.586		T2C5	160	72	0.449	
	T2U6	304	172	0.565		T2C6	306	134	0.437	
	T2U7	133	93	0.701		T2C7	58	24	0.417	
	T2U8	279	185	0.665		T2C8	159	73	0.459	
	T2U9	229	147	0.640		T2C9	310	148	0.478	0.463
	T2U10	184	115	0.624	0.627					
5610	T3U1	57	27	0.477		T3C1	266	117	0.442	
	T3U2	84	33	0.392		T3C2	134	95	0.711	
	T3U3	103	63	0.607		T3C3	51	15	0.304	
	T3U4	128	72	0.561		T3C4	256	148	0.577	
	T3U5	160	101	0.635		T3C5	134	50	0.370	
	T3U6	177	111	0.627		T3C6	55	13	0.227	
	T3U7	208	104	0.503		T3C7	260	113	0.435	
	T3U8	233	134	0.575		T3C8	132	64	0.488	
	T3U9	255	154	0.607		T3C9	54	15	0.279	0.426
	T3U10	285	137	0.482	0.547					
5670	T4U1	58	27	0.470		T4C1	57	13	0.222	
	T4U2	81	40	0.488		T4C2	136	57	0.419	
	T4U3	111	48	0.432		T4C3	264	92	0.348	
	T4U4	135	68	0.506		T4C4	133	71	0.534	
	T4U5	163	68	0.416		T4C5	259	117	0.452	
	T4U6	187	97	0.518		T4C6	58	18	0.321	
	T4U7	211	127	0.601		T4C7	264	123	0.465	
	T4U8	233	133	0.573		T4C8	55	15	0.271	
	T4U9	260	123	0.473		T4C9	135	51	0.377	0.379
	T4U10	286	158	0.554	0.503					

Table 2.7: Friction Test Results for Coated and Uncoated Reinforcing Bar Specimens with Formed-Surface Mortar at 7 days - Series 3 (Continued)

	Uncoated Specimens					Coated Specimens				
Mortar Strength (psi)	Test No.	Normal Force (lb)	Max. Shear Force (lb)	COF	Mean COF	Test No.	Normal Force (lb)	Max. Shear Force (lb)	COF	Mean COF
6860	T5U1	69	40	0.579		T5C1	71	50	0.702	
	T5U2	116	70	0.599		T5C2	120	50	*	
	T5U3	158	70	0.440		T5C3	172	79	0.463	
	T5U4	211	114	0.541		T5C4	230	99	0.431	
	T5U5	272	119	0.439		T5C5	278	50	*	
	T5U6	61	45	0.736		T5C6	75	30	0.397	
	T5U7	114	60	0.521		T5C7	121	55	0.451	
	T5U8	169	79	0.471		T5C8	176	79	0.451	
	T5U9	219	119	0.545		T5C9	228	89	*	
	T5U10	277	114	0.413	0.528	T5C10	281	20	*	0.483
6250	T6U1	64	40	0.624		T6C1	57	20	0.347	
	T6U2	118	50	0.424		T6C2	106	70	0.657	
	T6U3	211	95	0.449		T6C3	159	70	0.440	
	T6U4	262	179	0.685		T6C4	207	100	0.483	
	T6U5	63	30	0.474		T6C5	263	140	0.531	
	T6U6	118	70	0.589		T6C6	57	40	0.695	
	T6U7	146	60	0.408		T6C7	111	80	0.721	
	T6U8	213	130	0.610	0.533	T6C8	158	60	0.378	
						T6C9	211	100	0.472	
						T6C10	266	130	0.487	0.521
6420	T7U1	62	50	0.806		T7C1	114	60	0.524	
	T7U2	113	70	0.619		T7C2	163	110	0.675	
	T7U3	162	90	0.552		T7C3	210	125	0.593	
	T7U4	228	145	0.633		T7C4	264	140	0.528	
	T7U5	248	150	0.602		T7C5	69	40	0.575	
	T7U6	65	30	0.457		T7C6	113	50	0.441	
	T7U7	114	80	0.699		T7C7	161	80	0.494	
	T7U8	160	95	0.593		T7C8	211	120	0.569	
	T7U9	199	115	0.576		T7C9	267	160	0.597	0.555
	T7U10	265	145	0.545	0.608					

* Mortar specimen crushed.

Table 2.8: Friction Test Results Summary - Series 3

Test Group No.	Mortar Strength (psi)	Uncoated		Coated	
		No. of Tests	Mean COF	No. of Tests	Mean COF
T1	6420	10	0.573	10	0.591
T2	5770	10	0.627	9	0.463
T3	5610	10	0.546	9	0.426
T4	5670	10	0.503	9	0.379
T5	6860	10	0.528	6	0.483
T6	6250	8	0.533	10	0.521
T7	6420	10	0.608	9	0.555
	Wt. Mean		0.561		0.491
	Std. dev.		0.088		0.123
	COV		0.158		0.251

Table 3.1a: Properties and Designations of Machined Bars*

Bar Designation	Nominal Diameter (in.)	Rib Face Angle (deg.)	Rib Radius (in.)	Rib Spacing (in.)	Av. Rib Height*** (in.)	Relative Rib Area	Av. coating Thicknesses** (mils)
M1	1.00	90.00	0.030	0.550	0.100	0.200	9.9
M45.3	1.00	45.00	0.030	0.550	0.075	0.150	8.5
M45.4	1.00	45.00	0.040	0.550	0.075	0.150	8.5
M60.3	1.00	60.00	0.030	0.550	0.075	0.150	8.5
M60.4	1.00	60.00	0.040	0.550	0.075	0.150	8.5

Table 3.1b: Properties and Designations of Rolled Reinforcing Bars

Bar Designation	Yield Strength (ksi)	Nominal Diameter (in.)	Weight per foot (lb)	Rib Spacing (in.)	Rib Height ASTM (in.)	Rib Height Av.*** (in.)	Relative Rib Area	Av. coating Thicknesses** (mils)
C0		1.00	2.615	0.589	0.066	0.063	0.085	-
C1	60.00	1.00	2.529	0.504	0.064	0.060	0.101	13.3
F1	75.00	1.00	2.600	0.471	0.078	0.074	0.140	16.8
F2	75.00	1.00	2.551	1.006	0.086	0.080	0.072	16.8
N0	79.00	1.00	2.594	0.650	0.057	0.054	0.069	-
N3	81.00	1.00	2.730	0.487	0.072	0.068	0.119	12.1
SH0		1.00	2.618	0.637	0.054	0.052	0.065	-
S0	70.00	1.00	2.568	0.668	0.056	0.054	0.071	-

\- No coated bars tested.

* Machined bars were fabricated from 110 ksi yield strength ASTM A 311 (1990) cold-rolled steel.

** Average coating thicknesses for the coated bars belonging to the bar designation.

*** Average rib height between longitudinal ribs.

C0	Conventional Chaparral bar	N0	Conventional North Star bar
C1	New Chaparral bar	N3	New North Star bar
F1	New Florida Type 1 bar	SH0	Conventional Sheffield bar
F2	New Florida Type 2 bar	S0	Conventional Structural Metals Inc. bar

Table 3.2a: Concrete Mix Proportions (lb/yd^3) and Properties for Beam-End Specimens

Group	w/c Ratio	Cement	Water	Fine Agg*.	Coarse Agg. Type		wr (oz)	Slump (in.)	Concrete Temp (F)	Air Content (%)	Test Age (days)	Cylinder Strength (psi)
0	0.41	550	225	1564	L	1588	0	2.00			7	5180
1	0.41	550	225	1564	L	1588	0	1.75	50	4.25	9	4340
2	0.41	550	225	1564	L	1588	0	4.00	75	2.30	17	4900
3	0.36	575	205	1556	L	1588	3	2.00	88	3.70	8	5020
5	0.36	575	205	1556	L	1588	3	2.25	62	4.00	18	5440
8	0.36	575	205	1556	L	1588	3	2.75	57	2.80	7	4760

Table 3.2b: Concrete Mix Proportions (lb/yd^3) and Properties for Splice Tests

Group	w/c Ratio	Cement	Water	Fine Agg*.	Coarse Agg. Type		wr (oz)	Slump (in.)	Concrete Temp (F)	Air Content (%)	Test Age (days)	Cylinder Strength (psi)
1	0.41	550	225	1564	L	1588	0	2.00	80	3.50	14	5020
2	0.36	575	205	1556	L	1588	3	0.75	91.5	3.10	7	5250
3a	0.36	575	205	1556	L	1588	3	2.75	93	3.70	5	3810
3b	0.36	575	205	1556	L	1588	3	2.75	93	3.70	7	5110
4	0.36	575	205	1556	L	1588	3	1.75	95	4.50	5	4090
5	0.36	575	205	1556	L	1588	3	1.00	83	3.60	5	4190
6	0.36	575	205	1556	L	1588	3	2.25	77	4.70	5	4220
7	0.36	575	205	1556	L	1588	3	5.25	67	3.50	7	4160
8	0.45	556	250	1556	B	1670	0	1.25	86	3.00	8	3830
9	0.45	578	260	1512	B	1670	0	3.00	95	2.30	16	4230
10	0.42	578	240	1512	B	1670	0	2.50	91	2.50	10	4250
11	0.42	578	240	1512	B	1670	0	3.00	91	2.10	7	4380
14	0.44	511	225	1564	L	1661	0	2.50	90	2.90	10	4200

* Kansas River Sand - Lawrence Sand Co., Lawrence, KS.
Bulk Specific Gravity (SSD) = 2.62; Absorption = 0.5 %; Fineness Modulus = 2.89

L Crushed Limestone - Fogel's Quarry, Ottawa, KS.
Bulk Specific Gravity (SSD) = 2.58; Absorption = 2.7 %; Max. Size = 3/4 in.;
Unit Weight = 90.5 lb/cu ft

B Basalt - Iron Mountain Trap Rock Company
Bulk Specific Gravity (SSD) = 2.64; Absorption = 0.44 %; Max. Size = 3/4 in.;
Unit Weight = 95.5 lb/cu ft

wr Water Reducer per 100 lb Cement

Table 3.3: Beam-End Test Results

Specimen Label**	Concrete Cover (in.)	Concrete Strength (psi)	JUST BEFORE PEAK LOAD: Bond Force (kips)	Mod. Bond Force* (kips)	Crack Width (mils)	Av. Crack Width (mils)	PEAK LOAD: Crack Width (mils)	Bond Str. (kips)	Mod. Bond Str.* (kips)	Av. Mod. Bond Str.* (kips)
0M1-8UNA	2.250	5180						33.44	33.15	
0M1-8UNB	2.063	5180						25.16	24.94	
0M1-8UNC	2.250	5180						31.24	30.97	
1M1-8UNA	1.875	4340	29.76	30.83	13.71		18.10	29.83	30.90	
1M1-8UNB	2.000	4340	33.25	34.45	12.87		184.62	33.33	34.53	
1M1-8UNC	2.250	4340	25.70	26.63	12.57	13.05	28.39	25.74	26.67	30.19
0M1-8CNA	2.375	5180						27.10	26.86	
0M1-8CNB	1.875	5180						30.22	29.95	
0M1-8CNC	1.750	5180						29.54	29.28	
1M1-8CNA	2.063	4340	28.45	29.47	4.66		4.40	28.49	29.52	
1M1-8CNB	1.938	4340	30.31	31.40	11.39		14.31	30.39	31.48	
1M1-8CNC	2.063	4340	28.84	29.88	10.86	8.97	12.77	28.89	29.93	29.50
1C1-8UNA	2.188	4340	27.04	28.01	5.86		7.34	27.09	28.07	
1C1-8UNB	2.188	4340	28.19	29.21	2.64		3.76	28.24	29.26	
1C1-8UNC	2.125	4340	26.01	26.95	7.03		8.91	26.08	27.02	
1C1-8UND	2.188	4340	26.47	27.42	3.24		3.84	26.56	27.52	
1C1-8UNE	2.063	4340	27.50	28.49	5.97		124.33	27.52	28.51	
1C1-8UNF	2.000	4340	25.57	26.49	3.48		5.35	25.61	26.53	
2C1-8UNA	2.000	4900	28.83	28.98	1.74		100.90	29.01	29.16	
2C1-8UNB	2.125	4900	28.27	28.41	1.93		2.73	28.43	28.57	
2C1-8UNC	2.125	4900	29.24	29.39	3.31	3.91	8.50	29.50	29.65	28.25
1C1-8CNA	2.188	4340	25.18	26.09	5.05		5.95	25.23	26.14	
1C1-8CNB	2.250	4340	26.90	27.87	5.66		7.85	26.96	27.93	
1C1-8CNC	2.250	4340	26.27	27.22	5.37		12.86	26.41	27.36	
1C1-8CND	2.000	4340	23.76	24.62	8.63		157.75	23.78	24.64	
1C1-8CNE	2.063	4340	25.28	26.19	3.87		4.51	25.41	26.33	
1C1-8CNF	2.125	4340	23.14	23.97	6.60		12.25	23.20	24.04	
2C1-8CNA	2.250	4900	26.99	27.13	5.29		200.60	27.03	27.17	
2C1-8CNB	2.188	4900	26.54	26.67	3.98		9.58	26.71	26.85	
2C1-8CNC	2.125	4900	27.57	27.71	3.57	5.34	4.10	27.59	27.73	26.46
3F1-8UNA	2.125	5020	27.29	27.26	3.98		120.32	27.30	27.27	
3F1-8UNB	2.250	5020	27.31	27.28	4.64		6.40	27.38	27.35	
3F1-8UNC	2.063	5020	27.13	27.10	3.41	4.01	4.49	27.18	27.15	27.26
3F1-8CNA	2.250	5020	22.63	22.61	2.09		2.63	22.69	22.67	
3F1-8CNB	2.125	5020	23.58	23.56	3.72		6.05	23.62	23.60	
3F1-8CNC	2.063	5020	23.18	23.16	3.77	3.19	5.15	23.23	23.21	23.16

Note: Refer to last page of the table for footnotes.

Table 3.3: Beam-End Test Results (Continued)

Specimen Label**	Concrete Cover (in.)	Concrete Strength (psi)	JUST BEFORE PEAK LOAD: Bond Force (kips)	Mod. Bond Force* (kips)	Crack Width (mils)	Av. Crack Width (mils)	PEAK LOAD: Crack Width (mils)	Bond Str. (kips)	Mod. Bond Str.* (kips)	Av. Mod. Bond Str.* (kips)
3F2-8UNA	2.313	5020	27.20	27.17	4.08		5.10	27.26	27.23	
3F2-8UNB	2.125	5020	26.65	26.62	2.76		3.93	26.67	26.64	
3F2-8UNC	2.125	5020	27.46	27.43	0.92	2.59	1.77	27.52	27.49	27.12
3F2-8CNA	2.250	5020	23.24	23.22	2.25		2.85	23.32	23.30	
3F2-8CNB	2.313	5020	20.54	20.52	2.74		3.46	20.63	20.61	
3F2-8CNC	2.125	5020	22.83	22.81	1.94	2.31	2.44	22.92	22.90	22.27
5M45.3-8UN	2.063	5440	28.34	27.75	6.23		7.28	28.36	27.77	
8M45.3-8UN	2.063	4760	30.36	30.74	5.55	5.89	6.30	30.39	31.15	29.46
5M45.3-8CN	2.063	5440	25.88	25.34	6.85		8.16	25.88	25.34	
8M45.3-8CN	2.000	4760	22.57	22.85	6.32	6.59	8.11	22.57	23.13	24.24
5M45.4-8UN	2.125	5440	25.99	25.45	3.70		3.91	26.02	25.48	
8M45.4-8UN	2.250	4760	30.27	30.64	11.12	7.41	11.99	30.28	31.03	28.25
5M45.4-8CN	2.188	5440	26.65	26.09	4.49		5.05	26.67	26.11	
8M45.4-8CN	1.875	4760	28.35	28.70	5.22	4.86	6.08	28.35	29.06	27.59
5M60.3-8UN	2.250	5440	26.38	25.83	7.25		8.51	26.39	25.84	
8M60.3-8UN	1.938	4760	30.28	30.66	10.99	9.12	12.08	30.29	31.04	28.44
5M60.3-8CN	2.125	5440	27.34	26.77	3.62		4.02	27.37	26.80	
8M60.3-8CN	2.250	4760	30.88	31.27	6.94	5.28	7.75	30.90	31.66	29.23
5M60.4-8UN	2.063	5440	26.40	25.85	12.95		14.90	26.40	25.85	
8M60.4-8UN	2.125	4760	28.39	28.74	10.11	11.53	10.86	28.40	29.11	27.48
5M60.4-8CN	2.063	5440	25.08	24.56	0.00		0.00	25.09	25.71	
8M60.4-8CN	2.000	4760	26.82	27.15	7.46	3.73	8.38	26.82	27.15	26.43

* Modified Bond Strength (Force) = Bond Strength (Force) x $(5000 / f_c')^{1/4}$.

** Specimen Label

GBD-#SNR

G : Group number : 0, 1, 2, 3, 5, 8

BD : Bar designation : C1, F1, F2, M1, M45.3, M45.4, M60.3, M60.4

: Bar size : 8

S : Bar surface condition : C = coated, U = uncoated

N : No stirrups

R : Replication I.D. : blank, A, B, C, D, E, F

Table 3.4 : Splice Test Results

Specimen Label ++	Bar Designation	n_b	l_s (in.)	d_b (in.)	C_{so} (in.)	C_{si} (in.)	C_b (in.)	b (in.)	h (in.)	l (ft)	l_c (ft)	d (in.)	f'_c (psi)	N	d_s (in.)	f_{yt} (ksi)	P (kips)	M_u (k-in.)	f_s+ (ksi)
1.1	C1	2	16.0	1.034	2.969	2.938	2.938	16.08	17.22	13.00	4.00	13.77	5020				20.69	1021	51.63
1.2	C1	2*	16.0	1.034	2.032	2.281	1.938	24.06	16.25	13.00	4.00	13.80	5020				35.53	1746	44.60
1.3	C1	3	16.0	1.034	2.032	1.422	1.938	16.07	16.21	13.00	4.00	13.76	5020				26.74	1310	45.01
1.4	C1**	3	16.0	1.035	2.032	1.375	1.938	16.11	16.20	13.00	4.00	13.74	5020				21.93	1079	37.09
1.5	C1	3	16.0	1.037	2.063	1.375	1.938	16.07	16.19	13.00	4.00	13.73	5020	5	0.500	70.75	31.08	1518	52.22
1.6	C1	3	16.0	1.033	2.063	1.438	1.938	16.05	16.19	13.00	4.00	13.74	5020	3	0.500	70.75	30.93	1511	51.98
2.1	SM1	2	24.0	1.051	2.250	1.706	1.328	12.12	15.56	16.00	6.00	13.71	5250	7	0.375	69.92	22.12	1214	62.43
2.2	F1	2	24.0	1.067	2.125	1.801	1.406	12.12	15.52	16.00	6.00	13.58	5250	7	0.375	69.92	27.90	1526	77.60
2.3	F1	2	24.0	1.075	2.125	1.780	1.969	12.11	16.06	16.00	6.00	13.55	5250	4	0.375	69.92	25.77	1413	73.45
2.4	F1	2	24.0	1.075	2.000	1.914	1.313	12.13	15.64	16.00	6.00	13.79	5250				19.24	1059	54.08
2.5	F1	2	24.0	1.073	2.063	1.856	1.813	12.13	16.01	16.00	6.00	13.66	5250				20.69	1138	58.67
2.6	F1**	2	24.0	1.072	2.000	1.917	1.938	12.12	16.19	16.00	6.00	13.72	5250				17.41	961	49.37
3.4#	C0	2	24.0	1.051	2.110	1.857	2.000	12.14	16.26	16.00	6.00	13.73	5110	4	0.375	69.92	19.73	1087	55.77
3.5#	C0	3	28.0	1.052	1.001	0.965	1.906	12.17	16.17	16.00	6.00	13.74	3810	8	0.375	69.92	27.00	1479	52.02
4.1	SM1	2	24.0	1.046	2.063	1.926	1.250	12.16	15.49	16.00	6.00	13.72	4090	6	0.500	70.75	22.05	1211	62.51
4.2	F1	2	24.0	1.071	2.094	1.848	1.313	12.17	15.59	16.00	6.00	13.74	4090	8	0.375	69.92	25.61	1403	72.33
4.4	C1	2	24.0	1.032	2.032	1.978	1.219	12.15	15.47	16.00	6.00	13.74	4090	4	0.375	69.92	20.75	1141	58.85
4.5	C1	2	24.0	1.030	2.063	1.936	1.844	12.12	16.15	16.00	6.00	13.79	4090				18.02	994	51.06
4.6	C1**	2	24.0	1.031	2.094	1.926	2.000	12.16	16.23	16.00	6.00	13.71	4090				14.57	808	41.72
5.1	SH0	3	24.0	1.049	2.016	1.914	1.250	18.22	15.57	16.00	6.00	13.80	4190	7	0.375	69.92	34.41	1888	64.62
5.2	F1	3	24.0	1.072	2.078	1.867	1.359	18.12	15.62	16.00	6.00	13.73	4190	7	0.375	69.92	34.67	1902	65.41
5.3	F1	2	24.0	1.072	2.063	1.849	1.281	12.11	15.50	16.00	6.00	13.68	4190	7	0.375	69.92	23.90	1311	67.88
5.4	SH0	2	24.0	1.048	1.985	1.980	1.250	12.12	15.46	16.00	6.00	13.69	4190	7	0.375	69.92	20.69	1137	58.87
5.5	C0	2	24.0	1.047	2.063	1.904	1.406	12.12	15.60	16.00	6.00	13.67	4190	4	0.375	69.92	16.22	896	46.43
5.6	F1	2	22.0	1.078	2.094	1.807	1.313	12.11	15.69	16.00	6.00	13.84	4190	5	0.500	70.75	23.65	1297	66.34
6.1	SH0	3	24.0	1.048	2.063	0.422	1.906	12.18	16.12	16.00	6.00	13.69	4220	8	0.500	66.42	32.89	1797	63.26
6.2	F1	3	24.0	1.067	2.000	0.438	2.000	12.11	16.15	16.00	6.00	13.62	4220	8	0.500	66.42	38.79	2115	74.88
6.3	F1	2	16.0	1.061	2.000	1.906	1.344	12.13	15.51	16.00	6.00	13.64	4220	2	0.375	64.55	16.07	887	46.09
6.4	C0	2	16.0	1.048	2.094	1.844	1.344	12.11	15.45	16.00	6.00	13.58	4220	2	0.375	64.55	12.67	703	36.68
6.5	F1	2	24.0	1.075	2.000	1.906	1.969	12.10	16.13	16.00	6.00	13.62	4220				18.71	1031	53.59
6.6	F1**	2	24.0	1.075	2.032	1.875	1.969	12.15	16.13	16.00	6.00	13.62	4220				17.30	955	49.63
7.1	F1	2	16.0	1.066	2.079	1.797	1.875	12.00	16.18	16.00	6.00	13.77	4160	2	0.375	64.55	15.56	908	46.72
7.2	C1	2	18.0	1.021	1.469	2.531	1.313	12.06	15.54	16.00	6.00	13.72	4160	5	0.500	84.70	18.81	1081	55.82

Note: Refer to last page of the table for footnotes.

Table 3.4 : Splice Test Results (Continued)

Specimen Label ++	Bar Designation	n_b	l_s (in.)	d_b (in.)	C_{so} (in.)	C_{si} (in.)	C_b (in.)	b (in.)	h (in.)	l (ft)	l_c (ft)	d (in.)	f'_c (psi)	N	d_s (in.)	f_{yt} (ksi)	P (kips)	M_u (k-in.)	f_s+ (ksi)
7.5	F1	3	24.0	1.065	2.032	0.399	2.000	11.97	16.17	16.00	6.00	13.64	4160	8	0.500	84.70	37.07	2068	73.17
7.6	C1	2	16.0	1.024	2.032	1.969	1.938	12.01	16.22	16.00	6.00	13.77	4160	2	0.375	64.55	14.70	862	44.34
8.1	N0	3	24.0	1.049	2.032	0.453	1.953	12.13	16.23	16.00	6.00	13.75	3830	8	0.500	84.70	36.34	1983	69.67
8.2	N3	3	24.0	1.079	2.047	0.430	1.969	12.16	16.20	16.00	6.00	13.69	3830	8	0.500	84.70	41.23	2247	79.32
8.3	N0	2	24.0	1.049	2.000	1.953	2.000	12.11	16.05	16.00	6.00	13.53	3830				21.30	1171	61.47
8.4	N3	2	16.0	1.079	2.063	1.891	1.906	12.10	16.35	16.00	6.00	13.90	3830	2	0.375	64.55	17.38	959	48.90
9.1	N3	2	24.0	1.079	2.032	1.875	1.954	12.14	16.19	16.00	6.00	13.70	4230	2	0.375	64.55	22.33	1226	63.40
9.2	F1	2	18.0	1.071	2.063	1.844	1.290	12.10	15.67	16.00	6.00	13.84	4230	6	0.375	64.55	24.65	1351	69.06
9.3	N0	2	24.0	1.049	2.094	1.907	1.818	12.19	16.12	16.00	6.00	13.78	4230	2	0.375	64.55	19.54	1076	55.25
9.4	F1	2	24.0	1.071	2.016	1.891	1.915	12.11	16.17	16.00	6.00	13.72	4230	2	0.375	64.55	22.94	1259	65.00
10.1	N3**	2	26.0	1.079	2.016	1.907	1.896	12.15	16.16	16.00	6.00	13.72	4250				20.36	1120	57.79
10.2	N3	2	26.0	1.079	2.063	1.875	1.933	12.13	16.25	16.00	6.00	13.78	4250				21.66	1191	61.17
10.3	N0	2	26.0	1.049	2.094	1.844	1.798	12.11	16.09	16.00	6.00	13.77	4250	2	0.375	64.55	20.81	1144	58.85
10.4	N0	2	20.0	1.049	2.079	1.875	1.916	12.07	16.19	16.00	6.00	13.75	4250	5	0.500	84.70	21.91	1204	61.98
11.1	F1	3	18.0	1.071	2.000	0.453	1.928	12.20	16.14	16.00	6.00	13.68	4380	6	0.500	84.70	34.85	1902	66.94
11.2	N0	2	18.0	1.049	2.094	1.844	1.881	12.19	16.13	16.00	6.00	13.72	4380	4	0.500	84.70	21.88	1202	61.94
11.3	N3	2	18.0	1.079	2.063	1.844	1.943	12.13	16.08	16.00	6.00	13.60	4380	4	0.500	84.70	21.85	1200	62.44
11.4	F1	2	24.0	1.071	2.094	1.844	1.928	12.15	16.23	16.00	6.00	13.77	4380	2	0.375	64.55	22.14	1217	62.49
14.1	C1	3	36.0	1.032	2.032	0.484	1.877	12.12	16.26	16.00	6.00	13.87	4200	3	0.375	64.55	31.53	1725	59.96
14.2	C1	3	21.0	1.032	2.016	0.469	1.897	12.19	16.13	16.00	6.00	13.72	4200	7	0.500	84.70	32.73	1788	62.83

* Contained 2 splices and 2 continuous bars.

** Spliced bars were coated.

\# For specimen 3.4 see group 3a (Table 3.2b) for concrete properties.
For specimen 3.5 see group 3b (Table 3.2b) for concrete properties.

\+ Bar stress is computed using working stress if the stress does not exceed bar yield stress, otherwise ultimate strength method is used.

++ Specimen Label
G.P
G : Group number : 1, 2, 3, 4, 5, 6, 7, 8, 9, 10, 11, 14
P : Casting order in the group : 1, 2, 3, 4, 5, 6

Table 4.1a: Effect of Epoxy-Coating on Bond Strength, using Beam-End Tests

Bar	Group	No. of Test Specimens*	Rib Face Angle (deg.)	Relative Rib Area	Av. Modified Bond Strength		C/U^{+}	Average C/U^{+}
					Uncoated (kips)	Coated (kips)		
M1	0	3	90	0.200	29.68	28.70	0.97	
	1	3	90	0.200	30.70	30.31	0.99	0.98
C1	1	6	40	0.101	27.82	26.07	0.94	
	2	3	40	0.101	29.13	27.25	0.94	0.94
F1	3	3	40	0.140	27.26	23.16	0.85	0.85
F2	3	3	30	0.072	27.12	22.27	0.82	0.82
M45.3	5	1	45	0.150	27.77	25.34	0.91	
	8	1	45	0.150	31.15	23.13	0.74	0.83
M45.4	5	1	45	0.150	25.48	26.11	1.02	
	8	1	45	0.150	31.03	29.06	0.94	0.98
M60.3	5	1	60	0.150	25.84	26.80	1.04	
	8	1	60	0.150	31.04	31.66	1.02	1.03
M60.4	5	1	60	0.150	25.85	25.71	0.99	
	8	1	60	0.150	29.11	27.15	0.93	0.96
						Average		0.92

Table 4.1b : Effect of Epoxy Coating on Splice Strength**

Bar	Group	No. of Test Specimens*	Rib Face Angle (deg.)	Relative Rib Area	Bar Stress		C/U^{++}	Average C/U^{++}
					Uncoated (ksi)	Coated (ksi)		
C1	1	1	40	0.101	45.01	37.09	0.82	
	4	1	40	0.101	51.06	41.72	0.82	0.82
F1	2	1	40	0.140	58.67	49.37	0.84	
	6	1	40	0.140	53.59	49.63	0.93	0.88
N3	10	1	45	0.119	61.17	57.79	0.94	0.94
						Average		0.88

* Number of uncoated and coated specimens each.

** Splices had no transverse reinforcements.

C/U^{+} Ratio of average modified bond strengths of coated to uncoated bars at peak load.

C/U^{++} Ratio of bar stress of coated to uncoated specimens.

Table 4.2a: Effect of Epoxy-Coating on Bond Strength, using Beam-End Test Results from Choi et al. (1990, 1991)

Bar	Group	No. of Test Specimens		Relative Rib Area	Av. Modified Bond Strength		C/U*	Average C/U*
		Uncoated	Coated		Uncoated (kips)	Coated (kips)		
5S	9	3	6	0.057	14.15	11.75	0.83	
	21	3	6	0.057	14.60	12.01	0.82	0.83
5C	10	3	6	0.074	13.58	13.01	0.96	
	21	3	6	0.074	15.08	13.02	0.86	0.91
5N	11	3	3	0.086	12.96	12.00	0.93	
	12	3	3	0.086	14.00	12.43	0.89	
	13	3	3	0.086	13.11	11.98	0.91	0.91
6S	14	3	6	0.060	19.36	15.50	0.80	
	17	3	6	0.060	18.72	15.53	0.83	0.82
6C	14	3	6	0.079	18.73	18.11	0.97	
	17	3	6	0.079	18.76	16.06	0.86	0.92
6N	14	3	3	0.084	19.31	19.09	0.99	
	22	6	6	0.084	20.39	14.49	0.91	0.95
8S	3	3	9	0.064	41.38	29.47	0.71	
	6	2	2	0.064	45.10	34.51	0.77	
	15	2	6	0.064	42.68	31.60	0.74	
	18	3	3	0.064	41.31	34.06	0.82	0.76
8C	2	1	3	0.077	47.18	37.98	0.80	
	5	3	9	0.077	36.50	34.78	0.95	
	6	2	2	0.077	45.88	35.60	0.78	0.84
8N	4	3	3	0.080	46.10	37.21	0.81	
	6	2	2	0.080	43.30	41.30	0.95	
	18	3	3	0.080	48.26	38.80	0.80	0.85
11S	19	3	3	0.071	39.03	33.14	0.85	
	20	3	3	0.071	41.99	41.58	0.99	0.92
11C	19	3	3	0.069	40.44	30.56	0.76	
	20	3	3	0.069	40.42	36.16	0.89	0.83
11N	19	3	3	0.065	42.29	32.15	0.76	
	20	3	3	0.065	44.94	32.63	0.73	0.75
						Average		0.86

C/U* Ratio of average modified bond strengths of coated to uncoated bars at peak load.

Table 4.2b: Effect of Epoxy-Coating on Splice Strength, using Splice Test Results from Choi et al. (1990, 1991)**

Bar	Group	No. of Test Specimens		Relative Rib Area	Bars Stress		C/U*	Average C/U*
		Uncoated	Coated		Uncoated (kips)	Coated (kips)		
5N	SP1	1	1	0.086	45.50	34.13	0.75	0.75
6S	SP2	1	1	0.060	40.60	38.16	0.94	0.94
6C	SP2	1	1	0.079	36.90	28.04	0.76	0.76
8S	SP3	1	1	0.064	35.90	32.31	0.90	0.90
8N	SP3	1	1	0.080	34.40	29.58	0.86	0.86
11S	SP4	1	1	0.071	26.60	19.15	0.72	0.72
11C	SP4	1	1	0.069	28.60	23.45	0.82	0.82
						Average		0.82

Table 4.2c: Effect of Epoxy-Coating on Splice Strength, using Splice Test Results from Hester et al. (1991, 1993)**

Bar	Group	No. of Test Specimens		Relative Rib Area	Bars Stress		C/U*	Average C/U*
		Uncoated	Coated		Uncoated (kips)	Coated (kips)		
8C	B2	1	1	0.071	46.50	38.50	0.83	
	B5	1	1	0.071	39.80	31.90	0.80	
	B6	1	1	0.071	51.60	33.40	0.65	
	B7	1	1	0.071	45.20	38.70	0.86	0.79
8S	B3	1	1	0.070	47.00	30.90	0.66	
	B4	1	1	0.070	42.70	30.80	0.72	0.69
						Average		0.74

** Splices had no transverse reinforcement.

C/U* Ratio of bar stress of coated to uncoated specimens.

Table 4.3: Comparison of Splice Strengths for Conventional and High Relative Rib Area Bars

Specimen Label	Bar	Relative Rib Area	Stirrups	Bar Stress (ksi)
5.4	SH0	0.065	7-No. 3	58.87
5.3	F1	0.140	7-No. 3	67.88
6.1	SH0	0.065	8-No. 4	63.26
6.2	F1	0.140	8-No. 4	74.88
6.4	C0	0.085	2-No. 3	36.68
6.3	F1	0.140	2-No. 3	46.09
7.6	C1	0.101	2-No. 3	44.34
7.1	F1	0.140	2-No. 3	46.72
8.1	N0	0.069	8-No. 4	69.67
8.2	N3	0.119	8-No. 4	79.32
9.3	N0	0.069	2-No. 3	55.25
9.1	N3	0.119	2-No. 3	63.40
9.4	F1	0.140	2-No. 3	65.00
11.2	N0	0.069	4-No. 4	61.94
11.3	N3	0.119	4-No. 4	62.44

Table 4.4a: Tabulated Values of Increase in Modified Bond Force due to Stirrups for Splice Tests from Current Study

Specimen Label	Bar Designation	l_s (in.)	Stirrups	f'_c (psi)	f_s (ksi)	$A_b f_s$ (kips)	NA_{tr}/n ($in.^2$)	T_b (kips)	T_c (kips)	T_s* (kips)
1.5	C1	16.00	5-No. 4	5020	52.22	41.25	0.667	41.23	32.87	8.36
1.6	C1	16.00	3-No. 4	5020	51.98	41.06	0.400	41.04	33.28	7.76
2.1	SMI	24.00	7-No. 3	5250	62.43	49.32	0.770	48.72	38.99	9.72
2.2	F1	24.00	7-No. 3	5250	77.60	61.30	0.770	60.56	39.96	20.60
2.3	F1	24.00	4-No. 3	5250	73.45	58.02	0.440	57.32	45.63	11.69
3.4	C0	24.00	4-No. 3	5110	55.77	44.06	0.440	43.84	46.10	-2.26
3.5	C0	28.00	8-No. 3	3810	52.02	41.09	0.587	43.98	39.33	4.65
4.1	SMI	24.00	6-No. 4	4090	62.51	49.38	1.200	51.95	38.53	13.42
4.2	F1	24.00	8-No. 3	4090	72.33	57.14	0.880	60.09	39.19	20.90
4.4	C1	24.00	4-No. 3	4090	58.85	46.49	0.440	48.91	38.17	10.74
5.1	SH0	24.00	7-No. 3	4190	64.62	51.05	0.770	53.35	38.41	14.94
5.2	F1	24.00	7-No. 3	4190	65.41	51.67	0.770	54.00	39.58	14.43
5.3	F1	24.00	7-No. 3	4190	67.88	53.63	0.770	56.05	38.81	17.24
5.4	SH0	24.00	7-No. 3	4190	58.87	46.51	0.770	48.61	38.34	10.27
5.5	C0	24.00	4-No. 3	4190	46.43	36.68	0.440	38.33	39.99	-1.66
5.6	F1	22.00	5-No. 4	4190	66.34	52.41	1.000	54.78	37.12	17.66
6.1	SH0	24.00	8-No. 4	4220	63.26	49.98	1.067	52.14	33.85	18.29
6.2	F1	24.00	8-No. 4	4220	74.88	59.16	1.067	61.72	34.26	27.46
6.3	F1	16.00	2-No. 3	4220	46.09	36.41	0.220	37.99	31.24	6.75
6.4	C0	16.00	2-No. 3	4220	36.68	28.97	0.220	30.23	31.42	-1.19
7.1	F1	16.00	2-No. 3	4160	46.72	36.91	0.220	38.65	34.69	3.95
7.2	C1	18.00	5-No. 4	4160	55.82	44.10	1.000	46.17	31.95	14.22
7.5	F1	24.00	8-No. 4	4160	73.17	57.80	1.067	60.52	34.12	26.40
7.6	C1	16.00	2-No. 3	4160	44.34	35.03	0.220	36.68	35.10	1.58
8.1	N0	24.00	8-No. 4	3830	69.67	55.04	1.067	58.83	34.15	24.68
8.2	N3	24.00	8-No. 4	3830	79.32	62.66	1.067	66.98	34.11	32.87
8.4	N3	16.00	2-No. 3	3830	48.90	38.63	0.220	41.29	34.93	6.37
9.1	N3	24.00	2-No. 3	4230	63.40	50.09	0.220	52.22	45.47	6.75
9.2	F1	18.00	6-No. 3	4230	69.06	54.56	0.660	56.89	33.01	23.87
9.3	N0	24.00	2-No. 3	4230	55.25	43.65	0.220	45.51	44.18	1.33
9.4	F1	24.00	2-No. 3	4230	65.00	51.35	0.220	53.54	45.03	8.51
10.3	N0	26.00	2-No. 3	4250	58.85	46.49	0.220	48.42	46.41	2.01
10.4	N0	20.00	5-No. 4	4250	61.98	48.96	1.000	50.99	40.09	10.90
11.1	F1	18.00	6-No. 4	4380	66.94	52.88	0.800	54.66	29.74	24.92
11.2	N0	18.00	4-No. 4	4380	61.94	48.93	0.800	50.58	37.31	13.26
11.3	N3	18.00	4-No. 4	4380	62.44	49.33	0.800	50.99	37.74	13.25
11.4	F1	24.00	2-No. 3	4380	62.49	49.37	0.220	51.03	45.32	5.70
14.1	C1	36.00	3-No. 3	4200	59.96	47.37	0.220	49.48	42.78	6.70
14.2	C1	21.00	7-No. 4	4200	62.83	49.64	0.933	51.85	31.85	19.99

Note: Refer to Table 4.4b for footnote.

Table 4.4b: Tabulated Values of Increase in Modified Bond Force due to Stirrups for Splice Tests by Hester et al. (1991, 1993)**

Specimen Label	l_s (in.)	Stirrups	f'_c (psi)	f_s (ksi)	$A_b f_s$ (kips)	NA_{tr}/n (in.^{2})	T_b (kips)	T_c (kips)	T_s* (kips)
1-8N3-16-2-U	16.00	2-No. 3	5990	56.00	44.24	0.147	42.29	33.79	8.50
2-8C3-16-2-U	16.00	2-No. 3	6200	43.99	34.75	0.147	32.93	33.51	-0.58
3-8S3-16-2-U	16.00	2-No. 3	6020	46.47	36.71	0.147	35.05	33.92	1.13
4-8S3-16-2-U	16.00	2-No. 3	6450	47.06	37.17	0.147	34.88	33.85	1.03
4-8S3-16-3-U	16.00	3-No. 3	6450	50.04	39.53	0.220	37.09	33.95	3.14
5-8C3-16-2-U	16.00	2-No. 3	5490	46.51	36.75	0.147	35.90	33.89	2.01
5-8C3-16-3-U	16.00	3-No. 3	5490	43.31	34.22	0.220	33.43	33.89	-0.46
6-8C3-22 3/4-3-U	22.75	3-No. 3	5850	56.45	44.60	0.220	42.88	42.14	0.74
6-8C3-22 3/4-4-U	22.75	4-No. 3	5850	55.67	43.98	0.293	42.29	42.12	0.16
7-8C3-16-3-U	16.00	3-No. 3	5240	51.49	40.68	0.330	40.20	35.51	4.69

* $T_s = T_b - T_c$

** All spliced bars were conventional bars.

Table 5.1: Comparison of Results of Dummy Variables Analysis of Best-fit Equations for Test Bond Strength ($A_b f_s / f'^{p}_c$) versus Prediction Bond Strength (right side of Eq. 5.2) based on f'_c, for p = 1/4 and p = 1/2

f'_c Range (psi)	No. of Tests	Intercept	
		p = 1/4	p = 1/2
< 3000	6	-248.8	86.8
3000 - 4000	35	15.1	20.3
4000 - 5000	42	12.1	-15.2
5000 - 6000	25	-6.6	-48.3
> 6000	7	29.4	-46.1
	Slope	8.858	1.134
	r^2	0.9789	0.9771
	Wt. Std	58.6	34.4
	Min	663	81
	Max	18508	2589
	Range	17844	2508
	Wt. Std/Range	0.0033	0.0137

Wt. Std = weighted standard deviation for the intercepts

Min, Max = minimum and maximum, respectively, of the predicted bond strength

Range = Max - Min

Table 5.2: Comparisons of Test/Prediction Ratios obtained using Eq. 5.3 with C_{si} and C_{si} + 0.25 in. for p =1/4 and p = 1/2 for 34 of the 115 Bottom-Cast Bars Not Confined by Stirrups that C_{si} controls

Test No.	Test/Prediction			
	C_{si}, p = 1/4	C_{si}, p = 1/2	C_{si} + 0.25 in., p = 1/4	C_{si} + 0.25 in., p = 1/2
3c	1.021	1.083	1.050	1.122
SIV53	1.042	1.041	0.895	0.875
D3	1.141	1.221	1.061	1.118
D6	0.977	1.035	0.911	0.952
D8	1.046	1.094	0.975	1.005
6-12-4/2/2-6/6	1.084	1.104	1.095	1.118
D4	1.239	1.277	1.118	1.132
2a	1.180	1.197	1.084	1.088
2b	1.194	1.223	1.097	1.112
1-8N3-16-0-U	1.095	1.029	1.047	0.976
1.3	0.865	0.814	1.008	0.986
1.1	1.055	1.040	0.873	0.822
2-8C3-16-0U	1.004	0.935	0.959	0.887
3-8S3-16-0-U	1.023	0.960	0.978	0.911
4-8S3-16-0-U	0.911	0.840	0.871	0.797
5-8C3-16-0-U	0.891	0.855	0.852	0.812
8-18-4/3/2-6/6	1.083	1.052	1.097	1.067
8-18-4/3/2.5-4/6	1.071	1.171	1.022	1.111
6-8C3-22-0-U	0.940	0.863	0.884	0.806
6.5	0.908	0.890	0.900	0.881
8-24-4/2/2-6/6	0.904	0.953	0.911	0.962
8.1	1.054	1.056	1.049	1.051
10.2	0.990	0.964	0.981	0.954
9-53-B-N	1.186	1.154	1.146	1.108
5a	1.113	1.122	1.037	1.036
5b	1.159	1.172	1.069	1.072
N-N-80-B	0.985	1.045	0.977	1.035
4-11C0-24-0-U	0.821	0.774	0.836	0.791
4-11S0-24-0-U	0.873	0.823	0.889	0.841
11-30-4/2/2-6/6	0.873	0.967	0.886	0.983
11-30-4/2/2.7/4/6	1.188	1.180	0.995	1.062
11-30-4/2/4-6/6	0.981	1.045	1.205	1.199
14-6--4/2/4-5/5	1.003	1.051	0.830	0.894
14-60-4/2/2-5/5	0.824	0.887	1.012	1.060
Min	0.821	0.774	0.830	0.791
Max	1.239	1.277	1.205	1.199
Mean	1.021	1.027	0.988	0.989
Std	0.1147	0.1327	0.0977	0.1163
COV	0.1123	0.1292	0.0989	0.1176

Table 5.3: Results of Dummy Variables Analysis for $A_b f_s/f'^{p}_c$ versus $l_d(C_m + 0.5d_b)$ based on Bar Size for 115 Bottom-Cast Bars Not Confined by Stirrups

Bar Size	No. of Tests	Intercepts, K_2		nK_2/A_b	
	n	p = 1/4	p = 1/2	p = 1/4	p = 1/2
No. 3	2	412	44	7491	800
No. 4	16	517	52	41360	4160
No. 5	2	1229	119	7929	768
No. 6	33	995	98	74625	7350
No. 8	35	1648	146	73013	6468
No. 9	3	3068	309	9204	927
No. 11	22	4264	461	60133	6501
No. 14	2	4102	486	3646	432
			Wt. Mean	2412	238
			Slope, K_1	66.3	9.31
			r^2	0.9782	0.9732

Table 5.4: Results of Dummy Variables Analysis of Test/Prediction Ratio versus C_M/C_m, using Eqs. 5.4a and 5.4b based on Bar Size for 115 Bottom-Cast Bars Not Confined by Stirrups

Bar Size	No. of Tests	Intercepts			
	n	K_3	K_4	nK_3	nK_4
No. 3	2	1.077	1.060	2.154	2.120
No. 4	16	0.912	0.906	14.592	14.496
No. 5	2	1.114	1.032	2.228	2.064
No. 6	33	0.836	0.827	27.588	27.291
No. 8	35	0.847	0.817	29.645	28.595
No. 9	3	0.981	0.956	2.943	2.868
No. 11	22	0.862	0.859	18.964	18.898
No. 14	2	0.839	0.885	1.678	1.770
			Wt. Mean	0.868	0.853
			Slope	0.077	0.087
			r^2	0.4611	0.4494

Table 5.5a: Data and Test/Prediction Ratios for Bars Not Confined by Stirrups from Current Tests

Test No.	l_d	d_b	A_b	C_b	C_{so}	C_{si}	C_s	f'_c	f_y	f_s*	$T_d/f'^{1/4}_c$ Test	$T_d/f'^{1/2}_c$ Test	$T_d/f'^{1/4}_c$ Eq. 5.7a+	$T_d/f'^{1/2}_c$ Eq. 5.7b*	Test / Eq. 5.7a	Test / Eq. 5.7b
	(in.)	(in.)	(in.^{2})	(in.)	(in.)	(in.)	(in.)	(psi)	(ksi)	(ksi)	(in.^{2})	(in.^{2})	(in.^{2})	(in.^{2})		
1.1	16.00	1.000	0.790	2.938	2.969	2.938	2.969	5020	60.00	51.63	4846	576	5271	659	0.919	0.874
1.3	16.00	1.000	0.790	1.938	2.032	1.406	1.656	5020	60.00	45.01	4224	502	4030	485	1.048	1.035
2.4	24.00	1.000	0.790	1.313	2.000	1.914	2.000	5250	75.00	54.08	5019	590	4737	584	1.059	1.010
2.5	24.00	1.000	0.790	1.813	2.063	1.856	2.063	5250	75.00	58.67	5445	640	5358	671	1.016	0.954
4.5	24.00	1.000	0.790	1.844	2.063	1.936	2.063	4090	60.00	51.06	5044	631	5397	676	0.935	0.933
6.5	24.00	1.000	0.790	1.969	2.000	1.906	2.000	4220	75.00	53.59	5253	652	5541	696	0.948	0.936
8.1	24.00	1.000	0.790	2.000	2.000	1.953	2.000	3830	79.00	61.47	6173	785	5581	702	1.106	1.118
10.2	26.00	1.000	0.790	1.933	2.063	1.875	2.063	4250	81.00	61.17	5985	741	5818	735	1.029	1.008
														Min	0.919	0.874
														Max	1.106	1.118
														Mean	1.008	0.984
														Std	0.067	0.075
														COV	0.066	0.077

Table 5.5b: Data and Test/Prediction Ratios for Bars Not Confined by Stirrups from Choi et al. (1990, 1991)

Test No.	l_d	d_b	A_b	C_b	C_{so}	C_{si}	C_s	f'_c	f_y	f_s*	$T_d/f'^{1/4}_c$ Test	$T_d/f'^{1/2}_c$ Test	$T_d/f'^{1/4}_c$ Eq. 5.7a+	$T_d/f'^{1/2}_c$ Eq. 5.7b*	Test / Eq. 5.7a	Test / Eq. 5.7b
	(in.)	(in.)	(in.^{2})	(in.)	(in.)	(in.)	(in.)	(psi)	(ksi)	(ksi)	(in.^{2})	(in.^{2})	(in.^{2})	(in.^{2})		
1-5N0-12-0-U	12.00	0.625	0.310	1.000	2.000	2.000	2.000	5360	63.80	61.51	2229	260	1838	226	1.212	1.152
1-5N0-12-0-U	12.00	0.625	0.310	1.000	2.000	2.000	2.000	5360	63.80	63.99	2318	271	1838	226	1.261	1.199
2-6C0-12-0-U	12.00	0.750	0.440	1.000	2.000	2.000	2.000	6010	69.00	51.40	2568	292	2210	265	1.162	1.103
2-6S0-12-0-U	12.00	0.750	0.440	1.000	2.000	2.000	2.000	6010	70.90	45.75	2286	260	2210	265	1.034	0.982
3-8N0-16-0-U	16.00	1.000	0.790	1.500	2.000	2.000	2.000	5980	63.80	43.02	3865	440	3922	470	0.986	0.936
3-8S0-16-0-U	16.00	1.000	0.790	1.500	2.000	2.000	2.000	5980	67.00	42.82	3847	437	3922	470	0.981	0.932
4-11C0-24-0-U	24.00	1.410	1.560	2.000	2.000	2.000	2.000	5850	63.10	37.82	6746	771	7647	914	0.882	0.844
4-11S0-24-0-U	24.00	1.410	1.560	2.000	2.000	2.000	2.000	5850	64.60	40.22	7174	820	7647	914	0.938	0.897
														Min	0.882	0.844
														Max	1.261	1.199
														Mean	1.057	1.005
														Std	0.138	0.129
														COV	0.130	0.129

Table 5.5c: Data and Test/Prediction Ratios for Bars Not Confined by Stirrups from Hester et al. (1991, 1993)

Test No.	l_d	d_b	A_b	C_b	C_{so}	C_{si}	C_s	f'_c	f_y	f_s*	$T_d/f'^{1/4}_c$ Test	$T_d/f'^{1/2}_c$ Test	$T_d/f'^{1/4}_c$ Eq. 5.7a+	$T_d/f'^{1/2}_c$ Eq. 5.7b*	Test / Eq. 5.7a	Test / Eq. 5.7b
	(in.)	(in.)	(in.^{2})	(in.)	(in.)	(in.)	(in.)	(psi)	(ksi)	(ksi)	(in.^{2})	(in.^{2})	(in.^{2})	(in.^{2})		
1-8N3-16-0-U	16.00	1.000	0.790	2.000	2.000	1.500	1.750	5990	63.80	50.03	4493	511	4117	497	1.091	1.027
2-8C3-16-0U	16.00	1.000	0.790	1.840	2.000	1.500	1.750	6200	69.00	46.24	4117	464	4086	493	1.008	0.941
3-8S3-16-0-U	16.00	1.000	0.790	2.040	2.000	1.500	1.750	6020	71.10	46.81	4198	477	4124	498	1.018	0.957
4-8S3-16-0-U	16.00	1.000	0.790	2.100	2.000	1.500	1.750	6450	71.10	42.40	3737	417	4136	500	0.904	0.835
5-8C3-16-0-U	16.00	1.000	0.790	2.050	2.000	1.500	1.750	5490	69.00	39.82	3655	425	4126	498	0.886	0.852
7-8C3-16-0-U	16.00	1.000	0.790	2.120	2.000	4.000	2.000	5240	69.00	45.37	4212	495	4342	529	0.970	0.936
6-8C3-22-0-U	22.75	1.000	0.790	2.150	2.000	1.500	1.750	5850	69.00	51.85	4683	536	5120	638	0.915	0.840
														Min	0.886	0.835
														Max	1.091	1.027
														Mean	0.970	0.913
														Std	0.074	0.073
														COV	0.076	0.079

Note: Refer to last page of Table 5.5 for footnote.

Table 5.5d: Data and Test/Prediction Ratios for Bars Not Confined by Stirrups from Chinn et al. (1955)

Test No.	l_d	d_b	A_b	C_b	C_{so}	C_{si}	C_s	f'_c	f_y	f_s*	$T_\sigma/f'^{1/4}_c$ Test	$T_\sigma/f'^{1/2}_c$ Test	$T_\sigma/f'^{1/4}_c$ Eq. 5.7a*	$T_\sigma/f'^{1/2}_c$ Eq. 5.7b*	Test Eq. 5.7a	Test Eq. 5.7b
	(in.)	(in.)	(in.^{2})	(in.)	(in.)	(in.)	(in.)	(psi)	(ksi)	(ksi)	(in.^{2})	(in.^{2})	(in.^{2})	(in.^{2})		
D31	5.50	0.375	0.110	0.830	1.470		1.470	4700	79.00	60.35	805	97	643	79	1.253	1.234
D36	5.50	0.375	0.110	0.560	1.470		1.470	4410	79.00	48.95	663	81	579	70	1.146	1.169
D10	7.00	0.750	0.440	1.480	1.060		1.060	4370	57.00	26.27	1421	175	1689	192	0.841	0.910
D20	7.00	0.750	0.440	1.420	1.125		1.125	4230	57.00	26.95	1470	182	1700	194	0.865	0.941
D22	7.00	0.750	0.440	0.800	1.095		1.095	4480	57.00	23.89	1285	157	1567	175	0.820	0.897
D13	11.00	0.750	0.440	1.440	2.905		2.905	4820	57.00	48.93	2584	310	2450	298	1.055	1.040
D14	11.00	0.750	0.440	0.830	1.095		1.095	4820	57.00	32.63	1723	207	1886	220	0.913	0.941
D15	11.00	0.750	0.440	0.620	2.875		2.875	4290	57.00	42.24	2296	284	2198	258	1.045	1.098
D21	11.00	0.750	0.440	1.470	2.905		2.905	4480	57.00	43.35	2331	285	2464	300	0.946	0.949
D29	11.00	0.750	0.440	1.390	1.095		1.095	7480	57.00	44.60	2110	227	2067	245	1.021	0.926
D3	11.00	0.750	0.440	1.500	1.500	0.500	0.750	4350	57.00	36.86	1997	246	1929	225	1.035	1.094
D32	11.00	0.750	0.440	1.470	2.875		2.875	4700	57.00	46.05	2447	296	2461	300	0.994	0.986
D38	11.00	0.750	0.440	1.520	1.560		1.560	3160	57.00	28.16	1653	220	2321	281	0.712	0.785
D39	11.00	0.750	0.440	1.560	1.095		1.095	3160	57.00	27.62	1621	216	2092	249	0.775	0.870
D5	11.00	0.750	0.440	1.500	2.000		2.000	4180	57.00	44.34	2426	302	2366	287	1.026	1.052
D6	11.00	0.750	0.440	1.160	1.500	0.625	0.875	4340	57.00	33.17	1798	222	1919	224	0.937	0.987
D7	11.00	0.750	0.440	1.270	1.060		1.060	4450	57.00	33.85	1824	223	2030	240	0.898	0.930
D8	11.00	0.750	0.440	1.480	1.500	0.625	0.875	4570	57.00	35.95	1924	234	1975	232	0.974	1.009
D9	11.00	0.750	0.440	1.440	1.060		1.060	4380	57.00	34.98	1892	233	2056	244	0.920	0.955
D34	12.50	0.750	0.440	1.490	1.060		1.060	3800	57.00	36.86	2066	263	2204	264	0.937	0.996
D12	16.00	0.750	0.440	1.620	1.125		1.125	4530	57.00	45.70	2451	299	2606	321	0.940	0.932
D17	16.00	0.750	0.440	0.800	1.095		1.095	3580	57.00	39.74	2261	292	2254	271	1.003	1.077
D19	16.00	0.750	0.440	1.700	2.905		2.905	4230	57.00	59.93	3270	405	3275	415	0.998	0.978
D23	16.00	0.750	0.440	0.780	1.060		1.060	4450	57.00	39.23	2113	259	2231	268	0.947	0.965
D24	16.00	0.750	0.440	0.810	2.875		2.875	4450	57.00	43.18	2326	285	2657	326	0.875	0.873
D30	16.00	0.750	0.440	1.560	1.095		1.095	7480	57.00	52.88	2502	269	2571	316	0.973	0.852
D4	16.00	0.750	0.440	1.500	1.500	0.500	0.750	4470	57.00	46.84	2521	308	2312	279	1.090	1.105
D40	16.00	0.750	0.440	0.750	2.940		2.940	5280	57.00	50.55	2609	306	2649	325	0.985	0.943
D25	24.00	0.750	0.440	1.530	1.060		1.060	5100	57.00	58.25	3033	359	3288	416	0.922	0.862
D26	24.00	0.750	0.440	0.750	1.095		1.095	5100	57.00	55.87	2909	344	2806	349	1.037	0.987
D35	24.00	0.750	0.440	1.450	1.060		1.060	3800	57.00	54.99	3082	393	3269	414	0.943	0.949
D33	20.25	1.410	1.560	1.550	1.990		1.990	4830	57.00	28.20	5277	633	6583	765	0.802	0.828
														Min	0.712	0.785
														Max	1.253	1.234
														Mean	0.957	0.972
														Std	0.108	0.099
														COV	0.113	0.102

Table 5.5e: Data and Test/Prediction Ratios for Bars Not Confined by Stirrups from Chamberlin (1956)

Test No.	l_d	d_b	A_b	C_b	C_{so}	C_{si}	C_s	f'_c	f_y	f_s*	$T_\sigma/f'^{1/4}_c$ Test	$T_\sigma/f'^{1/2}_c$ Test	$T_\sigma/f'^{1/4}_c$ Eq. 5.7a*	$T_\sigma/f'^{1/2}_c$ Eq. 5.7b*	Test Eq. 5.7a	Test Eq. 5.7b
	(in.)	(in.)	(in.^{2})	(in.)	(in.)	(in.)	(in.)	(psi)	(ksi)	(ksi)	(in.^{2})	(in.^{2})	(in.^{2})	(in.^{2})		
SII15	6.00	0.500	0.200	1.000	0.500		0.500	4470	-	34.52	844	103	800	91	1.055	1.130
SII16	6.00	0.500	0.200	1.000	0.750		0.750	4470	-	38.11	932	114	857	100	1.088	1.142
SIII31	6.00	0.500	0.200	1.000	0.500		0.500	5870	-	39.66	906	104	800	91	1.132	1.133
SIII32	6.00	0.500	0.200	1.000	0.750		0.750	5870	-	46.37	1060	121	857	100	1.237	1.213
SIII33	6.00	0.500	0.200	1.000	1.000		1.000	5870	-	48.45	1107	126	929	110	1.192	1.150
SII11	10.67	0.500	0.200	1.000	0.500		0.500	3680	-	41.17	1057	136	1039	125	1.018	1.086
SIII27	10.67	0.500	0.200	1.000	0.500		0.500	5870	-	46.43	1061	121	1039	125	1.021	0.969
SIII28	10.67	0.500	0.200	1.000	0.750		0.750	5870	-	49.32	1127	129	1159	142	0.972	0.906
SIII29	10.67	0.500	0.200	1.000	1.000		1.000	5870	-	49.32	1127	129	1296	161	0.870	0.798
SIV53	12.00	0.500	0.200	1.000	2.000	0.500	0.750	4540	-	46.95	1144	139	1245	154	0.919	0.904
SII23	16.00	0.750	0.440	1.000	0.750		0.750	4470	-	41.89	2254	276	2196	263	1.027	1.048
														Min	0.870	0.798
														Max	1.237	1.213
														Mean	1.048	1.043
														Std	0.110	0.131
														COV	0.105	0.125

Note: Refer to last page of Table 5.5 for footnote.

Table 5.5f: Data and Test/Prediction Ratios for Bars Not Confined by Stirrups from Chamberlin (1958)

Test No.	l_d	d_b	A_b	C_b	C_{so}	C_{si}	C_s	f'_c	f_y	f_s^*	$T_d/f'^{1/4}_c$ Test	$T_d/f'^{1/2}_c$ Test	$T_d/f'^{1/4}_c$ Eq. 5.7a*	$T_d/f'^{1/2}_c$ Eq. 5.7b*	Test Eq. 5.7a	Test Eq. 5.7b
	(in.)	(in.)	(in.^{2})	(in.)	(in.)	(in.)	(in.)	(psi)	(ksi)	(ksi)	(in.^{2})	(in.^{2})	(in.^{2})	(in.^{2})		
3a	6.00	0.500	0.200	1.000	0.500	1.500	0.500	4450	50.00	32.78	803	98	800	91	1.003	1.076
3b	6.00	0.500	0.200	1.000	0.500	1.000	0.500	4450	50.00	33.00	808	99	800	91	1.010	1.083
3c	6.00	0.500	0.200	1.000	0.500	0.500	0.500	4450	50.00	33.48	820	100	800	91	1.025	1.099
4a	6.00	0.500	0.200	1.000	2.500		2.500	4370	50.00	42.64	1049	129	1043	125	1.006	1.029
4b	6.00	0.500	0.200	1.000	2.250		2.250	4370	50.00	43.89	1080	133	1024	123	1.055	1.082
4c	6.00	0.500	0.200	1.000	2.000		2.000	4370	50.00	43.32	1066	131	1005	120	1.061	1.090
														Min	1.003	1.029
														Max	1.061	1.099
														Mean	1.027	1.076
														Std	0.025	0.024
														COV	0.025	0.023

Table 5.5g: Data and Test/Prediction Ratios for Bars Not Confined by Stirrups from Ferguson and Breen (1965)

Test No.	l_d	d_b	A_b	C_b	C_{so}	C_{si}	C_s	f'_c	f_y	f_s^*	$T_d/f'^{1/4}_c$ Test	$T_d/f'^{1/2}_c$ Test	$T_d/f'^{1/4}_c$ Eq. 5.7a*	$T_d/f'^{1/2}_c$ Eq. 5.7b*	Test Eq. 5.7a	Test Eq. 5.7b
	(in.)	(in.)	(in.^{2})	(in.)	(in.)	(in.)	(in.)	(psi)	(ksi)	(ksi)	(in.^{2})	(in.^{2})	(in.^{2})	(in.^{2})		
8R18a	18.00	1.000	0.790	1.750	3.250	3.265	3.250	3470	99.00	41.32	4253	554	4659	572	0.913	0.968
8R24a	24.00	1.000	0.790	1.670	3.250	3.310	3.250	3530	99.00	58.88	6035	783	5477	688	1.102	1.138
8F30a	30.00	1.000	0.790	1.530	3.250	3.295	3.250	3030	74.00	52.78	5620	757	6158	784	0.913	0.966
8F36a	36.00	1.000	0.790	1.410	3.250	3.330	3.250	4650	63.50	66.34	6346	769	6789	873	0.935	0.880
8F36b	36.00	1.000	0.790	1.400	3.250	3.220	3.250	3770	74.00	61.30	6180	789	6773	871	0.912	0.905
8F36k	36.00	1.000	0.790	1.380	1.420	1.425	1.420	3460	74.00	54.65	5630	734	6079	771	0.926	0.951
8F39a	39.00	1.000	0.790	1.530	3.250	3.280	3.250	3650	63.50	72.90	7410	953	7415	962	0.999	0.991
8F42a	42.00	1.000	0.790	1.500	3.250	3.345	3.250	2660	63.50	65.93	7253	1010	7772	1012	0.933	0.998
8F42b	42.00	1.000	0.790	1.450	3.250	3.330	3.250	3830	63.50	73.54	7385	939	7669	998	0.963	0.941
8R42a	42.00	1.000	0.790	1.560	3.250	3.345	3.250	3310	99.00	71.01	7396	975	7896	1029	0.937	0.947
8R48a	48.00	1.000	0.790	1.480	3.250	3.265	3.250	3040	99.00	72.88	7754	1044	8553	1123	0.907	0.930
8R64a	64.00	1.000	0.790	1.520	3.250	3.295	3.250	3550	99.00	89.71	9181	1189	10874	1450	0.844	0.820
8R80a	80.00	1.000	0.790	1.500	3.250	3.265	3.250	3740	99.00	96.41	9740	1245	13018	1753	0.748	0.710
11R24a	33.00	1.410	0.790	1.670	4.590	4.635	4.590	3720	93.00	51.81	10349	1325	9712	1201	1.066	1.104
11R30a	41.25	1.410	0.790	1.310	4.590	4.635	4.590	4030	93.00	58.50	11454	1438	10599	1325	1.081	1.085
11F36a	49.50	1.410	0.790	1.500	4.590	4.635	4.590	4570	73.00	64.16	12173	1481	12195	1553	0.998	0.953
11F36b	49.50	1.410	0.790	1.470	4.590	4.605	4.590	3350	65.00	59.20	12139	1596	12139	1545	1.000	1.032
11F42a	57.75	1.410	0.790	1.480	4.590	4.590	4.590	3530	65.00	63.61	12874	1670	13489	1738	0.954	0.961
11F48a	66.00	1.410	0.790	1.530	4.590	4.620	4.590	3140	73.00	74.56	15537	2076	14957	1947	1.039	1.066
11F48b	66.00	1.410	0.790	1.580	4.590	4.665	4.590	3330	65.00	72.24	14836	1953	15098	1966	0.983	0.993
11R48a	66.00	1.410	0.790	1.500	4.590	4.670	4.590	5620	93.00	82.22	14813	1711	14875	1935	0.996	0.884
11R48b	66.00	1.410	0.790	2.060	4.590	4.700	4.590	3100	93.00	71.43	14934	2001	16570	2172	0.901	0.922
11F60a	82.50	1.410	0.790	1.590	4.590	4.575	4.590	2610	73.00	84.80	18508	2589	17881	2362	1.035	1.096
11F60b	82.50	1.410	0.790	1.500	4.590	4.590	4.590	4090	65.00	78.02	15219	1903	17554	2316	0.867	0.822
11R60a	82.50	1.410	0.790	1.410	4.590	4.590	4.590	2690	93.00	74.61	16161	2244	17240	2273	0.937	0.987
11R60b	82.50	1.410	0.790	1.750	4.590	4.575	4.590	3460	93.00	87.80	17858	2328	18488	2446	0.966	0.952
														Min	0.748	0.710
														Max	1.102	1.138
														Mean	0.956	0.962
														Std	0.077	0.095
														COV	0.080	0.099

Note: Refer to last page of Table 5.5 for footnote.

Table 5.5h: Data and Test/Prediction Ratios for Bars Not Confined by Stirrups from Thompson et al. (1975)

Test No.	l_d	d_b	A_b	C_b	C_{so}	C_{si}	C_s	f'_c	f_y	f_s*	$T_c/f'^{1/4}_c$ Test	$T_c/f'^{1/2}_c$ Test	$T_c/f'^{1/4}_c$ Eq. 5.7a+	$T_c/f'^{1/2}_c$ Eq. 5.7b#	Test Eq. 5.7a	Test Eq. 5.7b
	(in.)	(in.)	(in.^{2})	(in.)	(in.)	(in.)	(in.)	(psi)	(ksi)	(ksi)	(in.^{2})	(in.^{2})	(in.^{2})	(in.^{2})		
6-12-4/2/2-6/6	12.00	0.750	0.440	2.000	2.000	2.000	2.000	3731	61.70	57.40	3232	414	2799	348	1.155	1.190
8-18-4/3/2-6/6	18.00	1.000	0.790	3.000	2.000	2.000	2.000	4710	59.30	56.26	5365	648	4826	596	1.112	1.086
8-18-4/3/2.5-4/6	18.00	1.000	0.790	3.000	2.500	2.000	2.250	2920	59.30	49.33	5301	721	5054	628	1.049	1.148
8-24-4/2/2-6/6	24.00	1.000	0.790	2.000	2.000	2.000	2.000	3105	59.30	50.64	5359	718	5581	702	0.960	1.023
11-25-6/2/3-5/5	25.00	1.410	1.560	2.000	3.000	3.000	3.000	3920	66.30	44.19	8713	1101	8138	982	1.071	1.121
11-30-4/2/2-6/6	30.00	1.410	1.560	2.000	2.000	2.000	2.000	2865	60.50	37.99	8100	1107	8669	1057	0.934	1.047
11-30-4/2/4-6/6	30.00	1.410	1.560	2.000	4.000	2.000	2.250	3350	63.40	44.39	9102	1196	8758	1070	1.039	1.119
11-30-4/2/2.7/4/6	30.00	1.410	1.560	2.000	2.700	2.000	2.250	4420	63.30	57.59	11019	1351	8758	1070	1.258	1.263
11-45-4/1/2-6/6	45.00	1.410	1.560	1.000	2.000	2.000	2.000	3520	60.50	45.28	9171	1191	9078	1113	1.010	1.070
14-60-4/2/2-5/5	60.00	1.693	2.250	2.000	2.000	2.000	2.000	2865	57.70	45.23	13909	1901	15890	1998	0.875	0.952
14-6--4/2/4-5/5	60.00	1.693	2.250	2.000	4.000	2.000	2.250	3200	57.70	56.64	16944	2253	16053	2021	1.056	1.115
														Min	0.875	0.952
														Max	1.258	1.263
														Mean	1.047	1.103
														Std	0.106	0.084
														COV	0.101	0.076

Table 5.5i: Data and Test/Prediction Ratios for Bars Not Confined by Stirrups from Zekany et al. (1981)

Test No.	l_d	d_b	A_b	C_b	C_{so}	C_{si}	C_s	f'_c	f_y	f_s*	$T_c/f'^{1/4}_c$ Test	$T_c/f'^{1/2}_c$ Test	$T_c/f'^{1/4}_c$ Eq. 5.7a+	$T_c/f'^{1/2}_c$ Eq. 5.7b#	Test Eq. 5.7a	Test Eq. 5.7b
	(in.)	(in.)	(in.^{2})	(in.)	(in.)	(in.)	(in.)	(psi)	(ksi)	(ksi)	(in.^{2})	(in.^{2})	(in.^{2})	(in.^{2})		
9-53-B-N	16.00	1.128	1.000	2.000	2.000	1.423	1.673	5650	62.80	47.56	5485	633	4607	545	1.191	1.162
N-N-80-B	22.00	1.410	1.560	2.000	2.000	1.849	2.000	3825	60.10	37.96	7531	958	7306	867	1.031	1.105
														Min	1.031	1.105
														Max	1.191	1.162
														Mean	1.111	1.133
														Std	0.113	0.040
														COV	0.102	0.036

Table 5.5j: Data and Test/Prediction Ratios for Bars Not Confined by Stirrups from Rezansoff et al. (1993)

Test No.	l_d	d_b	A_b	C_b	C_{so}	C_{si}	C_s	f'_c	f_y	f_s*	$T_c/f'^{1/4}_c$ Test	$T_c/f'^{1/2}_c$ Test	$T_c/f'^{1/4}_c$ Eq. 5.7a+	$T_c/f'^{1/2}_c$ Eq. 5.7b#	Test Eq. 5.7a	Test Eq. 5.7b
	(in.)	(in.)	(in.^{2})	(in.)	(in.)	(in.)	(in.)	(psi)	(ksi)	(ksi)	(in.^{2})	(in.^{2})	(in.^{2})	(in.^{2})		
2a	29.53	0.992	0.775	2.008	1.827	0.994	1.244	3958	64.52	58.56	5721	721	5256	658	1.089	1.096
2b	29.53	0.992	0.775	2.008	1.827	0.994	1.244	3799	64.52	58.63	5787	737	5256	658	1.101	1.120
5a	35.43	1.177	1.085	2.008	1.819	1.183	1.433	4031	68.87	56.08	7636	958	7216	901	1.058	1.063
5b	44.29	1.177	1.085	2.008	1.819	1.183	1.433	3726	68.87	65.83	9142	1170	8382	1065	1.091	1.099
														Min	1.058	1.063
														Max	1.101	1.120
														Mean	1.085	1.094
														Std	0.018	0.023
														COV	0.017	0.021

* Bar stress is calculated based on the working stress of the bar if the stress does not exceed the yield stress, otherwise, ultimate strength method is used to calculate the bar stress.

\- Data is not available

\+ Eq. 5.7a $= \dfrac{T_c}{f'^{1/4}_c} = \dfrac{A_b f_s}{f'^{1/4}_c} = \left[6.3 l_d (C_m + 0.5 d_b) + 2280 A_b\right]\left(0.082\dfrac{C_M}{C_m} + 0.918\right)$

\# Eq. 5.7b $= \dfrac{T_c}{f'^{1/2}_c} = \dfrac{A_b f_s}{f'^{1/2}_c} = \left[8.8 l_d (C_m + 0.5 d_b) + 220 A_b\right]\left(0.093\dfrac{C_M}{C_m} + 0.907\right)$

Table 5.6: Summary of Comparison of Test/Prediction Ratios for Eqs. 5.7a and 5.7b for Bars Not Confined by Stirrups

Test Series	No. of Tests	Test/Prediction (Eq. 5.7a*)					Test/Prediction (Eq. 5.7b**)				
		Min	Max	Mean	Std	COV	Min	Max	Mean	Std	COV
Current Tests	8	0.919	1.106	1.008	0.067	0.066	0.874	1.118	0.984	0.075	0.077
Choi et al. (1990, 1991)	8	0.882	1.261	1.057	0.138	0.130	0.844	1.199	1.005	0.129	0.129
Hester et al. (1991, 1993)	7	0.886	1.091	0.970	0.074	0.076	0.835	1.027	0.913	0.073	0.079
Chinn et al. (1955)	32	0.712	1.253	0.957	0.108	0.113	0.785	1.234	0.972	0.099	0.102
Chamberlin (1956)	11	0.870	1.237	1.048	0.110	0.105	0.798	1.213	1.043	0.131	0.125
Chamberlin (1958)	6	1.003	1.061	1.027	0.025	0.025	1.029	1.099	1.076	0.024	0.023
Ferguson and Breen (1965)	26	0.748	1.102	0.956	0.077	0.080	0.710	1.138	0.962	0.095	0.099
Thompson et al. (1975)	11	0.875	1.258	1.047	0.106	0.101	0.952	1.263	1.103	0.084	0.076
Zekany et al. (1981)	2	1.031	1.191	1.111	0.113	0.102	1.105	1.162	1.133	0.040	0.036
Rezansoff et al. (1993)	4	1.058	1.101	1.085	0.018	0.017	1.063	1.120	1.094	0.023	0.021
All tests	115	0.712	1.261	0.996	0.103	0.103	0.710	1.263	1.001	0.108	0.108

$$* \quad \text{Eq. 5.7a} = \frac{T_c}{f_c'^{1/4}} = \frac{A_b f_s}{f_c'^{1/4}} = \left[63 l_d (C_m + 0.5 d_b) + 2280 A_b\right]\left(0.082\frac{C_M}{C_m} + 0.918\right)$$

$$** \quad \text{Eq. 5.7b} = \frac{T_c}{f_c'^{1/2}} = \frac{A_b f_s}{f_c'^{1/2}} = \left[8.8 l_d (C_m + 0.5 d_b) + 220 A_b\right]\left(0.093\frac{C_M}{C_m} + 0.907\right)$$

Table 5.7: Comparison of Dummy Variables Analysis Results for Test ($A_b f_s / f'^{p}_c$) versus Prediction (right side of equation) Bond Strengths for p = 1/4 (Eq. 5.7a) and p = 1/2 (Eq. 5.7b) based on f'_c

f'_c (ksi)	No. of Tests	Intercepts	
		Eq. 5.7a	Eq. 5.7b
< 3.0	6	-64.07	138.55
3.0 - 4.0	35	128.94	60.90
4.0 - 5.0	42	96.94	20.02
5.0 - 6.0	25	147.57	1.56
> 6.0	7	138.21	-1.85
	Slope	0.960	0.937
	r^2	0.9808	0.9757

Table 5.8: Comparison of Dummy Variables Analysis Results for Test ($A_b f_s / f'^{p}_c$) versus Prediction (right side of equation) Bond Strengths for p = 1/4 (Eq. 5.7a) and p = 1/2 (Eq. 5.7b) based on Bar Size

Bar Size	No. of Tests	Intercepts	
		Eq. 5.7a	Eq. 5.7b
No. 3	2	204.46	25.53
No. 4	16	159.56	20.56
No. 5	2	678.85	71.43
No. 6	33	234.76	32.62
No. 8	35	540.69	66.22
No. 9	3	1579.14	200.98
No. 11	22	1419.49	210.19
No. 14	2	1572.79	349.78
	Slope	0.867	0.859
	r^2	0.9845	0.9790

Table 5.9: Comparison of Dummy Variables Analyses Results for $T_s/f'_c{}^{1/4}$ versus $NA_{tr}f_{yt}/n$ based on Test Series for 102 Tests with Conventional Bars, using different Limiting f_{yt} values

Test Series	No. of Tests	Intercepts, with the following limits on f_{yt}			
		None	75 ksi	60 ksi	40 ksi
KU Basalt	5	-405	-345	-285	-313
KU Limestone	19	-387	-446	-480	-514
Rezansoff et al. (1993)	11	1196	1135	1092	1070
Rezansoff et al. (1991)	34	877	811	647	579
DeVries et al. (1991)	10	-40	-57	-12	-26
Zekany et al. (1981)	10	315	281	257	246
Thompson et al. (1975)	4	438	364	297	273
Ferguson & Breen (1965)	9	112	58	-83	-307
Slope		28.34	30.36	35.73	54.68
r^2		0.6840	0.6918	0.7034	0.7152

Table 5.10: Dummy Variables Analyses Results for $T_s/f'_c{}^{1/4}$ versus NA_{tr}/n based on Test Series for 102 Tests with Conventional Bars

Test Series	No. of Tests	Intercept
KU Basalt	5	-313
KU Limestone	19	-514
Rezansoff et al. (1993)	11	1070
Rezansoff et al. (1991)	34	579
DeVries et al. (1991)	10	-26
Zekany et al. (1981)	10	246
Thompson et al. (1975)	4	273
Ferguson & Breen (1965)	9	-307
	Wt. Mean Intercept	202
	Slope	2187
	r^2	0.7152

Table 5.11: Linear Regression Analyses Results for $T_s/f'^{1/4}_c$ versus NA_{tr}/n for KU Tests

	Basalt Coarse Aggregate				Limestone Coarse Aggregate			
Bar Type	No. of Tests	Slope	Intercept	R-Squared	No. of Tests	Slope	Intercept	R-Squared
$R_r = 0.140$ (F1) bars	4	3985	−124	0.9667	10	2683	−46	0.8753
$R_r = 0.119$ (N3) bars	4	3168	−170	0.8176				
$R_r = 0.101$ (C1) bars					7	1883	37	0.7317
KU Conventional bars	5	2458	−493	0.7861	19	1786	-339	0.6444

Table 5.12: Estimated Slopes and Intercepts from Linear Regression Analyses Results for $T_s/f'^{1/4}_c$ versus NA_{tr}/n for KU Tests

	Slope				Intercept			
Bar Type	Basalt	Limestone	Average	Estimated**	Basalt	Limestone	Average	Estimated**
$R_r = 0.140$ (F1) bars	3985	2683	3334	3399	−124	−46	−85	533
$R_r = 0.119$ (N3) bars	3168	2283#	2726	2791	−170	−5#	−87	531
$R_r = 0.101$ (C1) bars	2813*	1883	2348	2413	−332*	37	−147	471
KU Conventional bars	2458	1786	2122	2187	−493	−339	−416	202

* Estimated based on the average of N3 and KU Conventional bars.

\# Estimated based on the average of F1 and C1 bars.

** Estimated Slope = (Average Slope for Bar type) + [(Slope for all conventional bars) − (Average Slope for KU conventional bars)]
Estimated Intercept = (Average Intercept for Bar type) + [(Intercept for all conventional bars) − (Average Intercept for KU conventional bars)]

Table 5.13a: Data and Test/Prediction Ratios for Bars Confined by Stirrups from Current Tests, using concrete with Basalt Coarse Aggregate

Tests No.	n_b	l_d	d_b	C_{so}	C_{si}	C_b	d_s	N	N_l	A_b	A_v	f'_c	f_y	f_{yt}	f_s^*	NA_{tr}/n	Test $T_b/f'^{1/4}_c$	Pred. $T_b/f'^{1/4}_c$	Test/Pred.
		(in.)	(in.)	(in.)	(in.)	(in.)	(in.)			(in.^{2})	(in.^{2})	(psi)	(ksi)	(ksi)	(ksi)	(in.^{2})	(in.^{2})	(in.^{2})	
8.1	3	24.0	1.000	2.032	0.453	1.953	0.500	8	2	0.790	0.200	3830	79.00	84.70	69.67	1.067	6996	6683	1.047
9.3	2	24.0	1.000	2.094	1.907	1.818	0.375	2	2	0.790	0.110	4230	79.00	64.55	55.25	0.220	5412	6055	0.894
10.3	2	26.0	1.000	2.094	1.844	1.798	0.375	2	2	0.790	0.110	4250	79.00	64.55	58.85	0.220	5758	6324	0.911
10.4	2	20.0	1.000	2.079	1.875	1.916	0.500	5	2	0.790	0.200	4250	79.00	84.70	61.98	1.000	6064	7268	0.834
11.2	2	18.0	1.000	2.094	1.844	1.881	0.500	4	2	0.790	0.200	4380	79.00	84.70	61.94	0.800	6015	6495	0.926
																		Min	0.834
																		Max	1.047
																		Mean	0.922
																		Std	0.078
																		COV	0.084

Table 5.13b: Data and Test/Prediction Ratios for Bars Confined by Stirrups from Current Tests, using concrete with Limestone Coarse Aggregate

Tests No.	n_b	l_d	d_b	C_{so}	C_{si}	C_b	d_s	N	N_l	A_b	A_v	f'_c	f_y	f_{yt}	f_s^*	NA_{tr}/n	Test $T_b/f'^{1/4}_c$	Pred. $T_b/f'^{1/4}_c$	Test/Pred.
		(in.)	(in.)	(in.)	(in.)	(in.)	(in.)			(in.^{2})	(in.^{2})	(psi)	(ksi)	(ksi)	(ksi)	(in.^{2})	(in.^{2})	(in.^{2})	
5.5	2	24.0	1.000	2.063	1.904	1.406	0.375	4	2	0.790	0.110	4190	-	69.92	46.43	0.440	4559	6027	0.756
6.4	2	16.0	1.000	2.094	1.844	1.344	0.375	2	2	0.790	0.110	4220	-	64.55	36.68	0.220	3595	4511	0.797
3.4	2	24.0	1.000	2.110	1.857	2.000	0.375	4	2	0.790	0.110	5110	-	69.92	55.77	0.440	5211	6770	0.770
3.5	3	28.0	1.000	1.001	0.965	1.906	0.375	8	2	0.790	0.110	3810	-	69.92	52.02	0.587	5230	6263	0.835
5.1	3	24.0	1.000	2.016	1.914	1.250	0.375	7	2	0.790	0.110	4190	-	69.92	64.62	0.770	6345	6557	0.968
5.4	2	24.0	1.000	1.985	1.980	1.250	0.375	7	2	0.790	0.110	4190	-	69.92	58.87	0.770	5781	6547	0.883
6.1	3	24.0	1.000	2.063	0.422	1.906	0.500	8	2	0.790	0.200	4220	-	66.42	63.26	1.067	6201	6646	0.933
2.1	2	24.0	1.000	2.250	1.706	1.328	0.375	7	2	0.790	0.110	5250	70.00	69.92	62.43	0.770	5794	6628	0.874
4.1	2	24.0	1.000	2.063	1.926	1.250	0.500	6	2	0.790	0.200	4090	70.00	70.75	62.51	1.200	6175	7511	0.822
																		Min	0.756
																		Max	0.968
																		Mean	0.849
																		Std	0.072
																		COV	0.085

Table 5.13c: Data and Test/Prediction Ratios for Bars Confined by Stirrups from Hester et al. (1991, 1993)

Tests No.	n_b	l_d	d_b	C_{so}	C_{si}	C_b	d_s	N	N_l	A_b	A_v	f'_c	f_y	f_{yt}	f_s^*	NA_{tr}/n	Test $T_b/f'^{1/4}_c$	Pred. $T_b/f'^{1/4}_c$	Test/Pred.
		(in.)	(in.)	(in.)	(in.)	(in.)	(in.)			(in.^{2})	(in.^{2})	(psi)	(ksi)	(ksi)	(ksi)	(in.^{2})	(in.^{2})	(in.^{2})	
7-8C3-16-3-U	2	16.0	1.000	2.000	4.000	2.030	0.375	3	2	0.790	0.110	5240	69.00	54.10	51.49	0.330	4781	5250	0.911
4-8S3-16-2-U	3	16.0	1.000	2.000	1.500	2.040	0.375	2	2	0.790	0.110	6450	71.10	68.90	47.06	0.147	4148	4647	0.893
4-8S3-16-3-U	3	16.0	1.000	2.000	1.500	2.100	0.375	3	2	0.790	0.110	6450	71.10	68.90	50.04	0.220	4411	4819	0.915
5-8C3-16-2-U	3	16.0	1.000	2.000	1.500	2.060	0.375	2	2	0.790	0.110	5490	69.00	54.10	46.51	0.147	4269	4651	0.918
6-8C3-22 3/4-3-U	3	22.8	1.000	2.000	1.500	2.170	0.375	3	2	0.790	0.110	5850	69.00	54.10	56.45	0.220	5099	5808	0.878
1-8N3-16-2-U	3	16.0	1.000	2.000	1.500	2.000	0.375	2	2	0.790	0.110	5990	69.00	77.30	56.00	0.147	5029	4640	1.084
6-8C3-22 3/4-4-U	3	22.8	1.000	2.000	1.500	2.160	0.375	4	2	0.790	0.110	5850	69.00	54.10	55.67	0.293	5029	5966	0.843
5-8C3-16-3-U	3	16.0	1.000	2.000	1.500	2.060	0.375	3	2	0.790	0.110	5490	69.00	54.10	43.31	0.220	3975	4811	0.826
3-8S3-16-2-U	3	16.0	1.000	2.000	1.500	2.080	0.375	2	2	0.790	0.110	6020	71.10	68.90	46.47	0.147	4168	4655	0.895
2-8C3-16-2-U	3	16.0	1.000	2.000	1.500	1.830	0.375	2	2	0.790	0.110	6200	69.00	54.10	43.99	0.147	3916	4607	0.850
																		Min	0.826
																		Max	1.084
																		Mean	0.901
																		Std	0.072
																		COV	0.080

Note: Refer to last page of Table 5.13 for footnote.

Table 5.13d: Data and Test/Prediction Ratios for Bars Confined by Stirrups from Thompson et al. (1975)

Tests No.	n_b	l_s	d_b	C_{so}	C_{si}	C_b	d_s	N	N_l	A_b	A_v	f'_c	f_y	f_{yt}	f_s^*	NA_v/n	Test $T_b/f'^{1/4+}_c$	Pred. $T_b/f'^{1/4+}_c$	Test/Pred.
		(in.)	(in.)	(in.)	(in.)	(in.)	(in.)			(in.^{2})	(in.^{2})	(psi)	(ksi)	(ksi)	(ksi)	(in.^{2})	(in.^{2})	(in.^{2})	
11-30-4/2/2-6/6-S5	6	30.0	1.410	2.000	2.000	2.000	0.375	6	6	1.560	0.110	3063	65.00	68.00	46.47	0.660	9745	10315	0.945
11-20-4/2/2/-6/6-SF	6	20.0	1.410	2.000	2.000	2.000	0.375	7	6	1.560	0.110	3260	67.30	67.30	42.34	0.770	8741	8851	0.988
11-20-4/2/2-6/6-S5	6	20.0	1.410	2.000	2.000	2.000	0.375	4	6	1.560	0.110	3400	67.30	67.30	40.61	0.440	8296	8129	1.021
8-15-4/2/2-6/6-S5	6	15.0	1.000	2.000	2.000	2.000	0.375	3	6	0.790	0.110	3507	61.10	61.10	57.31	0.330	5883	5087	1.156
																		Min	0.945
																		Max	1.156
																		Mean	1.027
																		Std	0.091
																		COV	0.089

Table 5.13e: Data and Test/Prediction Ratios for Bars Confined by Stirrups from Ferguson and Breen (1965)

Tests No.	n_b	l_s	d_b	C_{so}	C_{si}	C_b	d_s	N	N_l	A_b	A_v	f'_c	f_y	f_{yt}	f_s^*	NA_v/n	Test $T_b/f'^{1/4+}_c$	Pred. $T_b/f'^{1/4+}_c$	Test/Pred.
		(in.)	(in.)	(in.)	(in.)	(in.)	(in.)			(in.^{2})	(in.^{2})	(psi)	(ksi)	(ksi)	(ksi)	(in.^{2})	(in.^{2})	(in.^{2})	
11R36a	2	49.5	1.410	4.590	4.620	2.020	0.375	11	2	1.560	0.110	3020	93.00	42.00	82.35	1.210	17330	16161	1.072
8F36c	2	36.0	1.000	3.250	3.295	1.470	0.252	6	2	0.790	0.050	2740	74.00	52.00	61.33	0.300	6697	7750	0.864
8F36d	2	36.0	1.000	3.250	3.280	1.530	0.252	10	2	0.790	0.050	3580	74.00	52.00	74.31	0.500	7589	8291	0.915
8F36e	2	36.0	1.000	3.250	3.310	1.470	0.252	6	2	0.790	0.050	4170	74.00	52.00	77.44	0.300	7613	7750	0.982
8F36f	2	36.0	1.000	3.250	3.280	1.500	0.252	10	2	0.790	0.050	3780	74.00	52.00	78.15	0.500	7873	8239	0.956
8F36g	2	36.0	1.000	3.250	3.265	1.530	0.252	6	2	0.790	0.050	3070	74.00	52.00	75.78	0.300	8042	7854	1.024
8F36h	2	36.0	1.000	3.250	3.265	1.590	0.252	14	2	0.790	0.050	1910	74.00	52.00	56.02	0.700	6695	8834	0.758
8F36j	2	36.0	1.000	3.250	3.310	1.500	0.252	14	2	0.790	0.050	1820	74.00	52.00	64.09	0.700	7751	8676	0.893
8F30b	2	30.0	1.000	3.250	3.270	1.500	0.252	6	2	0.790	0.050	2610	74.00	52.00	57.47	0.300	6352	6973	0.911
																		Min	0.758
																		Max	1.072
																		Mean	0.931
																		Std	0.092
																		COV	0.099

Table 5.13f: Data and Test/Prediction Ratios for Bars Confined by Stirrups from Zekany et al. (1981)

Tests No.	n_b	l_s	d_b	C_{so}	C_{si}	C_b	d_s	N	N_l	A_b	A_v	f'_c	f_y	f_{yt}	f_s^*	NA_v/n	Test $T_b/f'^{1/4+}_c$	Pred. $T_b/f'^{1/4+}_c$	Test/Pred.
		(in.)	(in.)	(in.)	(in.)	(in.)	(in.)			(in.^{2})	(in.^{2})	(psi)	(ksi)	(ksi)	(ksi)	(in.^{2})	(in.^{2})	(in.^{2})	
11-40-B-A	4	22.0	1.410	2.000	2.000	2.000	0.236	5	2	1.560	0.044	5425	60.10	70.00	44.94	0.219	8168	7986	1.023
2-4.5-80-B	4	22.0	1.410	2.000	2.000	2.000	0.236	5	2	1.560	0.044	4200	60.10	74.50	42.54	0.219	8243	7986	1.032
2-5-40-B(4)	4	22.0	1.410	2.000	2.000	2.000	0.236	4	4	1.560	0.044	3850	60.10	70.00	41.59	0.175	8236	7891	1.044
3-5-53-B	4	22.0	1.410	2.000	2.000	2.000	0.375	4	2	1.560	0.110	3775	60.10	60.30	39.44	0.440	7850	8470	0.927
2-4.5-53-B	4	22.0	1.410	2.000	2.000	2.000	0.236	5	2	1.560	0.044	4125	60.10	74.50	42.00	0.219	8175	7986	1.024
11-53-B	4	22.0	1.410	2.000	2.000	2.000	0.236	5	2	1.560	0.044	4025	60.10	70.00	42.32	0.219	8289	7986	1.038
11-40-B	4	22.0	1.410	2.000	2.000	2.000	0.236	5	2	1.560	0.044	5050	60.10	70.00	45.58	0.219	8435	7986	1.056
11-53-B-D	4	22.0	1.410	2.000	2.000	2.000	0.236	5	2	1.560	0.044	4125	60.10	70.00	33.89	0.219	6597	7986	0.826
3-5-40-B	4	22.0	1.410	2.000	2.000	2.000	0.375	4	2	1.560	0.110	3750	60.10	60.30	38.21	0.440	7617	8470	0.899
9-53-B	5	16.0	1.128	2.000	1.500	2.000	0.236	4	2	1.000	0.044	5700	62.80	70.00	57.36	0.070	6601	5022	1.315
																		Min	0.826
																		Max	1.315
																		Mean	1.018
																		Std	0.129
																		COV	0.127

Note: Refer to last page of Table 5.13 for footnote.

Table 5.13g: Data and Test/Prediction Ratios for Bars Confined by Stirrups from DeVries et al. (1991)

Tests No.	n_b	l_s	d_b	C_{so}	C_{si}	C_b	d_s	N	N_l	A_b	A_v	f'_c	f_y	f_{yt}	f_t*	NA_{tr}/n	Test $T_b/f'^{1/4}_c$	Pred. $T_b/f'^{1/4}_c$	Test/Pred.
		(in.)	(in.)	(in.)	(in.)	(in.)	(in.)			(in.^{2})	(in.^{2})	(psi)	(ksi)	(ksi)	(ksi)	(in.^{2})	(in.^{2})	(in.^{2})	
8G-9B-P6	2	9.0	0.750	1.875	2.125	1.125	0.375	3	2	0.440	0.110	8850	76.63	78.58	70.39	0.330	3193	2879	1.109
8N-9B-P6	2	9.0	0.750	1.625	2.438	1.250	0.375	3	2	0.440	0.110	8300	76.63	78.58	56.55	0.330	2607	2896	0.900
8G-22B-P9	2	22.0	1.128	1.500	1.744	1.125	0.375	4	2	1.000	0.110	7460	66.40	78.58	52.76	0.440	5677	5912	0.960
8N-18B-P9	2	18.0	1.128	1.375	1.932	1.500	0.375	3	2	1.000	0.110	7660	70.35	78.58	51.68	0.330	5524	5436	1.016
8G-16B-P9	2	16.0	1.128	1.375	1.869	1.063	0.375	3	2	1.000	0.110	7460	66.40	78.58	42.44	0.330	4567	4938	0.925
8G-18B-P9	2	18.0	1.128	1.688	1.557	1.250	0.375	3	2	1.000	0.110	8610	70.35	78.58	52.38	0.330	5437	5385	1.010
10N-12B-P9	2	12.0	1.128	1.938	1.307	1.188	0.375	3	2	1.000	0.110	9780	70.35	78.58	37.63	0.330	3784	4620	0.819
10G-12B-P9	2	12.0	1.128	1.625	1.619	1.250	0.375	3	2	1.000	0.110	9680	70.35	78.58	37.61	0.330	3792	4665	0.813
15G-12B-P9	2	12.0	1.128	1.375	1.932	1.188	0.375	3	2	1.000	0.110	16100	70.35	78.58	49.09	0.330	4358	4575	0.953
15N-12B-P9	2	12.0	1.128	1.500	1.807	1.250	0.375	3	2	1.000	0.110	13440	70.35	78.58	50.77	0.330	4716	4635	1.017
																		Min	0.813
																		Max	1.109
																		Mean	0.952
																		Std	0.092
																		COV	0.097

Table 5.13h: Data and Test/Prediction Ratios for Bars Confined by Stirrups from Rezansoff et al. (1991)

Tests No.	n_b	l_s	d_b	C_{so}	C_{si}	C_b	d_s	N	N_l	A_b	A_v	f'_c	f_y	f_{yt}	f_t*	NA_{tr}/n	Test $T_b/f'^{1/4}_c$	Pred. $T_b/f'^{1/4}_c$	Test/Pred.
		(in.)	(in.)	(in.)	(in.)	(in.)	(in.)			(in.^{2})	(in.^{2})	(psi)	(ksi)	(ksi)	(ksi)	(in.^{2})	(in.^{2})	(in.^{2})	
20-6-2	2	18.1	0.768	1.000	2.980	1.000	0.313	5	2	0.465	0.077	4277	72.50	62.08	70.12	0.384	4032	3684	1.095
20-6-3	2	15.4	0.768	1.000	2.980	1.000	0.313	6	2	0.465	0.077	3886	72.50	62.08	75.55	0.460	4449	3611	1.232
20-6-1	2	22.1	0.768	1.000	2.980	1.000	0.313	3	2	0.465	0.077	4045	72.50	62.08	78.49	0.230	4576	3691	1.240
20-8-11	2	16.3	0.992	1.000	2.530	1.000	0.313	13	2	0.775	0.077	4466	65.54	62.08	75.00	0.998	7110	5691	1.249
20-8-9	2	18.7	0.992	1.500	2.030	1.500	0.313	9	2	0.775	0.077	4205	65.54	62.08	60.05	0.691	5780	5831	0.991
20-8-10	2	15.1	0.992	1.500	2.030	1.500	0.313	12	2	0.775	0.077	4408	65.54	62.08	64.03	0.921	6090	5884	1.035
20-8-1	2	18.7	0.992	1.000	2.530	1.000	0.313	13	2	0.775	0.077	5220	65.54	62.08	71.05	0.998	6478	5914	1.095
20-8-12	2	16.3	0.992	1.500	2.030	1.500	0.313	11	2	0.775	0.077	4350	65.54	62.08	64.20	0.844	6126	5870	1.044
20-8-2	2	21.8	0.992	1.000	2.530	1.000	0.313	11	2	0.775	0.077	5742	65.54	62.08	64.84	0.844	5773	5867	0.984
20-8-3	2	26.1	0.992	1.000	2.530	1.000	0.313	9	2	0.775	0.077	5510	65.54	62.08	64.02	0.691	5759	5940	0.969
20-8-6	2	26.1	0.992	1.000	2.530	1.000	0.313	9	2	0.775	0.077	4770	65.54	62.08	75.37	0.691	7028	5940	1.183
20-8-7	2	26.1	0.992	1.500	2.030	1.500	0.313	4	2	0.775	0.077	4495	65.54	62.08	61.35	0.307	5806	5923	0.980
20-8-8	2	21.8	0.992	1.500	2.030	1.500	0.313	7	2	0.775	0.077	4350	65.54	62.08	59.58	0.537	5686	5882	0.967
20-8-5	2	21.8	0.992	1.000	2.530	1.000	0.313	11	2	0.775	0.077	4770	65.54	62.08	76.01	0.844	7088	5867	1.208
20-8-4	2	18.7	0.992	1.000	2.530	1.000	0.313	13	2	0.775	0.077	4335	65.54	62.08	71.94	0.998	6871	5914	1.162
20-8-21	2	15.4	0.992	1.260	2.270	1.500	0.313	7	2	0.775	0.077	3378	60.90	52.21	45.76	0.537	4652	4897	0.950
20-8-13	2	28.7	0.992	1.180	2.350	1.000	0.313	4	2	0.775	0.077	3509	64.38	52.21	51.22	0.307	5158	5411	0.953
20-8-14	2	23.1	0.992	1.180	2.350	1.000	0.313	6	2	0.775	0.077	3277	64.38	52.21	53.28	0.460	5458	5212	1.047
20-8-15	2	20.3	0.992	1.180	2.350	1.000	0.313	7	2	0.775	0.077	3625	64.38	52.21	54.68	0.537	5462	5113	1.068
20-8-16	2	28.7	0.992	1.180	2.350	1.000	0.313	4	2	0.775	0.077	3291	60.90	52.21	54.82	0.307	5609	5411	1.037
20-8-18	2	17.4	0.992	1.180	2.350	1.000	0.313	8	2	0.775	0.077	3349	60.90	52.21	54.80	0.614	5582	5006	1.115
20-8-19	2	21.7	0.992	1.260	2.270	1.500	0.313	4	2	0.775	0.077	3219	60.90	52.21	44.56	0.307	4584	5101	0.899
20-8-17	2	20.3	0.992	1.180	2.350	1.000	0.313	7	2	0.775	0.077	3480	60.90	52.21	60.78	0.537	6133	5113	1.199
20-8-20	2	17.3	0.992	1.260	2.270	1.500	0.313	6	2	0.775	0.077	3291	60.90	52.21	44.95	0.460	4599	4950	0.929
20-11-4	2	18.9	1.406	2.020	1.670	1.508	0.444	10	2	1.550	0.155	4350	67.28	83.40	47.51	1.549	9067	9894	0.916
20-11-2	2	26.6	1.406	2.020	1.670	2.295	0.444	11	2	1.550	0.155	4335	67.28	83.40	70.91	1.704	13545	11980	1.131
20-11-1	2	38.0	1.406	2.020	1.670	2.295	0.444	5	2	1.550	0.155	4770	66.12	83.40	68.59	0.774	12792	11865	1.078
20-11-3	2	26.6	1.406	2.020	1.670	1.508	0.444	7	2	1.550	0.155	4466	69.02	83.40	52.37	1.084	9930	9976	0.995
20-11-8	2	34.3	1.406	2.000	1.690	1.000	0.444	10	2	1.550	0.155	3349	69.02	60.05	61.36	1.549	12502	11358	1.101
20-11-5	2	27.0	1.406	2.000	1.690	2.000	0.444	9	2	1.550	0.155	3625	66.12	60.05	63.81	1.394	12746	11302	1.128
20-11-6	2	34.7	1.406	2.000	1.690	2.000	0.444	6	2	1.550	0.155	3625	66.12	60.05	54.54	0.929	10895	11574	0.941
20-11-7	2	27.2	1.406	2.000	1.690	1.000	0.444	12	2	1.550	0.155	3291	66.12	60.05	51.38	1.859	10515	11217	0.937
20-9-1	2	19.7	1.177	2.000	2.140	1.500	0.444	7	2	1.085	0.155	3538	66.12	60.05	58.74	1.084	8264	7776	1.063
20-9-2	2	25.6	1.177	2.000	2.140	1.500	0.444	5	2	1.085	0.155	3378	66.12	60.05	64.82	0.774	9225	7896	1.168
																		Min	0.899
																		Max	1.249
																		Mean	1.062
																		Std	0.103
																		COV	0.097

Note: Refer to last page of Table 5.13 for footnote.

Table 5.13i: Data and Test/Prediction Ratios for Bars Confined by Stirrups from Rezansoff et al. (1993)

Tests No.	n_b	l_d	d_b	C_{so}	C_{si}	C_b	d_s	N	N_l	A_b	A_v	f'_c	f_y	f_{yt}	f_s^*	NA_{tr}/n	Test $T_b/f'^{1/4}_c$	Pred. $T_b/f'^{1/4}_c$	Test/Pred.
		(in.)	(in.)	(in.)	(in.)	(in.)	(in.)			($in.^2$)	($in.^2$)	(psi)	(ksi)	(ksi)	(ksi)	($in.^2$)	($in.^2$)	($in.^2$)	
6	3	22.0	0.992	1.827	0.502	2.008	0.313	8	2	0.775	0.077	3625	64.52	84.10	50.77	0.409	5071	5077	0.999
1b	2	29.5	0.992	1.827	0.520	2.008	0.250	6	2	0.775	0.049	3799	64.52	63.80	69.82	0.295	6892	5512	1.251
1a	2	29.5	0.992	1.827	0.520	2.008	0.250	6	2	0.775	0.049	3958	64.52	63.80	74.05	0.295	7235	5512	1.313
7	3	14.8	0.992	1.827	0.502	2.008	0.630	4	2	0.775	0.312	3625	64.52	68.15	46.60	0.831	4654	5348	0.870
3a	3	29.5	0.992	1.827	0.502	2.008	0.250	6	2	0.775	0.049	3958	64.52	63.80	69.76	0.196	6816	5280	1.291
3b	3	29.5	0.992	1.827	0.502	2.008	0.250	6	2	0.775	0.049	3799	64.52	63.80	59.03	0.196	5827	5280	1.104
8	3	11.8	0.992	1.827	0.994	2.008	0.630	3	2	0.775	0.312	3625	64.52	68.15	34.05	0.623	3401	4781	0.711
4b	3	44.3	1.177	1.819	0.573	2.008	0.250	5	2	1.085	0.049	3726	68.87	63.80	67.65	0.164	9395	7730	1.215
9	3	33.5	1.177	1.819	0.573	2.008	0.445	10	2	1.085	0.155	3886	68.87	68.87	76.40	1.036	10500	8562	1.226
10	3	22.0	1.177	1.819	0.573	2.008	0.630	7	2	1.085	0.312	4089	68.87	68.15	70.99	1.454	9632	8341	1.155
4a	3	35.4	1.177	1.819	0.573	2.008	0.250	4	2	1.085	0.049	4031	68.87	63.80	61.08	0.131	8318	6777	1.227
																		Min	0.711
																		Max	1.313
																		Mean	1.124
																		Std	0.190
																		COV	0.169

Table 5.13j: Data and Test/Prediction Ratios for R_r = 0.140 (F1) Bars Confined by Stirrups from Current Tests, using concrete with Basalt Coarse Aggregate

Tests No.	n_b	l_d	d_b	C_{so}	C_{si}	C_b	d_s	N	N_l	A_b	A_v	f'_c	f_y	f_{yt}	f_s^*	NA_{tr}/n	Test $T_b/f'^{1/4}_c$	Pred. $T_b/f'^{1/4}_c$	Test/Pred.
		(in.)	(in.)	(in.)	(in.)	(in.)	(in.)			($in.^2$)	($in.^2$)	(psi)	(ksi)	(ksi)	(ksi)	($in.^2$)	($in.^2$)	($in.^2$)	
9.2	2	18.0	1.000	2.063	1.844	1.290	0.375	6	2	0.790	0.110	4230	75.00	64.55	69.06	0.660	6765	6796	0.995
9.4	2	24.0	1.000	2.016	1.891	1.915	0.375	2	2	0.790	0.110	4230	75.00	64.55	65.00	0.220	6367	6757	0.942
11.1	3	18.0	1.000	2.000	0.453	1.928	0.500	6	2	0.790	0.200	4380	75.00	84.70	66.94	0.800	6500	6870	0.946
11.4	2	24.0	1.000	2.094	1.844	1.928	0.375	2	2	0.790	0.110	4380	75.00	64.55	62.49	0.220	6068	6792	0.893
																		Min	0.893
																		Max	0.995
																		Mean	0.944
																		Std	0.042
																		COV	0.044

Table 5.13k: Data and Test/Prediction Ratios for R_r = 0.140 (F1) Bars Confined by Stirrups from Current Tests, using concrete with Limestone Coarse Aggregate

Tests No.	n_b	l_d	d_b	C_{so}	C_{si}	C_b	d_s	N	N_l	A_b	A_v	f'_c	f_y	f_{yt}	f_s^*	NA_{tr}/n	Test $T_b/f'^{1/4}_c$	Pred. $T_b/f'^{1/4}_c$	Test/Pred.
		(in.)	(in.)	(in.)	(in.)	(in.)	(in.)			($in.^2$)	($in.^2$)	(psi)	(ksi)	(ksi)	(ksi)	($in.^2$)	($in.^2$)	($in.^2$)	
2.2	2	24.0	1.000	2.125	1.801	1.406	0.375	7	2	0.790	0.110	5250	75.00	69.92	77.60	0.770	7202	8009	0.899
2.3	2	24.0	1.000	2.125	1.780	1.969	0.375	4	2	0.790	0.110	5250	75.00	69.92	73.45	0.440	6817	7577	0.900
4.2	2	24.0	1.000	2.094	1.848	1.313	0.375	8	2	0.790	0.110	4090	75.00	69.92	72.33	0.880	7145	8288	0.862
5.2	3	24.0	1.000	2.078	1.867	1.359	0.375	7	2	0.790	0.110	4190	75.00	69.92	65.41	0.770	6422	7962	0.807
5.3	2	24.0	1.000	2.063	1.849	1.281	0.375	7	2	0.790	0.110	4190	75.00	69.92	67.88	0.770	6665	7869	0.847
5.6	2	22.0	1.000	2.094	1.807	1.313	0.500	5	2	0.790	0.200	4190	75.00	70.75	66.34	1.000	6514	8446	0.771
6.2	3	24.0	1.000	2.000	0.438	2.000	0.500	8	2	0.790	0.200	4220	75.00	66.42	74.88	1.067	7340	8319	0.882
6.3	2	16.0	1.000	2.000	1.906	1.344	0.375	2	2	0.790	0.110	4220	75.00	64.55	46.09	0.220	4518	5087	0.888
7.1	2	16.0	1.000	2.079	1.797	1.875	0.375	2	2	0.790	0.110	4160	75.00	64.55	46.72	0.220	4596	5508	0.834
7.5	3	24.0	1.000	2.032	0.399	2.000	0.500	8	2	0.790	0.200	4160	75.00	84.70	73.17	1.067	7198	8301	0.867
																		Min	0.771
																		Max	0.900
																		Mean	0.856
																		Std	0.042
																		COV	0.049

Note: Refer to last page of Table 5.14 for footnote.

Table 5.13l: Data and Test/Prediction Ratios for R_r = 0.119 (N3) Bars Confined by Stirrups from Current Tests, using concrete with Basalt Coarse Aggregate

Tests No.	n_b	l_s	d_b	C_{so}	C_{si}	C_b	d_s	N	N_l	A_b	A_v	f'_c	f_y	f_{yt}	f_s*	NA_{tr}/n	Test $T_b/f'^{1/4}_c$	Pred. $T_b/f'^{1/4}_c$	Test/Pred.
		(in.)	(in.)	(in.)	(in.)	(in.)	(in.)			(in.^{2})	(in.^{2})	(psi)	(ksi)	(ksi)	(ksi)	(in.^{2})	(in.^{2})	(in.^{2})	
8.2	3	24.0	1.000	2.047	0.430	1.969	0.500	8	2	0.790	0.200	3830	81.00	84.70	79.32	1.067	7965	7581	1.051
8.4	2	16.0	1.000	2.063	1.891	1.906	0.375	2	2	0.790	0.110	3830	81.00	64.55	48.90	0.220	4911	5386	0.912
9.1	2	24.0	1.000	2.032	1.875	1.954	0.375	2	2	0.790	0.110	4230	81.00	64.55	63.40	0.220	6211	6660	0.932
11.3	2	18.0	1.000	2.063	1.844	1.943	0.500	4	2	0.790	0.200	4380	81.00	84.70	62.44	0.800	6063	7307	0.830
																		Min	0.830
																		Max	1.051
																		Mean	0.931
																		Std	0.091
																		COV	0.098

Table 5.13m: Data and Test/Prediction Ratios for R_r = 0.101 (C1) Bars Confined by Stirrups from Current Tests, using concrete with Limestone Coarse Aggregate

Tests No.	n_b	l_s	d_b	C_{so}	C_{si}	C_b	d_s	N	N_l	A_b	A_v	f'_c	f_y	f_{yt}	f_s*	NA_{tr}/n	Test $T_b/f'^{1/4}_c$	Pred. $T_b/f'^{1/4}_c$	Test/Pred.
		(in.)	(in.)	(in.)	(in.)	(in.)	(in.)			(in.^{2})	(in.^{2})	(psi)	(ksi)	(ksi)	(ksi)	(in.^{2})	(in.^{2})	(in.^{2})	
1.5	3	16.0	1.000	2.063	1.375	1.938	0.500	5	2	0.790	0.200	5020	60.00	70.75	52.22	0.667	4901	6085	0.805
1.6	3	16.0	1.000	2.063	1.438	1.938	0.500	3	2	0.790	0.200	5020	60.00	70.75	51.98	0.400	4879	5492	0.888
4.4	2	24.0	1.000	2.032	1.978	1.219	0.375	4	2	0.790	0.110	4090	60.00	69.92	58.85	0.440	5814	6174	0.942
7.2	2	18.0	1.000	1.469	2.531	1.313	0.500	5	2	0.790	0.200	4160	60.00	84.70	55.82	1.000	5491	6779	0.810
7.6	2	16.0	1.000	2.032	1.969	1.938	0.375	2	2	0.790	0.110	4160	60.00	64.55	44.34	0.220	4362	5277	0.826
14.1	3	36.0	1.000	2.032	0.484	1.877	0.375	3	2	0.790	0.110	4200	60.00	64.55	59.96	0.220	5884	6189	0.951
14.2	3	21.0	1.000	2.016	0.469	1.897	0.500	7	2	0.790	0.200	4200	60.00	84.70	62.83	0.933	6166	6596	0.935
																		Min	0.805
																		Max	0.951
																		Mean	0.880
																		Std	0.065
																		COV	0.074

* Bar stress is calculated based on the working stress of the bar if the stress does not exceed the yield stress, otherwise, ultimate strength method is used to calculate the bar stress.

\- Data is not available

\+ For Conventional bars:

$$\frac{T_b}{f_c'^{1/4}} = \frac{A_b f_s}{f_c'^{1/4}} = \left[631_d(C_m + 0.5d_b) + 2280A_b\left(0.082\frac{C_M}{C_m} + 0.918\right) + 2187\frac{NA_{tr}}{n} + 202\right]$$

For R_r = 0.140 (F1) bars:

$$\frac{T_b}{f_c'^{1/4}} = \frac{A_b f_s}{f_c'^{1/4}} = \left[631_d(C_m + 0.5d_b) + 2280A_b\left(0.082\frac{C_M}{C_m} + 0.918\right) + 3399\frac{NA_{tr}}{n} + 533\right]$$

For R_r = 0.140 (N3) bars:

$$\frac{T_b}{f_c'^{1/4}} = \frac{A_b f_s}{f_c'^{1/4}} = \left[631_d(C_m + 0.5d_b) + 2280A_b\left(0.082\frac{C_M}{C_m} + 0.918\right) + 2791\frac{NA_{tr}}{n} + 531\right]$$

For R_r = 0.140 (C1) bars:

$$\frac{T_b}{f_c'^{1/4}} = \frac{A_b f_s}{f_c'^{1/4}} = \left[631_d(C_m + 0.5d_b) + 2280A_b\left(0.082\frac{C_M}{C_m} + 0.918\right) + 2413\frac{NA_{tr}}{n} + 471\right]$$

Table 5.14a: Test/Prediction Ratios for Bars Not Confined by Stirrups and $f_s \leq 40$ ksi

Test No.	f_y (ksi)	f_s (ksi)	Test/Prediction
D22	57.00	23.89	0.820
D10	57.00	26.27	0.841
D20	57.00	26.95	0.865
D39	57.00	27.62	0.775
D38	57.00	28.16	0.712
D33	57.00	28.20	0.802
D14	57.00	32.63	0.913
3a	50.00	32.78	1.003
3b	50.00	33.00	1.010
D6	57.00	33.17	0.937
3c	50.00	33.48	1.025
D7	57.00	33.85	0.898
SII15	-	34.52	1.055
D9	57.00	34.98	0.920
D8	57.00	35.95	0.974
D3	57.00	36.86	1.035
D34	57.00	36.86	0.937
4-11C0-24-0-U	69.00	37.82	0.882
N-N-80-B	60.10	37.96	1.031
11-30-4/2/2-6/6	60.50	37.99	0.934
SII16	-	38.11	1.088
D23	57.00	39.23	0.947
SIII31	-	39.66	1.132
D17	57.00	39.74	1.003
5-8C3-16-0-U	69.00	39.82	0.886
		Min	0.712
		Max	1.132
		Mean	0.937
		Std	0.102
		COV	0.109

Table 5.14b: Test/Prediction Ratios for Bars Not Confined by Stirrups and 40 ksi < f_s ≤ 50 ksi

Test No.	f_y (ksi)	f_s (ksi)	Test/Prediction
4-11S0-24-0-U	71.00	40.22	0.938
SII11	-	41.17	1.018
8R18a	99.00	41.32	0.913
SII23	-	41.89	1.027
D15	57.00	42.24	1.045
4-8S3-16-0-U	71.00	42.40	0.904
4a	50.00	42.64	1.006
3-8S0-16-0-U	71.00	42.82	0.981
3-8N0-16-0-U	63.80	43.02	0.986
D24	57.00	43.18	0.875
4c	50.00	43.32	1.061
D21	57.00	43.35	0.946
4b	50.00	43.89	1.055
11-25-6/2/3-5/5	66.30	44.19	1.071
D5	57.00	44.34	1.026
11-30-4/2/4-6/6	63.40	44.39	1.039
D29	57.00	44.60	1.021
1.3	60.00	45.01	1.048
14-60-4/2/2-5/5	57.70	45.23	0.875
11-45-4/1/2-6/6	60.50	45.28	1.010
7-8C3-16-0-U	69.00	45.37	0.970
D12	57.00	45.70	0.940
2-6S0-12-0-U	71.00	45.75	1.034
D32	57.00	46.05	0.994
2-8C3-16-0U	69.00	46.24	1.008
SIII32	-	46.37	1.237
SIII27	-	46.43	1.021
3-8S3-16-0-U	71.00	46.81	1.018
D4	57.00	46.84	1.090
SIV53	-	46.95	0.919
9-53-B-N	62.80	47.56	1.191
SIII33	-	48.45	1.192
D13	57.00	48.93	1.055
D36	79.00	48.95	1.146
SIII28	-	49.32	0.972
SIII29	-	49.32	0.870
8-18-4/3/2.5-4/6	59.30	49.33	1.049
		Min	0.870
		Max	1.237
		Mean	1.015
		Std	0.085
		COV	0.084

Table 5.14c: Test/Prediction Ratios for Bars Not Confined by Stirrups and 50 ksi < $f_s \leq$ 60 ksi

Test No.	f_y (ksi)	f_s (ksi)	Test/Prediction
1-8N3-16-0-U	63.80	50.03	1.091
D40	57.00	50.55	0.985
8-24-4/2/2-6/6	59.30	50.64	0.960
4.5	60.00	51.06	0.935
2-6C0-12-0-U	69.00	51.40	1.162
1.1	60.00	51.63	0.919
11R24a	93.00	51.81	1.066
6-8C3-22-0-U	69.00	51.85	0.915
8F30a	74.00	52.78	0.913
D30	57.00	52.88	0.973
6.5	75.00	53.59	0.948
2.4	75.00	54.08	1.059
8F36k	74.00	54.65	0.926
D35	57.00	54.99	0.943
D26	57.00	55.87	1.037
5a	68.87	56.08	1.058
8-18-4/3/2-6/6	59.30	56.26	1.112
14-6--4/2/4-5/5	57.70	56.64	1.056
6-12-4/2/2-6/6	61.70	57.40	1.155
11-30-4/2/2.7/4/6	63.30	57.59	1.258
D25	57.00	58.25	0.922
11R30a	93.00	58.50	1.081
2a	64.52	58.56	1.089
2b	64.52	58.63	1.101
2.5	75.00	58.67	1.016
8R24a	99.00	58.88	1.102
11F36b	65.00	59.20	1.000
D19	57.00	59.93	0.998
		Min	0.913
		Max	1.258
		Mean	1.028
		Std	0.089
		COV	0.086

Table 5.14d: Test/Prediction Ratios for Bars Not Confined by Stirrups and $f_s > 60$ ksi

Test No.	f_y (ksi)	f_s (ksi)	Test/Prediction
D31	79.00	60.35	1.253
10.2	81.00	61.17	1.029
8F36b	74.00	61.30	0.912
8.1	79.00	61.47	1.106
1-5N0-12-0-U	63.80	61.51	1.212
11F42a	65.00	63.61	0.954
1-5N0-12-0-U	63.80	63.99	1.261
11F36a	73.00	64.16	0.998
5b	68.87	65.83	1.091
8F42a	63.50	65.93	0.933
8F36a	63.00	66.34	0.935
8R42a	99.00	71.01	0.937
11R48b	93.00	71.43	0.901
11F48b	65.00	72.24	0.983
8R48a	99.00	72.88	0.907
8F39a	63.50	72.90	0.999
8F42b	63.50	73.54	0.963
11F48a	73.00	74.56	1.039
11R60a	93.00	74.61	0.937
11F60b	65.00	78.02	0.867
11R48a	93.00	82.22	0.996
11F60a	73.00	84.80	1.035
11R60b	93.00	87.80	0.966
8R64a	99.00	89.71	0.844
8R80a	99.00	96.41	0.748
		Min	0.748
		Max	1.261
		Mean	0.992
		Std	0.121
		COV	0.122

Table 5.15a: Test/Prediction Ratios for Conventional Bars Confined by Stirrups and $f_s \leq 50$ ksi

Tests No.	f_y (ksi)	f_s (ksi)	Test/Prediction
11-53-B-D	60.10	33.89	0.826
8	64.52	34.05	0.711
6.4	-	36.68	0.797
10G-12B-P9	70.35	37.61	0.813
10N-12B-P9	70.35	37.63	0.819
3-5-40-B	60.10	38.21	0.899
3-5-53-B	60.10	39.44	0.927
11-20-4/2/2-6/6-S5	67.30	40.61	1.021
2-5-40-B(4)	60.10	41.59	1.044
2-4.5-53-B	60.10	42.00	1.024
11-53-B	60.10	42.32	1.038
11-20-4/2/2/-6/6-SP	67.30	42.34	0.988
8G-16B-P9	66.40	42.44	0.925
2-4.5-80-B	60.10	42.54	1.032
5-8C3-16-3-U	69.00	43.31	0.826
2-8C3-16-2-U	69.00	43.99	0.850
20-8-19	60.90	44.56	0.899
11-40-B-A	60.10	44.94	1.023
20-8-20	60.90	44.95	0.929
11-40-B	60.10	45.58	1.056
20-8-21	60.90	45.76	0.950
5.5	-	46.43	0.756
11-30-4/2/2-6/6-S5	65.00	46.47	0.945
3-8S3-16-2-U	71.10	46.47	0.895
5-8C3-16-2-U	69.00	46.51	0.918
7	64.52	46.60	0.870
4-8S3-16-2-U	71.10	47.06	0.893
20-11-4	67.28	47.51	0.916
15G-12B-P9	70.35	49.09	0.953
		Min	0.711
		Max	1.056
		Mean	0.915
		Std	0.091
		COV	0.100

Table 5.15b: Test/Prediction Ratios for Conventional Bars Confined by Stirrups and 50 ksi < fs ≤ 60 ksi

Tests No.	f_y (ksi)	f_s (ksi)	Test/Prediction
4-8S3-16-3-U	71.10	50.04	0.915
6	64.52	50.77	0.999
15N-12B-P9	70.35	50.77	1.017
20-8-13	64.38	51.22	0.953
20-11-7	66.12	51.38	0.937
7-8C3-16-3-U	69.00	51.49	0.911
8N-18B-P9	70.35	51.68	1.016
3.5	-	52.02	0.835
20-11-3	69.02	52.37	0.995
8G-18B-P9	70.35	52.38	1.010
8G-22B-P9	66.40	52.76	0.960
20-8-14	64.38	53.28	1.047
20-11-6	66.12	54.54	0.941
20-8-15	64.38	54.68	1.068
20-8-18	60.90	54.80	1.115
20-8-16	60.90	54.82	1.037
9.3	79.00	55.25	0.894
6-8C3-22 3/4-4-U	69.00	55.67	0.843
3.4	-	55.77	0.770
1-8N3-16-2-U	69.00	56.00	1.084
8F36h	74.00	56.02	0.758
6-8C3-22 3/4-3-U	69.00	56.45	0.878
8N-9B-P6	76.63	56.55	0.900
8-15-4/2/2-6/6-S5	61.10	57.31	1.156
9-53-B	62.80	57.36	1.315
8F30b	74.00	57.47	0.911
20-9-1	66.12	58.74	1.063
10.3	79.00	58.85	0.911
5.4	-	58.87	0.883
3b	64.52	59.03	1.104
20-8-8	65.54	59.58	0.967
		Min	0.758
		Max	1.315
		Mean	0.974
		Std	0.116
		COV	0.119

Table 5.15c: Test/Prediction Ratios for Conventional Bars Confined by Stirrups and $f_s > 60$ ksi

Tests No.	f_y (ksi)	f_s (ksi)	Test/Prediction
20-8-9	65.54	60.05	0.991
20-8-17	60.90	60.78	1.199
4a	68.87	61.08	1.227
8F36c	74.00	61.33	0.864
20-8-7	65.54	61.35	0.980
20-11-8	69.02	61.36	1.101
11.2	79.00	61.94	0.926
10.4	79.00	61.98	0.834
2.1	70.00	62.43	0.874
4.1	70.00	62.51	0.822
6.1	-	63.26	0.933
20-11-5	66.12	63.81	1.128
20-8-3	65.54	64.02	0.969
20-8-10	65.54	64.03	1.035
8F36j	74.00	64.09	0.893
20-8-12	65.54	64.20	1.044
5.1	-	64.62	0.968
20-9-2	66.12	64.82	1.168
20-8-2	65.54	64.84	0.984
4b	68.87	67.65	1.215
20-11-1	66.12	68.59	1.078
8.1	79.00	69.67	1.047
3a	64.52	69.76	1.291
1b	64.52	69.82	1.251
20-6-2	72.50	70.12	1.095
8G-9B-P6	76.63	70.39	1.109
20-11-2	67.28	70.91	1.131
10	68.87	70.99	1.155
20-8-1	65.54	71.05	1.095
20-8-4	65.54	71.94	1.162
1a	64.52	74.05	1.313
8F36d	74.00	74.31	0.915
20-8-11	65.54	75.00	1.249
20-8-6	65.54	75.37	1.183
20-6-3	72.50	75.55	1.232
8F36g	74.00	75.78	1.024
20-8-5	65.54	76.01	1.208
9	68.87	76.40	1.226
8F36e	74.00	77.44	0.982
8F36f	74.00	78.15	0.956
20-6-1	72.50	78.49	1.240
11R36a	93.00	82.35	1.072
		Min	0.822
		Max	1.313
		Mean	1.076
		Std	0.134
		COV	0.125

Table 5.16a: Test/Prediction Ratios for Bars Not Confined by Stirrups and $f_s/f_y \leq 1/2$*

Test No.	f_y (ksi)	f_s (ksi)	f_s/f_y	Test/Prediction
8R18a	99.00	41.32	0.417	0.913
D22	57.00	23.89	0.419	0.820
D10	57.00	26.27	0.461	0.841
D20	57.00	26.95	0.473	0.865
D39	57.00	27.62	0.485	0.775
D38	57.00	28.16	0.494	0.712
D33	57.00	28.20	0.495	0.802
			Min	0.712
			Max	0.913
			Mean	0.818
			Std	0.065
			COV	0.079

Table 5.16b: Test/Prediction Ratios for Bars Not Confined by Stirrups and $1/2 < f_s/f_y \leq 3/4$*

Test No.	f_y (ksi)	f_s (ksi)	f_s/f_y	Test/Prediction
4-11C0-24-0-U	69.00	37.82	0.548	0.882
11R24a	93.00	51.81	0.557	1.066
4-11S0-24-0-U	71.00	40.22	0.566	0.938
D14	57.00	32.63	0.572	0.913
5-8C3-16-0-U	69.00	39.82	0.577	0.886
D6	57.00	33.17	0.582	0.937
D7	57.00	33.85	0.594	0.898
8R24a	99.00	58.88	0.595	1.102
4-8S3-16-0-U	71.00	42.40	0.597	0.904
3-8S0-16-0-U	71.00	42.82	0.603	0.981
D9	57.00	34.98	0.614	0.920
D36	79.00	48.95	0.620	1.146
11-30-4/2/2-6/6	60.50	37.99	0.628	0.934
11R30a	93.00	58.50	0.629	1.081
D8	57.00	35.95	0.631	0.974
N-N-80-B	60.10	37.96	0.632	1.031
2-6S0-12-0-U	71.00	45.75	0.644	1.034
D3	57.00	36.86	0.647	1.035
D34	57.00	36.86	0.647	0.937
3a	50.00	32.78	0.656	1.003
7-8C3-16-0-U	69.00	45.37	0.657	0.970

Note: Refer to last page of Table 16 for footnote.

Table 5.16b (Continued): Test/Prediction Ratios for Bars Not Confined by Stirrups and 1/2 < $f_s/f_y \leq 3/4$*

Test No.	f_y (ksi)	f_s (ksi)	f_s/f_y	Test/Prediction
3-8S3-16-0-U	71.00	46.81	0.659	1.018
3b	50.00	33.00	0.660	1.010
11-25-6/2/3-5/5	66.30	44.19	0.667	1.071
3c	50.00	33.48	0.670	1.025
2-8C3-16-0U	69.00	46.24	0.670	1.008
3-8N0-16-0-U	63.80	43.02	0.674	0.986
D23	57.00	39.23	0.688	0.947
D17	57.00	39.74	0.697	1.003
11-30-4/2/4-6/6	63.40	44.39	0.700	1.039
8F30a	74.00	52.78	0.713	0.913
6.5	75.00	53.59	0.715	0.948
8R42a	99.00	71.01	0.717	0.937
2.4	75.00	54.08	0.721	1.059
8R48a	99.00	72.88	0.736	0.907
8F36k	74.00	54.65	0.739	0.926
D15	57.00	42.24	0.741	1.045
2-6C0-12-0-U	69.00	51.40	0.745	1.162
11-45-4/1/2-6/6	60.50	45.28	0.748	1.010
1.3	60.00	45.01	0.750	1.048
			Min	0.882
			Max	1.162
			Mean	0.991
			Std	0.071
			COV	0.071

Table 5.16c: Test/Prediction Ratios for Bars Not Confined by Stirrups and 3/4 < $f_s/f_y \leq 1$*

Test No.	f_y (ksi)	f_s (ksi)	f_s/f_y	Test/Prediction
6-8C3-22-0-U	69.00	51.85	0.751	0.915
10.2	81.00	61.17	0.755	1.029
9-53-B-N	62.80	47.56	0.757	1.191
D24	57.00	43.18	0.757	0.875
D21	57.00	43.35	0.761	0.946
D31	79.00	60.35	0.764	1.253
11R48b	93.00	71.43	0.768	0.901
D5	57.00	44.34	0.778	1.026

Note: Refer to last page of Table 16 for footnote.

Table 5.16c (Continued): Test/Prediction Ratios for Bars Not Confined by Stirrups and $3/4 < f_s/f_y \leq 1$*

Test No.	f_y (ksi)	f_s (ksi)	f_s/f_y	Test/Prediction
8.1	79.00	61.47	0.778	1.106
2.5	75.00	58.67	0.782	1.016
D29	57.00	44.60	0.782	1.021
14-60-4/2/2-5/5	57.70	45.23	0.784	0.875
1-8N3-16-0-U	63.80	50.03	0.784	1.091
D12	57.00	45.70	0.802	0.940
11R60a	93.00	74.61	0.802	0.937
D32	57.00	46.05	0.808	0.994
5a	68.87	56.08	0.814	1.058
D4	57.00	46.84	0.822	1.090
8F36b	74.00	61.30	0.828	0.912
8-18-4/3/2.5-4/6	59.30	49.33	0.832	1.049
4.5	60.00	51.06	0.851	0.935
4a	50.00	42.64	0.853	1.006
8-24-4/2/2-6/6	59.30	50.64	0.854	0.960
D13	57.00	48.93	0.858	1.055
1.1	60.00	51.63	0.861	0.919
4c	50.00	43.32	0.866	1.061
4b	50.00	43.89	0.878	1.055
11F36a	73.00	64.16	0.879	0.998
11R48a	93.00	82.22	0.884	0.996
D40	57.00	50.55	0.887	0.985
8R64a	99.00	89.71	0.906	0.844
2a	64.52	58.56	0.908	1.089
2b	64.52	58.63	0.909	1.101
11-30-4/2/2.7/4/6	63.30	57.59	0.910	1.258
11F36b	65.00	59.20	0.911	1.000
D30	57.00	52.88	0.928	0.973
6-12-4/2/2-6/6	61.70	57.40	0.930	1.155
11R60b	93.00	87.80	0.944	0.966
8-18-4/3/2-6/6	59.30	56.26	0.949	1.112
5b	68.87	65.83	0.956	1.091
1-5N0-12-0-U	63.80	61.51	0.964	1.212
D35	57.00	54.99	0.965	0.943
8R80a	99.00	96.41	0.974	0.748
11F42a	65.00	63.61	0.979	0.954
D26	57.00	55.87	0.980	1.037
14-6--4/2/4-5/5	57.70	56.64	0.982	1.056
			Min	0.748
			Max	1.258
			Mean	1.016
			Std	0.104
			COV	0.102

Note: Refer to last page of Table 5.16 for footnote.

Table 5.16d: Test/Prediction Ratios for Bars Not Confined by Stirrups and $f_s/f_y > 1$*

Test No.	f_y (ksi)	f_s (ksi)	f_s/f_y	Test/Prediction
1-5N0-12-0-U	63.80	63.99	1.003	1.261
11F48a	73.00	74.56	1.021	1.039
D25	57.00	58.25	1.022	0.922
8F42a	63.50	65.93	1.038	0.933
D19	57.00	59.93	1.051	0.998
8F36a	63.00	66.34	1.053	0.935
11F48b	65.00	72.24	1.111	0.983
8F39a	63.50	72.90	1.148	0.999
8F42b	63.50	73.54	1.158	0.963
11F60a	73.00	84.80	1.162	1.035
11F60b	65.00	78.02	1.200	0.867
			Min	0.867
			Max	1.261
			Mean	0.994
			Std	0.102
			COV	0.103

* For only tests whose f_y are known

Table 5.17a: Test/Prediction Ratios for Conventional Bars Confined by Stirrups and $1/2 < f_s/f_y \leq 3/4$*

Tests No.	f_y (ksi)	f_s (ksi)	f_s/f_y	Test/Prediction
8	64.52	34.05	0.528	0.711
10G-12B-P9	70.35	37.61	0.535	0.813
10N-12B-P9	70.35	37.63	0.535	0.819
11-53-B-D	60.10	33.89	0.564	0.826
11-20-4/2/2-6/6-S5	67.30	40.61	0.603	1.021
5-8C3-16-3-U	69.00	43.31	0.628	0.826
11-20-4/2/2/-6/6-SP	67.30	42.34	0.629	0.988
3-5-40-B	60.10	38.21	0.636	0.899
2-8C3-16-2-U	69.00	43.99	0.638	0.850
8G-16B-P9	66.40	42.44	0.639	0.925
3-8S3-16-2-U	71.10	46.47	0.654	0.895
3-5-53-B	60.10	39.44	0.656	0.927
4-8S3-16-2-U	71.10	47.06	0.662	0.893
5-8C3-16-2-U	69.00	46.51	0.674	0.918
2-5-40-B(4)	60.10	41.59	0.692	1.044
15G-12B-P9	70.35	49.09	0.698	0.953
2-4.5-53-B	60.10	42.00	0.699	1.024
9.3	79.00	55.25	0.699	0.894
4-8S3-16-3-U	71.10	50.04	0.704	0.915
11-53-B	60.10	42.32	0.704	1.038
20-11-4	67.28	47.51	0.706	0.916
2-4.5-80-B	60.10	42.54	0.708	1.032
11-30-4/2/2-6/6-S5	65.00	46.47	0.715	0.945
15N-12B-P9	70.35	50.77	0.722	1.017
7	64.52	46.60	0.722	0.870
20-8-19	60.90	44.56	0.732	0.899
8N-18B-P9	70.35	51.68	0.735	1.016
8N-9B-P6	76.63	56.55	0.738	0.900
20-8-20	60.90	44.95	0.738	0.929
8G-18B-P9	70.35	52.38	0.745	1.010
10.3	79.00	58.85	0.745	0.911
7-8C3-16-3-U	69.00	51.49	0.746	0.911
11-40-B-A	60.10	44.94	0.748	1.023
			Min	0.711
			Max	1.044
			Mean	0.926
			Std	0.079
			COV	0.085

Note: Refer to last page of Table 5.17 for footnote.

Table 5.17b: Test/Prediction Ratios for Conventional Bars Confined by Stirrups and $3/4 < f_s/f_y \leq 1$*

Tests No.	f_y (ksi)	f_s (ksi)	f_s/f_y	Test/Prediction
20-8-21	60.90	45.76	0.751	0.950
8F36h	74.00	56.02	0.757	0.758
11-40-B	60.10	45.58	0.758	1.056
20-11-3	69.02	52.37	0.759	0.995
8F30b	74.00	57.47	0.777	0.911
20-11-7	66.12	51.38	0.777	0.937
11.2	79.00	61.94	0.784	0.926
10.4	79.00	61.98	0.785	0.834
6	64.52	50.77	0.787	0.999
8G-22B-P9	66.40	52.76	0.795	0.960
20-8-13	64.38	51.22	0.796	0.953
6-8C3-22 3/4-4-U	69.00	55.67	0.807	0.843
1-8N3-16-2-U	69.00	56.00	0.812	1.084
6-8C3-22 3/4-3-U	69.00	56.45	0.818	0.878
20-11-6	66.12	54.54	0.825	0.941
20-8-14	64.38	53.28	0.828	1.047
8F36c	74.00	61.33	0.829	0.864
20-8-15	64.38	54.68	0.849	1.068
8F36j	74.00	64.09	0.866	0.893
8.1	79.00	69.67	0.882	1.047
11R36a	93.00	82.35	0.886	1.072
4a	68.87	61.08	0.887	1.227
20-9-1	66.12	58.74	0.888	1.063
20-11-8	69.02	61.36	0.889	1.101
2.1	70.00	62.43	0.892	0.874
4.1	70.00	62.51	0.893	0.822
20-8-18	60.90	54.80	0.900	1.115
20-8-16	60.90	54.82	0.900	1.037
20-8-8	65.54	59.58	0.909	0.967
9-53-B	62.80	57.36	0.913	1.315
3b	64.52	59.03	0.915	1.104
20-8-9	65.54	60.05	0.916	0.991
8G-9B-P6	76.63	70.39	0.919	1.109
20-8-7	65.54	61.35	0.936	0.980
8-15-4/2/2-6/6-S5	61.10	57.31	0.938	1.156
20-11-5	66.12	63.81	0.965	1.128
20-6-2	72.50	70.12	0.967	1.095
20-8-3	65.54	64.02	0.977	0.969
20-8-10	65.54	64.03	0.977	1.035
20-8-12	65.54	64.20	0.979	1.044
20-9-2	66.12	64.82	0.980	1.168
4b	68.87	67.65	0.982	1.215
20-8-2	65.54	64.84	0.989	0.984
20-8-17	60.90	60.78	0.998	1.199
			Min	0.758
			Max	1.315
			Mean	1.016
			Std	0.120
			COV	0.118

Note: Refer to last page of Table 5.17 for footnote.

Table 5.17c: Test/Prediction Ratios for Conventional Bars Confined by Stirrups and $f_s/f_y > 1$*

Tests No.	f_y (ksi)	f_s (ksi)	f_s/f_y	Test/Prediction
8F36d	74.00	74.31	1.004	0.915
8F36g	74.00	75.78	1.024	1.024
10	68.87	70.99	1.031	1.155
20-11-1	66.12	68.59	1.037	1.078
20-6-3	72.50	75.55	1.042	1.232
8F36e	74.00	77.44	1.047	0.982
20-11-2	67.28	70.91	1.054	1.131
8F36f	74.00	78.15	1.056	0.956
3a	64.52	69.76	1.081	1.291
1b	64.52	69.82	1.082	1.251
20-6-1	72.50	78.49	1.083	1.240
20-8-1	65.54	71.05	1.084	1.095
20-8-4	65.54	71.94	1.098	1.162
9	68.87	76.40	1.109	1.226
20-8-11	65.54	75.00	1.144	1.249
1a	64.52	74.05	1.148	1.313
20-8-6	65.54	75.37	1.150	1.183
20-8-5	65.54	76.01	1.160	1.208
			Min	0.915
			Max	1.313
			Mean	1.149
			Std	0.118
			COV	0.103

* For only tests whose f_y are known

Table 6.1: Data for Monte Carlo Simulations of Beams Containing Bars Not Confined by Transverse Reinforcement

Beam	b (in.)	h (in.)	f'_c (psi)	C_b (in.)	C_{so} (in.)	n_b	d_b (in.)	A_b (in.^{2})	l_s* (in.)
1	8.00	12.00	4000	2.00	2.00	2	0.75	0.44	31.63
2	12.00	12.00	4000	2.00	2.00	2	0.75	0.44	17.95
3	12.00	12.00	4000	2.00	2.00	2	1.00	0.79	30.61
4	12.00	12.00	4000	2.00	2.00	2	1.27	1.27	51.47
5	12.00	12.00	4000	2.00	2.00	2	1.41	1.56	67.70
6	24.00	12.00	4000	2.00	2.00	2	0.75	0.44	17.95
7	24.00	12.00	4000	2.00	2.00	4	0.75	0.44	17.95
8	24.00	12.00	4000	2.00	2.00	6	0.75	0.44	23.42
9	24.00	12.00	4000	2.00	2.00	8	0.75	0.44	30.47
10	24.00	12.00	4000	2.00	2.00	2	1.00	0.79	30.61
11	24.00	12.00	4000	2.00	2.00	4	1.00	0.79	30.61
12	24.00	12.00	4000	2.00	2.00	6	1.00	0.79	44.69
13	24.00	12.00	4000	2.00	2.00	2	1.27	1.27	46.69
14	24.00	12.00	4000	2.00	2.00	4	1.27	1.27	48.41
15	24.00	12.00	4000	2.00	2.00	2	1.41	1.56	55.87
16	24.00	12.00	4000	2.00	2.00	4	1.41	1.56	61.53
17	12.00	24.00	3000	2.00	2.00	2	0.75	0.44	19.78
18	12.00	24.00	4000	2.00	2.00	2	0.75	0.44	17.95
19	12.00	24.00	6000	2.00	2.00	2	0.75	0.44	15.57
20	12.00	24.00	3000	2.00	2.00	2	1.00	0.79	33.75
21	12.00	24.00	4000	2.00	2.00	2	1.00	0.79	30.61
22	12.00	24.00	6000	2.00	2.00	2	1.00	0.79	26.56
23	12.00	24.00	3000	2.00	2.00	2	1.27	1.27	56.77
24	12.00	24.00	4000	2.00	2.00	2	1.27	1.27	51.47
25	12.00	24.00	6000	2.00	2.00	2	1.27	1.27	44.62
26	12.00	24.00	3000	2.00	2.00	2	1.41	1.56	74.73
27	12.00	24.00	4000	2.00	2.00	2	1.41	1.56	67.70
28	12.00	24.00	6000	2.00	2.00	2	1.41	1.56	58.63
29	18.00	24.00	4000	2.00	2.00	4	0.75	0.44	21.13
30	18.00	24.00	4000	2.00	2.00	6	0.75	0.44	31.63
31	18.00	24.00	4000	2.00	2.00	2	1.00	0.79	30.61
32	18.00	24.00	4000	2.00	2.00	4	1.00	0.79	40.91
33	18.00	24.00	4000	2.00	2.00	2	1.27	1.27	46.69
34	18.00	24.00	4000	2.00	2.00	4	1.27	1.27	70.39
35	18.00	24.00	4000	2.00	2.00	2	1.41	1.56	55.87

* Computed using Eq. 6.1 with the right side multiplied by $\phi_d = 0.90$.

Table 6.2: Monte Carlo Simulation Results (average of 1000 runs) for Beams Containing Bars Not Confined by Transverse Reinforcement

Beam	b	f'_c	C_b	C_{so}	C_{si}	l_s	n_b	d_b	A_b	$A_b f_s$	$\overline{R}$	V_R	Cumulative	
	(in.)	(psi)	(in.)	(in.)	(in.)	(in.)		(in.)	($in.^2$)	(lb)			$\overline{R}$	V_R
1	8.07	3556	1.98	2.08	0.53	31.61	2	0.75	0.44	28593	0.975	0.127	0.975	0.127
2	12.17	3550	2.00	1.99	2.55	17.94	2	0.75	0.44	27521	0.938	0.102	0.956	0.117
3	11.94	3539	2.00	2.32	2.05	30.60	2	1.00	0.79	49235	0.935	0.101	0.949	0.113
4	11.90	3595	1.99	1.82	1.51	51.47	2	1.27	1.27	81395	0.961	0.094	0.952	0.109
5	12.21	3558	1.98	2.34	1.23	67.72	2	1.41	1.56	101102	0.972	0.101	0.956	0.107
6	24.04	3567	1.99	2.11	8.55	17.97	2	0.75	0.44	27541	0.939	0.109	0.953	0.108
7	24.19	3576	1.99	1.97	2.35	17.93	4	0.75	0.44	27404	0.934	0.109	0.951	0.108
8	24.67	3571	1.98	1.77	1.11	23.44	6	0.75	0.44	28412	0.969	0.094	0.953	0.107
9	23.88	3552	1.99	2.04	0.58	30.46	8	0.75	0.44	28319	0.966	0.094	0.954	0.105
10	24.14	3565	1.99	1.65	8.05	30.61	2	1.00	0.79	49297	0.936	0.103	0.952	0.105
11	23.86	3589	1.98	2.01	2.01	30.59	4	1.00	0.79	49393	0.938	0.100	0.951	0.105
12	24.15	3564	2.00	1.65	0.81	44.69	6	1.00	0.79	51160	0.971	0.090	0.953	0.104
13	24.05	3545	1.99	1.43	7.53	46.67	2	1.27	1.27	79001	0.933	0.101	0.951	0.104
14	24.20	3578	1.99	1.79	1.65	48.37	4	1.27	1.27	79771	0.942	0.092	0.951	0.103
15	24.11	3590	1.98	2.04	7.23	55.86	2	1.41	1.56	97927	0.942	0.103	0.950	0.103
16	23.85	3569	1.99	1.94	1.47	61.51	4	1.41	1.56	99916	0.961	0.089	0.951	0.102
17	12.10	2637	2.00	2.44	2.55	19.76	2	0.75	0.44	27245	0.929	0.114	0.949	0.103
18	12.14	3557	1.99	2.05	2.55	17.94	2	0.75	0.44	27321	0.931	0.106	0.948	0.103
19	12.13	5433	1.97	2.13	2.54	15.55	2	0.75	0.44	27608	0.941	0.103	0.948	0.103
20	12.00	2640	1.98	1.70	2.05	33.76	2	1.00	0.79	48628	0.923	0.103	0.947	0.103
21	12.06	3574	1.97	2.06	2.04	30.65	2	1.00	0.79	48968	0.930	0.106	0.946	0.104
22	12.04	5443	1.99	2.26	2.05	26.54	2	1.00	0.79	49356	0.937	0.100	0.946	0.104
23	11.93	2656	1.98	2.01	1.51	56.77	2	1.27	1.27	80519	0.951	0.101	0.946	0.103
24	12.13	3564	1.99	1.99	1.51	51.47	2	1.27	1.27	81184	0.959	0.098	0.946	0.103
25	12.09	5449	1.98	1.80	1.51	44.65	2	1.27	1.27	81280	0.960	0.092	0.947	0.103
26	11.87	2645	1.99	1.71	1.24	74.72	2	1.41	1.56	101364	0.975	0.103	0.948	0.103
27	12.14	3597	1.98	1.88	1.22	67.68	2	1.41	1.56	101135	0.973	0.099	0.949	0.103
28	12.01	5435	1.98	1.69	1.22	58.62	2	1.41	1.56	101755	0.978	0.096	0.950	0.103
29	17.77	3566	1.97	2.55	1.35	21.08	4	0.75	0.44	28270	0.964	0.100	0.950	0.103
30	18.38	3563	1.98	1.75	0.51	31.60	6	0.75	0.44	28424	0.969	0.092	0.951	0.103
31	18.45	3580	1.99	1.76	5.05	30.58	2	1.00	0.79	49038	0.931	0.105	0.950	0.103
32	17.69	3557	1.97	2.35	1.02	40.87	4	1.00	0.79	51000	0.968	0.093	0.951	0.102
33	17.64	3566	1.97	2.19	4.51	46.74	2	1.27	1.27	79005	0.933	0.111	0.950	0.103
34	18.22	3573	2.00	1.78	0.66	70.40	4	1.27	1.27	82593	0.976	0.093	0.951	0.103
35	18.46	3571	2.00	2.42	4.23	55.88	2	1.41	1.56	97950	0.942	0.101	0.951	0.103

Table 6.3: Data for Monte Carlo Simulations of Beams Containing Bars Confined by Transverse Reinforcement

Beam	b	h	f'_c	C_b	C_{so}	n_d	d_b	A_b	A_v	s	l_s*
	(in.)	(in.)	(psi)	(in.)	(in.)		(in.)	($in.^2$)	($in.^2$)	(in.)	(in.)
1	8.00	12.00	4000	2.00	2.00	2	0.75	0.44	0.11	4.81	17.97
2	12.00	12.00	4000	2.00	2.00	2	0.75	0.44	0.11	4.81	12.44
3	12.00	12.00	4000	2.00	2.00	2	1.00	0.79	0.11	4.75	22.19
4	12.00	12.00	4000	2.00	2.00	2	1.27	1.27	0.11	4.68	37.32
5	12.00	12.00	4000	2.00	2.00	2	1.41	1.56	0.11	4.65	48.26
6	24.00	12.00	4000	2.00	2.00	2	0.75	0.44	0.11	4.81	12.44
7	24.00	12.00	4000	2.00	2.00	4	0.75	0.44	0.11	4.81	14.22
8	24.00	12.00	4000	2.00	2.00	6	0.75	0.44	0.11	4.81	18.85
9	24.00	12.00	4000	2.00	2.00	8	0.75	0.44	0.11	4.81	24.45
10	24.00	12.00	4000	2.00	2.00	2	1.00	0.79	0.11	4.75	22.19
11	24.00	12.00	4000	2.00	2.00	4	1.00	0.79	0.11	4.75	25.27
12	24.00	12.00	4000	2.00	2.00	6	1.00	0.79	0.11	4.75	36.84
13	24.00	12.00	4000	2.00	2.00	2	1.27	1.27	0.11	4.68	34.73
14	24.00	12.00	4000	2.00	2.00	4	1.27	1.27	0.11	4.68	40.61
15	24.00	12.00	4000	2.00	2.00	2	1.41	1.56	0.11	4.65	41.94
16	24.00	12.00	4000	2.00	2.00	4	1.41	1.56	0.11	4.65	51.55
17	12.00	24.00	3000	2.00	2.00	2	0.75	0.44	0.11	10.81	16.05
18	12.00	24.00	4000	2.00	2.00	2	0.75	0.44	0.11	10.81	14.45
19	12.00	24.00	6000	2.00	2.00	2	0.75	0.44	0.11	10.81	12.38
20	12.00	24.00	3000	2.00	2.00	2	1.00	0.79	0.11	10.75	28.43
21	12.00	24.00	4000	2.00	2.00	2	1.00	0.79	0.11	10.75	25.68
22	12.00	24.00	6000	2.00	2.00	2	1.00	0.79	0.11	10.75	22.13
23	12.00	24.00	3000	2.00	2.00	2	1.27	1.27	0.11	10.68	48.18
24	12.00	24.00	4000	2.00	2.00	2	1.27	1.27	0.11	10.68	43.58
25	12.00	24.00	6000	2.00	2.00	2	1.27	1.27	0.11	10.68	37.62
26	12.00	24.00	3000	2.00	2.00	2	1.41	1.56	0.11	10.65	63.02
27	12.00	24.00	4000	2.00	2.00	2	1.41	1.56	0.11	10.65	56.98
28	12.00	24.00	6000	2.00	2.00	2	1.41	1.56	0.11	10.65	49.18
29	18.00	24.00	4000	2.00	2.00	4	0.75	0.44	0.20	10.81	16.83
30	18.00	24.00	4000	2.00	2.00	6	0.75	0.44	0.20	10.81	24.95
31	18.00	24.00	4000	2.00	2.00	2	1.00	0.79	0.20	10.75	23.31
32	18.00	24.00	4000	2.00	2.00	4	1.00	0.79	0.20	10.75	33.31
33	18.00	24.00	4000	2.00	2.00	2	1.27	1.27	0.20	10.68	36.48
34	18.00	24.00	4000	2.00	2.00	4	1.27	1.27	0.20	10.68	57.39
35	18.00	24.00	4000	2.00	2.00	2	1.41	1.56	0.20	10.65	44.06

* Computed using Eq. 6.2b with the right side multiplied by $\phi_d = 0.90$.

Table 6.4: Monte Carlo Simulation Results (average of 1000 runs) for Beams Containing Bars Confined by Transverse Reinforcement

Beam	b	f'_c	C_b	C_{so}	C_{si}	l_s	n_b	d_b	A_b	A_{tr}	s	$A_b f_s$	$\overline{R}$	V_R	Cumulative	
	(in.)	(psi)	(in.)	(in.)	(in.)	(in.)		(in.)	($in.^2$)	($in.^2$)	(in.)	(lb)			$\overline{R}$	V_R
1	8.15	3571	2.00	2.05	0.55	17.99	2	0.75	0.44	0.11	4.81	28743	0.980	0.136	0.980	0.136
2	11.82	3592	1.98	2.01	2.54	12.43	2	0.75	0.44	0.11	4.81	27898	0.951	0.132	0.965	0.135
3	12.04	3593	2.00	1.90	2.05	22.13	2	1.00	0.79	0.11	4.75	50000	0.949	0.134	0.960	0.135
4	12.11	3554	2.00	2.22	1.52	37.34	2	1.27	1.27	0.11	4.68	81674	0.965	0.126	0.961	0.133
5	11.91	3589	1.99	1.79	1.22	48.28	2	1.41	1.56	0.11	4.65	101769	0.979	0.130	0.965	0.132
6	24.15	3558	1.99	2.24	8.57	12.40	2	0.75	0.44	0.11	4.81	27704	0.944	0.141	0.961	0.134
7	23.87	3542	1.99	2.16	2.35	14.22	4	0.75	0.44	0.11	4.81	29079	0.904	0.145	0.953	0.137
8	24.19	3541	1.99	1.81	1.11	18.83	6	0.75	0.44	0.04	4.81	28440	0.970	0.135	0.955	0.137
9	24.39	3570	2.00	1.79	0.58	24.44	8	0.75	0.44	0.03	4.81	28561	0.974	0.125	0.957	0.136
10	24.20	3569	1.99	1.68	8.05	22.18	2	1.00	0.79	0.11	4.75	50248	0.954	0.133	0.957	0.135
11	23.96	3568	1.98	1.86	2.01	25.29	4	1.00	0.79	0.06	4.75	52011	0.900	0.143	0.952	0.137
12	24.14	3577	1.98	1.66	0.81	36.81	6	1.00	0.79	0.04	4.75	51295	0.974	0.123	0.954	0.136
13	24.17	3563	1.99	2.19	7.51	34.73	2	1.27	1.27	0.11	4.68	80628	0.952	0.130	0.954	0.136
14	23.96	3553	2.00	1.50	1.66	40.63	4	1.27	1.27	0.06	4.68	82189	0.971	0.135	0.955	0.136
15	23.99	3564	1.99	2.12	7.24	41.89	2	1.41	1.56	0.11	4.65	98474	0.947	0.130	0.954	0.135
16	24.18	3574	1.99	1.98	1.47	51.55	4	1.41	1.56	0.06	4.65	101739	0.978	0.121	0.956	0.135
17	12.27	2636	2.00	2.57	2.55	16.06	2	0.75	0.44	0.11	10.81	27671	0.943	0.141	0.955	0.135
18	12.04	3562	1.98	2.13	2.55	14.42	2	0.75	0.44	0.11	10.81	27667	0.943	0.138	0.954	0.135
19	12.20	5428	1.99	2.05	2.54	12.38	2	0.75	0.44	0.11	10.81	27810	0.948	0.139	0.954	0.135
20	12.16	2630	1.99	1.77	2.04	28.42	2	1.00	0.79	0.11	10.75	49241	0.935	0.131	0.953	0.135
21	11.99	3572	1.99	1.95	2.04	25.70	2	1.00	0.79	0.11	10.75	49529	0.940	0.132	0.952	0.135
22	12.01	5423	1.99	1.94	2.04	22.17	2	1.00	0.79	0.11	10.75	50021	0.950	0.129	0.952	0.135
23	12.15	2633	1.98	1.78	1.51	48.18	2	1.27	1.27	0.11	10.68	80655	0.953	0.131	0.952	0.135
24	12.32	3566	1.99	2.03	1.50	43.58	2	1.27	1.27	0.11	10.68	81513	0.963	0.133	0.953	0.135
25	12.14	5449	1.99	1.51	1.51	37.61	2	1.27	1.27	0.11	10.68	82495	0.974	0.131	0.954	0.135
26	11.96	2635	1.98	1.98	1.23	62.98	2	1.41	1.56	0.11	10.65	100802	0.969	0.132	0.954	0.135
27	12.17	3553	2.00	2.05	1.23	56.97	2	1.41	1.56	0.11	10.65	100823	0.969	0.134	0.955	0.135
28	11.98	5409	1.98	2.13	1.24	49.17	2	1.41	1.56	0.11	10.65	102222	0.983	0.128	0.956	0.134
29	17.87	3545	1.99	2.23	1.35	16.79	4	0.75	0.44	0.10	10.81	28535	0.973	0.132	0.956	0.134
30	17.78	3559	2.00	2.12	0.51	24.92	6	0.75	0.44	0.07	10.81	28654	0.977	0.125	0.957	0.134
31	17.94	3569	1.99	1.99	5.04	23.33	2	1.00	0.79	0.20	10.75	50064	0.951	0.138	0.957	0.134
32	17.83	3566	1.98	1.84	1.01	33.25	4	1.00	0.79	0.10	10.75	51171	0.972	0.126	0.957	0.134
33	18.14	3555	1.99	2.11	4.50	36.45	2	1.27	1.27	0.20	10.68	80263	0.948	0.131	0.957	0.134
34	17.84	3570	1.99	2.16	0.66	57.37	4	1.27	1.27	0.10	10.68	82999	0.980	0.127	0.958	0.134
35	18.38	3591	1.98	1.90	4.23	44.07	2	1.41	1.56	0.20	10.65	98349	0.946	0.128	0.957	0.134

Table 6.5: Calculated Resistance Factors

	Without stirrups			With stirrups		
$\bar{r}$		0.951			0.957	
V_r		0.103			0.134	
$(Q_L/Q_D)_n$	0.5	1.0	1.5	0.5	1.0	1.5
$\bar{q}$	0.675	0.647	0.631	0.675	0.647	0.631
V_q	0.102	0.131	0.152	0.102	0.131	0.152
ϕ_b	0.849	0.821	0.793	0.787	0.769	0.747
$\phi_d = \phi_d/0.9$	0.943	0.912	0.881	0.874	0.854	0.830

Table 6.6: Comparison of Development/Splice Lengths for Bars Not Confined by Transverse Reinforcement*

Beam	Eq. 6.40	ACI 95		Eq. 6.40/ACI 95	
	l_d (in.)	l_d (in.)	l_s (in.)	l_d	l_s
1	34.32	36.59	47.57	0.938	0.722
2	19.40	17.08	22.20	1.136	0.874
3	33.08	28.46	37.00	1.162	0.894
4	55.66	54.78	71.21	1.016	0.782
5	73.24	75.04	97.56	0.976	0.751
6	19.40	17.08	22.20	1.136	0.874
7	19.40	17.08	22.20	1.136	0.874
8	25.34	21.71	28.22	1.167	0.898
9	33.05	33.83	43.98	0.977	0.751
10	33.08	28.46	37.00	1.162	0.894
11	33.08	28.46	37.00	1.162	0.894
12	48.40	54.73	71.15	0.884	0.680
13	50.46	43.55	56.62	1.159	0.891
14	52.32	50.44	65.58	1.037	0.798
15	60.38	52.29	67.98	1.155	0.888
16	66.53	65.54	85.20	1.015	0.781
17	21.34	19.72	25.63	1.082	0.833
18	19.40	17.08	22.20	1.136	0.874
19	16.88	13.94	18.13	1.211	0.931
20	36.40	32.86	42.72	1.108	0.852
21	33.08	28.46	37.00	1.162	0.894
22	28.79	23.24	30.21	1.239	0.953
23	61.27	63.25	82.23	0.969	0.745
24	55.66	54.78	71.21	1.016	0.782
25	48.40	44.73	58.14	1.082	0.832
26	80.68	86.65	112.65	0.931	0.716
27	73.24	75.04	97.56	0.976	0.751
28	63.63	61.27	79.65	1.039	0.799
29	22.86	18.74	24.36	1.219	0.938
30	34.32	36.59	47.57	0.938	0.722
31	33.08	28.46	37.00	1.162	0.894
32	44.28	47.43	61.66	0.934	0.718
33	50.46	43.55	56.62	1.159	0.891
34	76.31	90.01	117.01	0.848	0.652
35	60.38	52.29	67.98	1.155	0.888
			Average	1.074	0.826

* Refer to Table 6.1 for beam data.

Table 6.7: Comparison of Development/Splice Lengths for Bars Confined by Transverse Reinforcement**

	Development or Splice Length*				ACI 95		Conv./ACI 95		High R_r/Conv.			High R_r/ACI 95 l_d			High R_r/ACI 95 l_s		
Beam	Conv. (in.)	$R_r = 0.140$ (in.)	$R_r = 0.119$ (in.)	$R_r = 0.101$ (in.)	l_d (in.)	l_s (in.)	l_d	l_s	$R_r = 0.140$	$R_r = 0.119$	$R_r = 0.101$	$R_r = 0.140$	$R_r = 0.119$	$R_r = 0.101$	$R_r = 0.140$	$R_r = 0.119$	$R_r = 0.101$
1	19.63	14.10	15.48	16.90	17.89	23.26	1.097	0.844	0.718	0.788	0.861	0.788	0.865	0.945	0.606	0.665	0.727
2	13.53	10.42	11.11	11.87	17.08	22.20	0.792	0.609	0.770	0.821	0.878	0.610	0.651	0.695	0.470	0.501	0.535
3	24.06	19.80	21.07	22.21	28.46	37.00	0.846	0.650	0.823	0.875	0.923	0.696	0.740	0.780	0.535	0.569	0.600
4	40.44	33.98	36.25	38.09	37.82	49.16	1.069	0.823	0.840	0.896	0.942	0.899	0.958	1.007	0.691	0.737	0.775
5	52.30	43.95	47.05	49.50	49.95	64.94	1.047	0.805	0.840	0.900	0.946	0.880	0.942	0.991	0.677	0.724	0.762
6	13.53	10.42	11.11	11.87	17.08	22.20	0.792	0.609	0.770	0.821	0.878	0.610	0.651	0.695	0.470	0.501	0.535
7	13.53	10.42	11.11	11.87	17.08	22.20	0.792	0.609	0.770	0.821	0.878	0.610	0.651	0.695	0.470	0.501	0.535
8	20.53	16.78	17.37	18.21	17.99	23.39	1.141	0.878	0.817	0.846	0.887	0.933	0.966	1.012	0.717	0.743	0.779
9	26.69	21.72	22.49	23.60	27.25	35.42	0.980	0.754	0.814	0.843	0.884	0.797	0.825	0.866	0.613	0.635	0.666
10	24.06	19.80	21.07	22.21	28.46	37.00	0.846	0.650	0.823	0.875	0.923	0.696	0.740	0.780	0.535	0.569	0.600
11	24.06	19.80	21.07	22.21	28.46	37.00	0.846	0.650	0.823	0.875	0.923	0.696	0.740	0.780	0.535	0.569	0.600
12	40.03	34.65	35.96	37.29	44.23	57.50	0.905	0.696	0.866	0.898	0.931	0.784	0.813	0.843	0.603	0.625	0.649
13	37.61	31.90	33.88	35.50	36.14	46.99	1.040	0.800	0.848	0.901	0.944	0.883	0.937	0.982	0.679	0.721	0.756
14	43.99	39.20	40.66	41.94	41.81	54.35	1.052	0.809	0.891	0.924	0.953	0.938	0.973	1.003	0.721	0.748	0.772
15	45.40	38.89	41.27	43.15	40.13	52.17	1.131	0.870	0.857	0.909	0.950	0.969	1.028	1.075	0.746	0.791	0.827
16	55.83	50.00	51.94	53.54	53.75	69.88	1.039	0.799	0.896	0.930	0.959	0.930	0.966	0.996	0.716	0.743	0.766
17	17.40	14.44	14.96	15.63	19.72	25.63	0.883	0.679	0.830	0.859	0.898	0.732	0.758	0.793	0.563	0.583	0.610
18	15.71	12.86	13.32	13.96	17.08	22.20	0.920	0.708	0.819	0.848	0.888	0.753	0.780	0.817	0.579	0.600	0.629
19	13.52	10.82	11.21	11.80	13.94	18.13	0.970	0.746	0.800	0.829	0.873	0.776	0.804	0.846	0.597	0.618	0.651
20	30.75	27.05	27.96	28.89	32.86	42.72	0.936	0.720	0.880	0.909	0.939	0.823	0.851	0.879	0.633	0.655	0.676
21	27.85	24.33	25.15	26.02	28.46	37.00	0.978	0.753	0.874	0.903	0.934	0.855	0.884	0.914	0.658	0.680	0.703
22	24.09	20.81	21.52	22.31	23.24	30.21	1.037	0.797	0.864	0.893	0.926	0.896	0.926	0.960	0.689	0.712	0.738
23	52.09	46.78	48.43	49.85	52.86	68.72	0.985	0.758	0.898	0.930	0.957	0.885	0.916	0.943	0.681	0.705	0.725
24	47.21	42.23	43.72	45.04	45.78	59.51	1.031	0.793	0.895	0.926	0.954	0.922	0.955	0.984	0.710	0.735	0.757
25	40.90	36.35	37.64	38.82	37.38	48.59	1.094	0.842	0.889	0.920	0.949	0.972	1.007	1.039	0.748	0.775	0.799
26	68.14	61.33	63.64	65.53	71.07	92.39	0.959	0.737	0.900	0.934	0.962	0.863	0.895	0.922	0.664	0.689	0.709
27	61.74	55.40	57.49	59.22	61.55	80.01	1.003	0.772	0.897	0.931	0.959	0.900	0.934	0.962	0.692	0.718	0.740
28	53.48	47.73	49.53	51.08	50.25	65.33	1.064	0.819	0.892	0.926	0.955	0.950	0.986	1.016	0.731	0.758	0.782
29	18.31	14.91	15.47	16.24	17.08	22.20	1.072	0.825	0.814	0.845	0.887	0.873	0.906	0.951	0.672	0.697	0.732
30	27.25	21.99	22.85	24.04	28.55	37.11	0.955	0.734	0.807	0.838	0.882	0.770	0.800	0.842	0.592	0.616	0.648
31	25.27	21.19	22.35	23.42	28.46	37.00	0.888	0.683	0.839	0.884	0.927	0.745	0.785	0.823	0.573	0.604	0.633
32	36.17	31.16	32.42	33.68	38.01	49.41	0.952	0.732	0.861	0.896	0.931	0.820	0.853	0.886	0.631	0.656	0.682
33	39.50	34.16	35.95	37.44	36.14	46.99	1.093	0.841	0.865	0.910	0.948	0.945	0.995	1.036	0.727	0.765	0.797
34	62.35	54.81	57.18	59.23	69.57	90.45	0.896	0.689	0.879	0.917	0.950	0.788	0.822	0.851	0.606	0.632	0.655
35	47.70	41.65	43.79	45.51	40.93	53.20	1.165	0.896	0.873	0.918	0.954	1.018	1.070	1.112	0.783	0.823	0.855
						Average	0.980	0.754	0.844	0.884	0.924	0.829	0.868	0.906	0.637	0.668	0.697

* Development or splice length based on the appropriate recommended design equation (Eqs. 6.27 to 6.30).

** Refer to Table 6.3 for beam data.

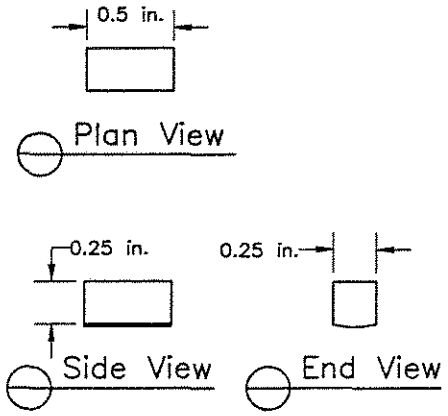

Fig. 2.1 Reinforcing steel specimen for friction test

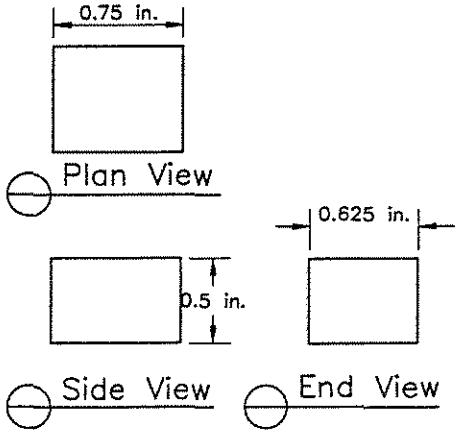

Fig. 2.2 Mortar specimen for friction test

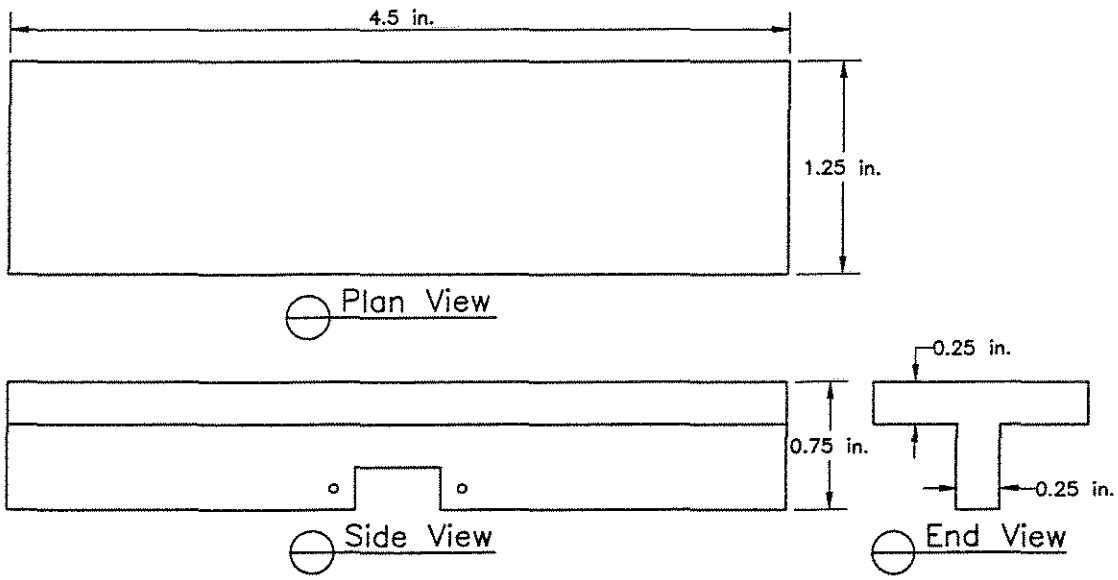

Fig. 2.3 Steel yoke for mounting reinforcing steel specimen for friction test

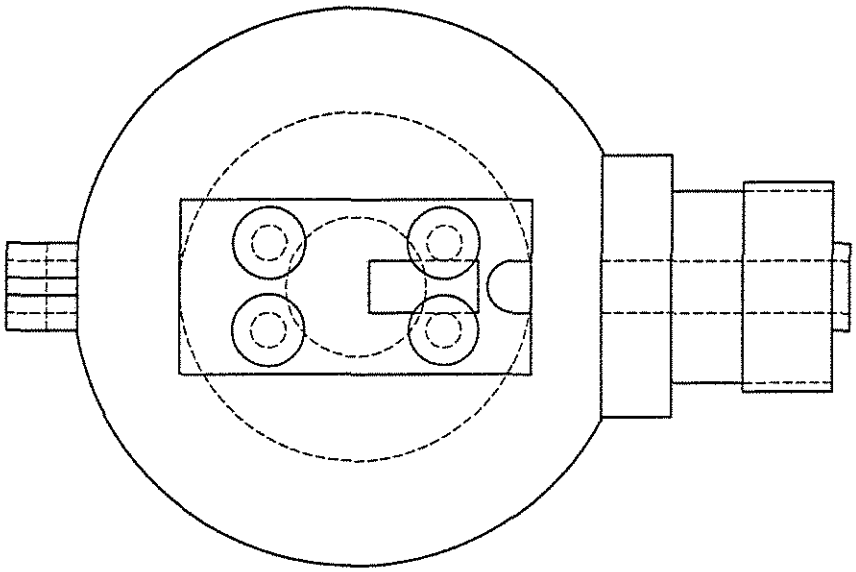

(a)

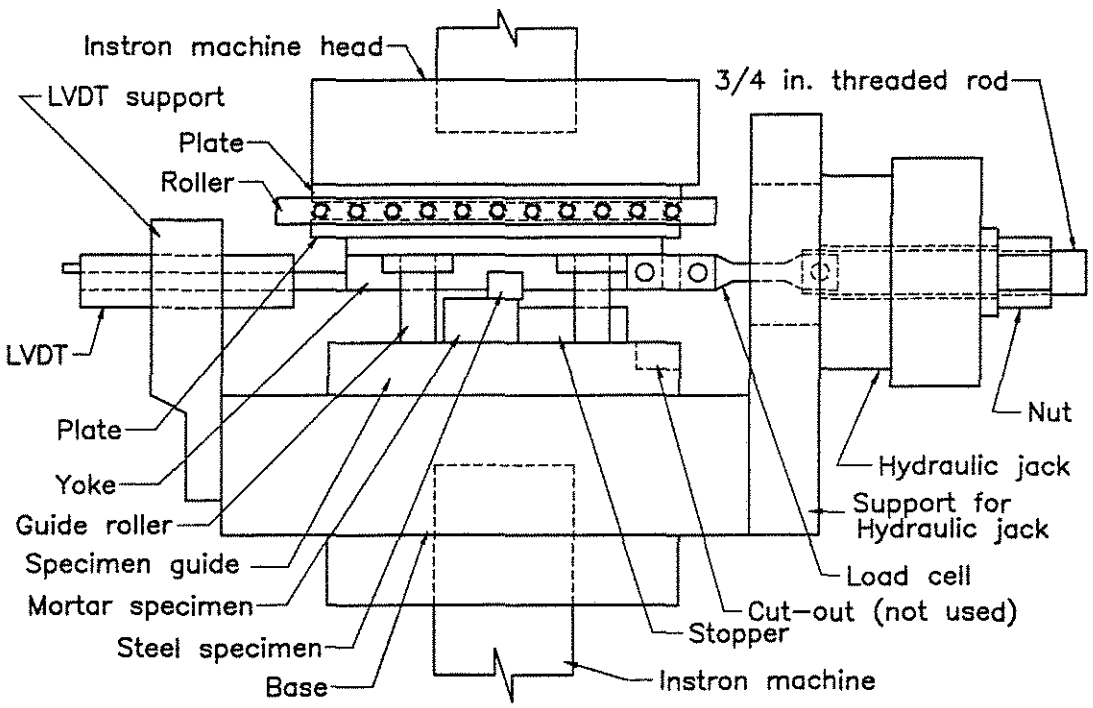

(b)

Fig. 2.4 Friction test apparatus, (a) plan view of hydraulic jack, support for hydraulic jack, specimen guide, stopper, and LVDT support for friction test apparatus, (b) side view of assembled friction test apparatus

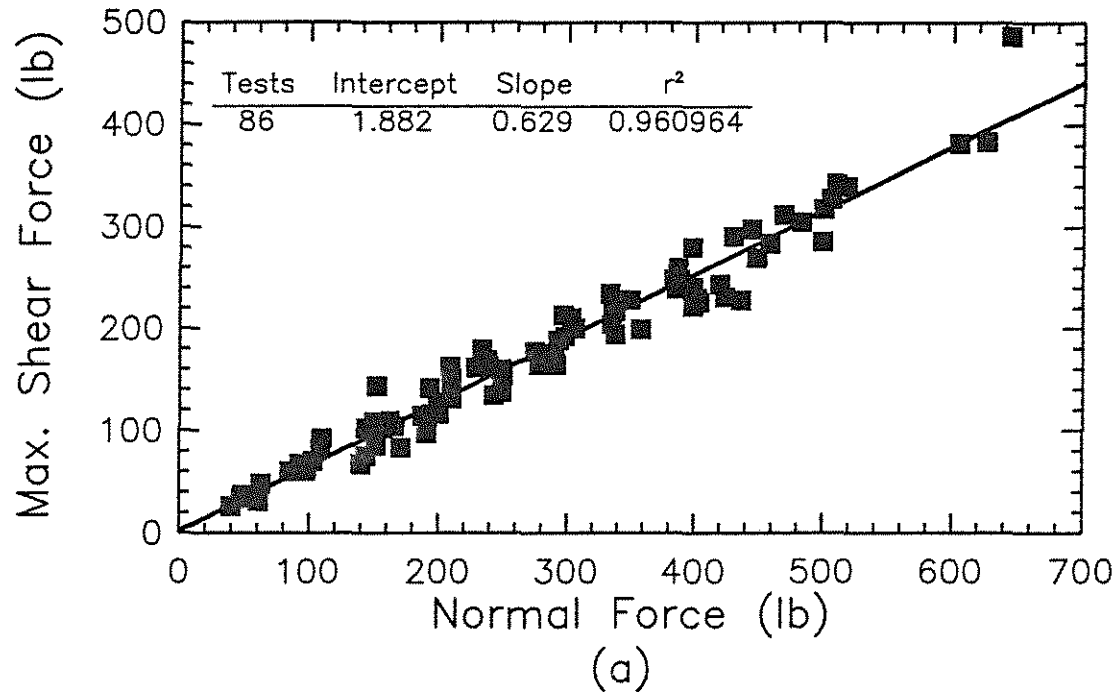

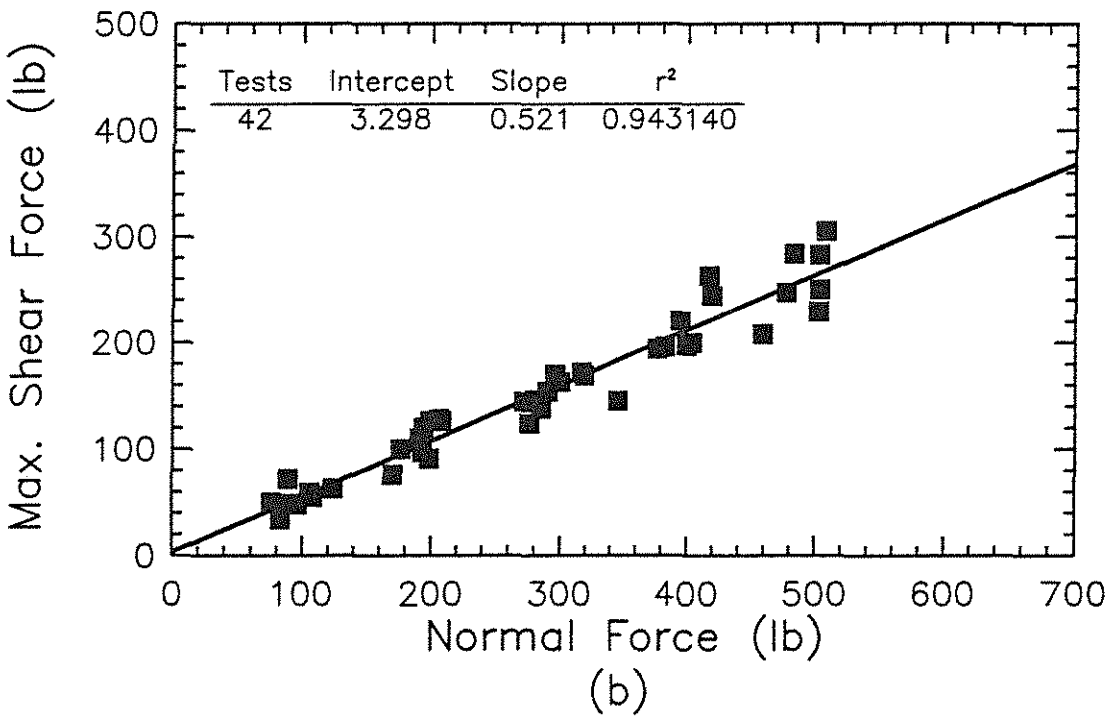

Fig. 2.5 Maximum shear force versus normal force for uncoated reinforcing bar specimens at 7 days - Series 1, (a) formed-surface mortar, (b) hand finished-surface mortar

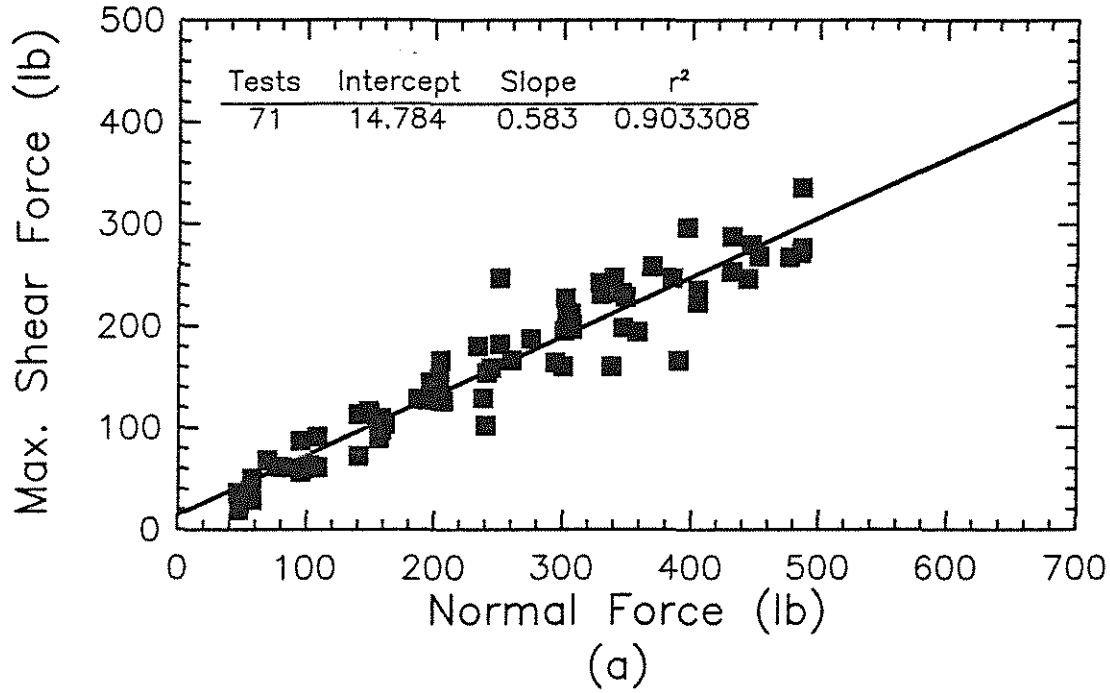

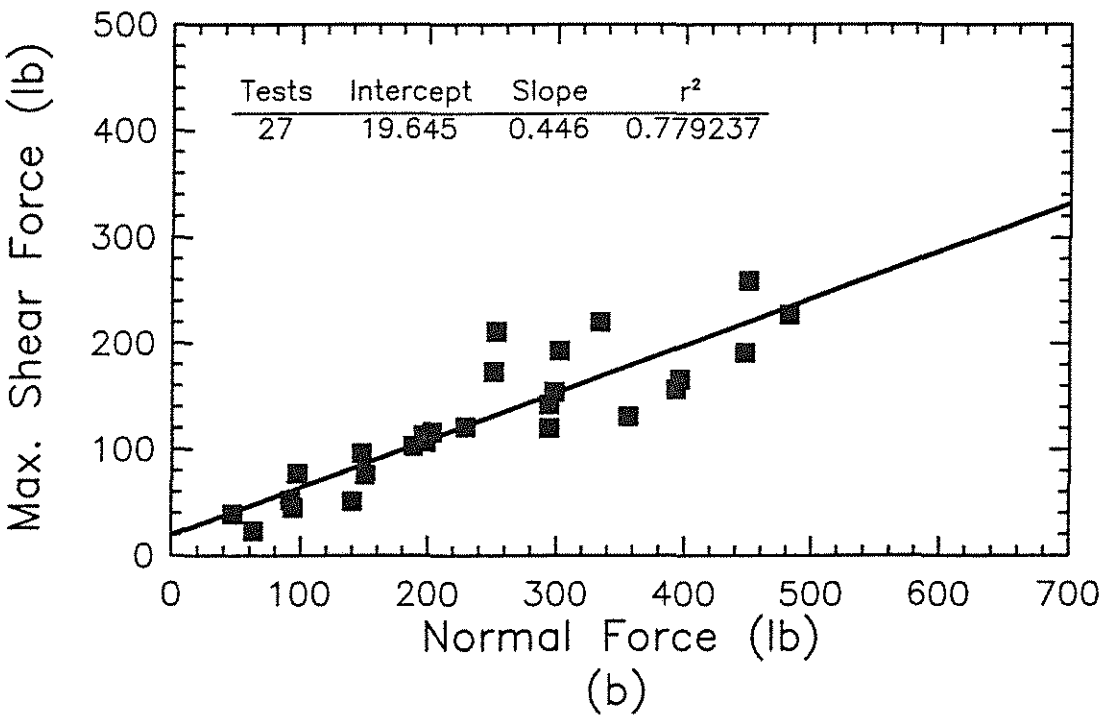

Fig. 2.6 Maximum shear force versus normal force for uncoated reinforcing bar specimens at 28 days - Series 1, (a) formed-surface mortar, (b) hand finished-surface mortar

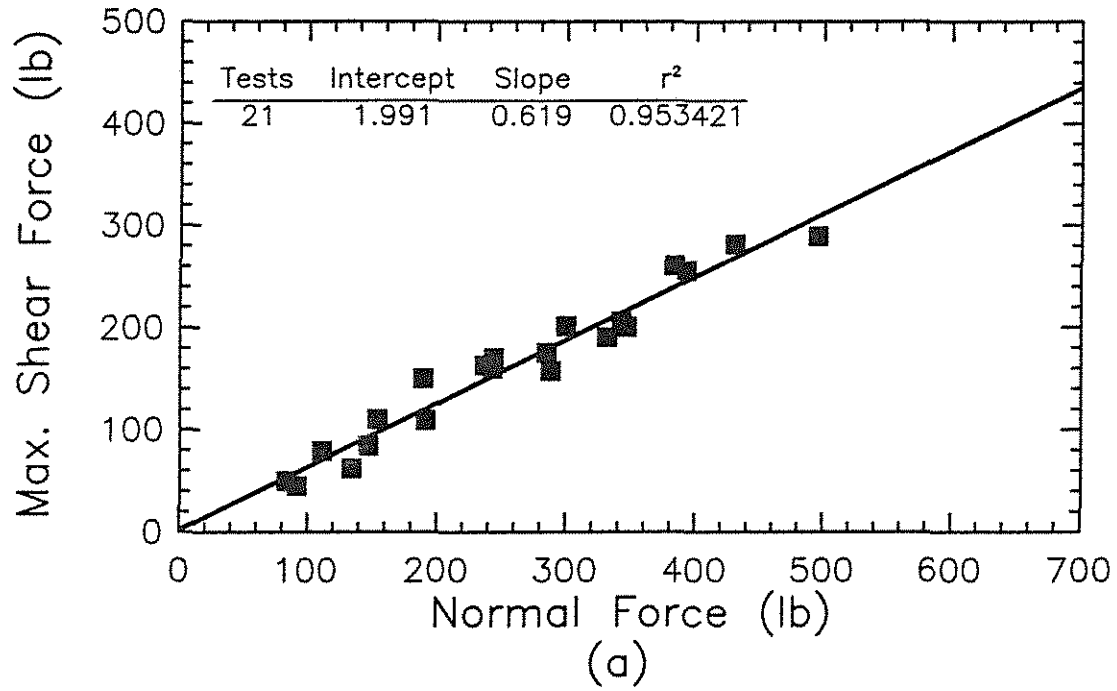

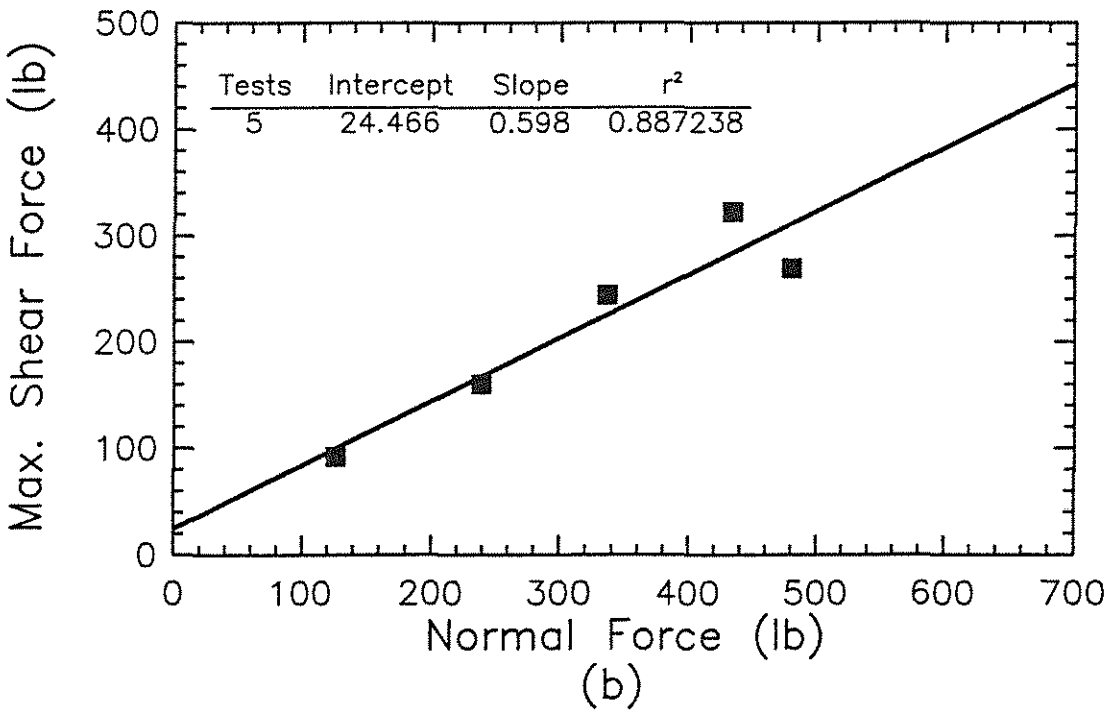

Fig. 2.7 Maximum shear force versus normal force for uncoated reinforcing bar specimens using mortar mix 1 (w/c = 0.4, s/c = 1.5) at 7 days - Series 2, (a) formed-surface mortar, (b) hand finished-surface mortar

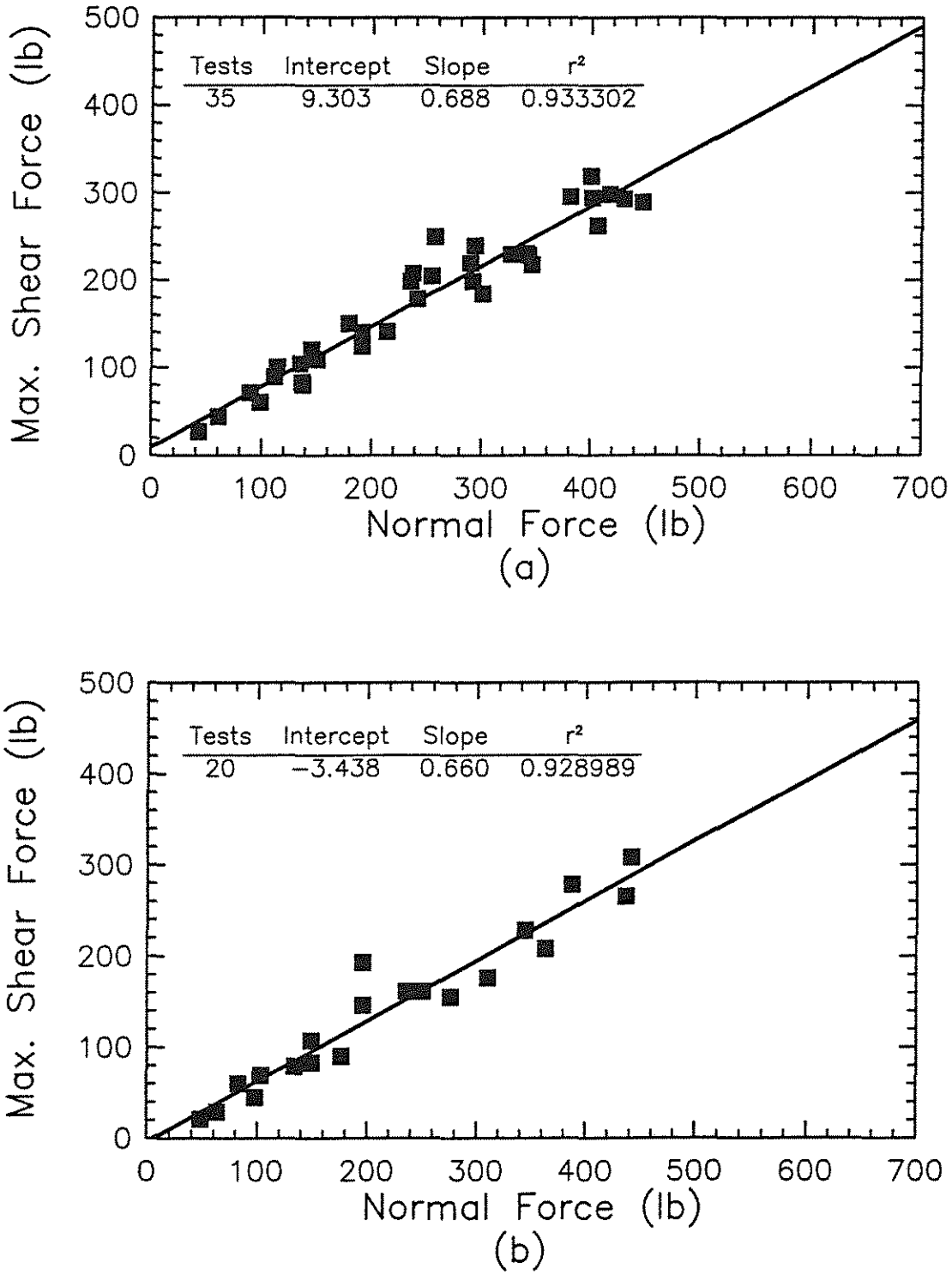

Fig. 2.8 Maximum shear force versus normal force for uncoated reinforcing bar specimens using mortar mix 2 (w/c = 0.5, s/c = 1.5) at 7 days - Series 2, (a) formed-surface mortar, (b) hand finished-surface mortar

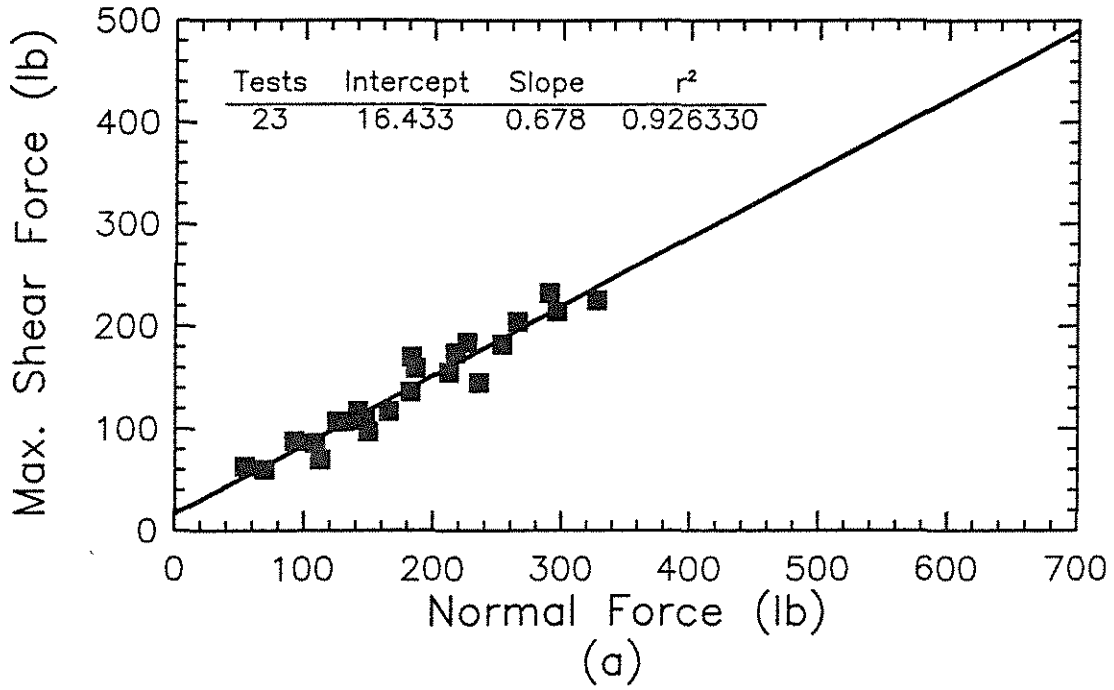

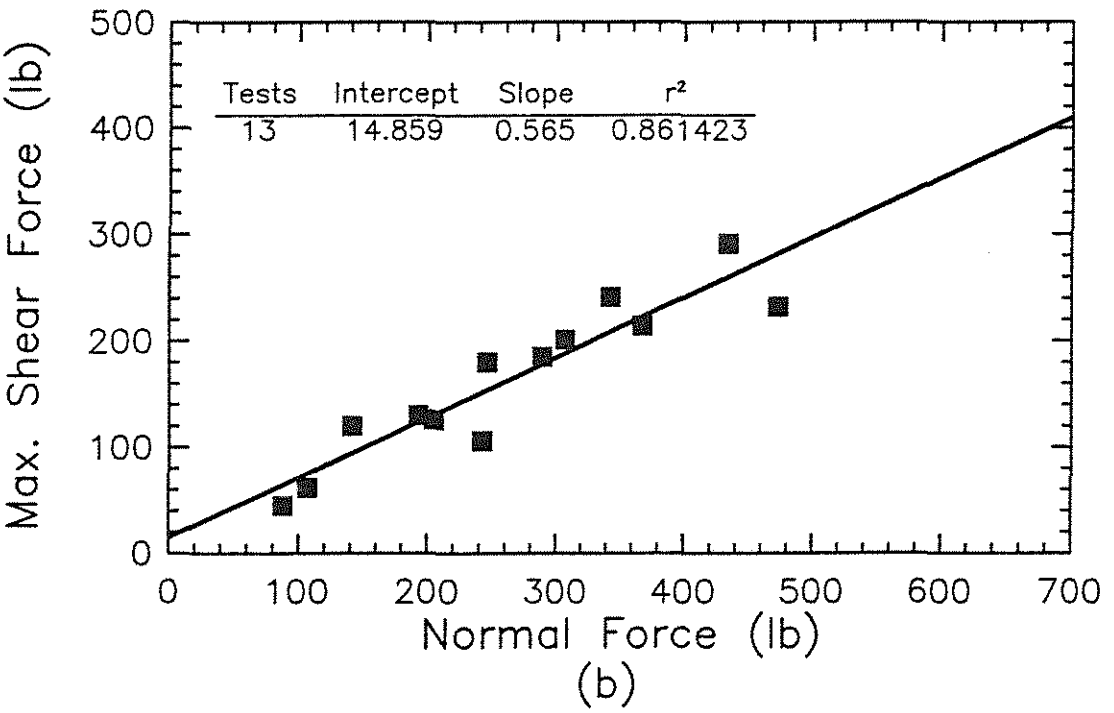

Fig. 2.9 Maximum shear force versus normal force for uncoated reinforcing bar specimens using mortar mix 3 (w/c = 0.6, s/c = 1.5) at 7 days - Series 2, (a) formed-surface mortar, (b) hand finished-surface mortar

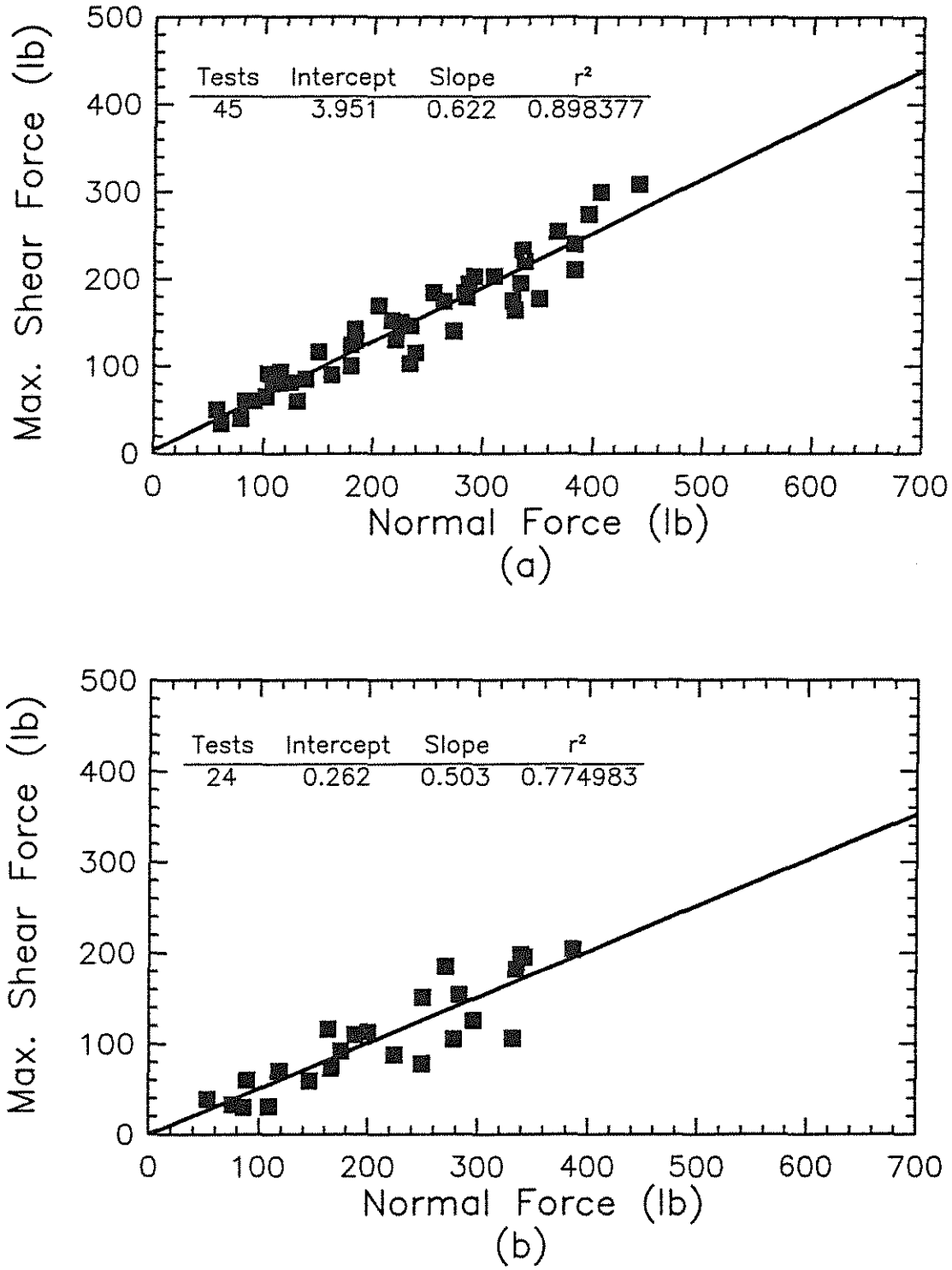

Fig. 2.10 Maximum shear force versus normal force for uncoated reinforcing bar specimens using mortar mix 4 (w/c = 0.5, s/c = 2.0) at 7 days - Series 2, (a) formed-surface mortar, (b) hand finished-surface mortar

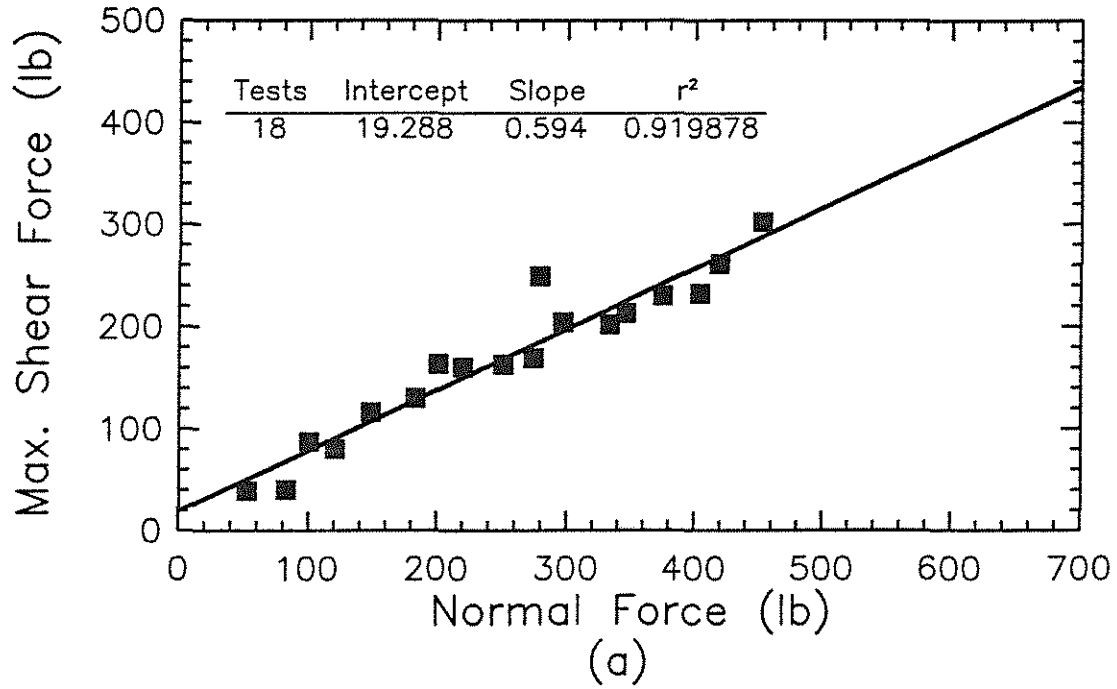

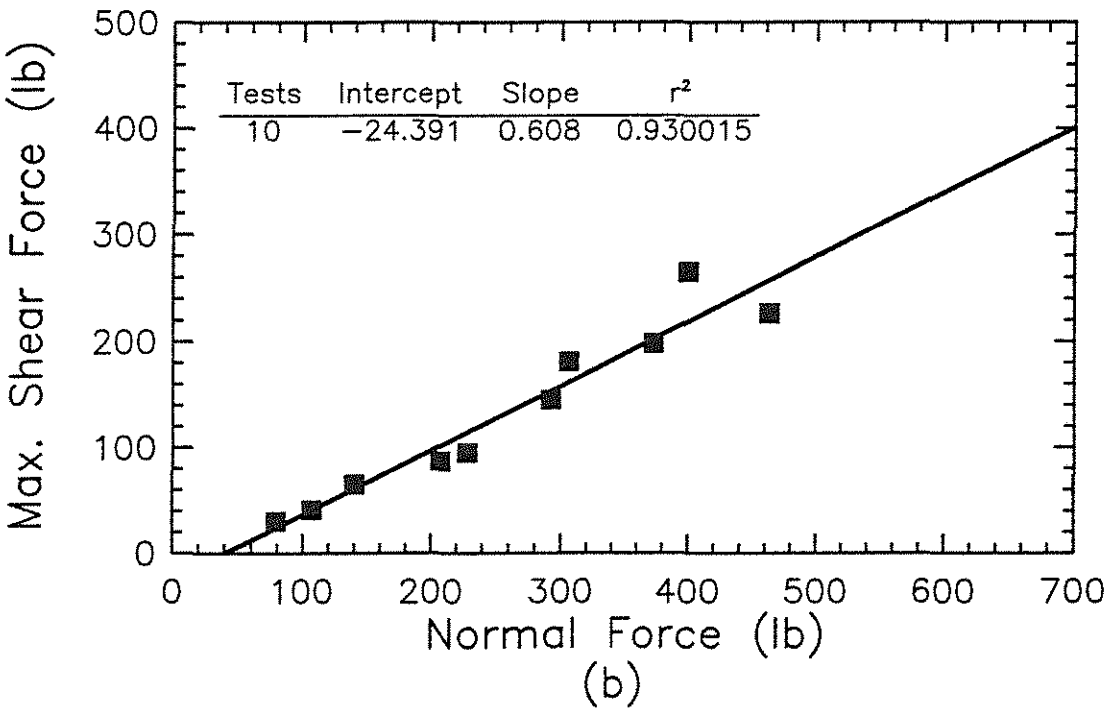

Fig. 2.11 Maximum shear force versus normal force for uncoated reinforcing bar specimens using mortar mix 5 (w/c = 0.5, s/c = 2.5) at 7 days - Series 2, (a) formed-surface mortar, (b) hand finished-surface mortar

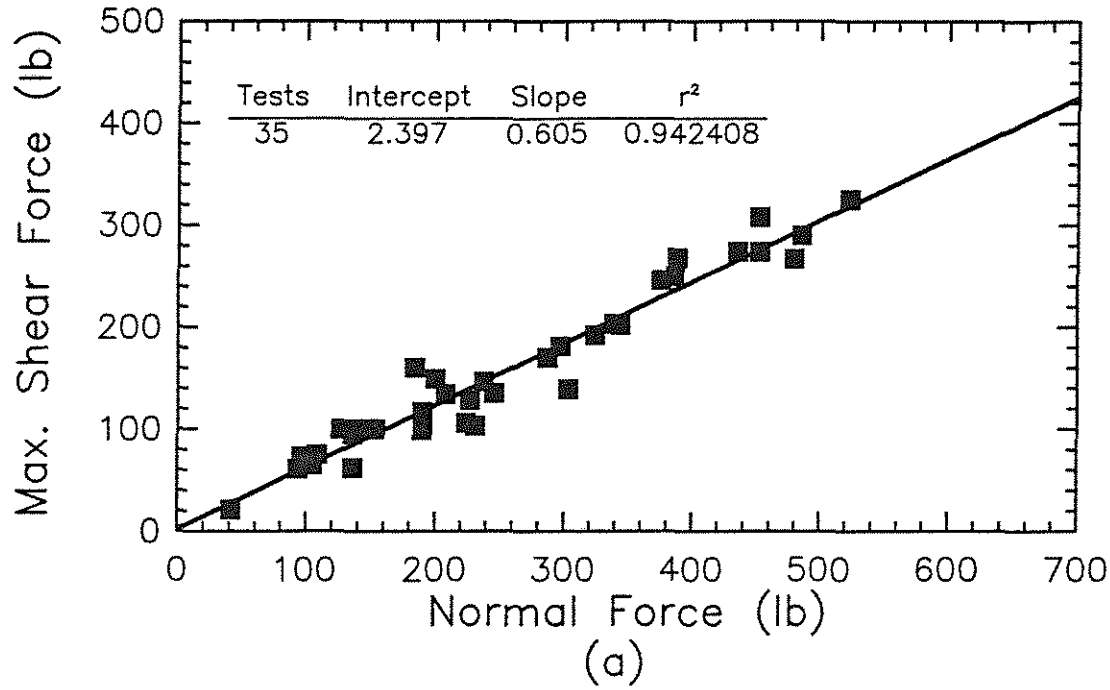

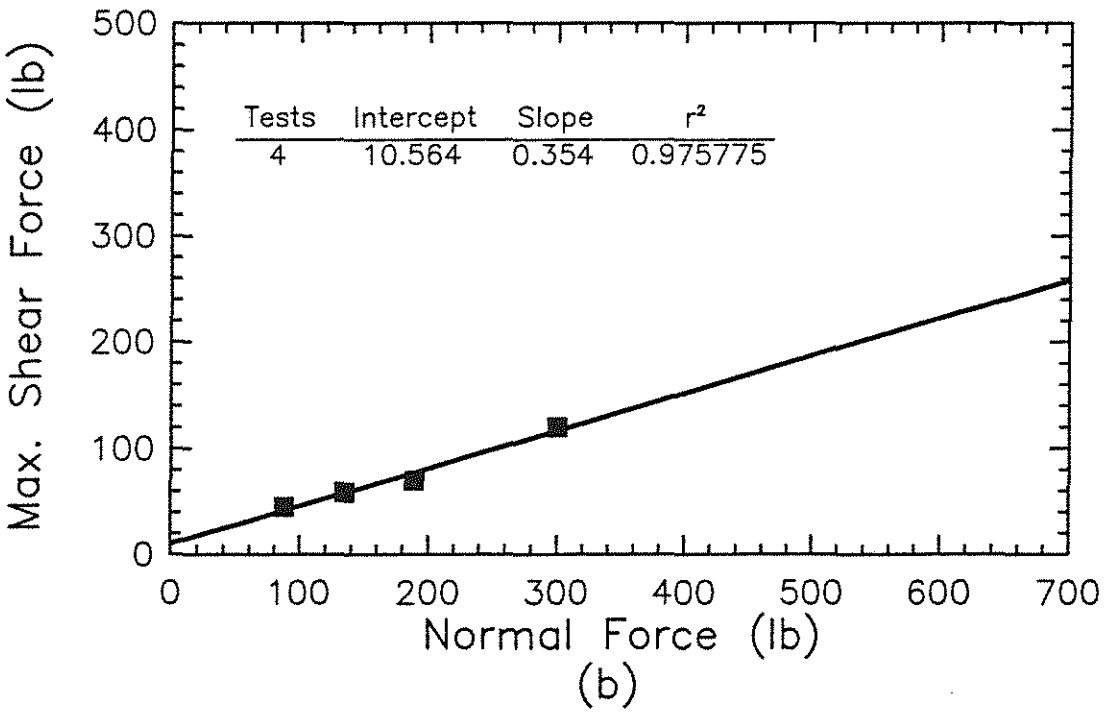

Fig. 2.12 Maximum shear force versus normal force for uncoated reinforcing bar specimens using mortar mix 1 (w/c = 0.4, s/c = 1.5) at 28 days - Series 2, (a) formed-surface mortar, (b) hand finished-surface mortar

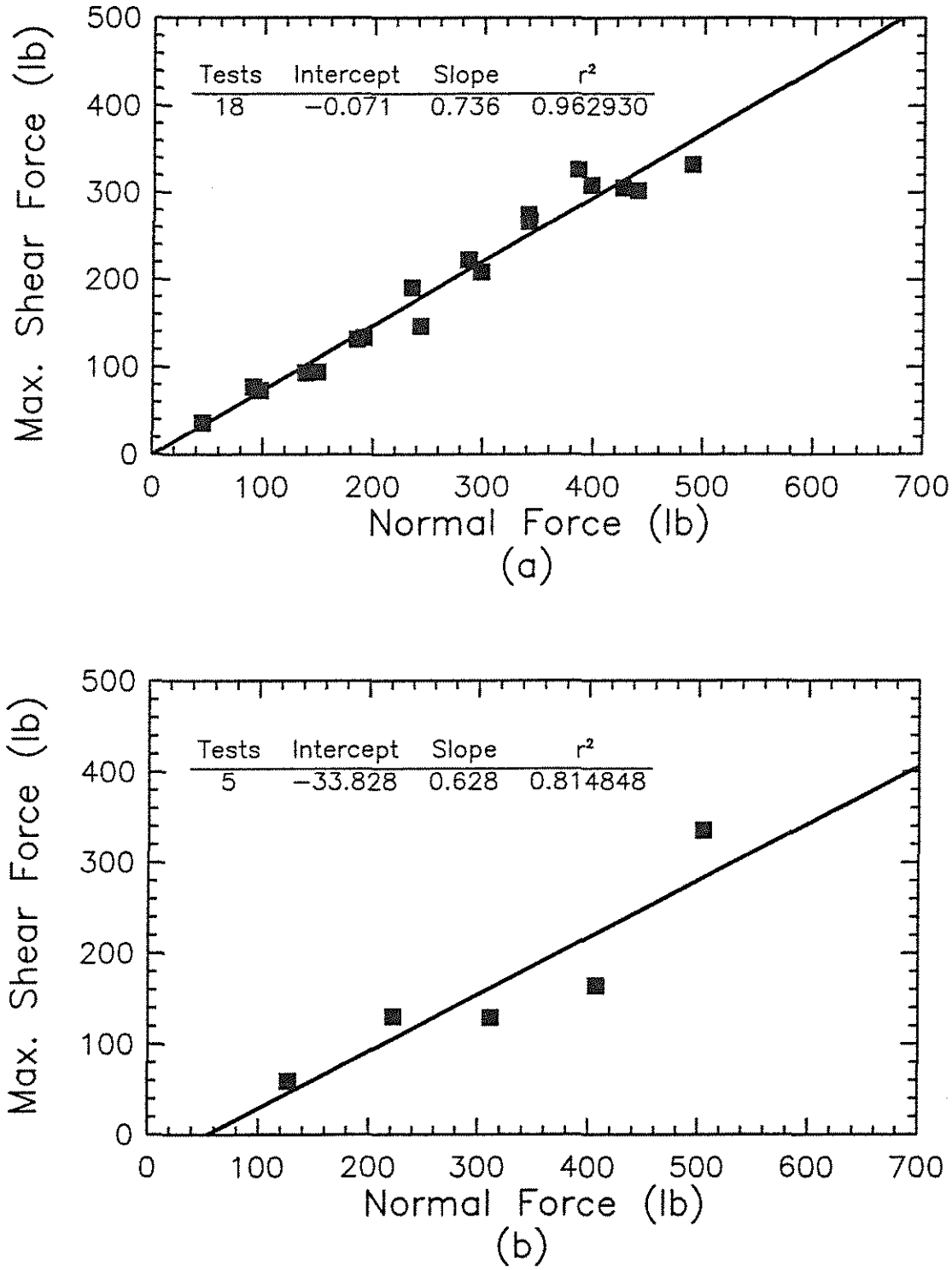

Fig. 2.13 Maximum shear force versus normal force for uncoated reinforcing bar specimens using mortar mix 2 (w/c = 0.5, s/c = 1.5) at 28 days - Series 2, (a) formed-surface mortar, (b) hand finished-surface mortar

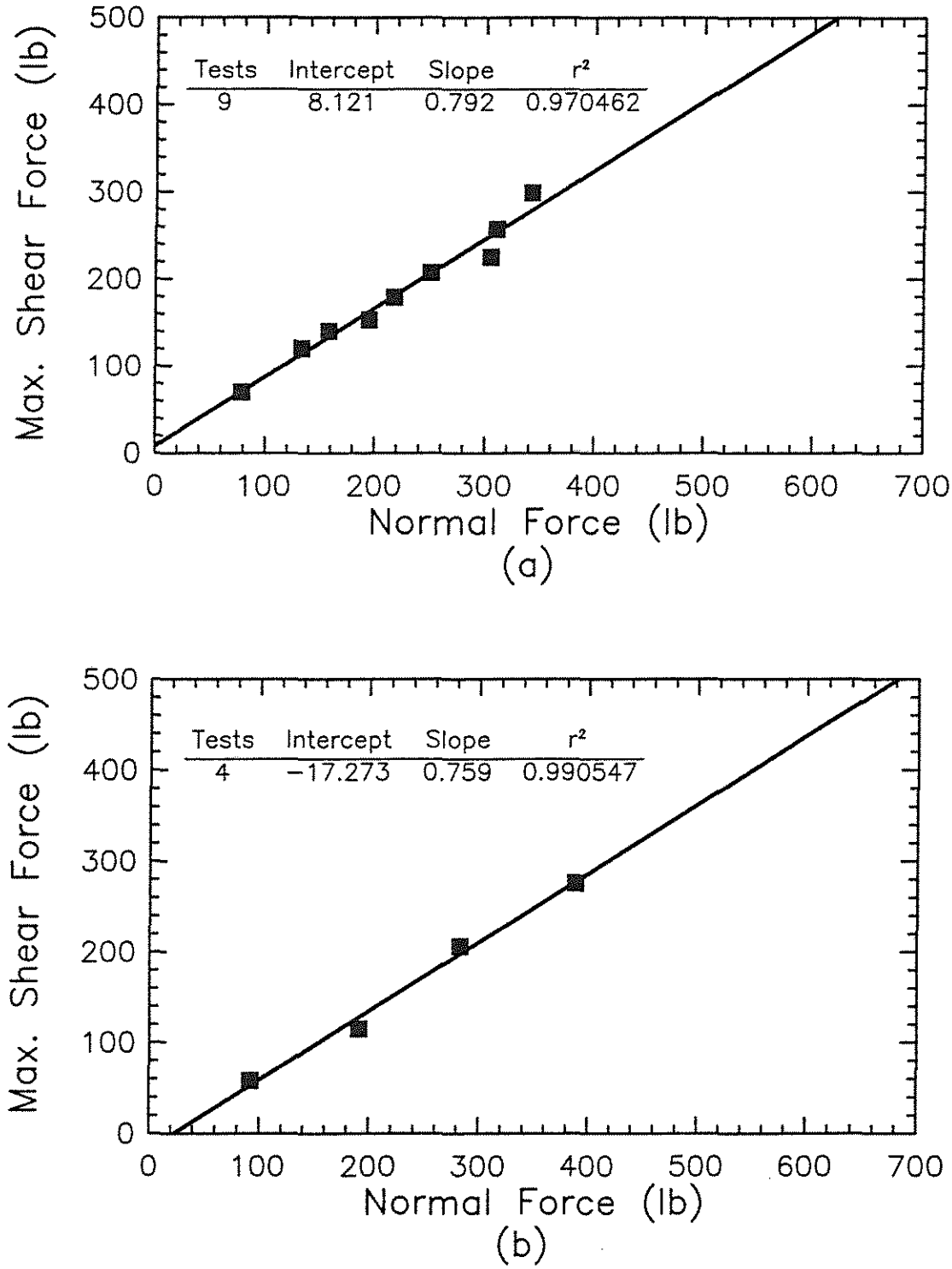

Fig. 2.14 Maximum shear force versus normal force for uncoated reinforcing bar specimens using mortar mix 3 (w/c = 0.6, s/c = 1.5) at 28 days - Series 2, (a) formed-surface mortar, (b) hand finished-surface mortar

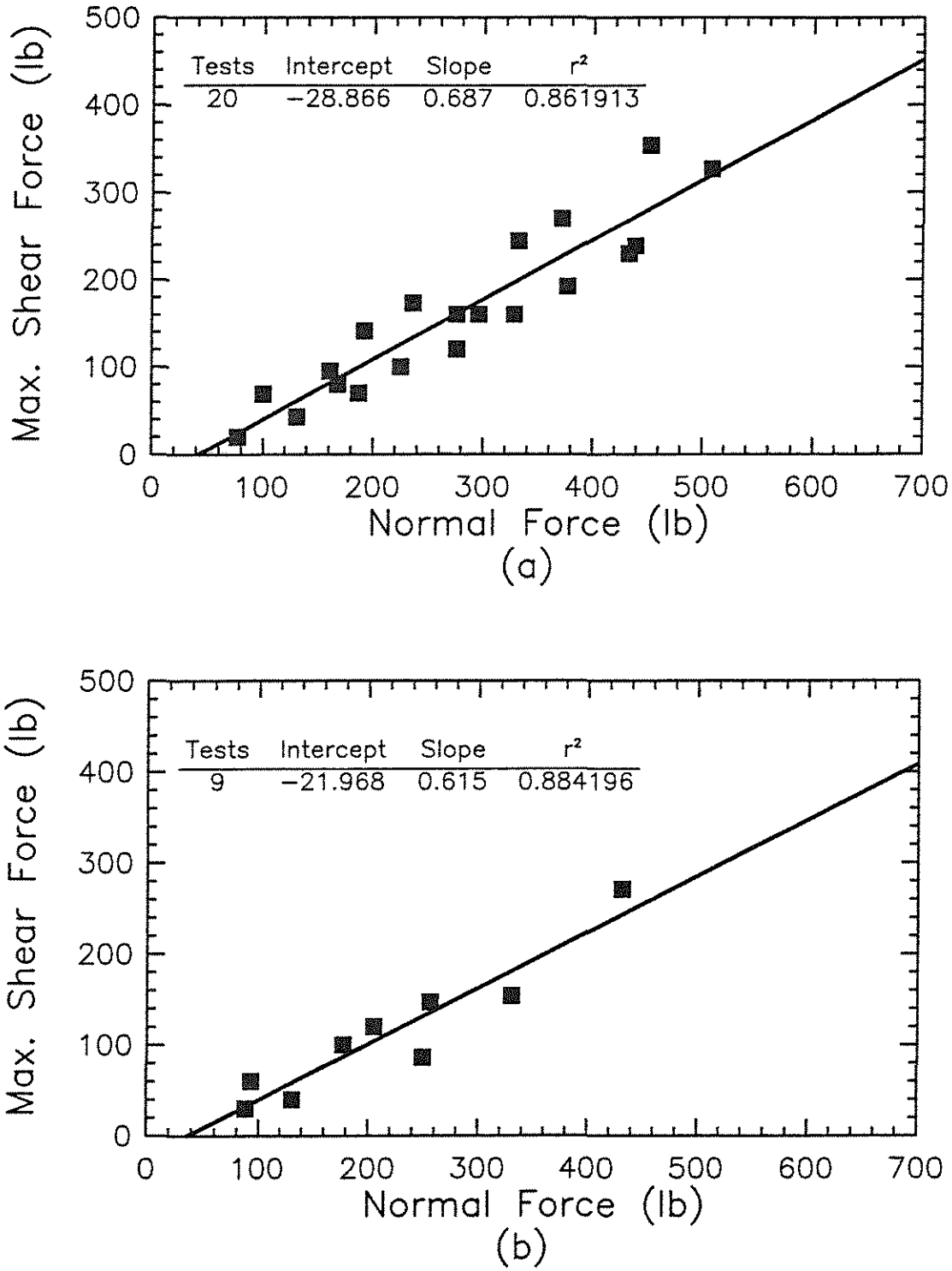

Fig. 2.15 Maximum shear force versus normal force for uncoated reinforcing bar specimens using mortar mix 4 (w/c = 0.5, s/c = 2.0) at 28 days - Series 2, (a) formed-surface mortar, (b) hand finished-surface mortar

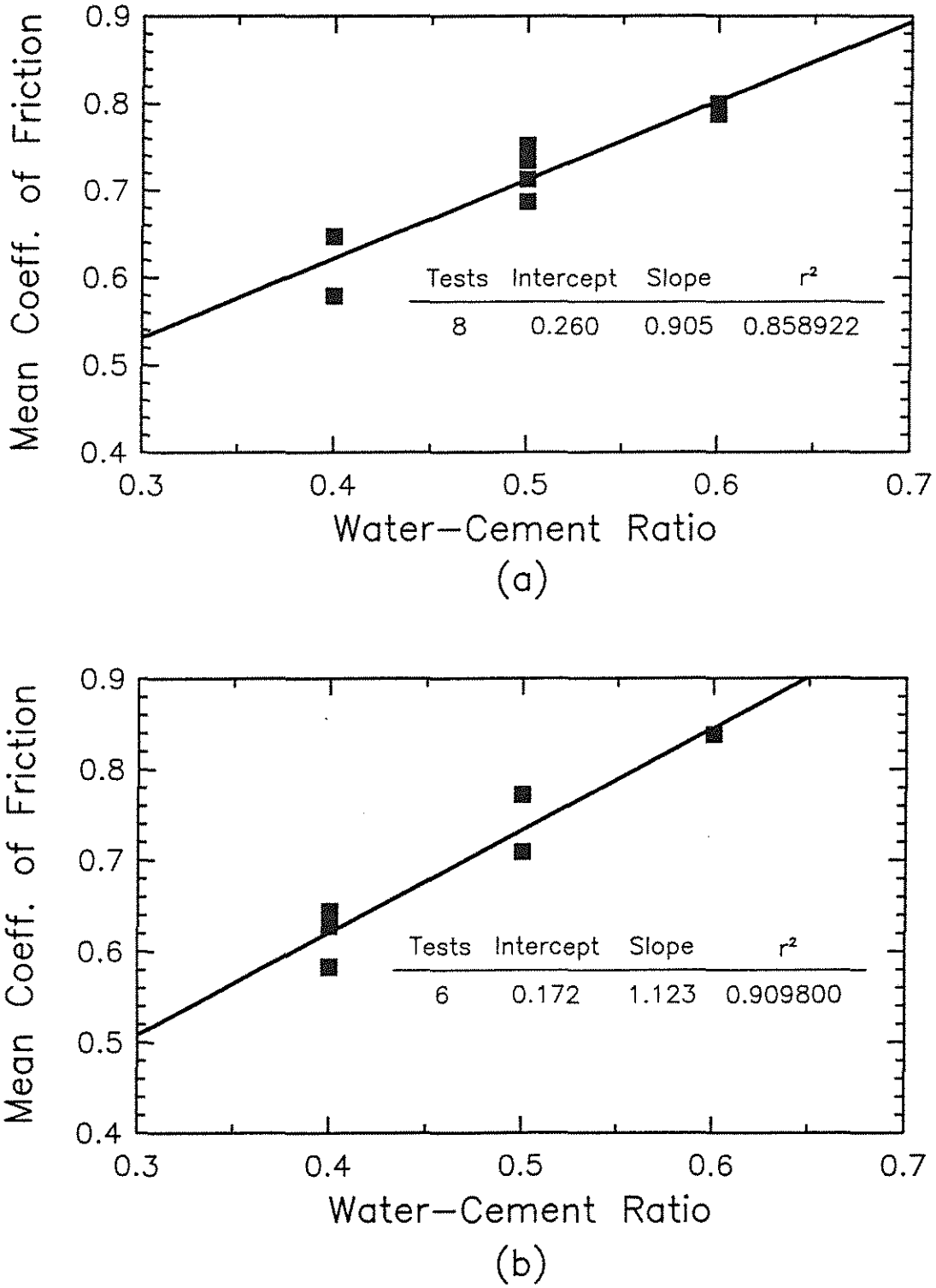

Fig. 2.16 Mean coefficient of friction versus water-cement ratio for uncoated reinforcing bar specimens with formed-surface mortar and c/s of 2.0 - Series 2, (a) 7 day tests, (b) 28 day tests

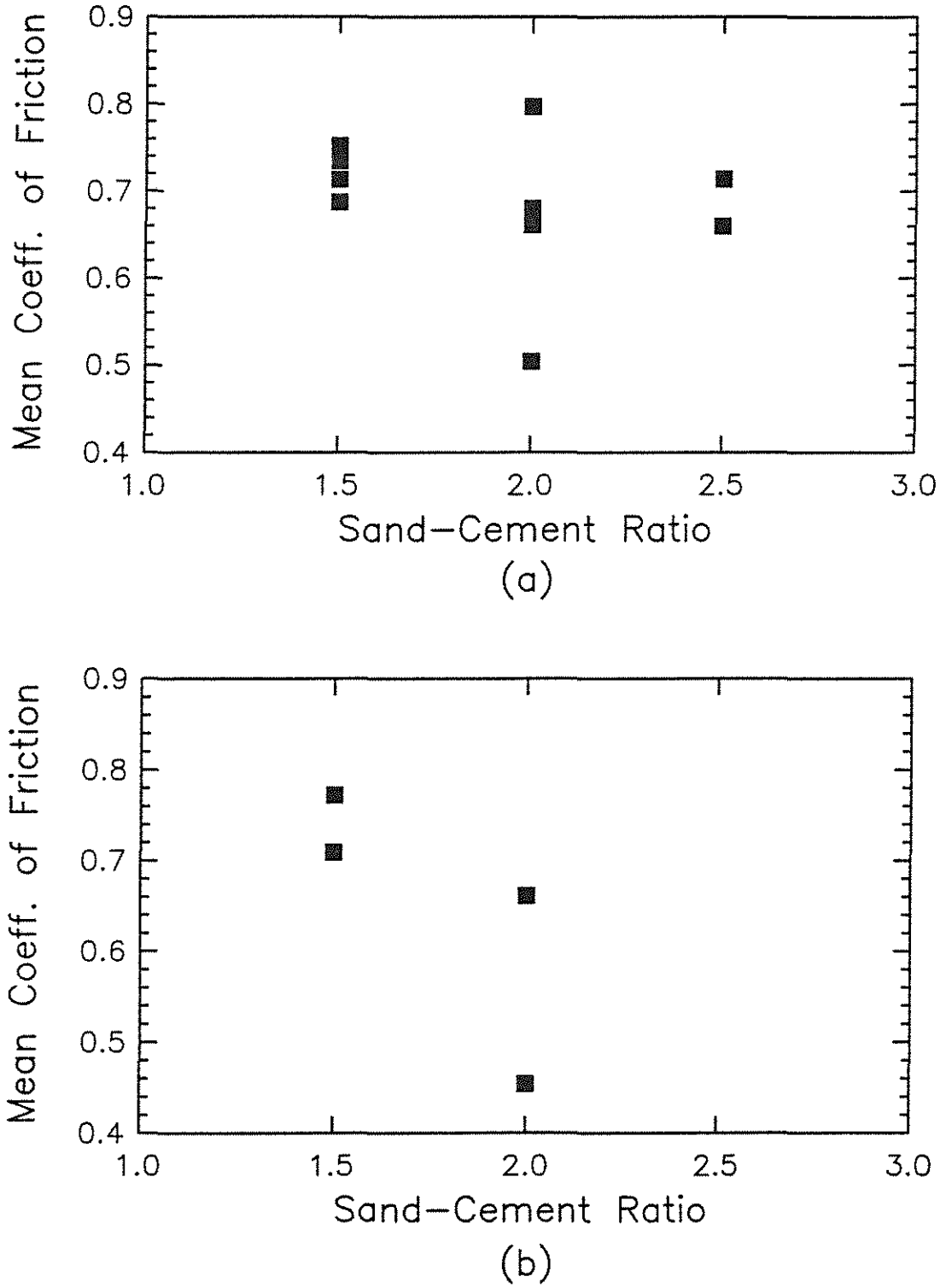

Fig. 2.17 Mean coefficient of friction versus sand-cement ratio for uncoated reinforcing bar specimens with formed-surface mortar and w/c of 0.5 - Series 2, (a) 7 day tests, (b) 28 day tests

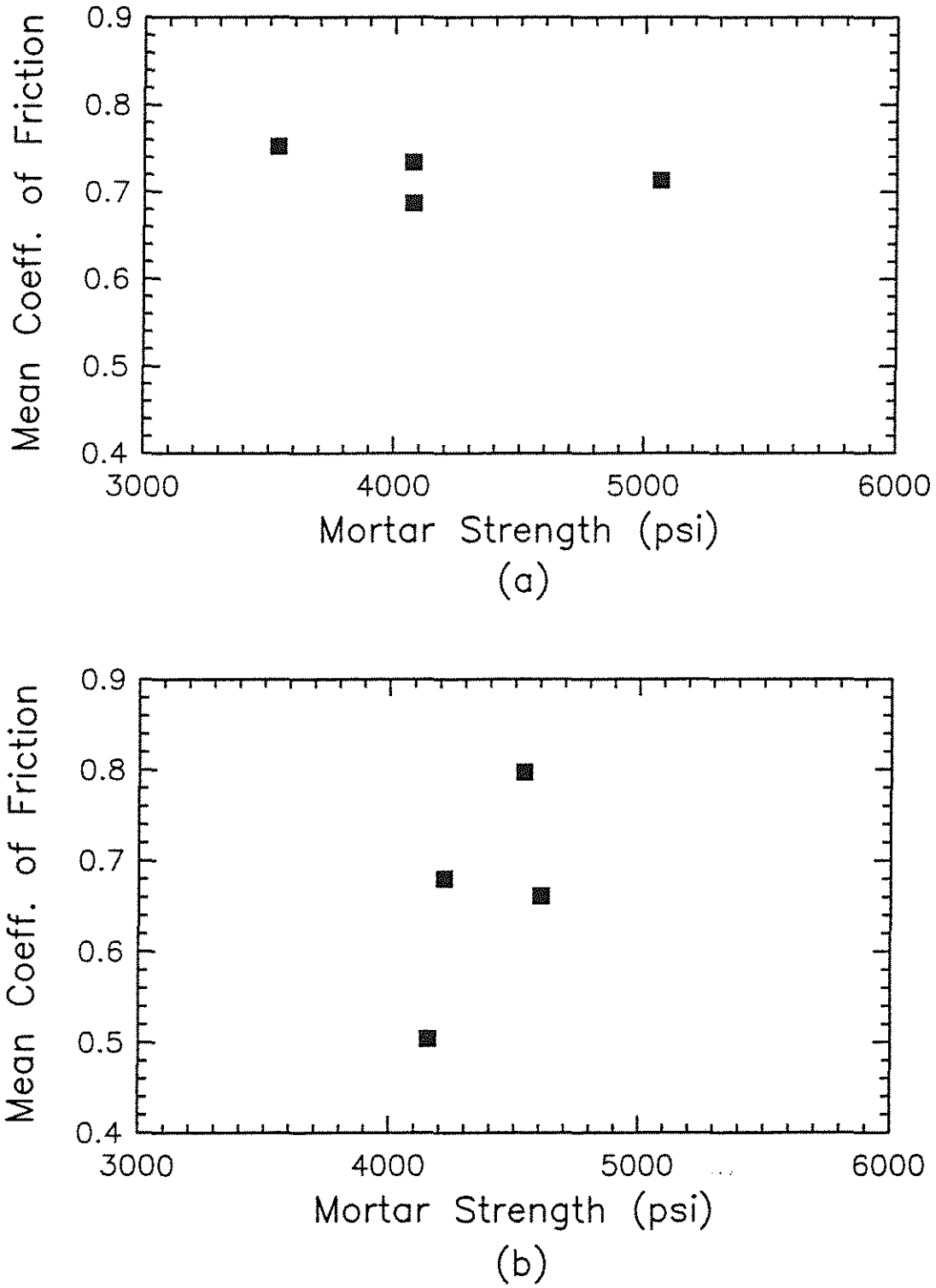

Fig. 2.18 Mean coefficient of friction versus mortar strength for uncoated reinforcing bar specimens with formed-surface mortar at 7 days - Series 2, (a) mix 2 (w/c = 0.5, s/c = 2.0), (b) mix 4 (w/c = 0.5, s/c = 1.5)

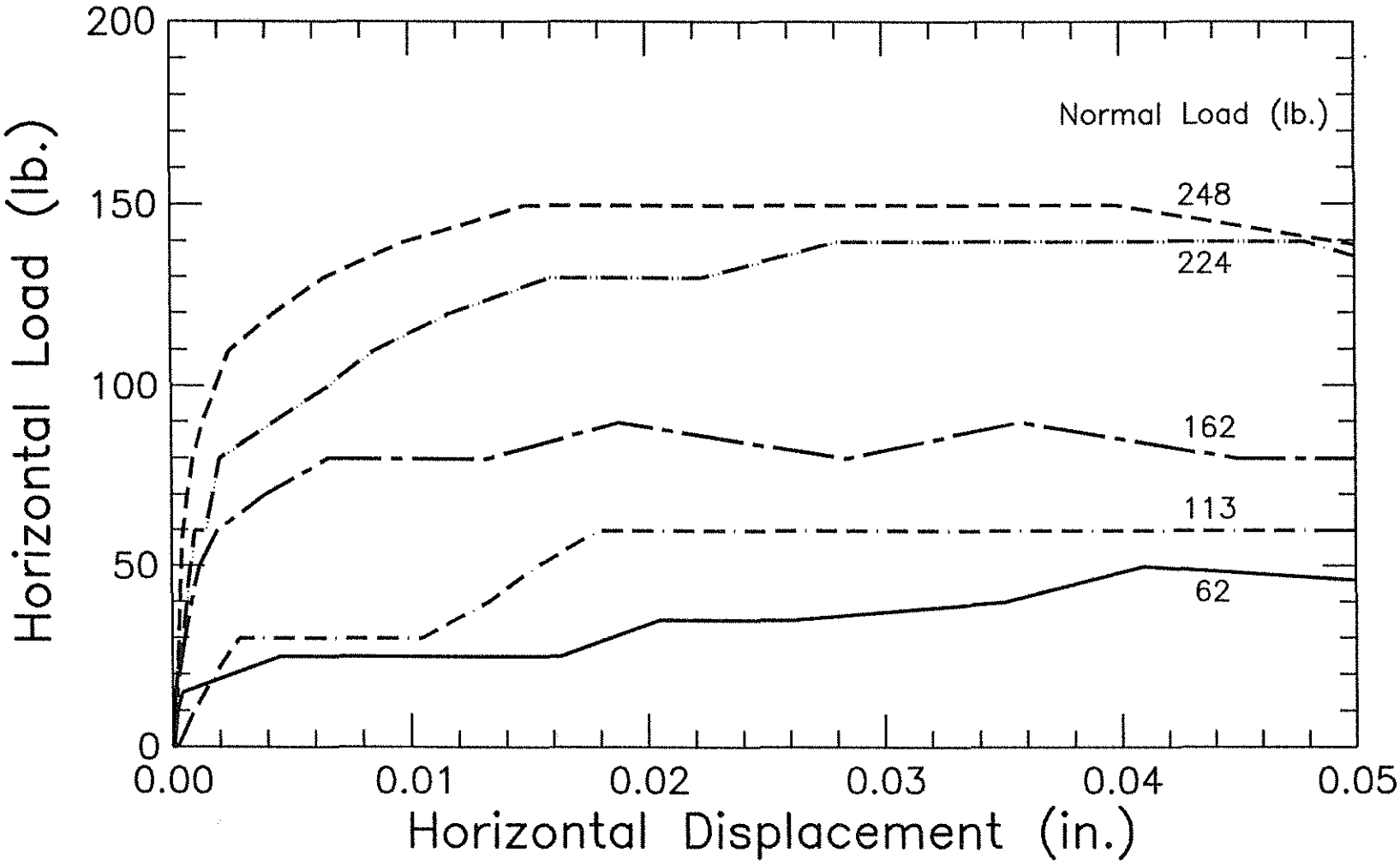

Fig. 2.19a Typical horizontal load versus horizontal displacement curves for uncoated reinforcing bar specimens with formed-surface mortar at 7 days - Series 3

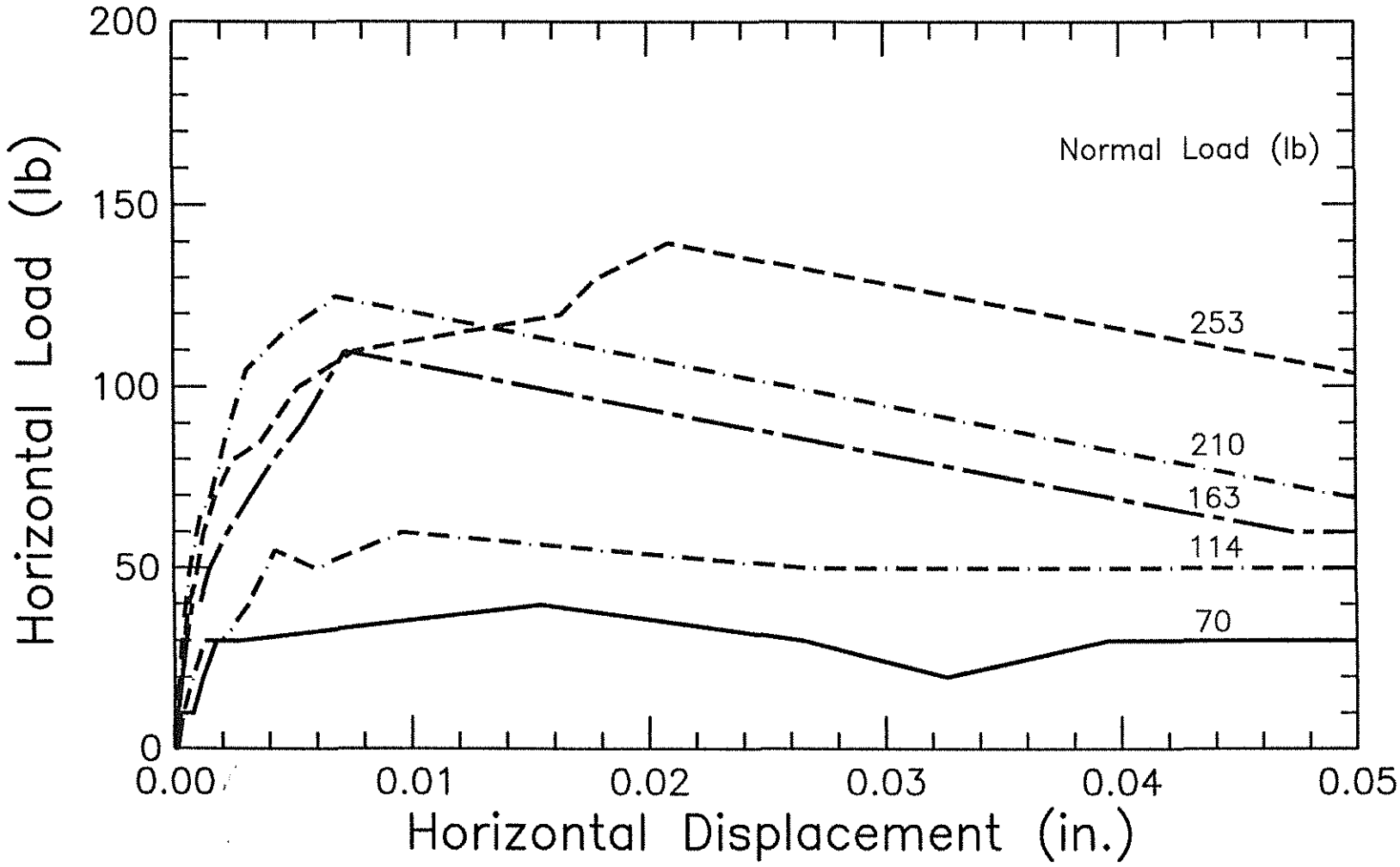

Fig. 2.19b Typical horizontal load versus horizontal displacement curves for coated reinforcing bar specimens with formed-surface mortar at 7 days - Series 3

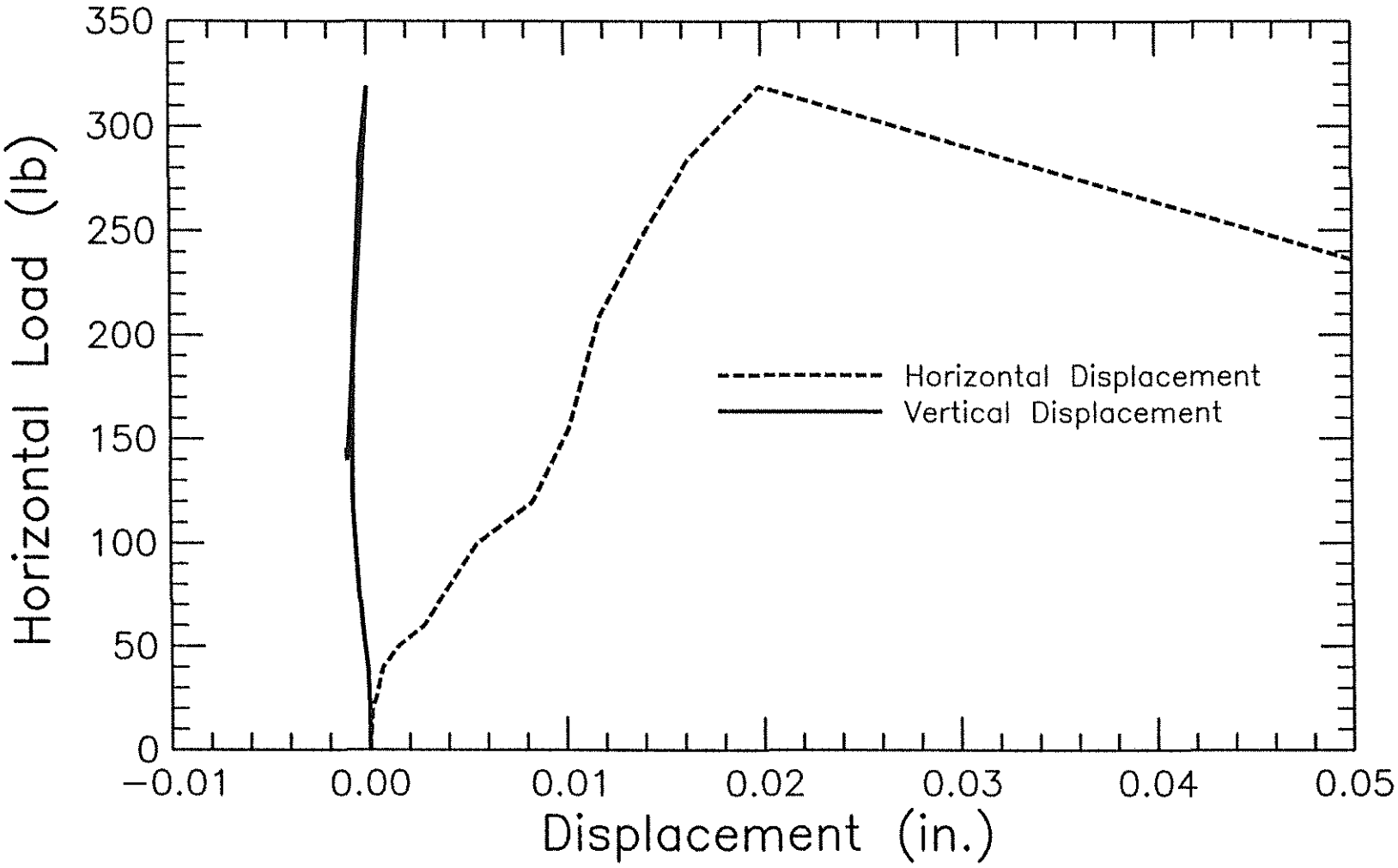

Fig. 2.20 Typical horizontal load versus horizontal and vertical displacements curves for uncoated reinforcing bar specimens and 75 lb. constant vertical load with formed-surface mortar at 7 days - Series 3

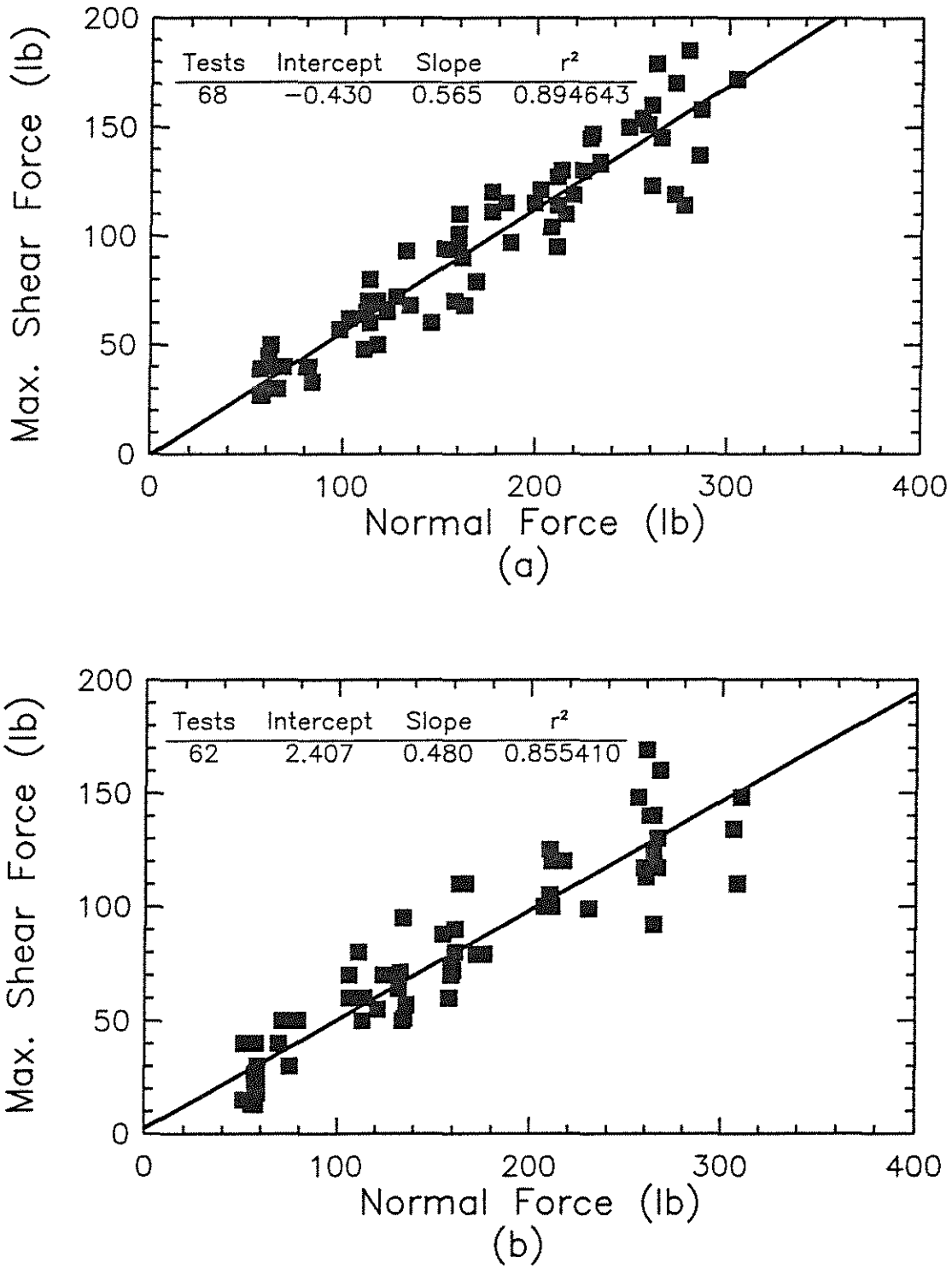

Fig. 2.21 Maximum shear force versus normal force for reinforcing bar specimens with formed-surface mortar at 7 days, using mix 2 (w/c = 0.5, s/c = 1.5) - Series 3, (a) uncoated, (b) epoxy coated

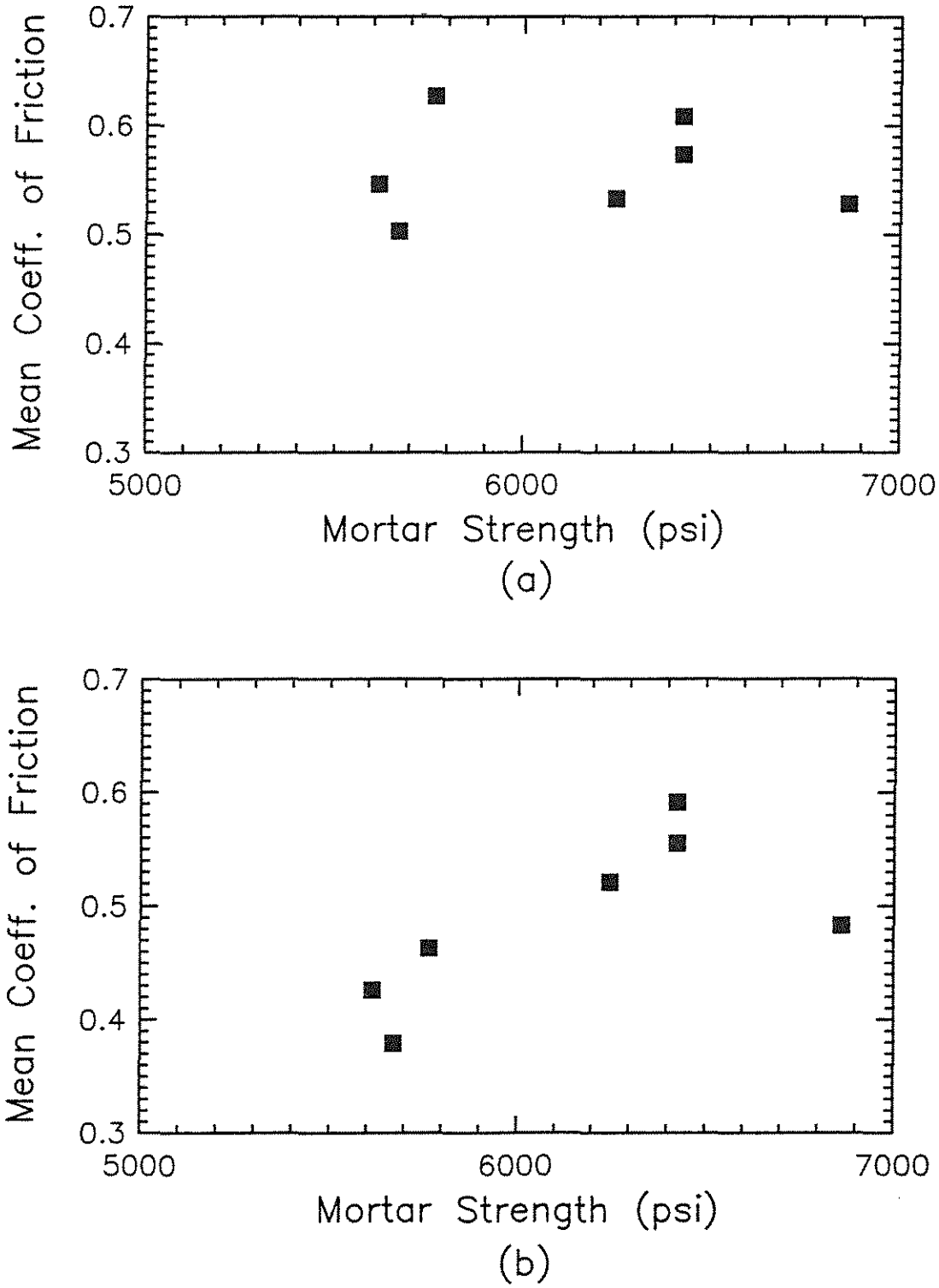

Fig. 2.22 Mean coefficient of friction versus mortar strength for reinforcing bar specimens with formed-surface mortar at 7 days, using mix 2 (w/c = 0.5, s/c = 1.5) - Series 3, (a) uncoated, (b) coated

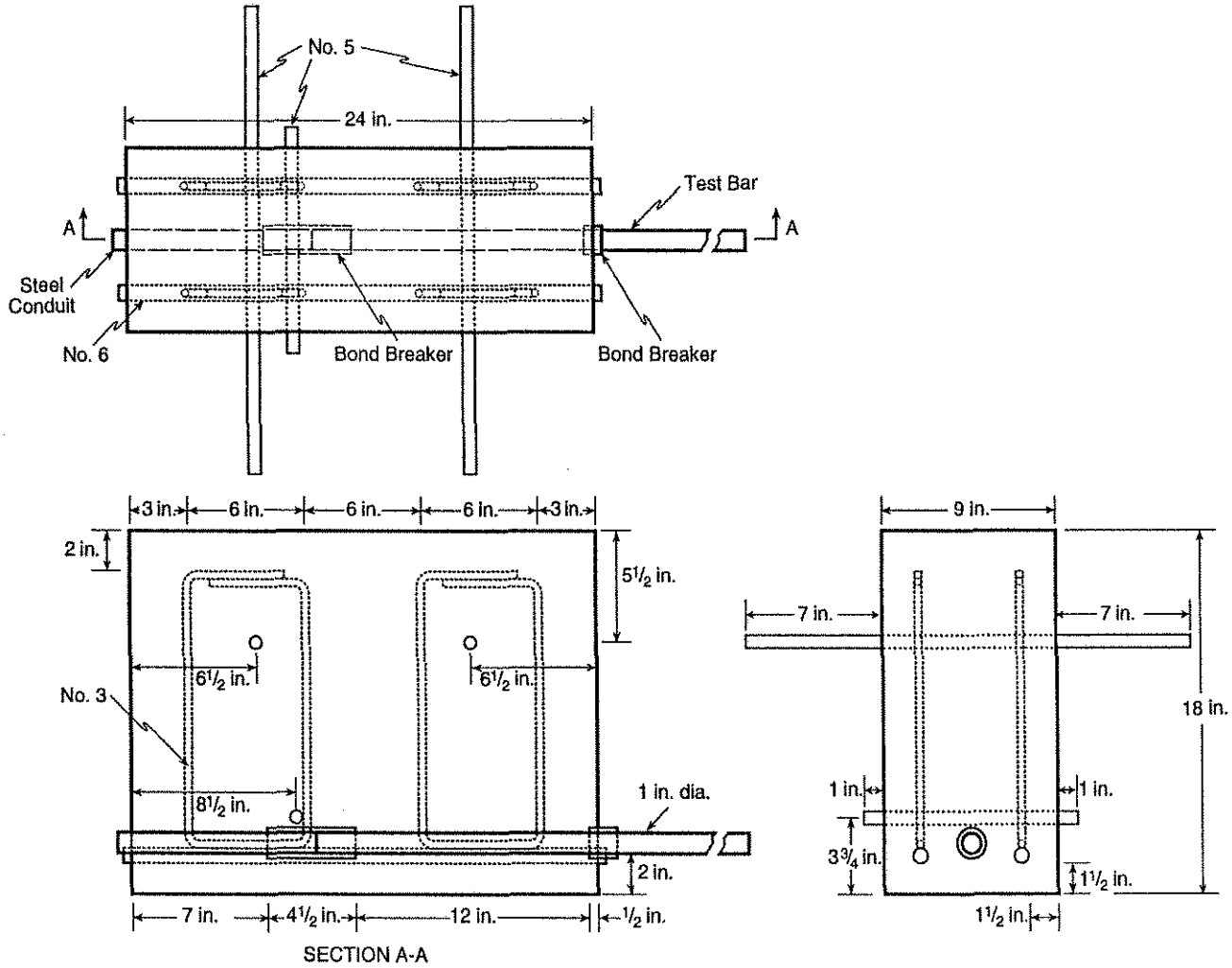

Fig. 3.1 Typical beam-end test specimen

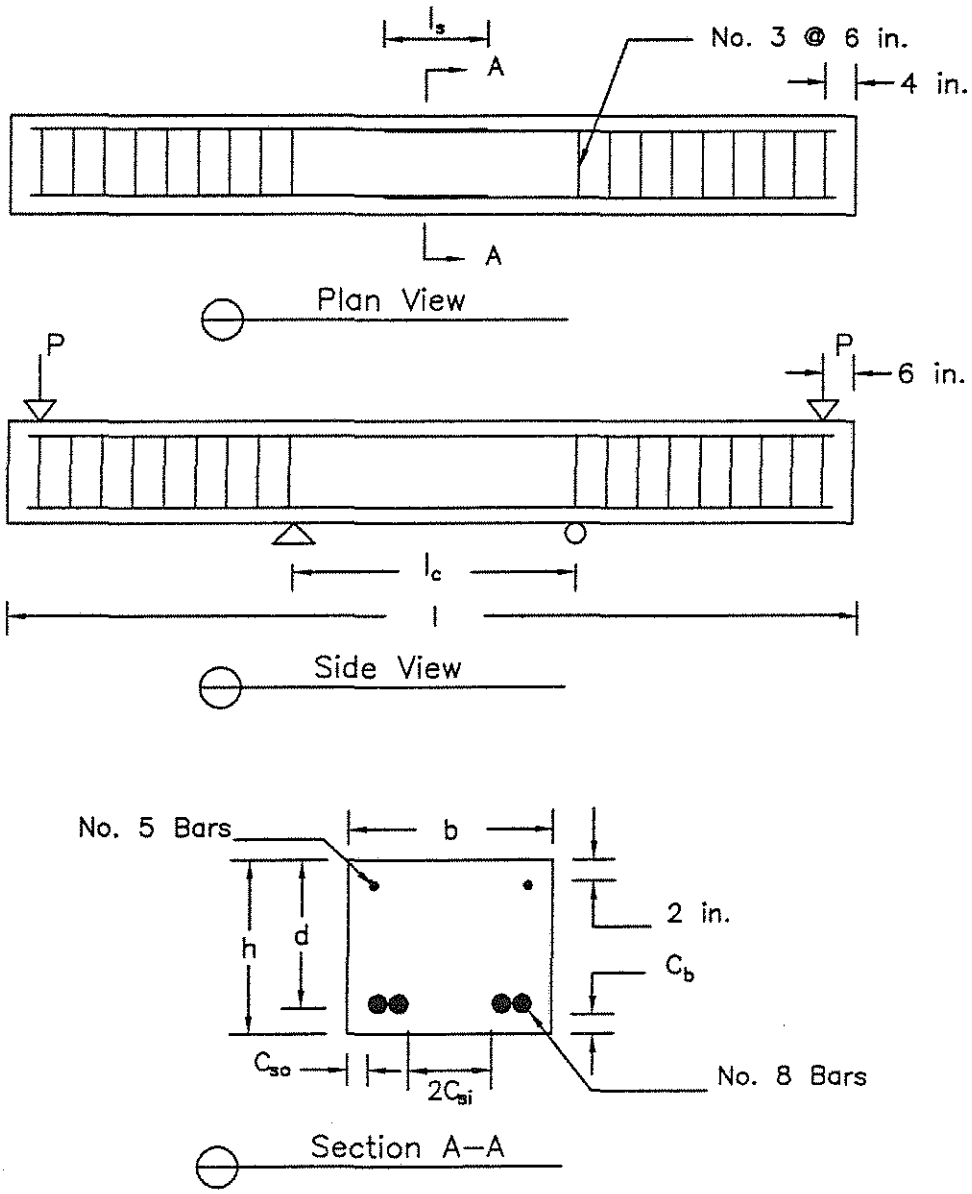

Fig. 3.2a Typical beam splice test specimen with 2 splices and no stirrups

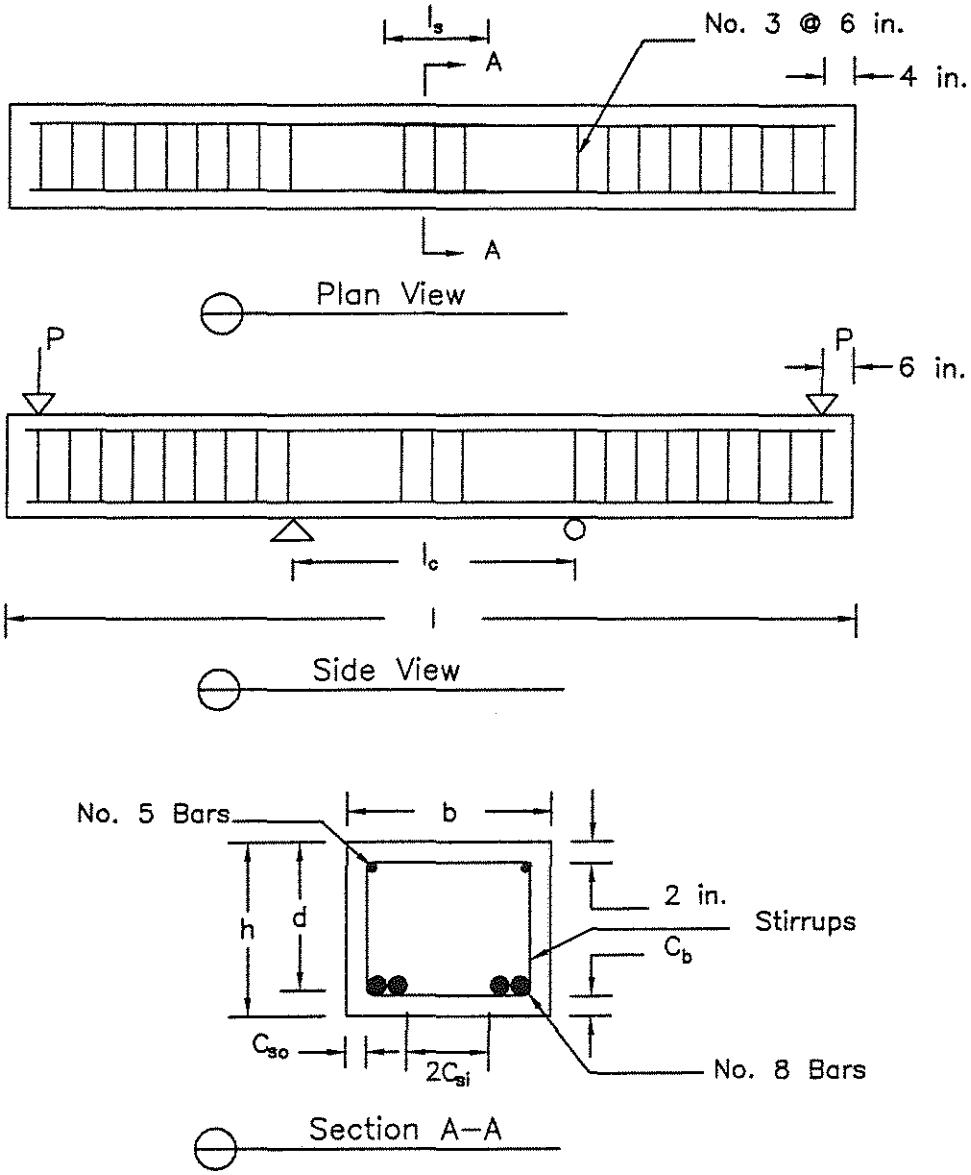

Fig. 3.2b Typical beam splice test specimen with 2 splices and stirrups

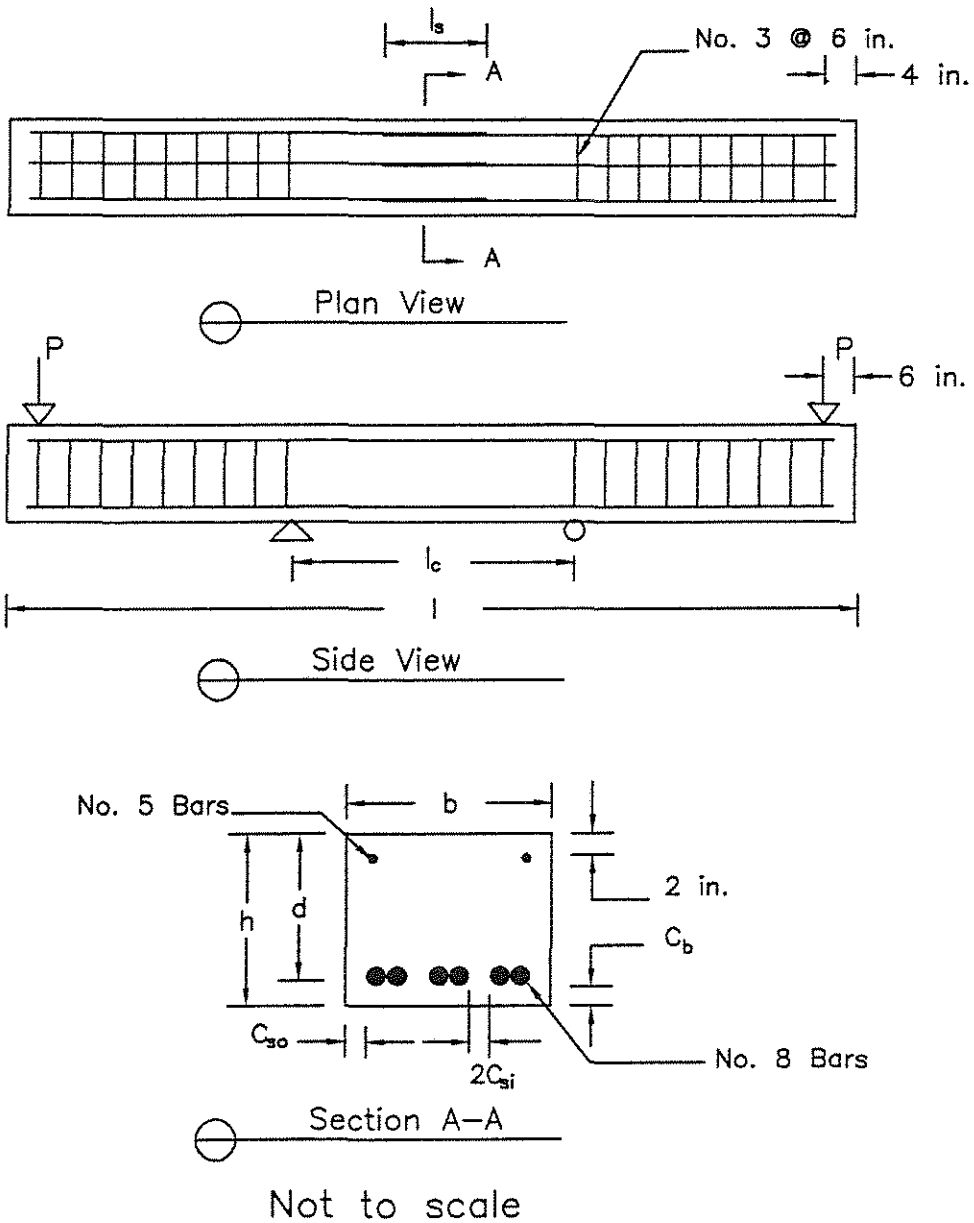

Fig. 3.2c Typical beam splice test specimen with 3 splices and no stirrups

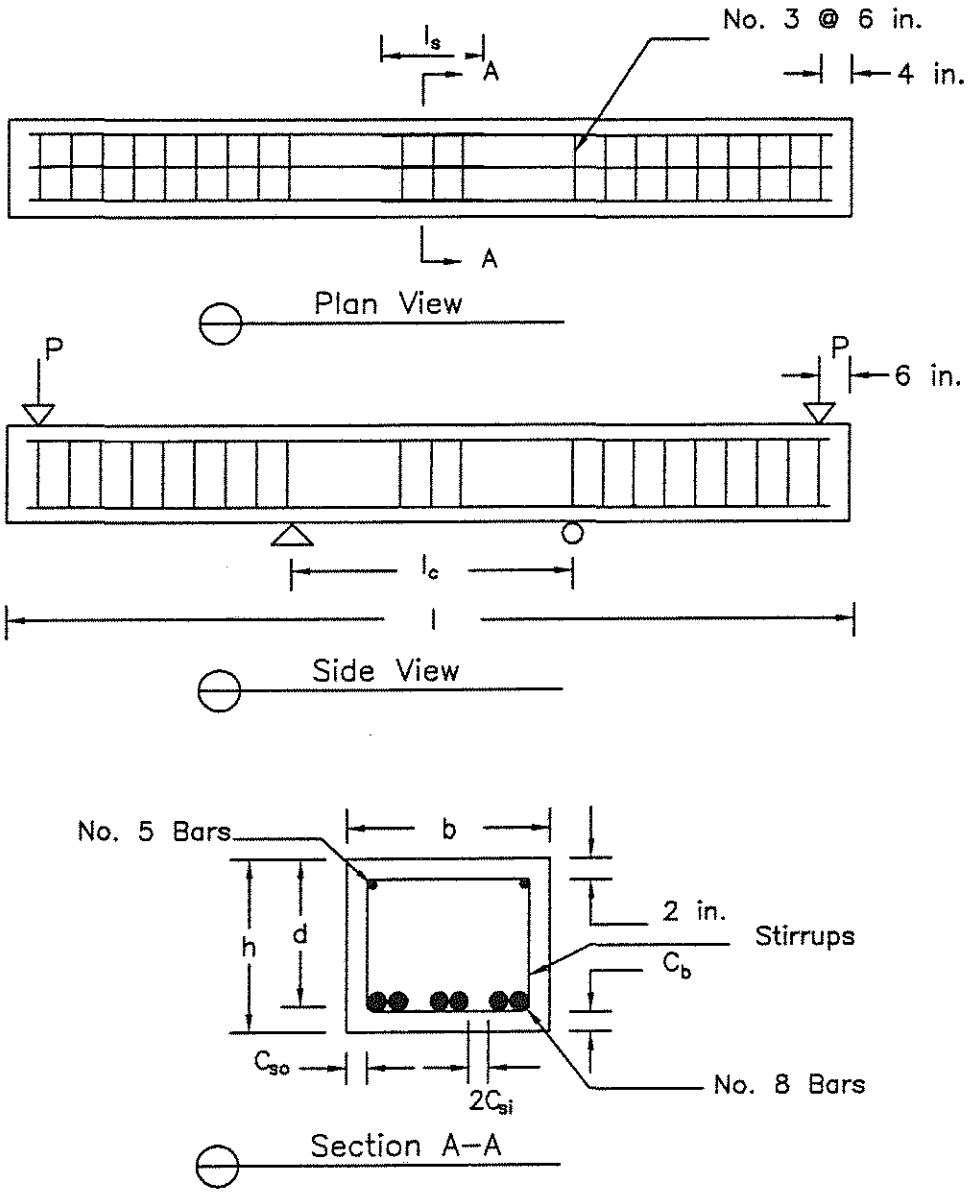

Fig. 3.2d Typical beam splice test specimen with 3 splices and stirrups

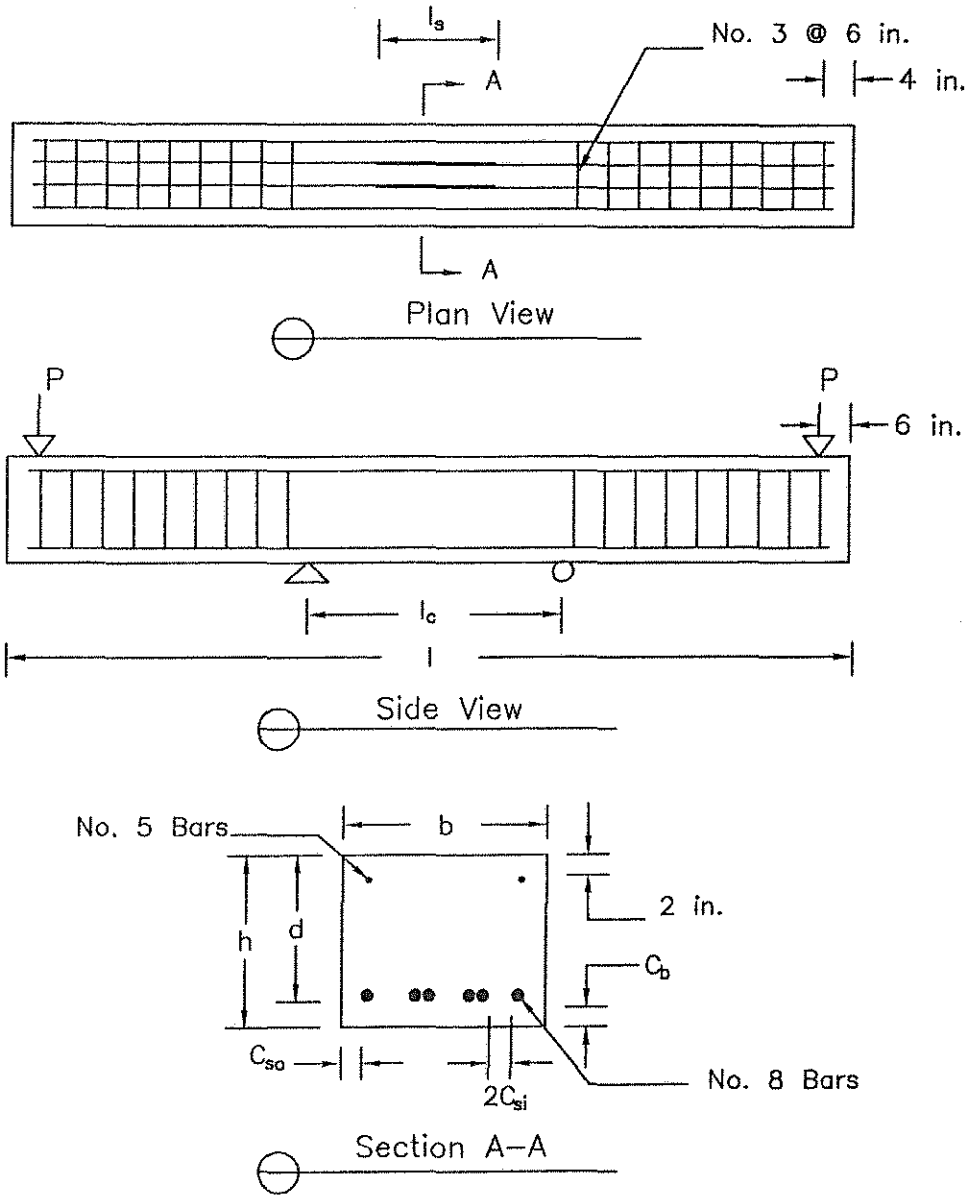

Fig. 3.2e Beam splice test specimen with 2 splices and 2 continuous bars

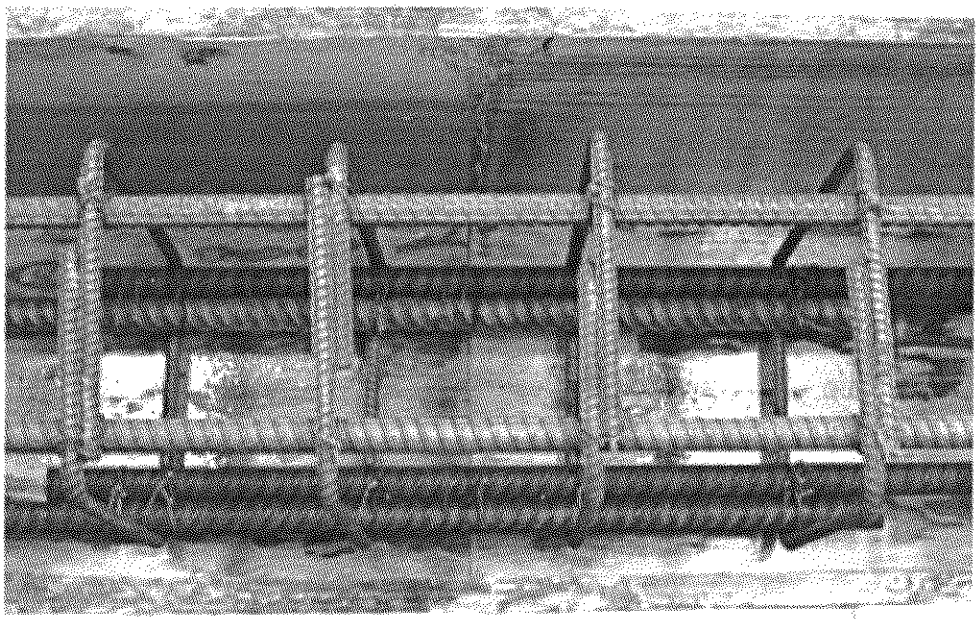

(a)

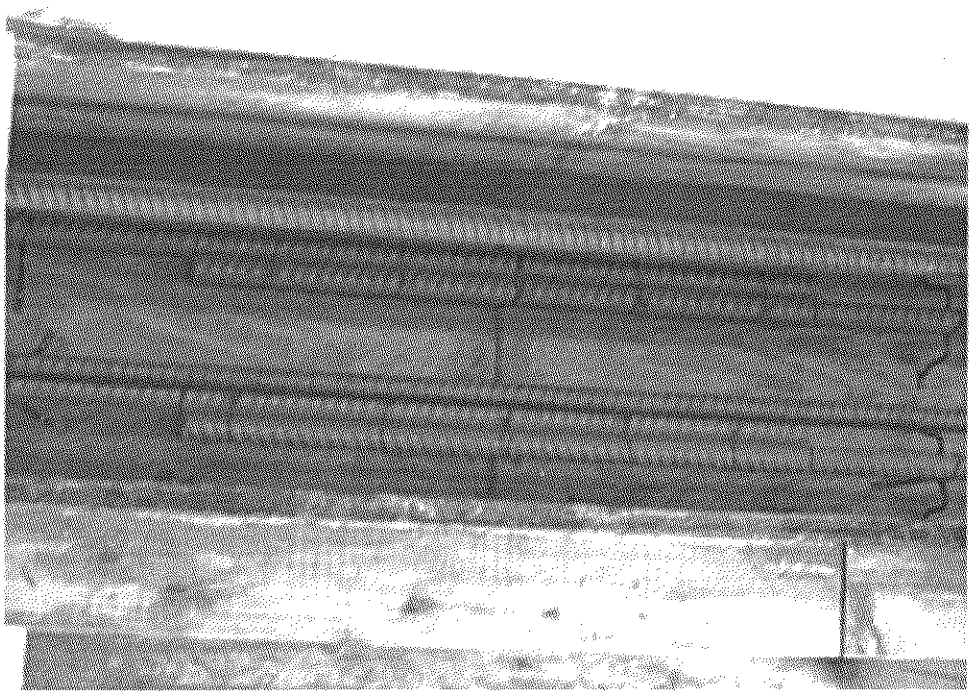

(b)

Fig. 3.3 Typical arrangement of splices, (a) with stirrups, (b) without stirrups

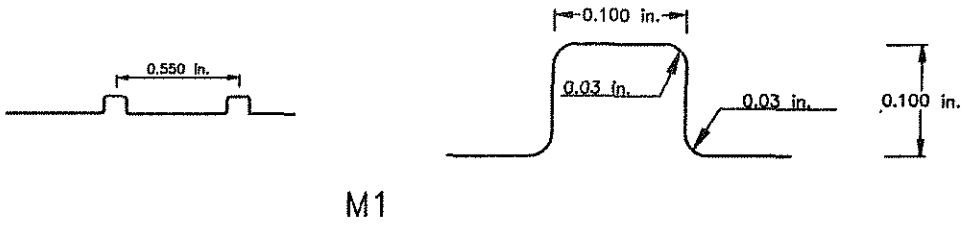

M1

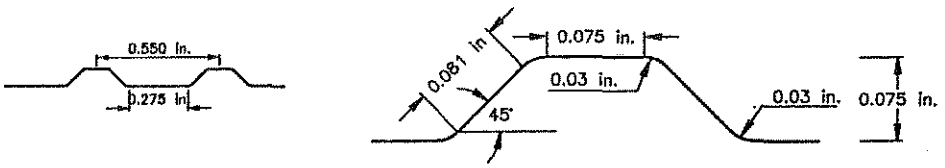

M45.3

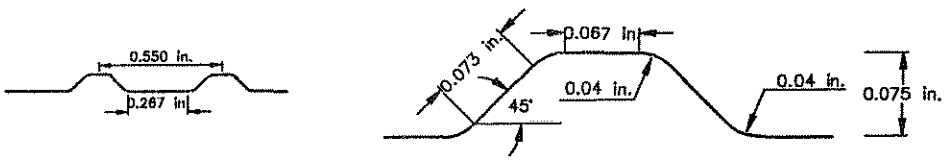

M45.4

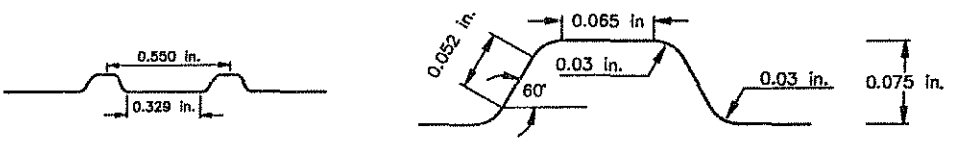

M60.3

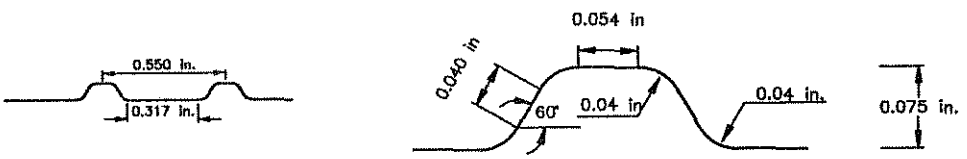

M60.4

Fig. 3.4 Machined bar deformation patterns

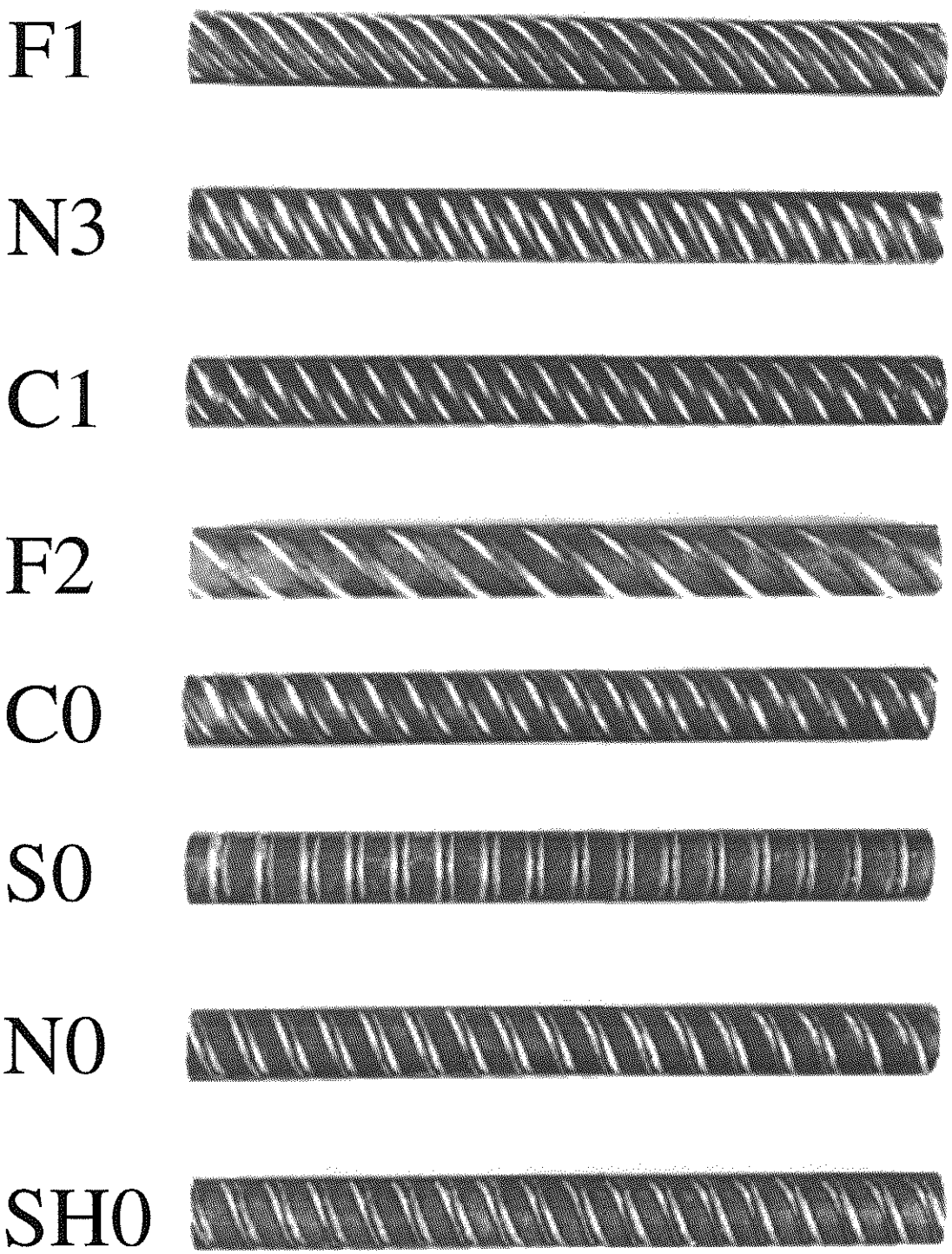

Fig. 3.5 ASTM A 615 No. 8 rolled bar deformation patterns

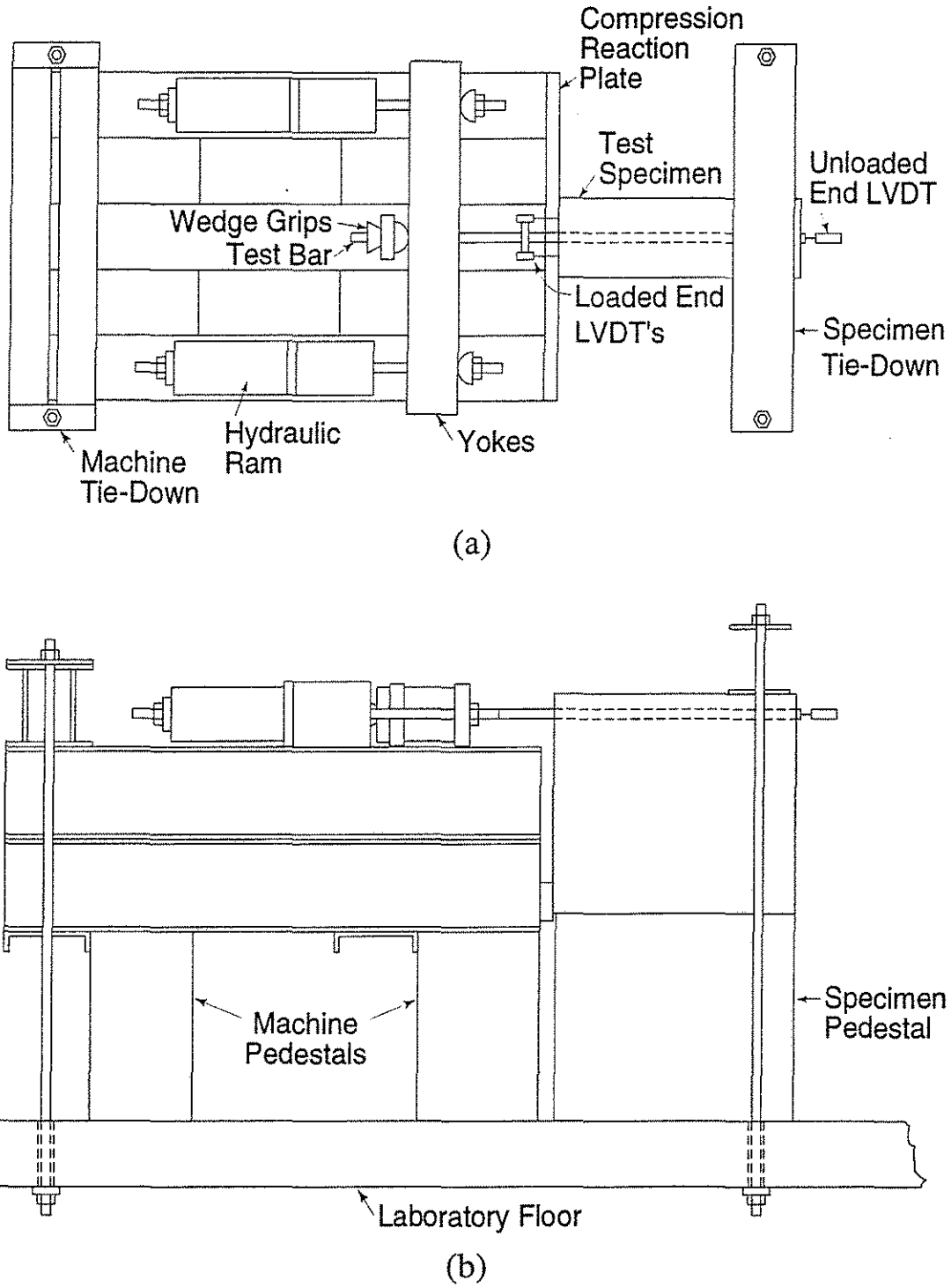

Fig. 3.6 Schematic of beam-end test apparatus, (a) plan view, (b) side view

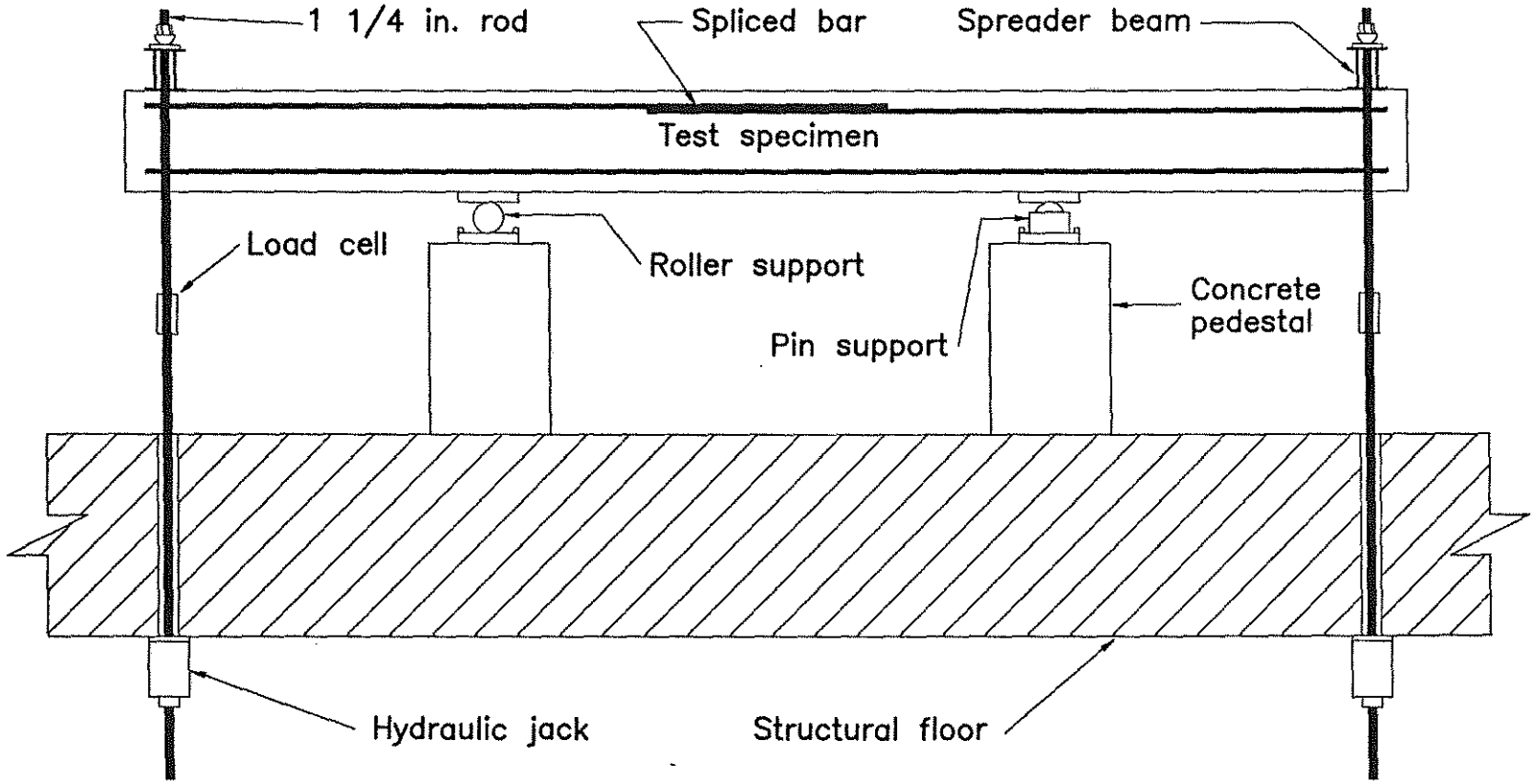

Fig. 3.7 Schematic of splice test setup

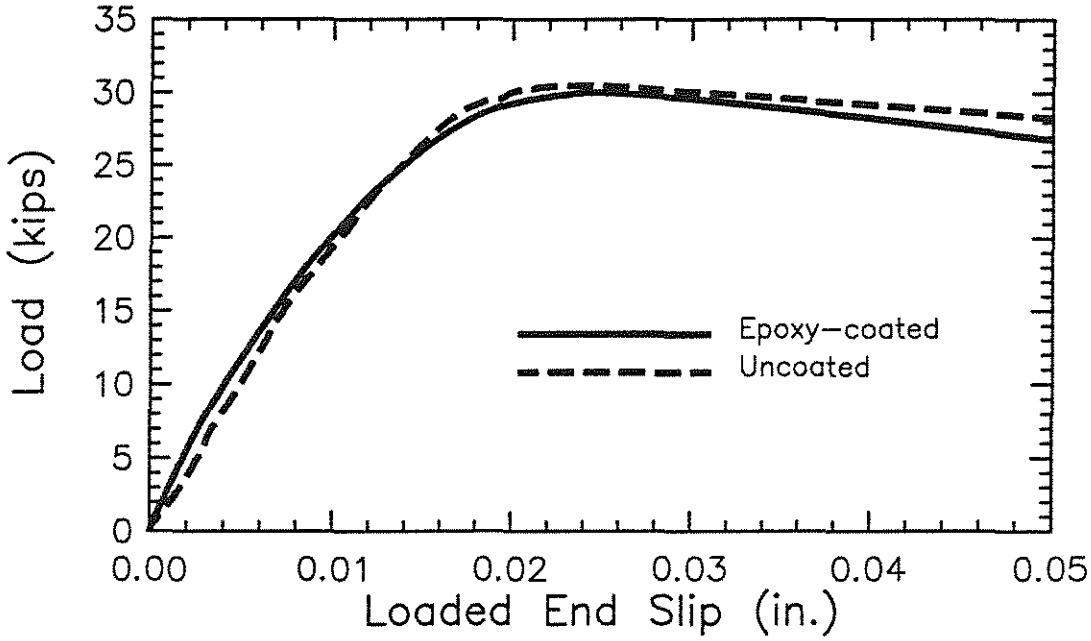

Fig. 3.8a Average load-loaded end slip curves for beam-end specimens containing M1 test bars

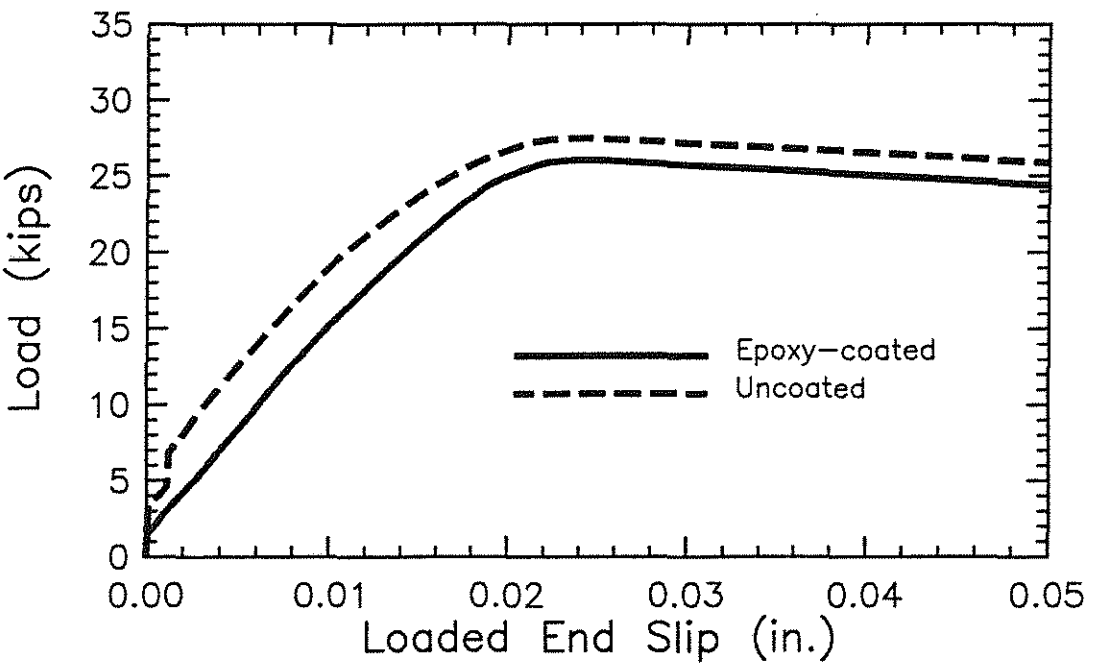

Fig. 3.8b Average load-loaded end slip curves for beam-end specimens containing C1 test bars

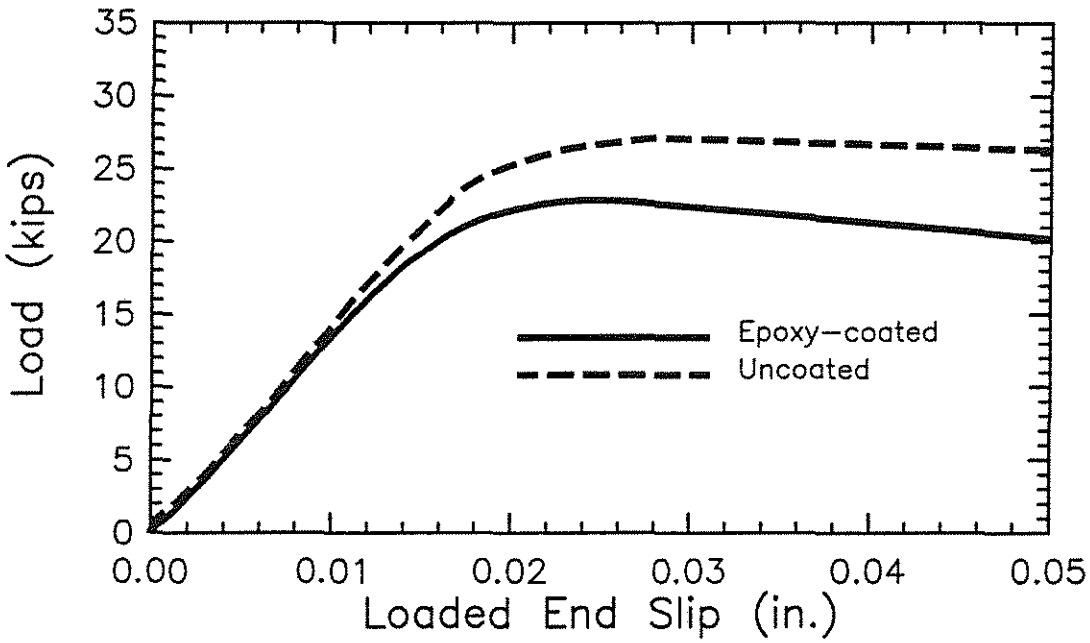

Fig. 3.8c Average load-loaded end slip curves for beam-end specimens containing F1 test bars

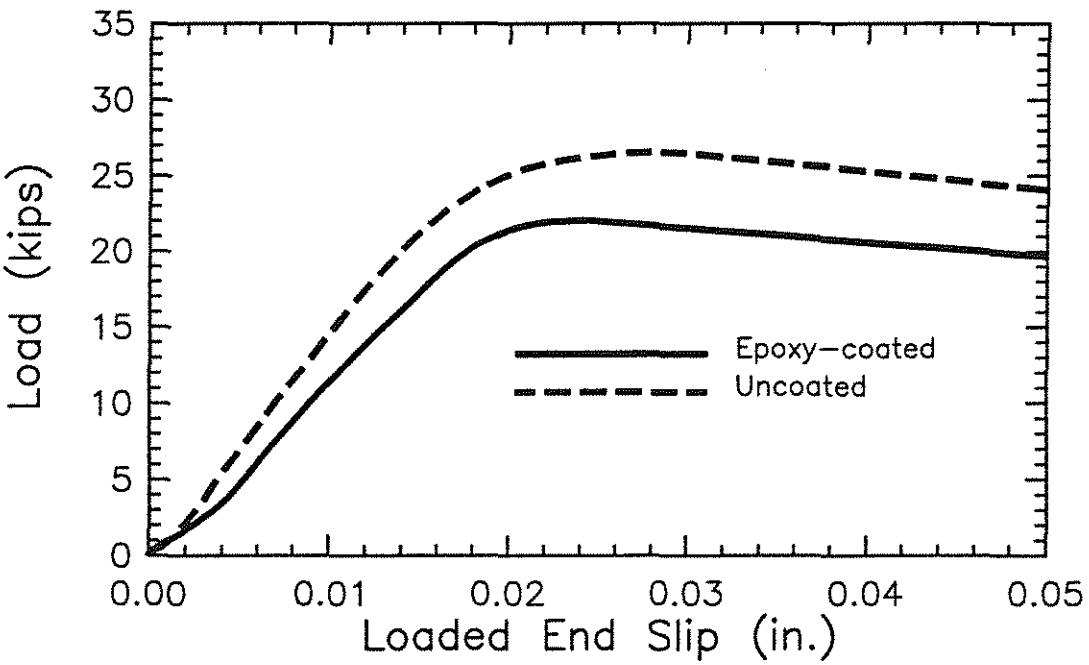

Fig. 3.8d Average load-loaded end slip curves for beam-end specimens containing F2 test bars

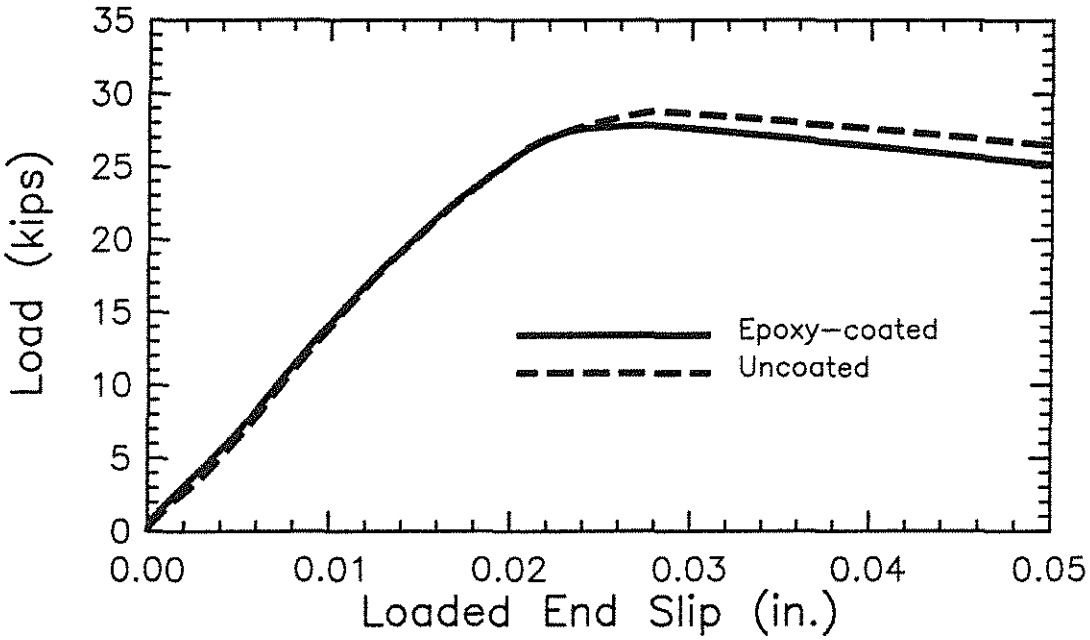

Fig. 3.8e Average load-loaded end slip curves for beam-end specimens containing M45.3 test bars

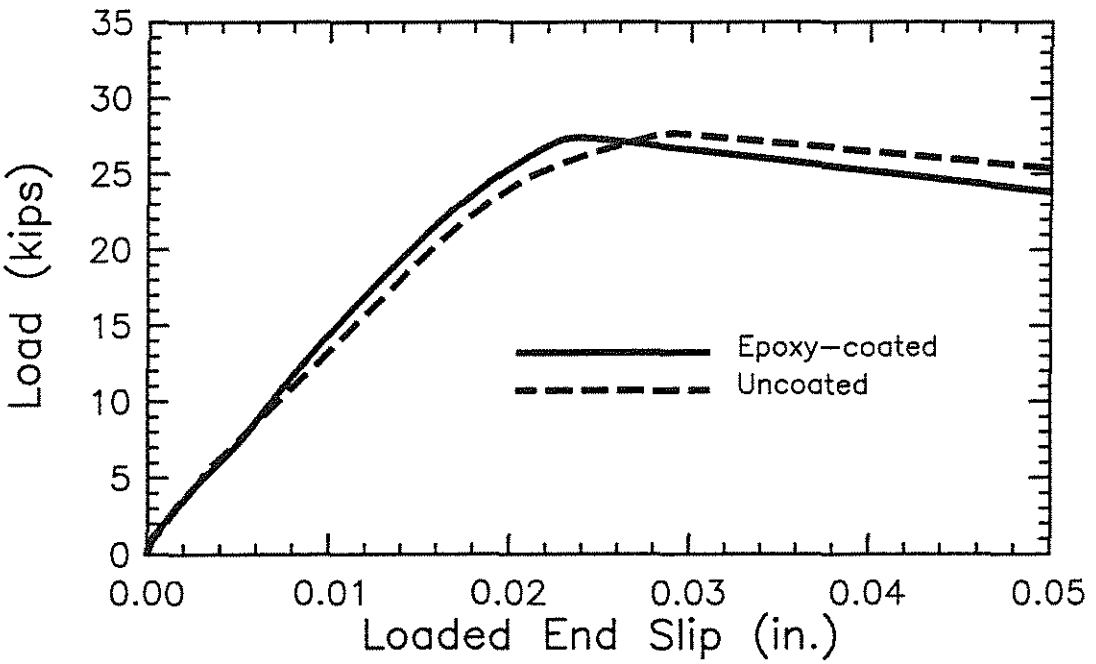

Fig. 3.8f Average load-loaded end slip curves for beam-end specimens containing M45.4 test bars

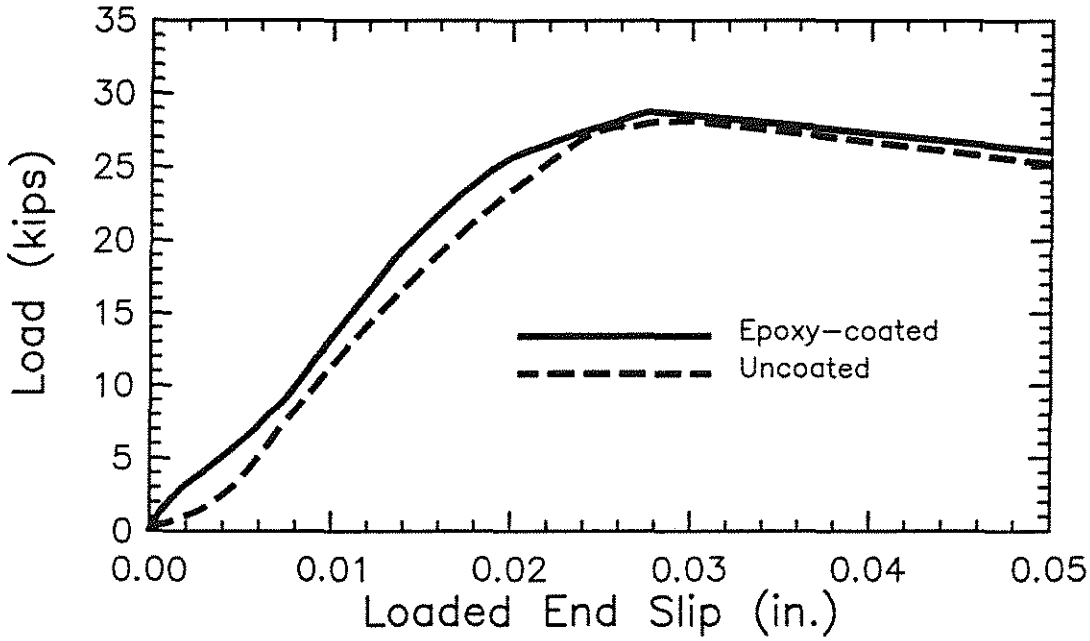

Fig. 3.8g Average load-loaded end slip curves for beam-end specimens containing M60.3 test bars

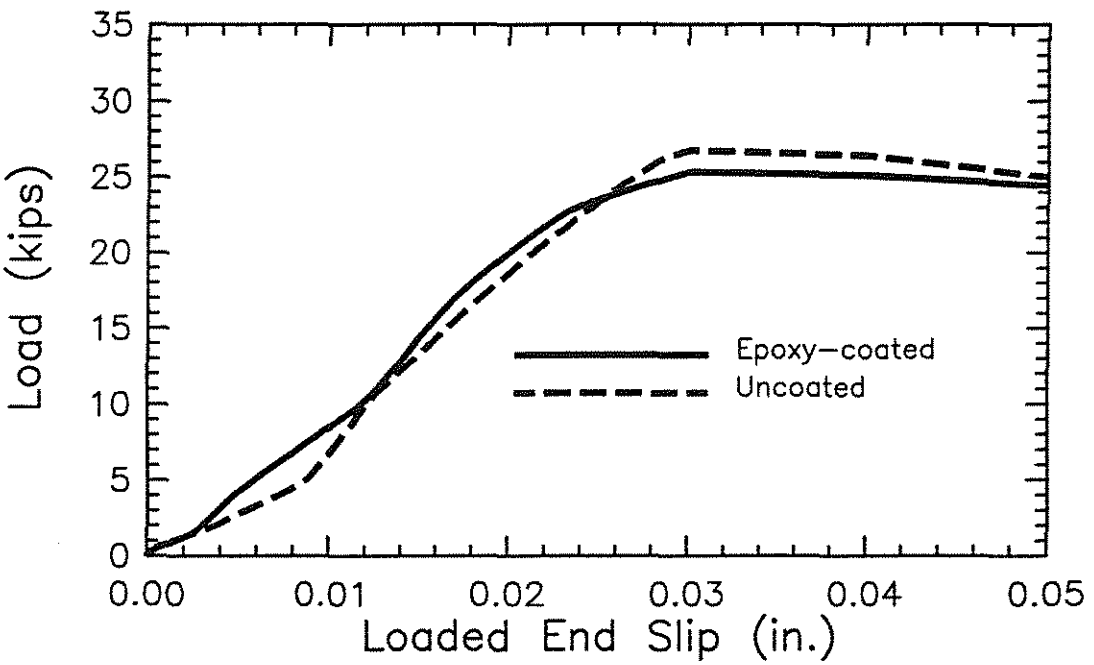

Fig. 3.8h Average load-loaded end slip curves for beam-end specimens containing M60.4 test bars

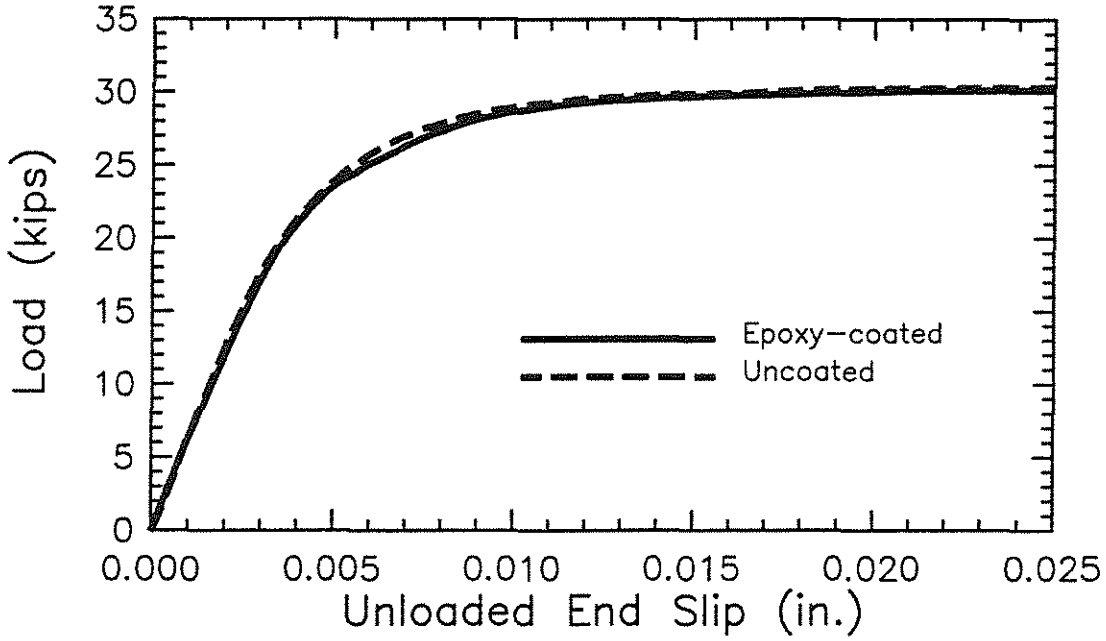

Fig. 3.9a Average load-unloaded end slip curves for beam-end specimens containing M1 test bars

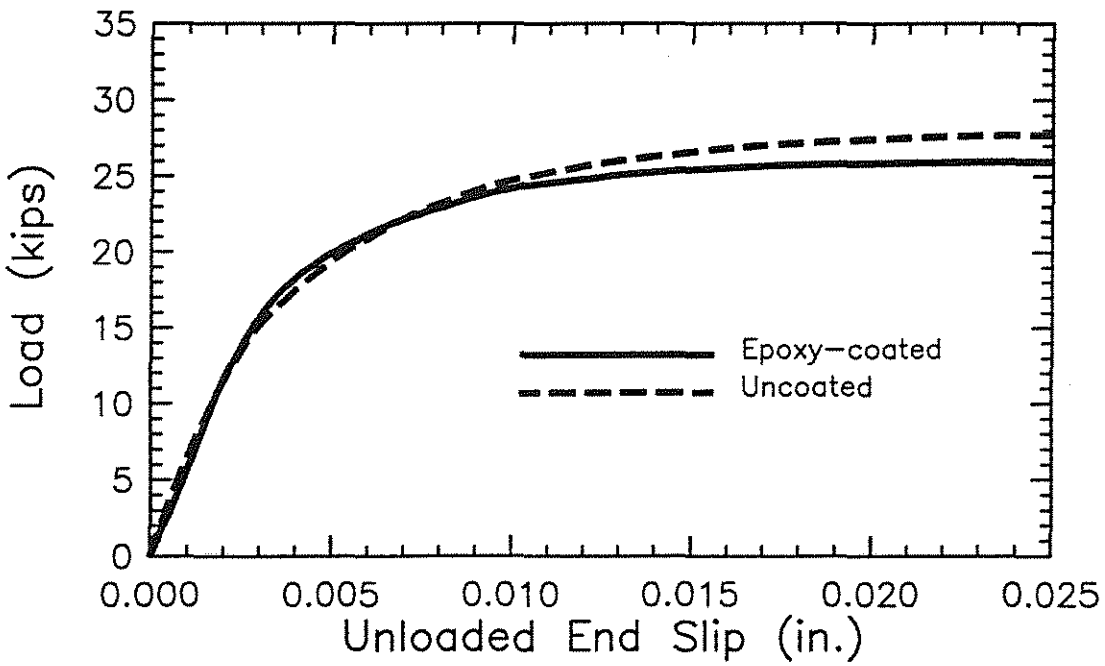

Fig. 3.9b Average load-unloaded end slip curves for beam-end specimens containing C1 test bars

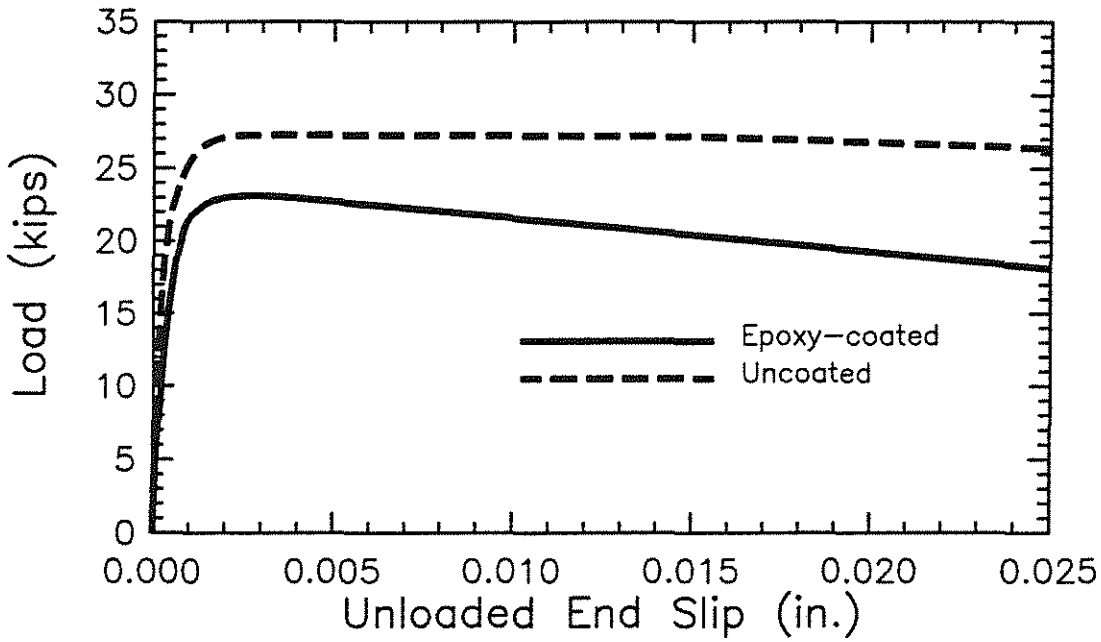

Fig. 3.9c Average load-unloaded end slip curves for beam-end specimens containing F1 test bars

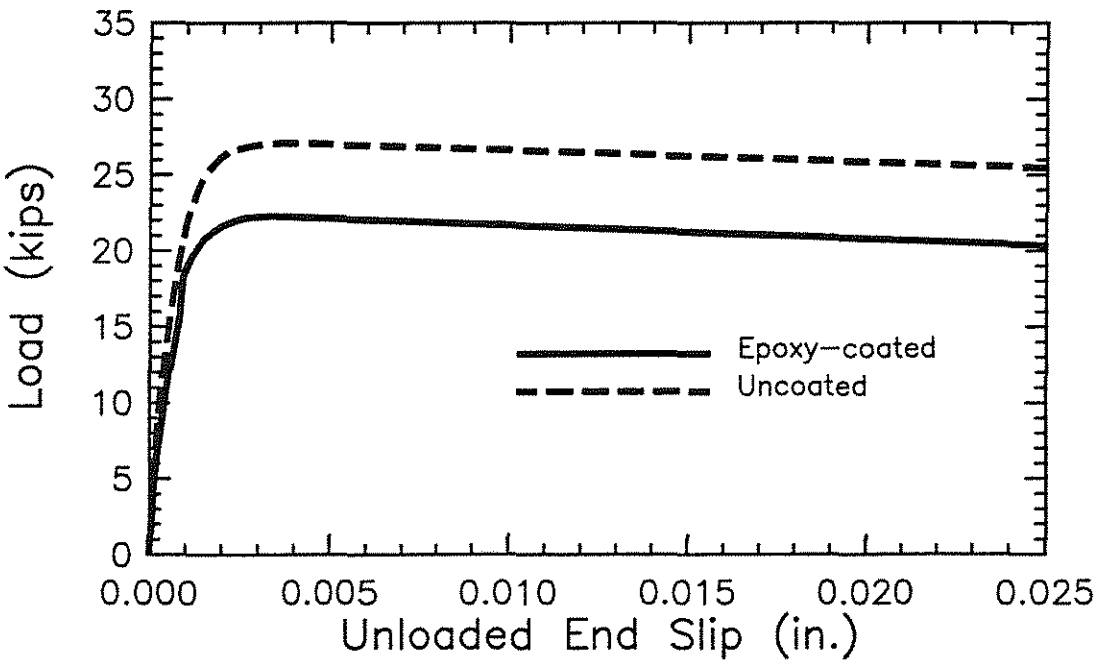

Fig. 3.9d Average load-unloaded end slip curves for beam-end specimens containing F2 test bars

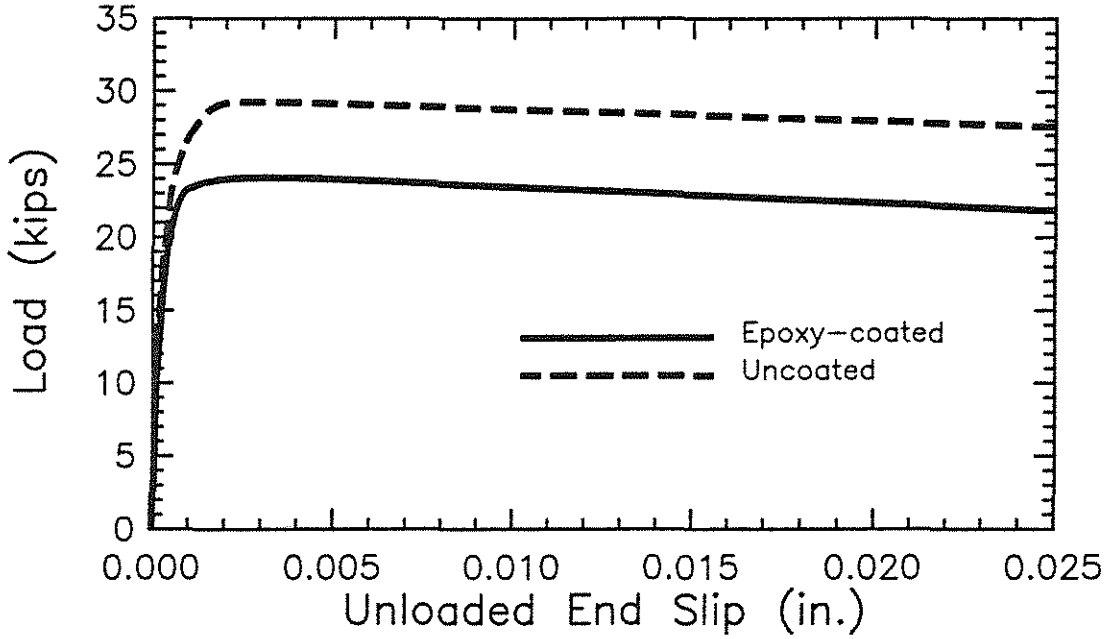

Fig. 3.9e Average load-unloaded end slip curves for beam-end specimens containing M45.3 test bars

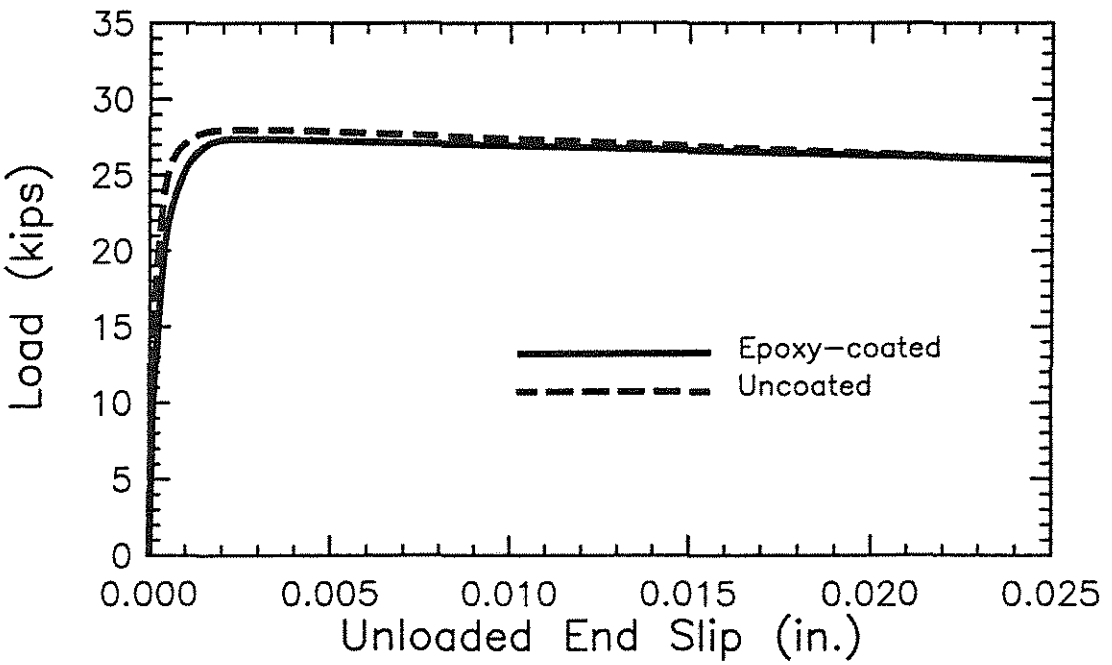

Fig. 3.9f Average load-unloaded end slip curves for beam-end specimens containing M45.4 test bars

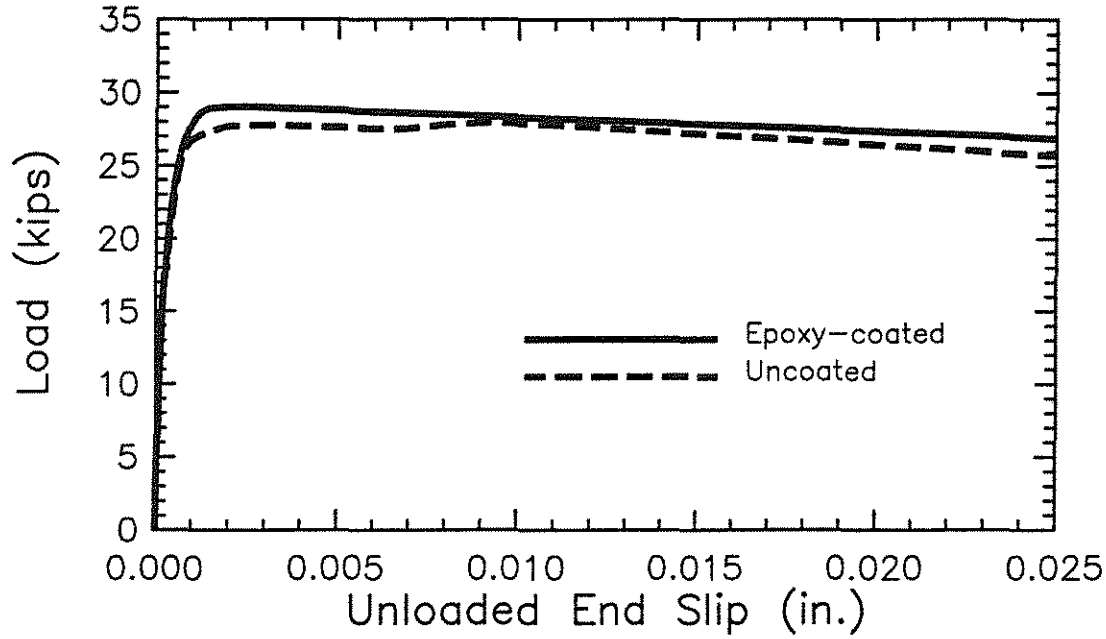

Fig. 3.9g Average load-unloaded end slip curves for beam-end specimens containing M60.3 test bars

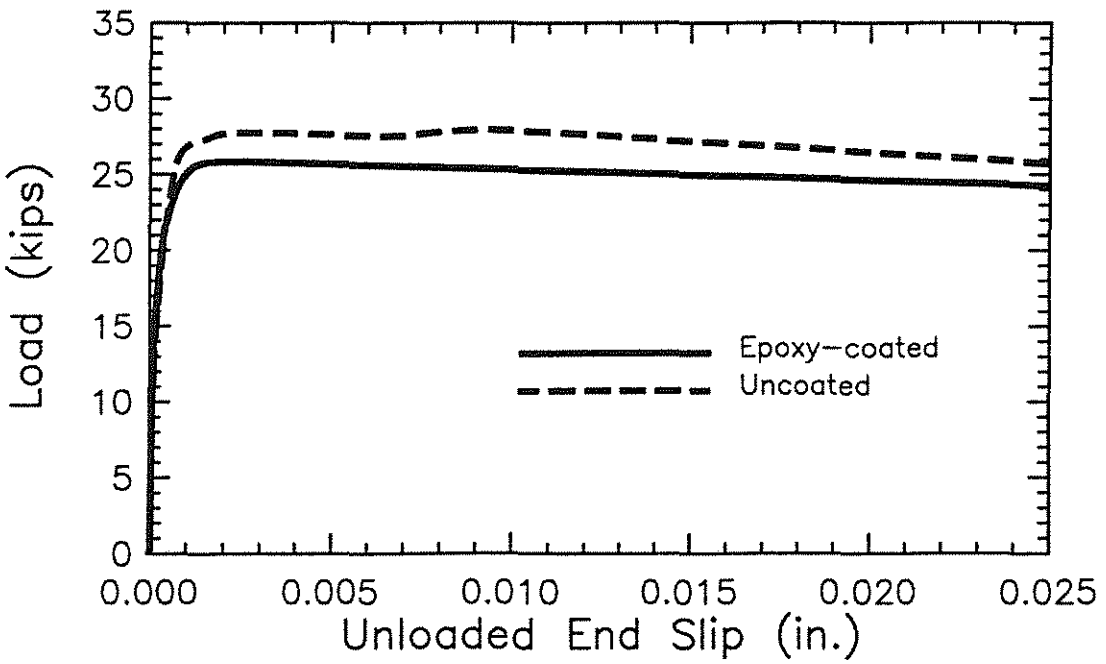

Fig. 3.9h Average load-unloaded end slip curves for beam-end specimens containing M60.4 test bar

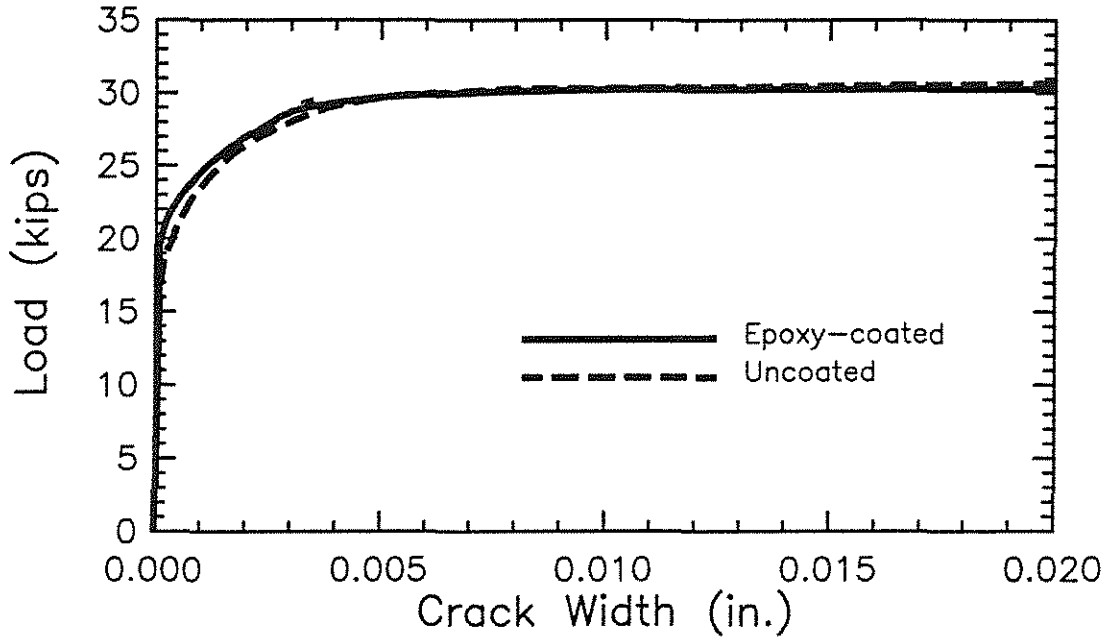

Fig. 3.10a Average load-crack width curves for beam-end specimens containing M1 test bars

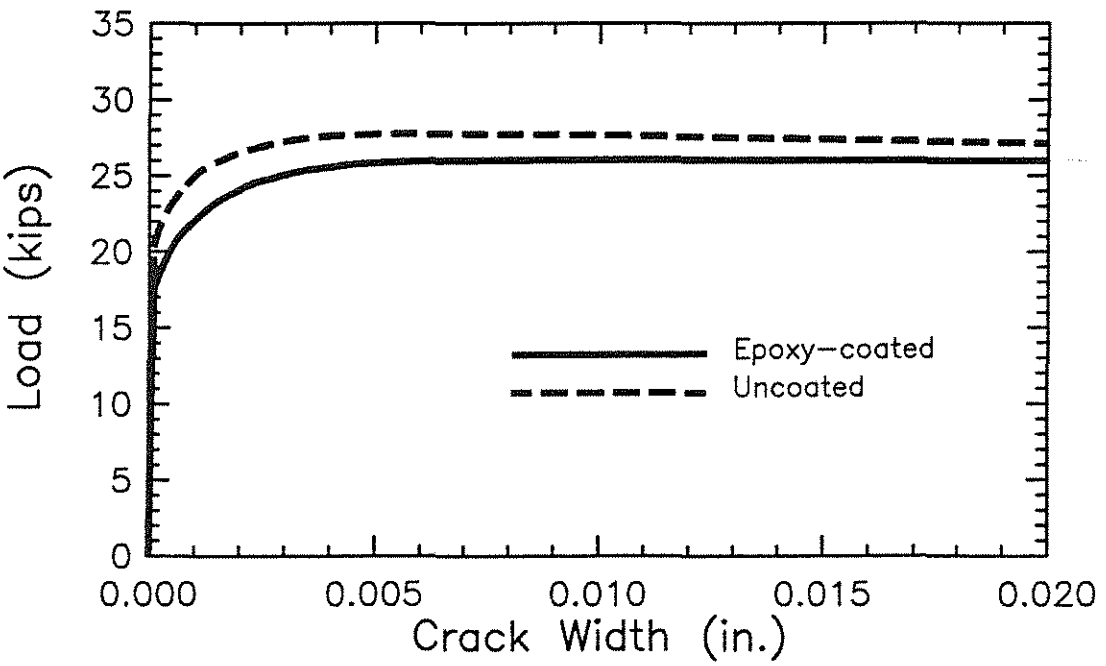

Fig. 3.10b Average load-crack width curves for beam-end specimens containing C1 test bars

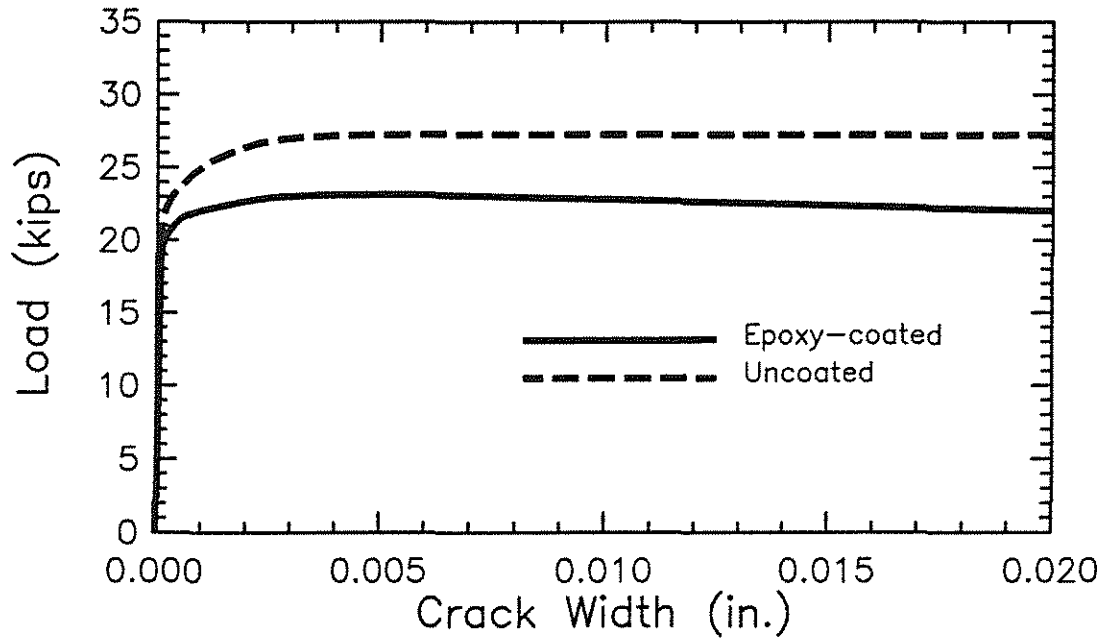

Fig. 3.10c Average load-crack width curves for beam-end specimens containing F1 test bars

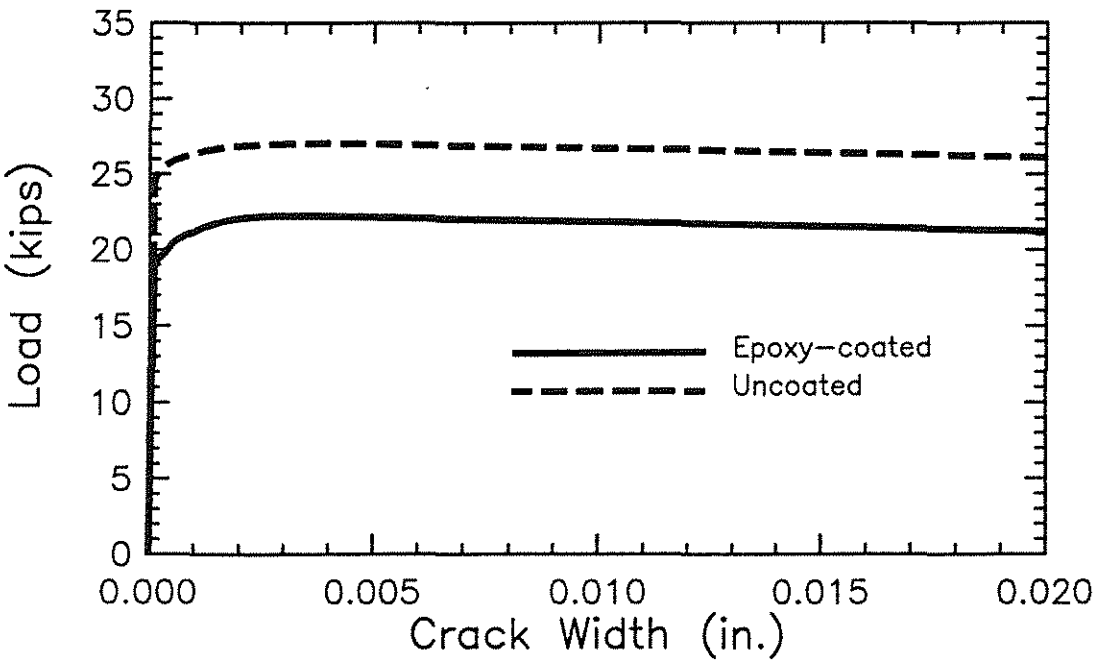

Fig. 3.10d Average load-crack width curves for beam-end specimens containing F2 test bars

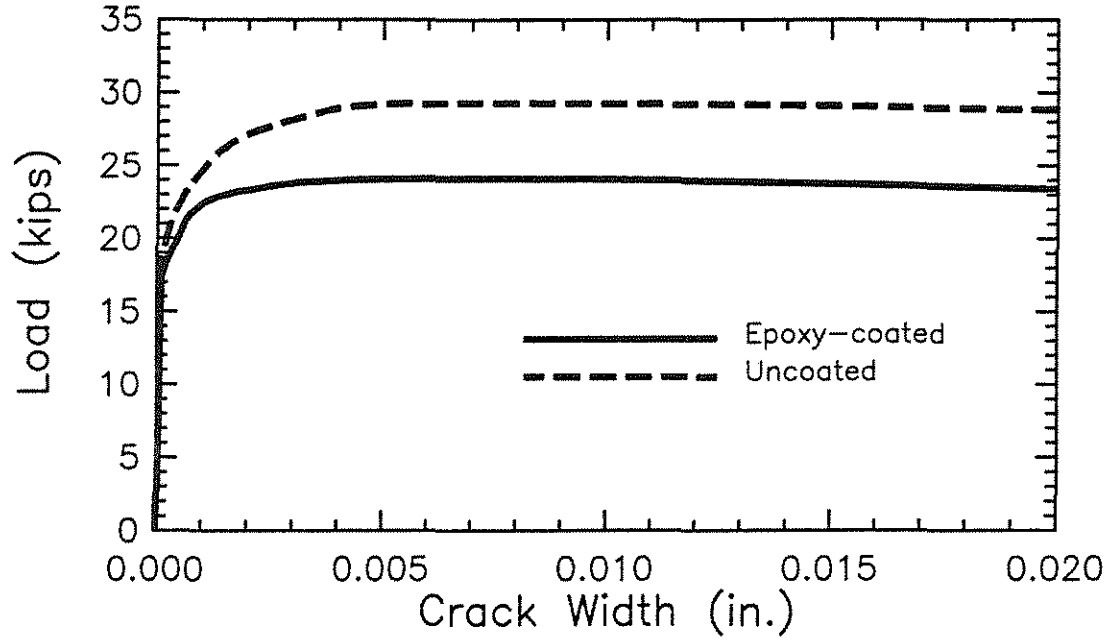

Fig. 3.10e Average load-crack width curves for beam-end specimens containing M45.3 test bars

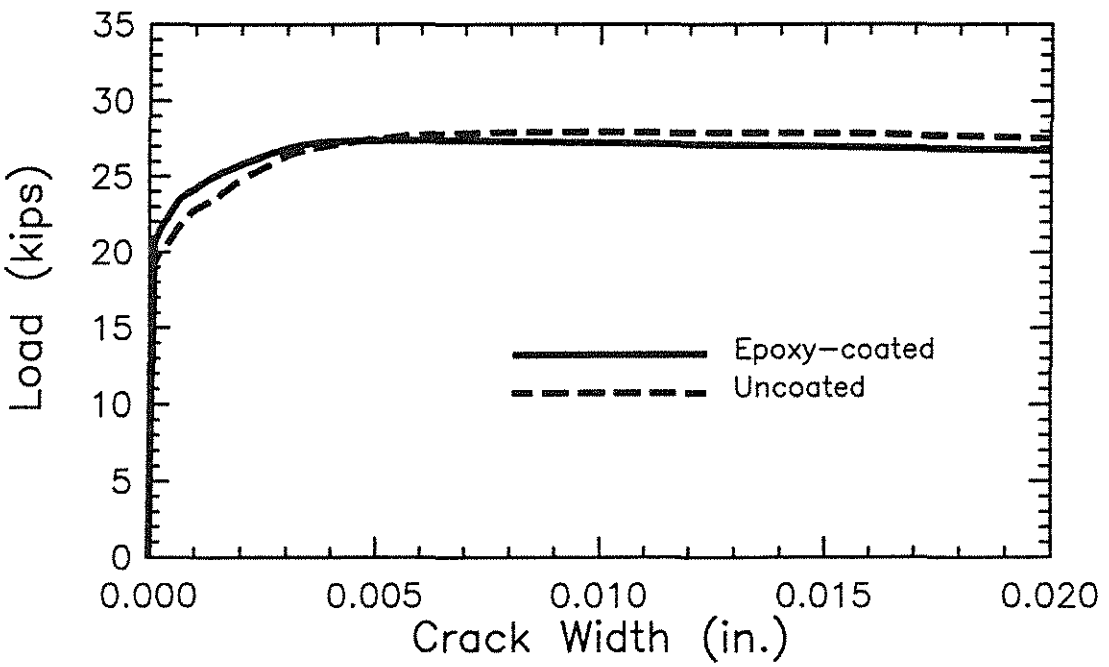

Fig. 3.10f Average load-crack width curves for beam-end specimens containing M45.4 test bars

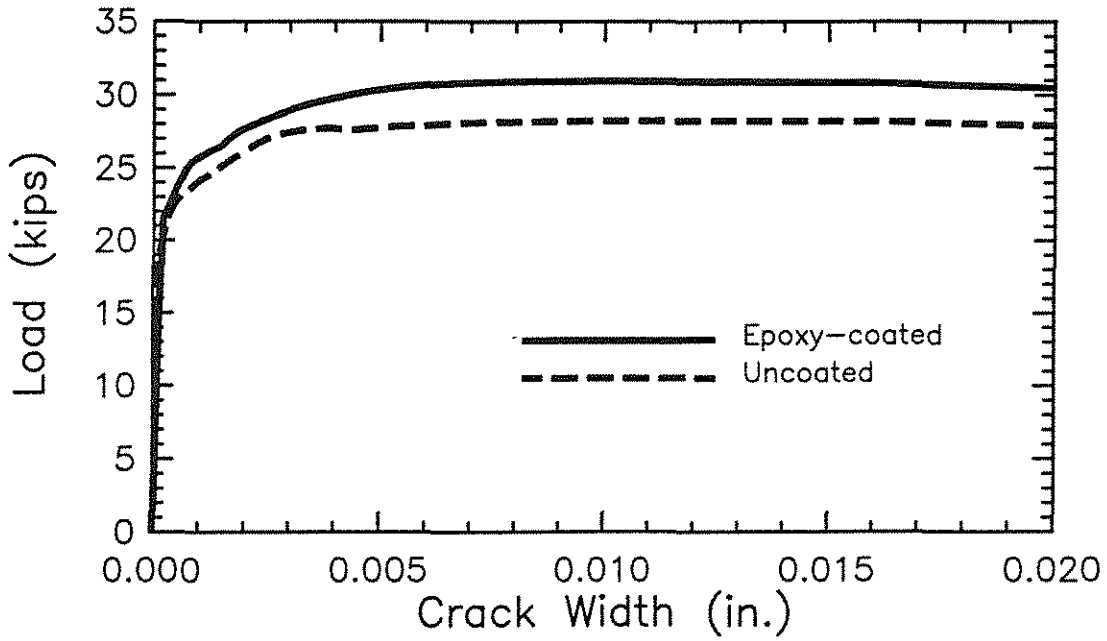

Fig. 3.10g Average load-crack width curves for beam-end specimens containing M60.3 test bars

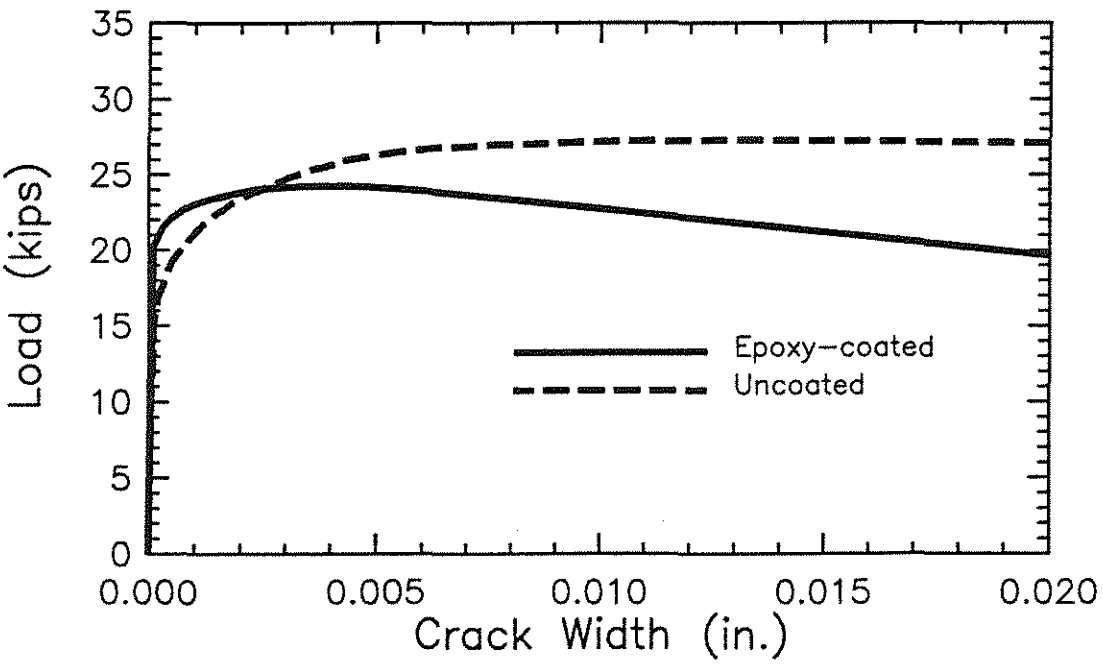

Fig. 3.10h Average load-crack width curves for beam-end specimens containing M60.4 test bars

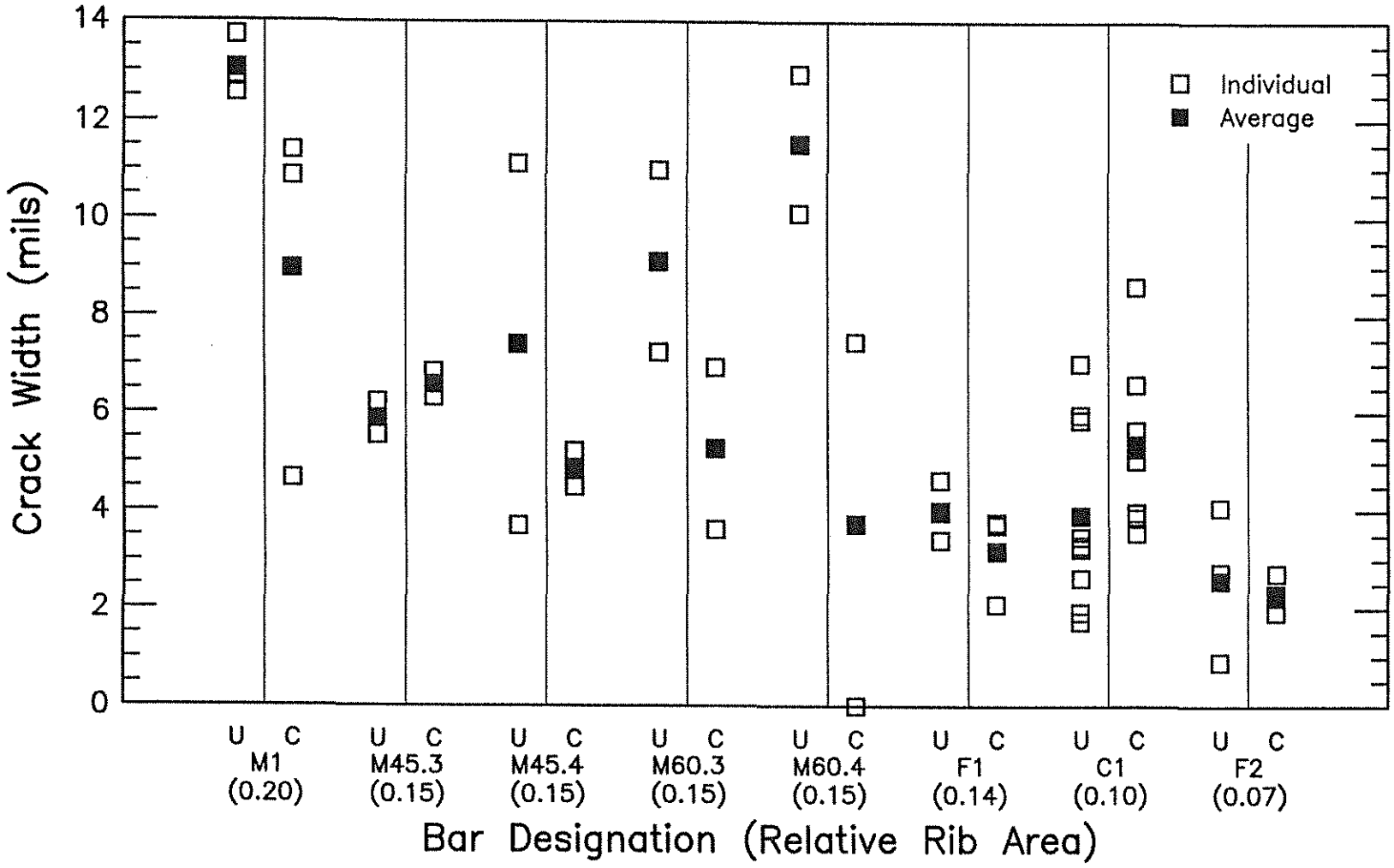

Fig. 3.11 Width of splitting crack just prior of peak for beam-end test bars

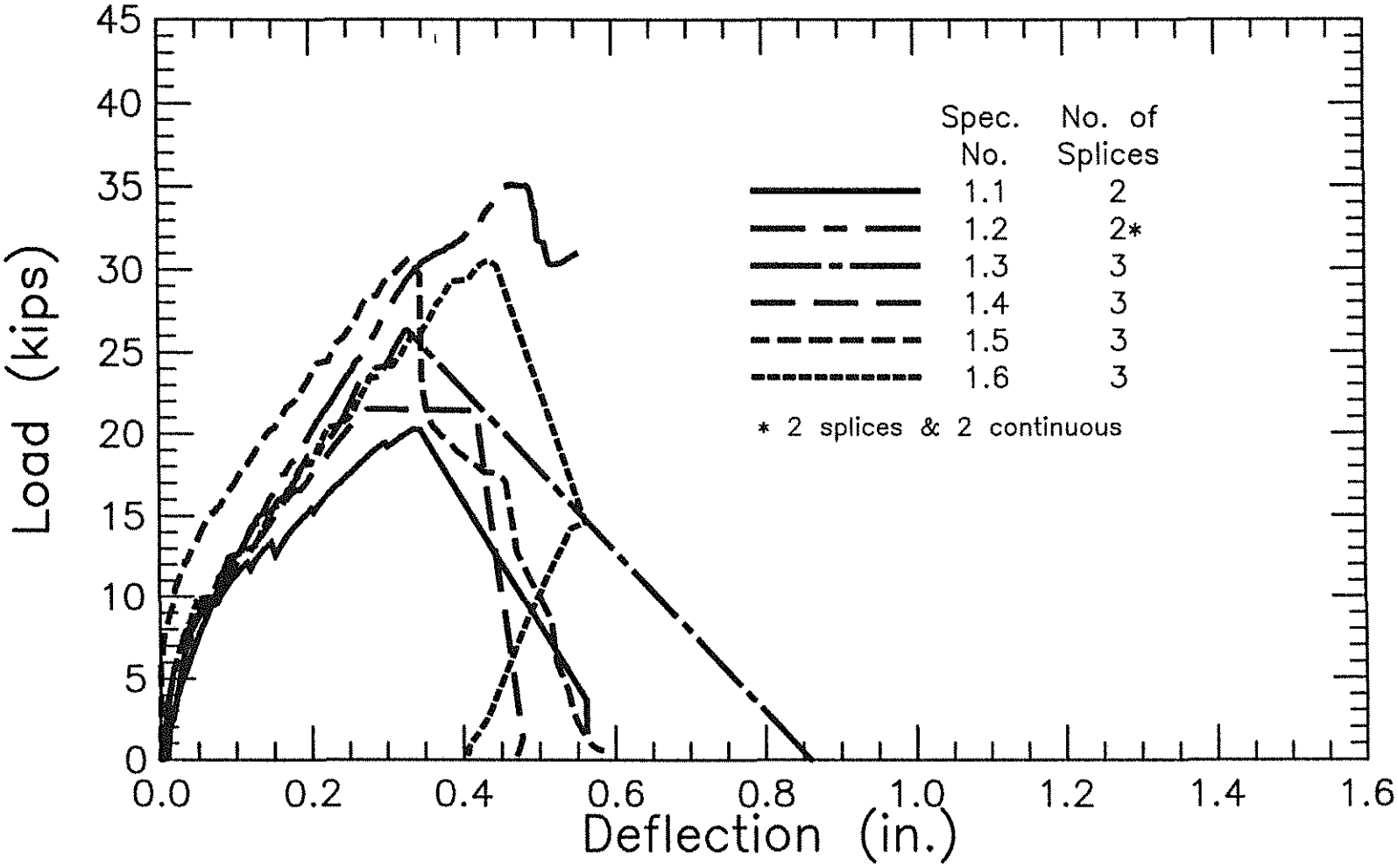

Fig. 3.12a Load-deflection curves for splice specimens in group 1

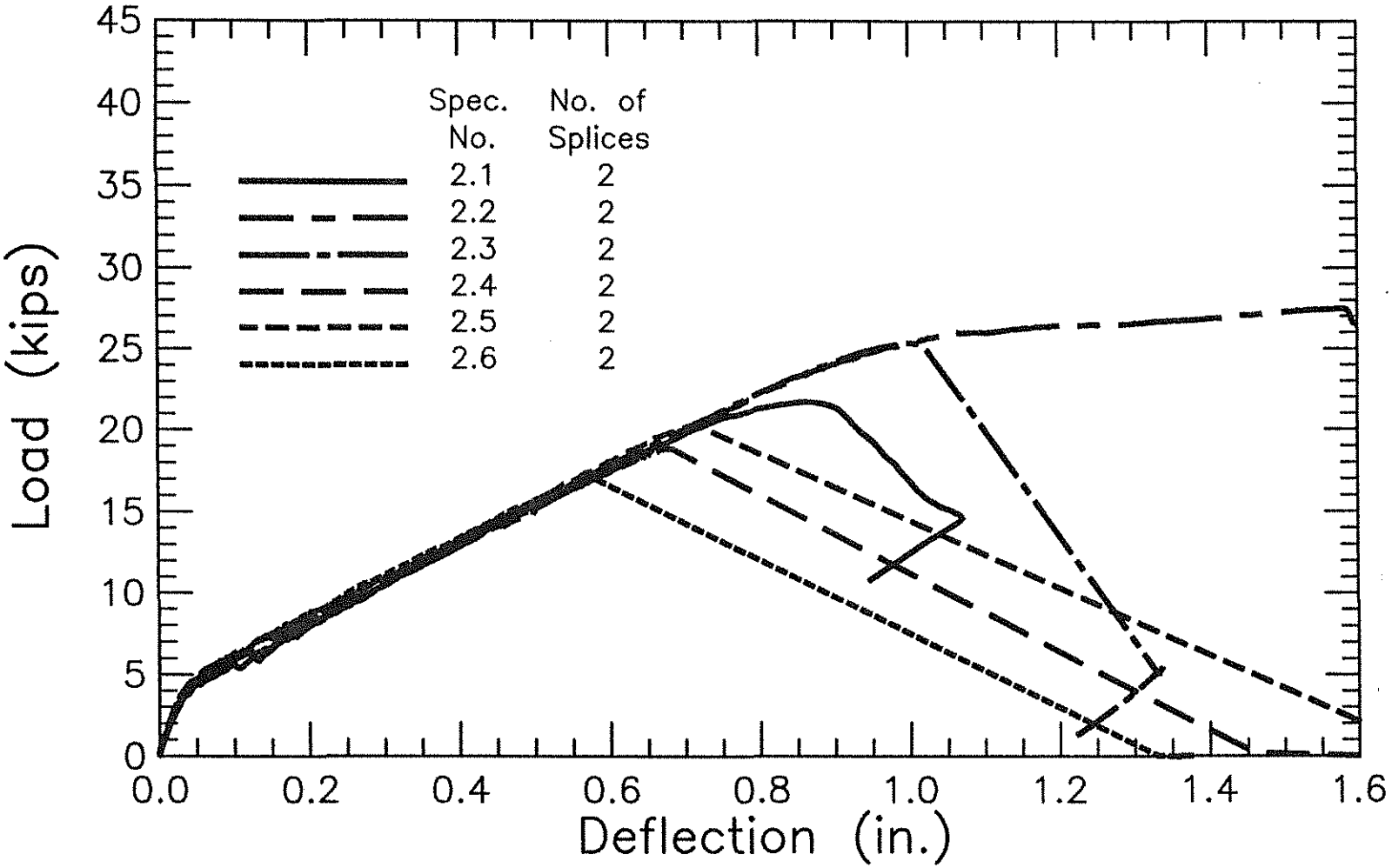

Fig. 3.12b Load-deflection curves for splice specimens in group 2

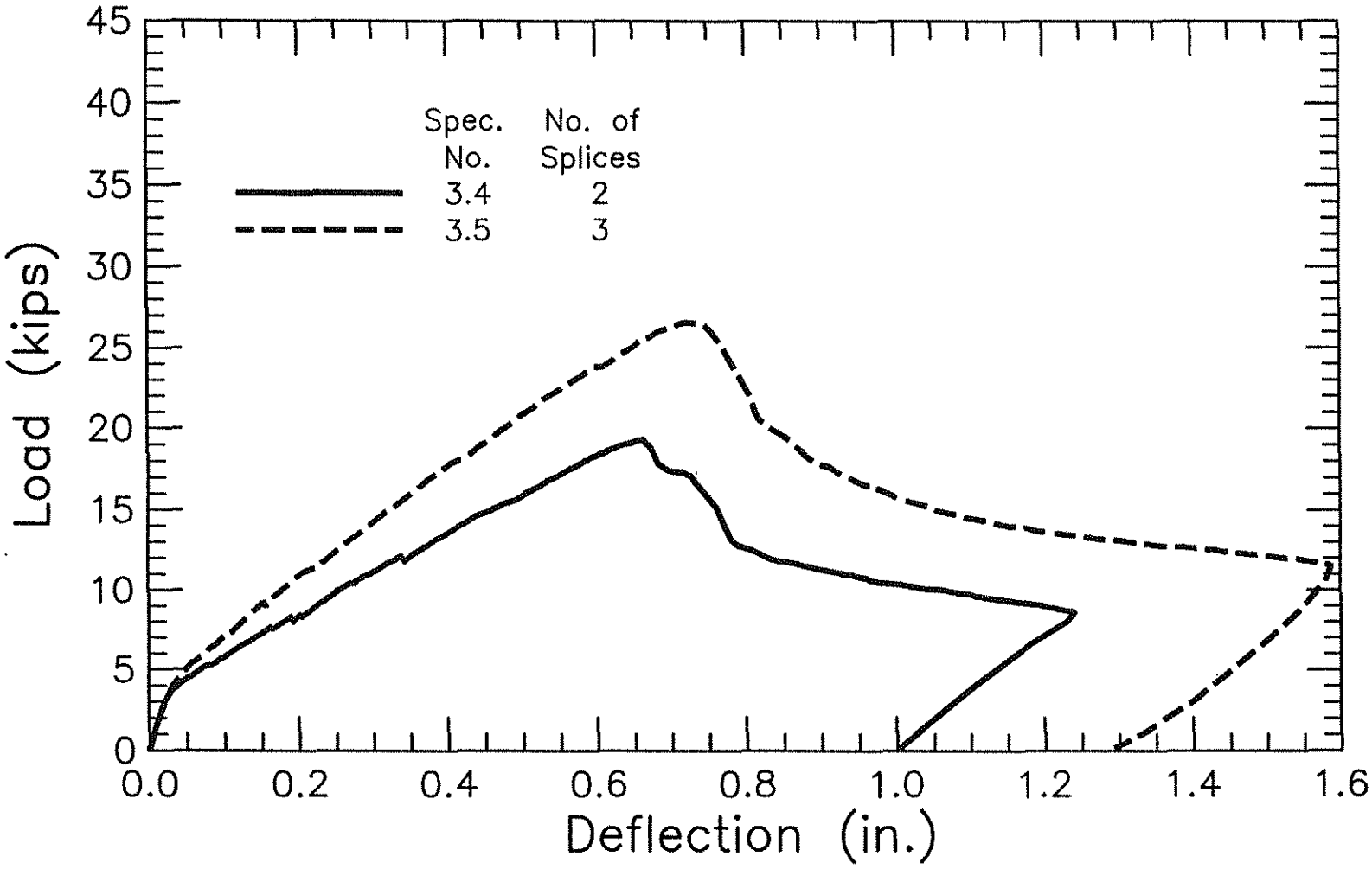

Fig. 3.12c Load-deflection curves for splice specimens in group 3

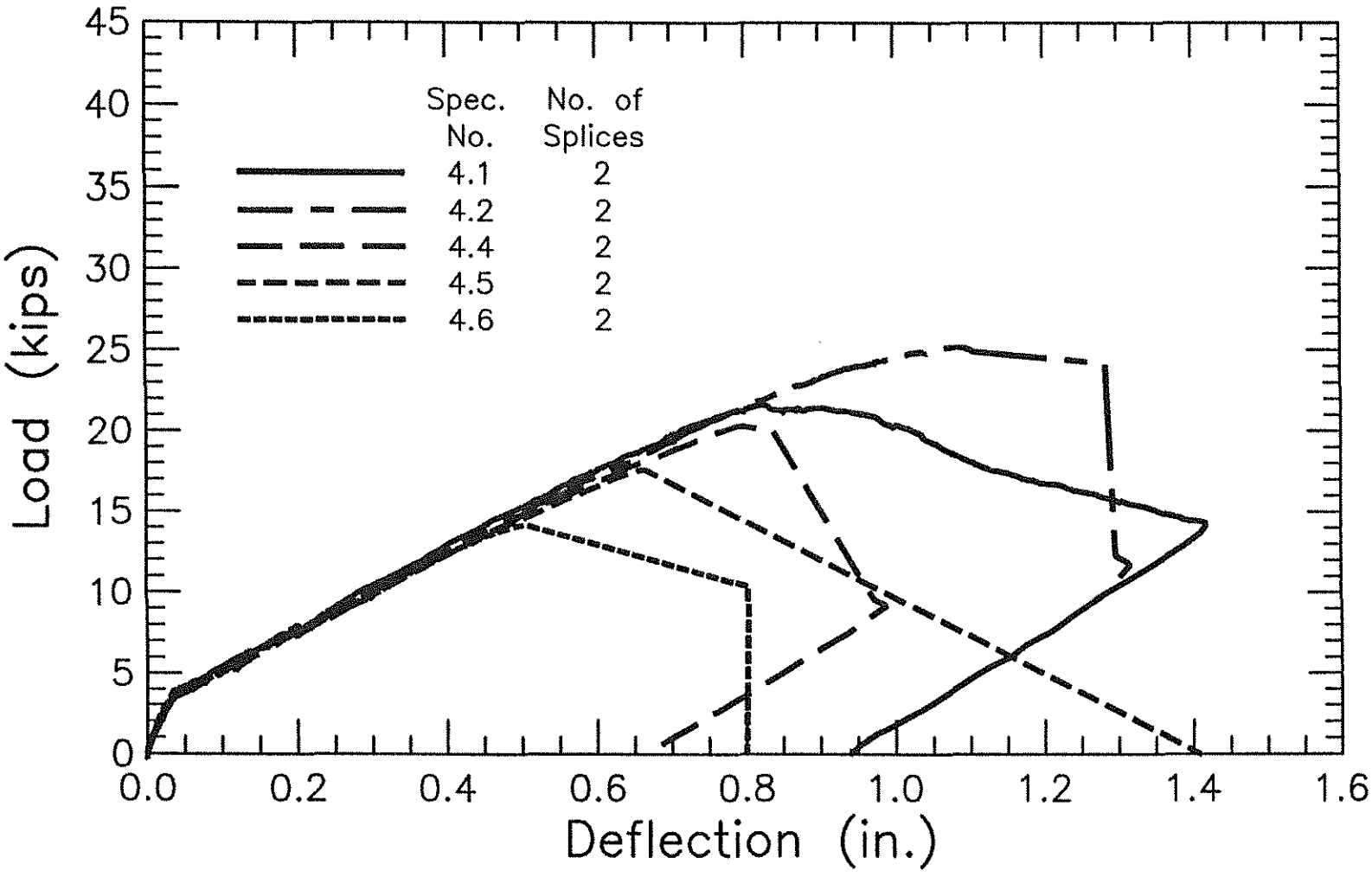

Fig. 3.12d Load-deflection curves for splice specimens in group 4

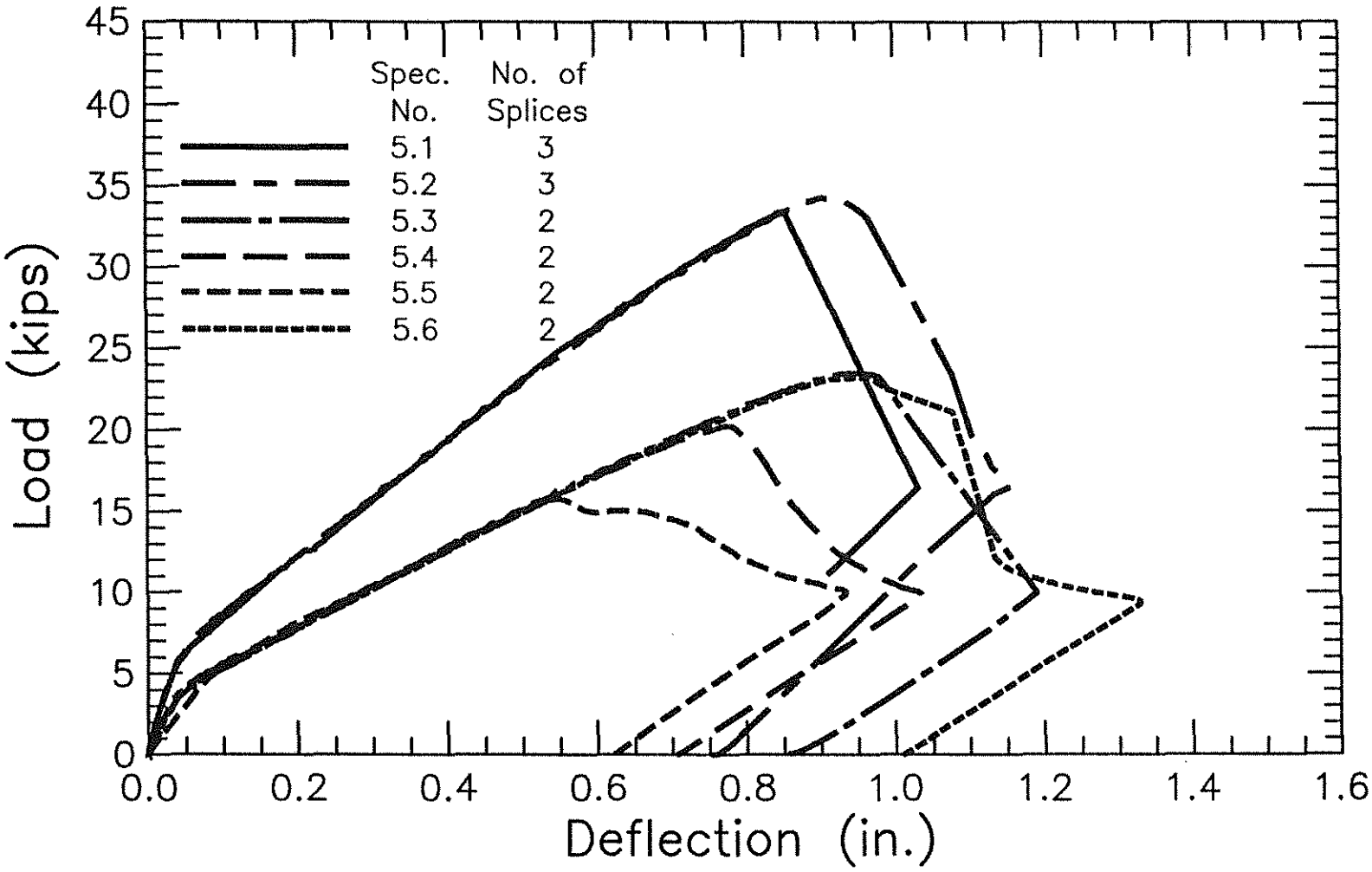

Fig. 3.12e Load-deflection curves for splice specimens in group 5

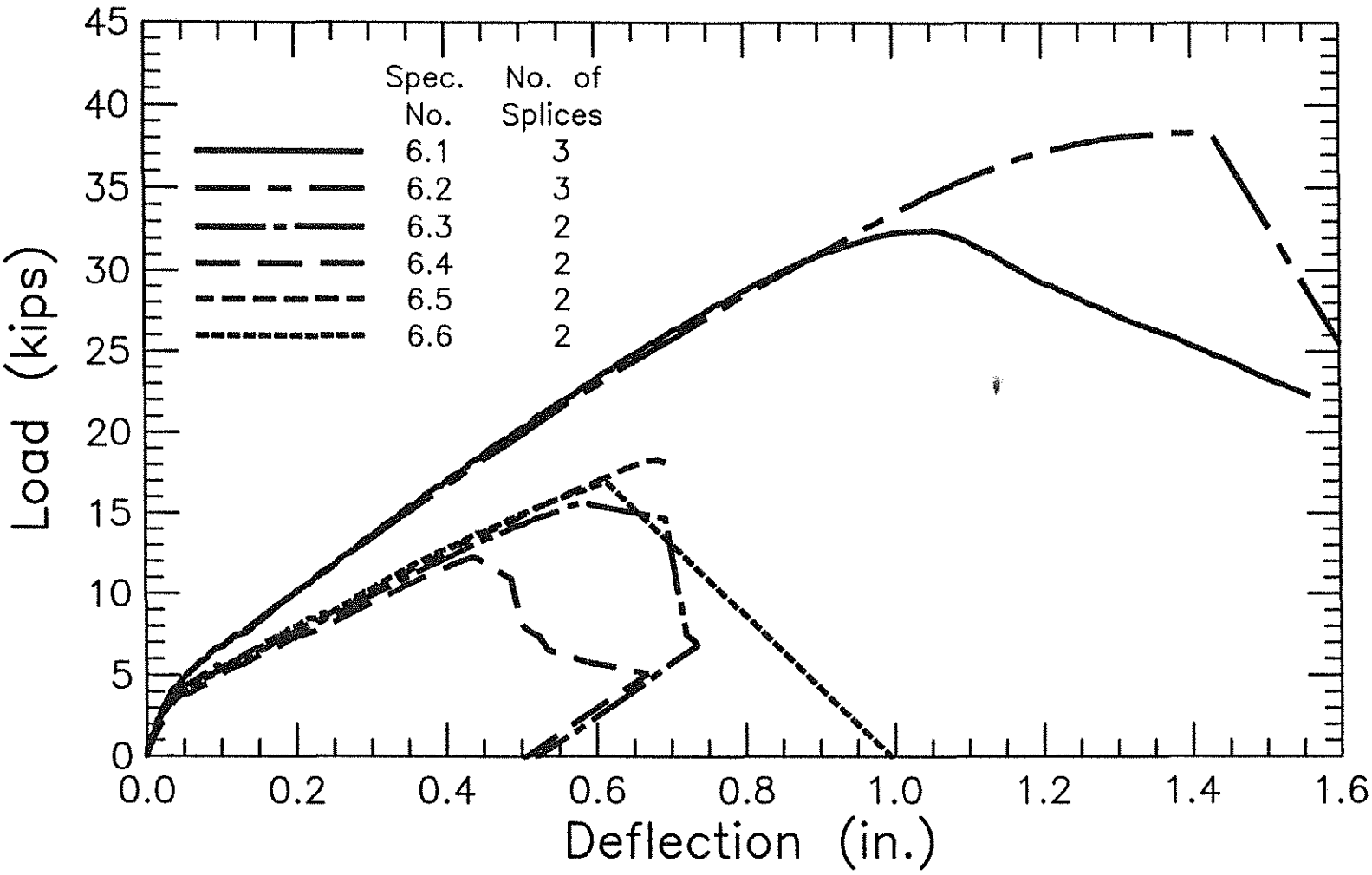

Fig. 3.12f Load-deflection curves for splice specimens in group 6

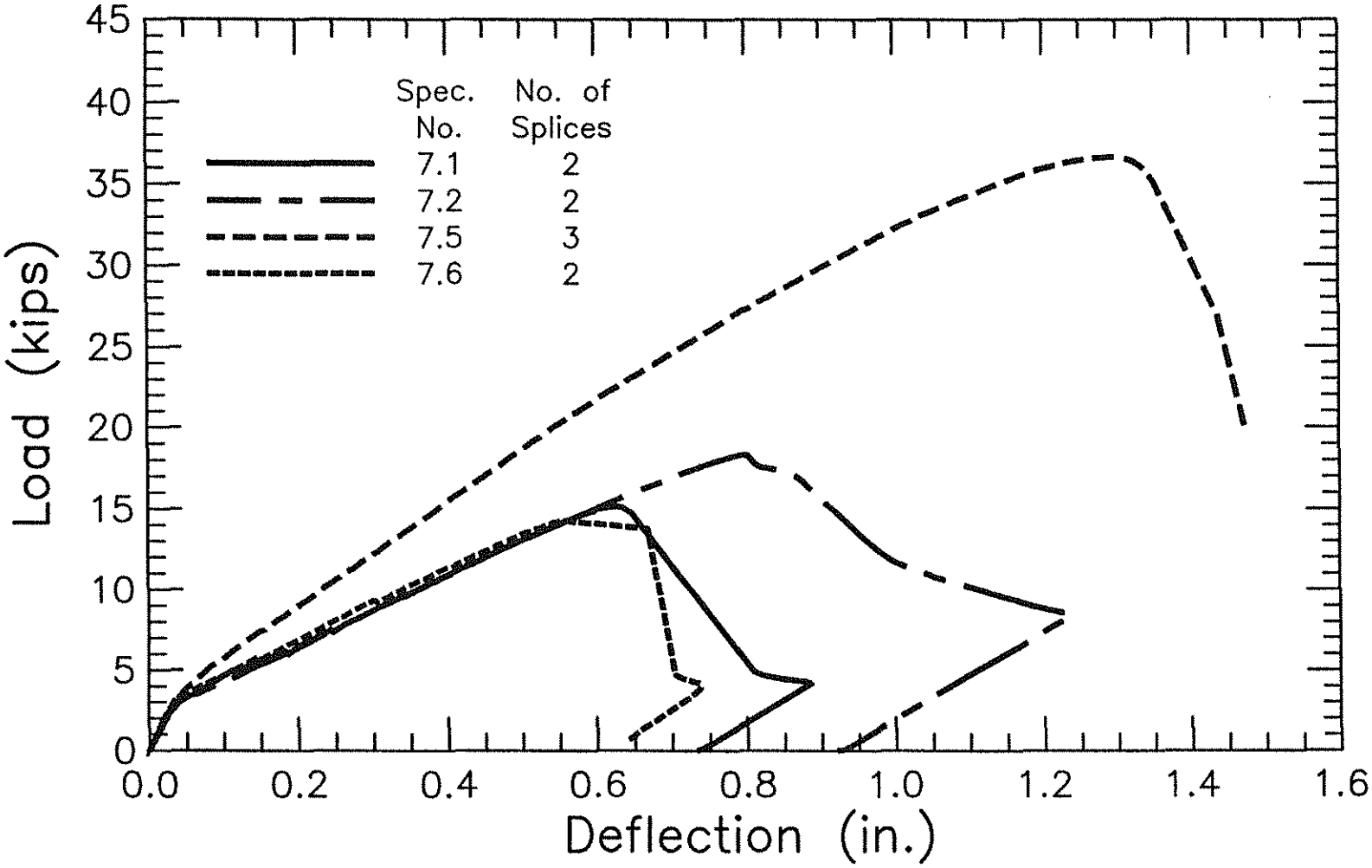

Fig. 3.12g Load-deflection curves for splice specimens in group 7

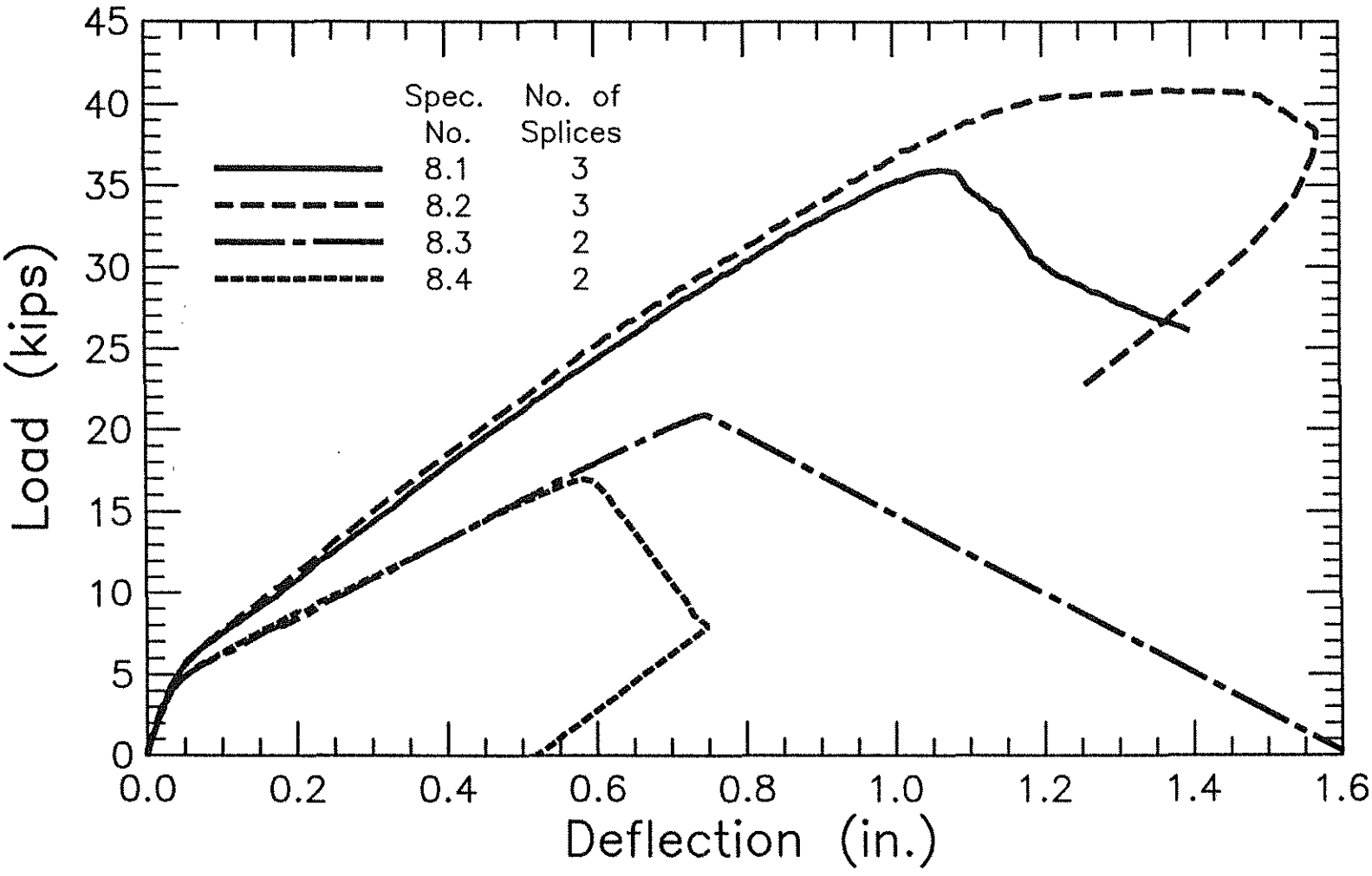

Fig. 3.12h Load-deflection curves for splice specimens in group 8

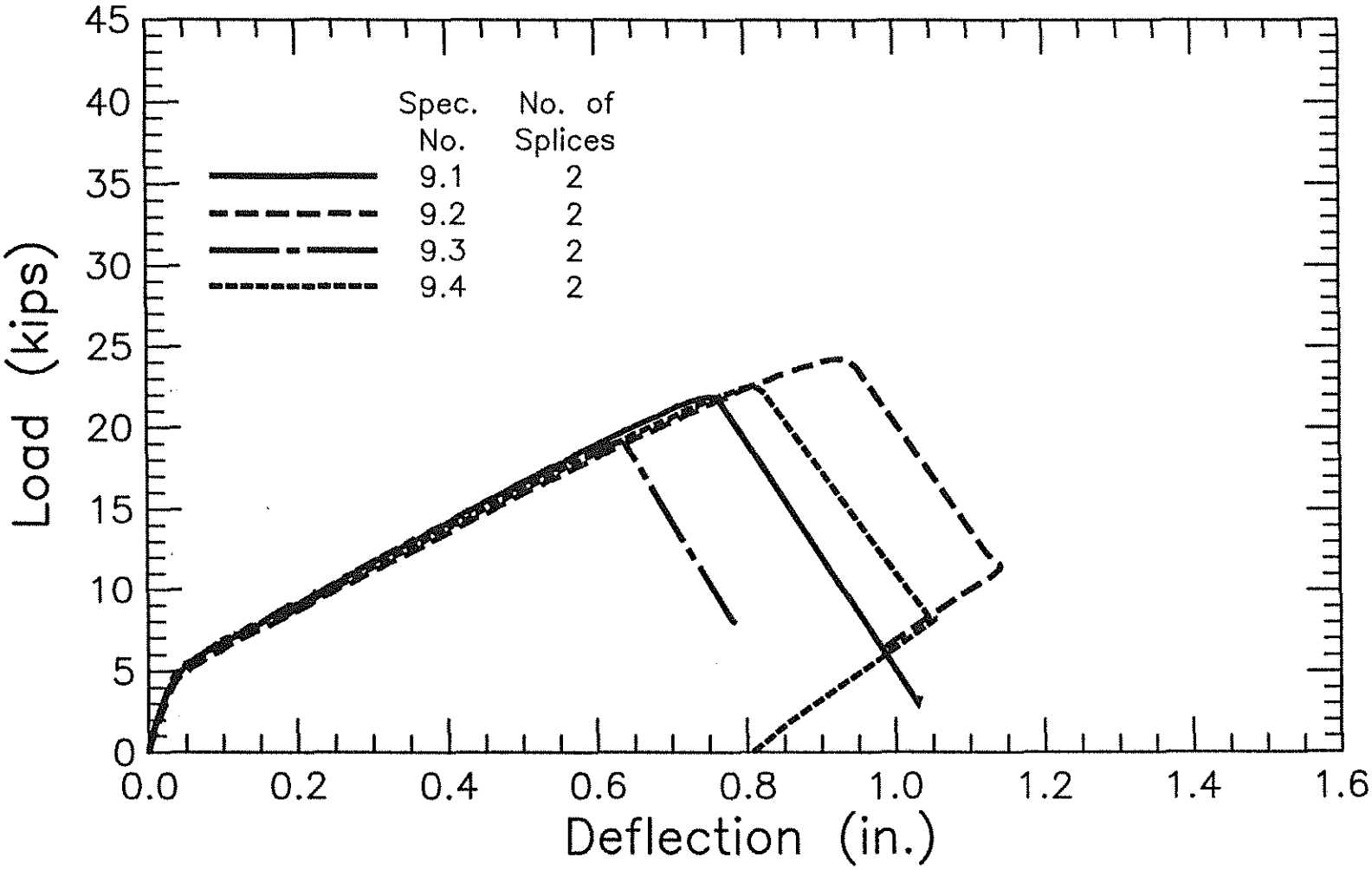

Fig. 3.12i Load-deflection curves for splice specimens in group 9

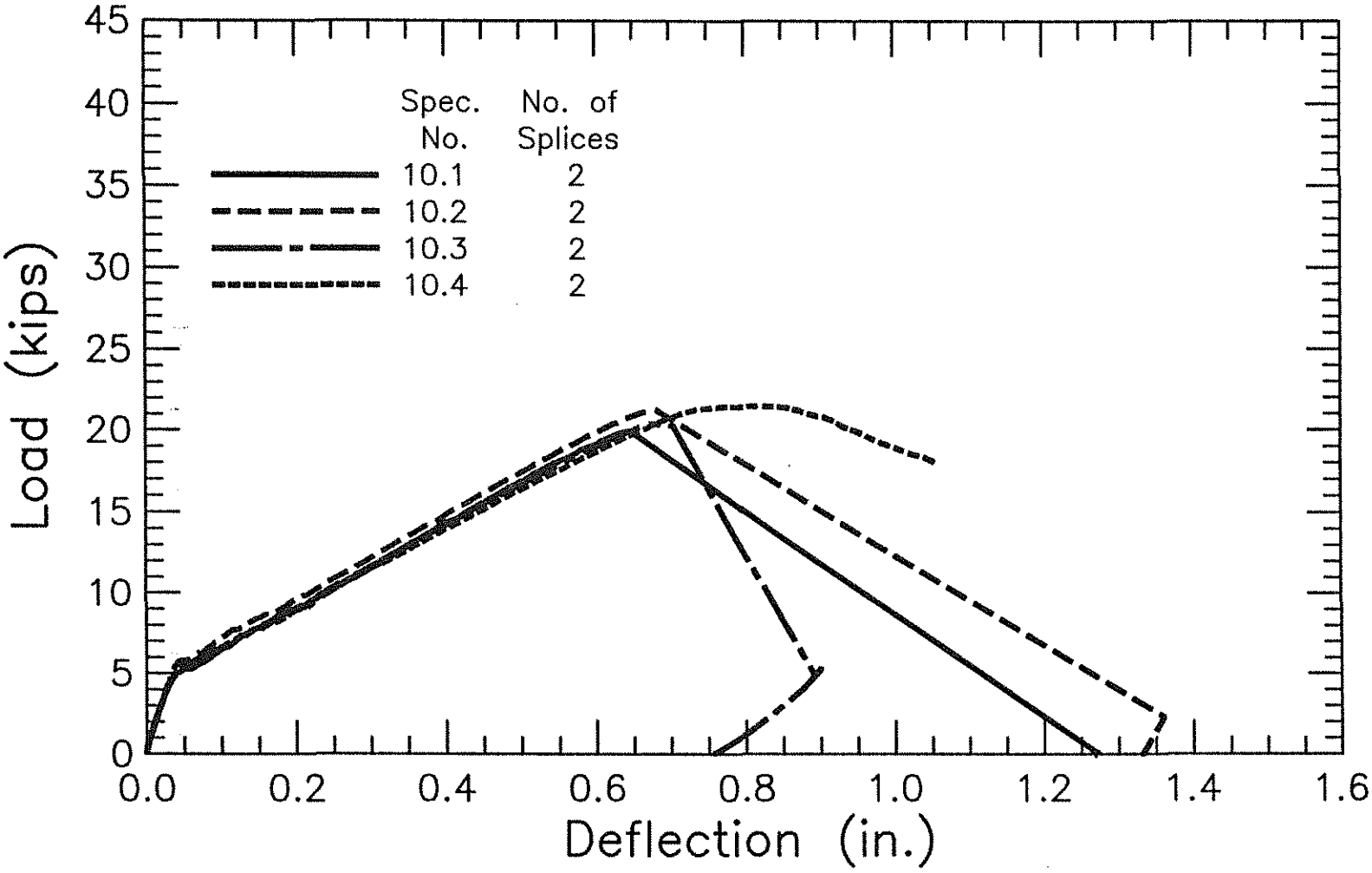

Fig. 3.12j Load-deflection curves for splice specimens in group 10

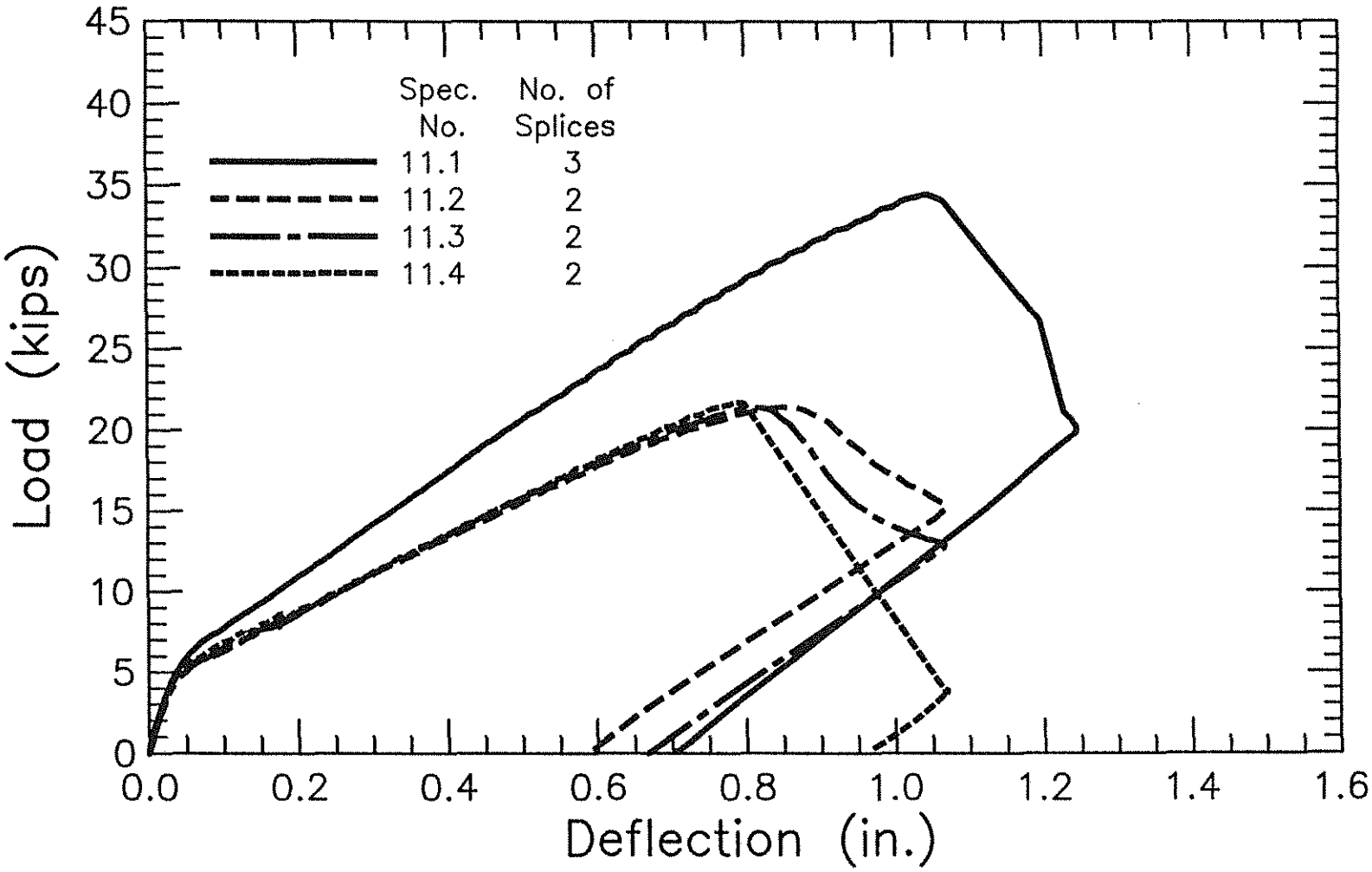

Fig. 3.12k Load-deflection curves for splice specimens in group 11

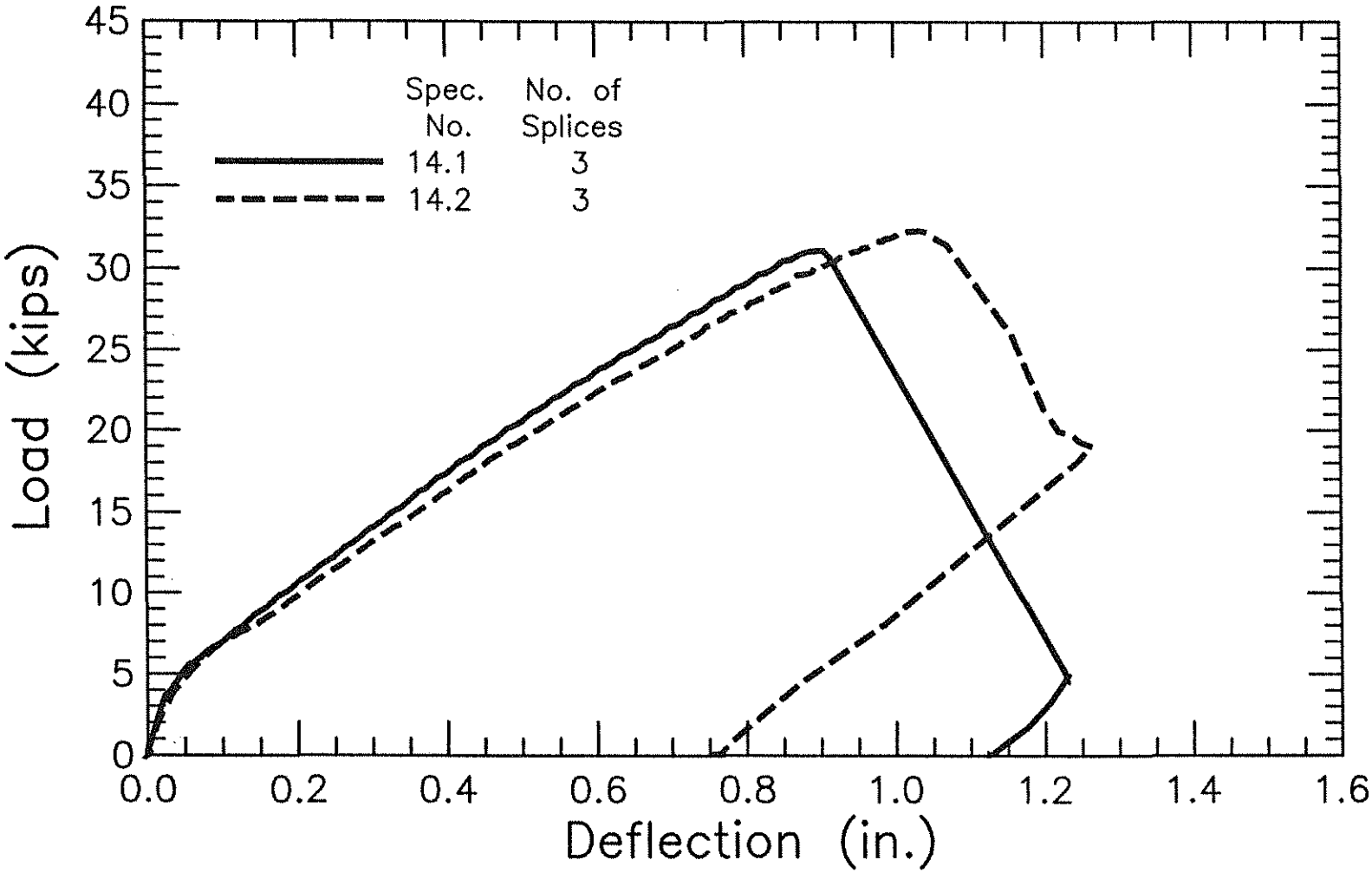

Fig. 3.12l Load-deflection curves for splice specimens in group 14

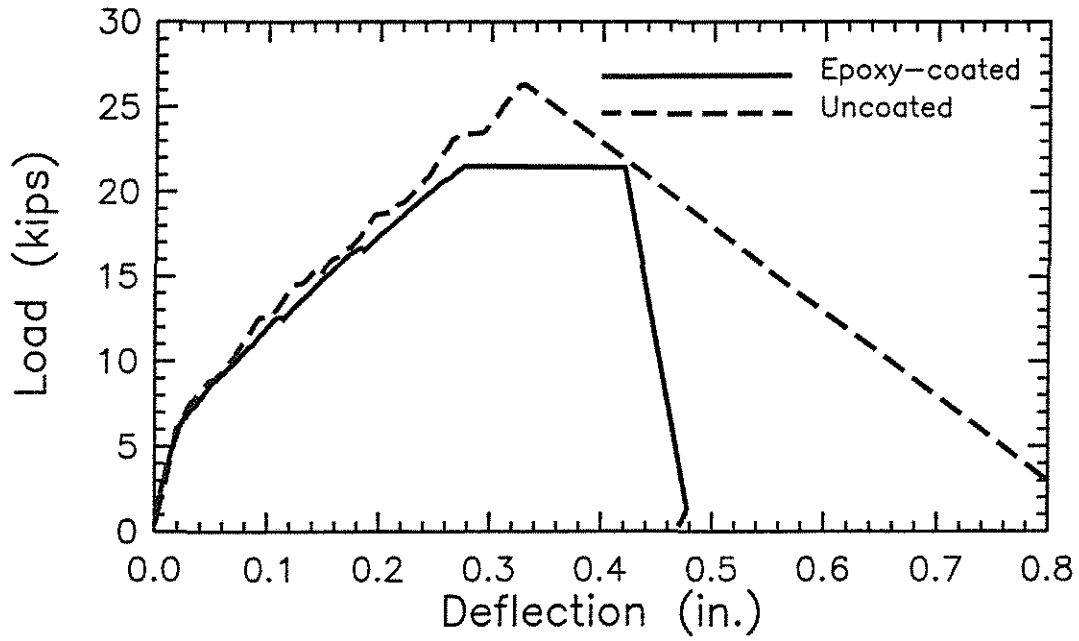

Fig. 3.13a Load-deflection curves for comparing the behavior of splice specimens containing epoxy-coated and uncoated bars in group 1 (without stirrups)

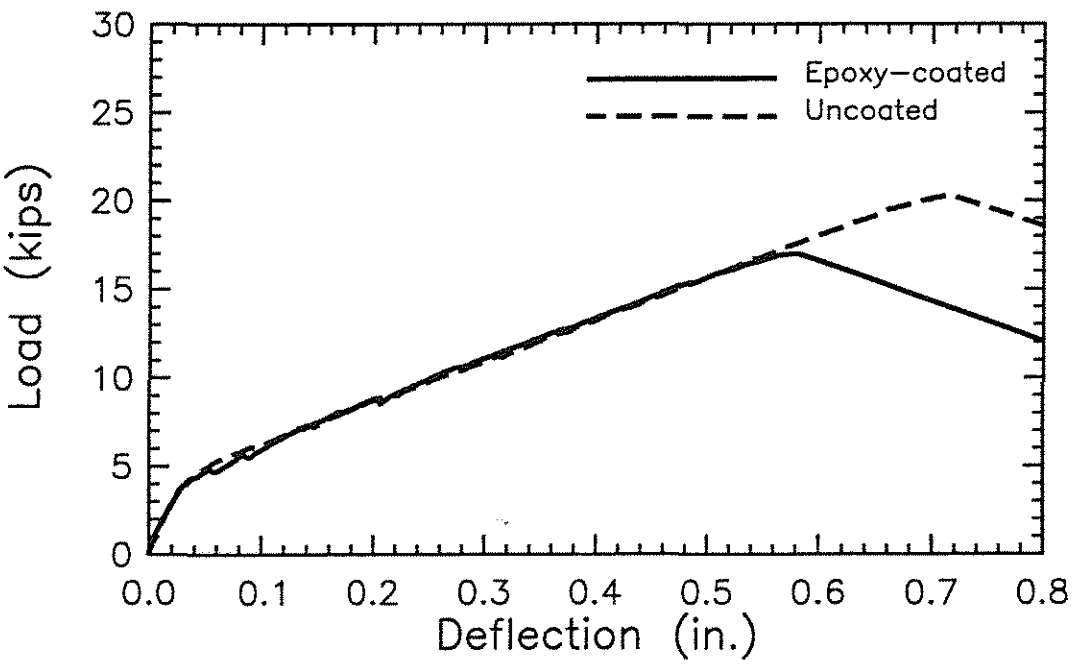

Fig. 3.13b Load-deflection curves for comparing the behavior of splice specimens containing epoxy-coated and uncoated bars in group 2 (without stirrups)

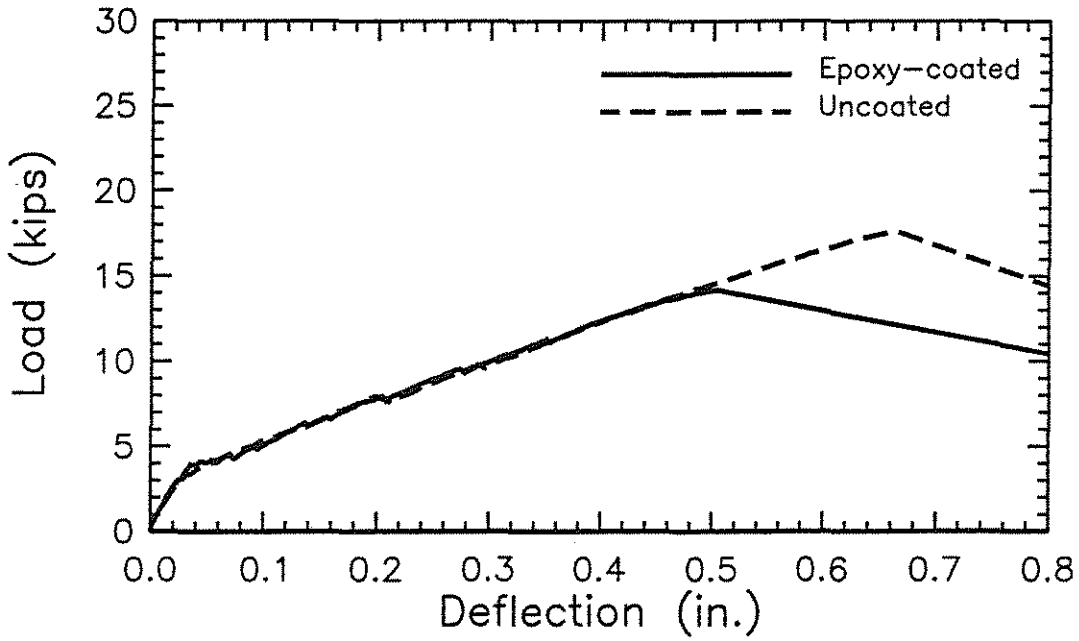

Fig. 3.13c Load-deflection curves for comparing the behavior of splice specimens containing epoxy-coated and uncoated bars in group 4 (without stirrups)

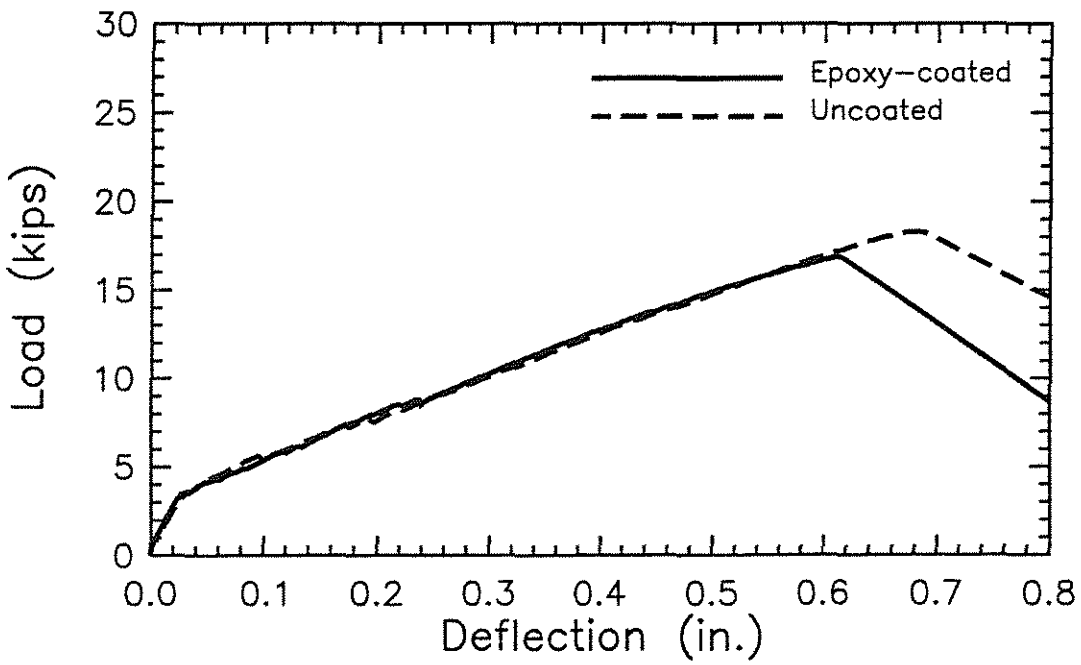

Fig. 3.13d Load-deflection curves for comparing the behavior of splice specimens containing epoxy-coated and uncoated bars in group 6 (without stirrups)

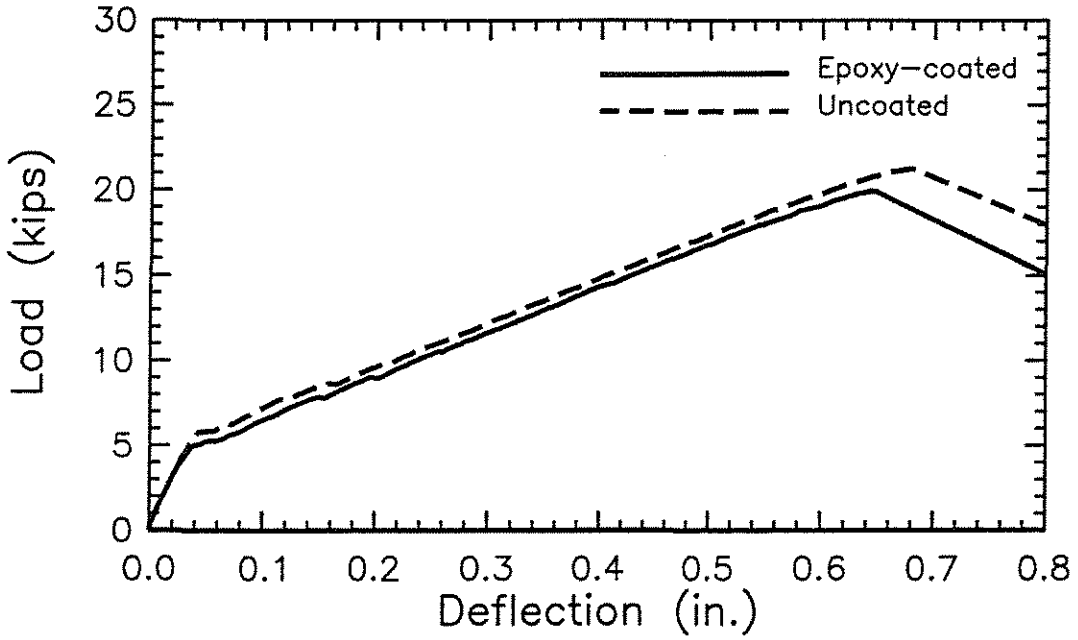

Fig. 3.13e Load-deflection curves for comparing the behavior of splice specimens containing epoxy-coated and uncoated bars in group 10 (without stirrups)

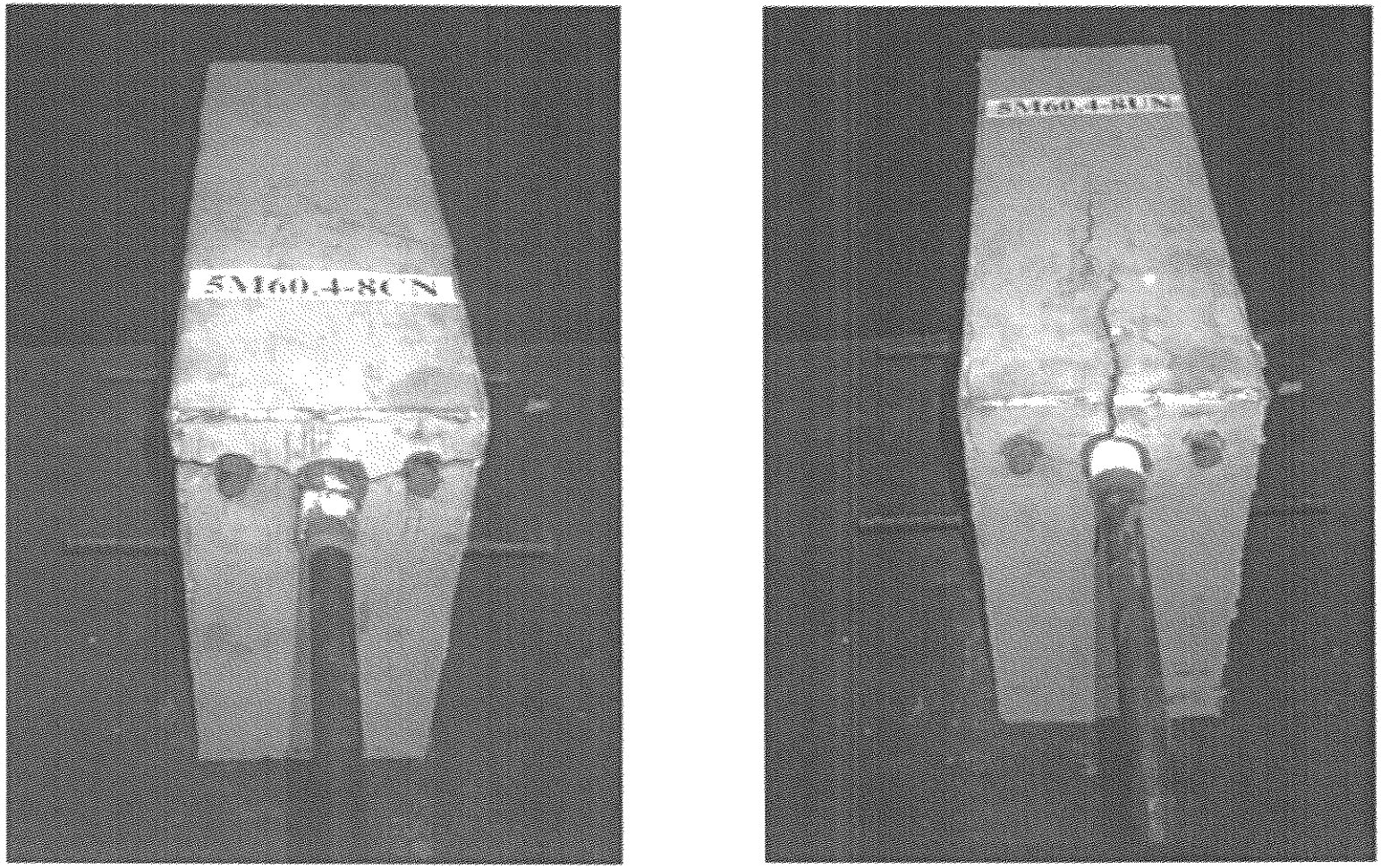

(a) (b)

Fig. 3.14 Cracked beam-end specimens, (a) specimen 5M60.4-8CN, (b) typical specimen

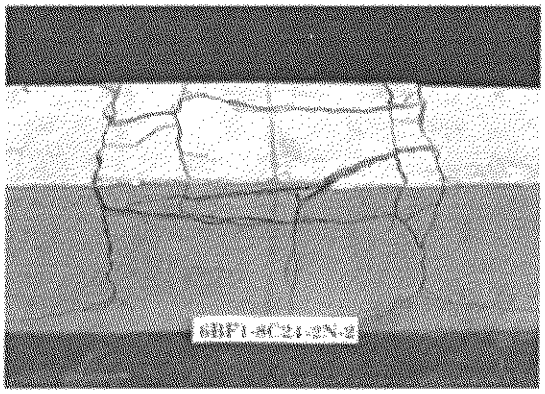

(a)

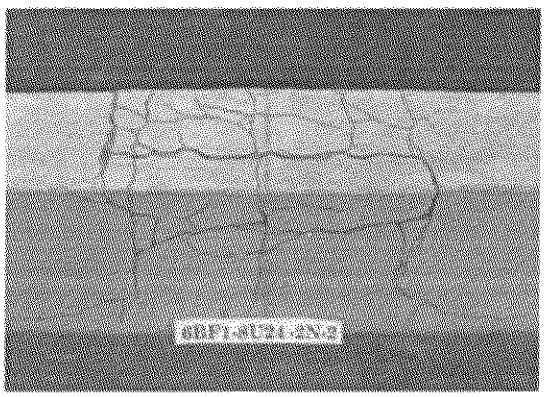

(b)

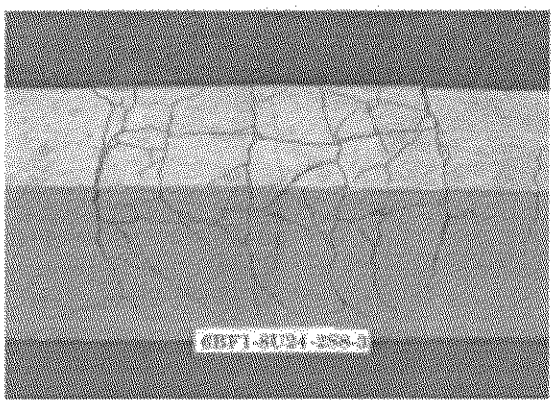

(c)

Fig. 3.15 Cracked splice specimens, (a) epoxy-coated bars without stirrups, (b) uncoated bars without stirrups, (c) uncoated bars with stirrups

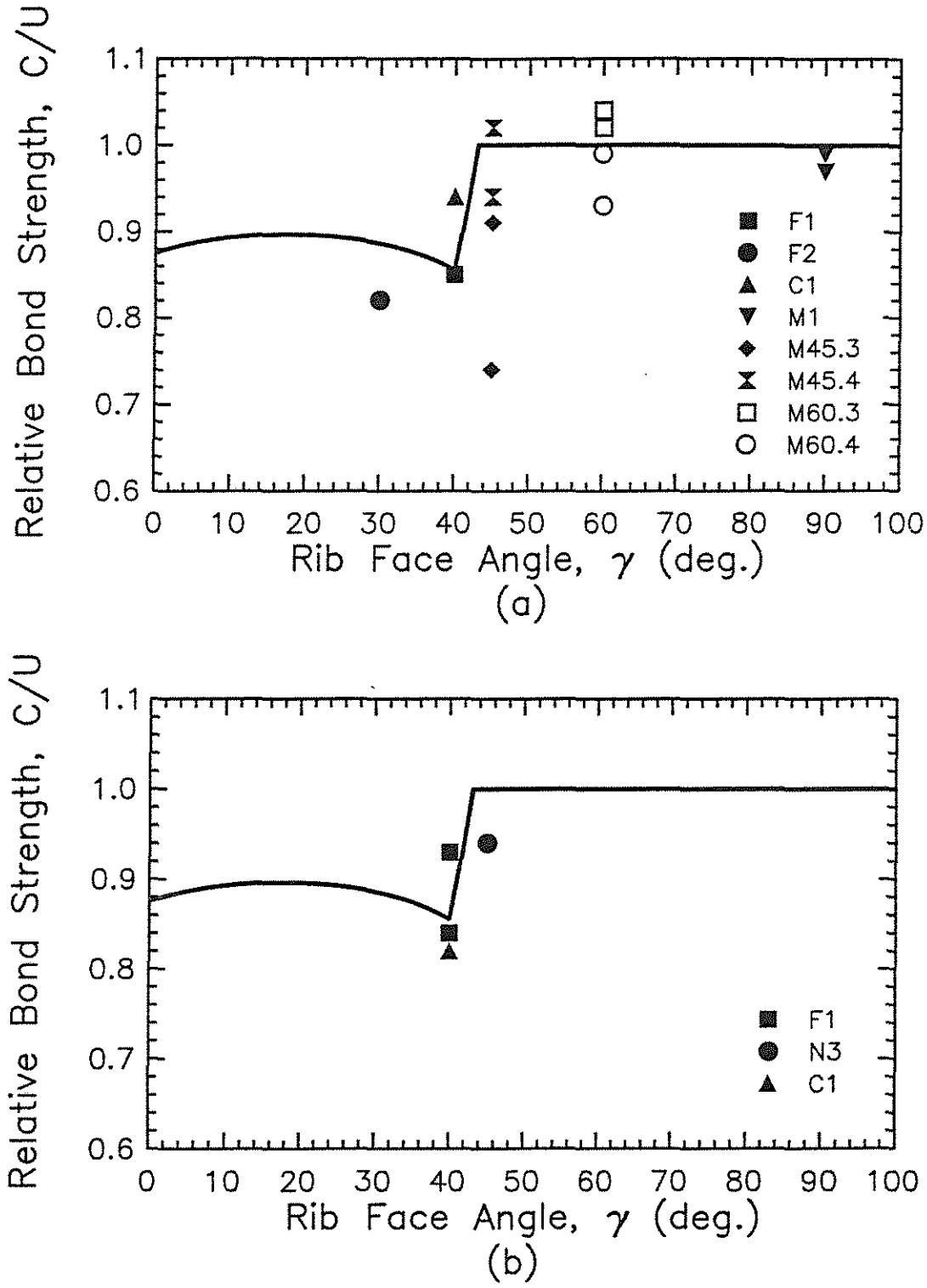

Fig. 4.1 Relative bond strength of epoxy-coated bars to uncoated bars, C/U, versus rib face angle, γ, (a) beam-end test results, (b) splice test results

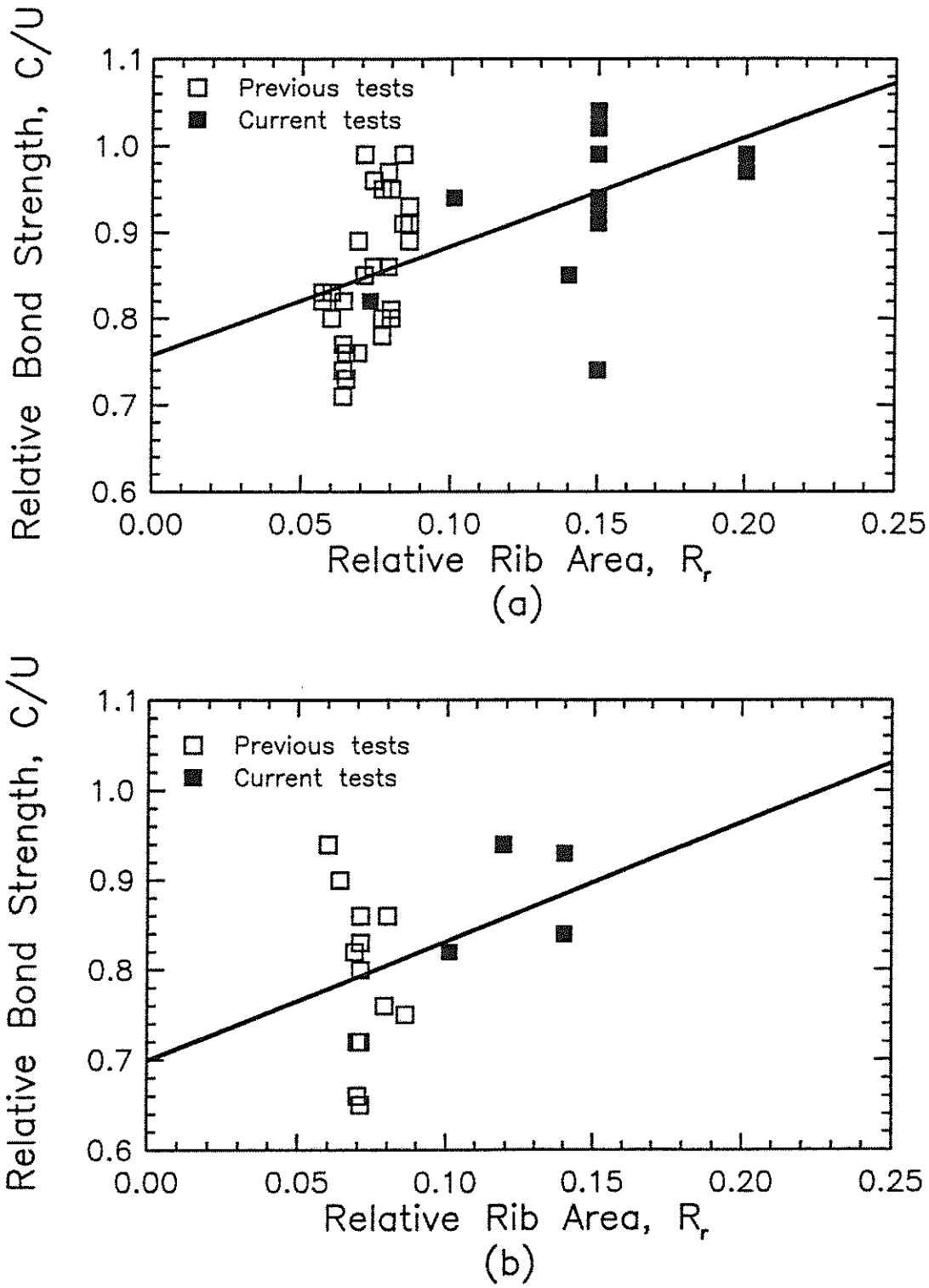

Fig. 4.2 Relative bond strength of epoxy-coated bars to uncoated bars, C/U, versus relative rib area, R_r, (a) beam-end test results, (b) splice test results

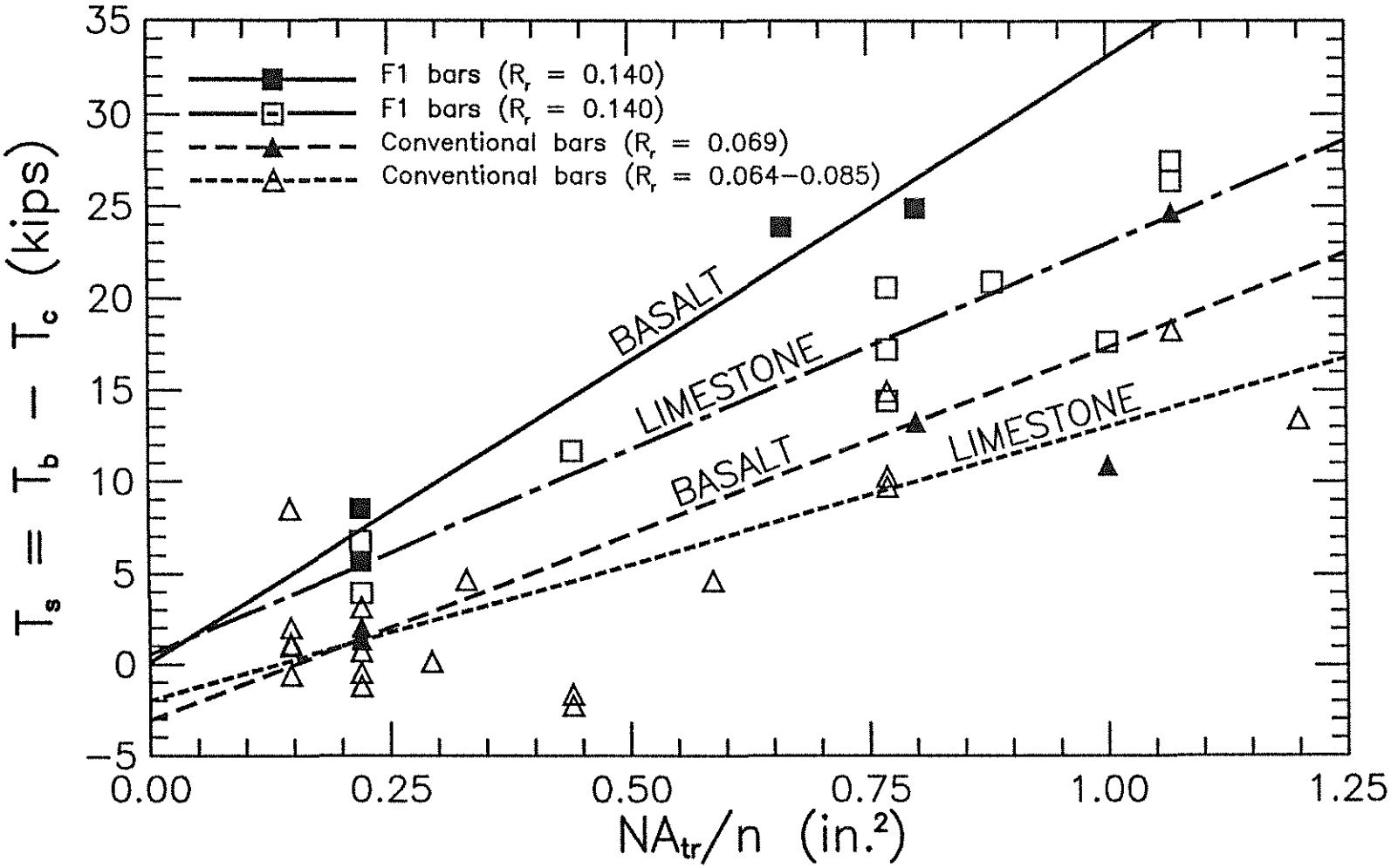

Fig. 4.3 Increase in modified bond force, T_s, versus total effective stirrup area, NA_{tr}/n, for F1 and conventional bar types cast in concrete with basalt or limestone coarse aggregate

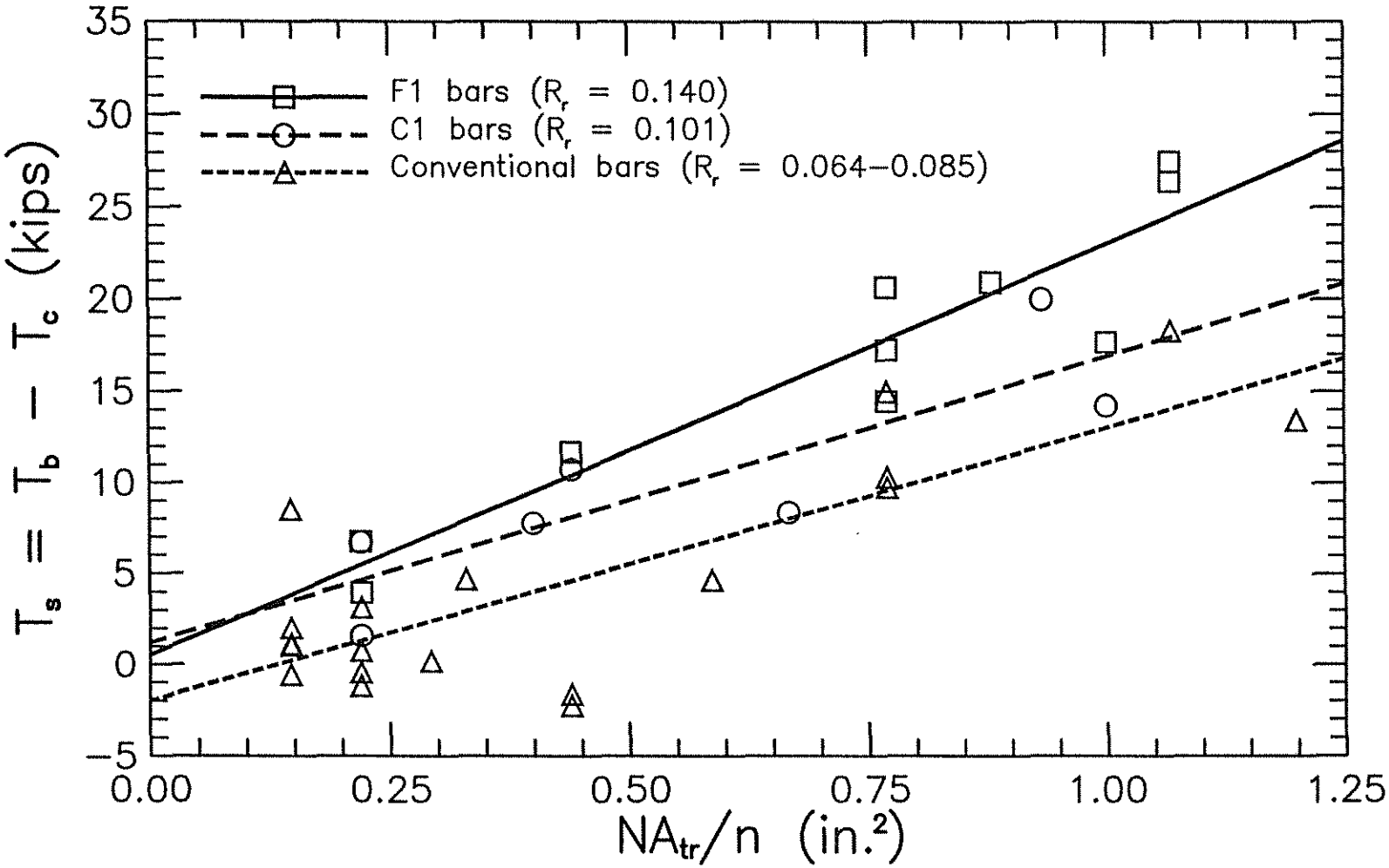

Fig. 4.4a Increase in modified bond force, T_s, versus total effective stirrup area, NA_{tr}/n, for F1, C1 and conventional bar types cast in concrete with limestone coarse aggregate

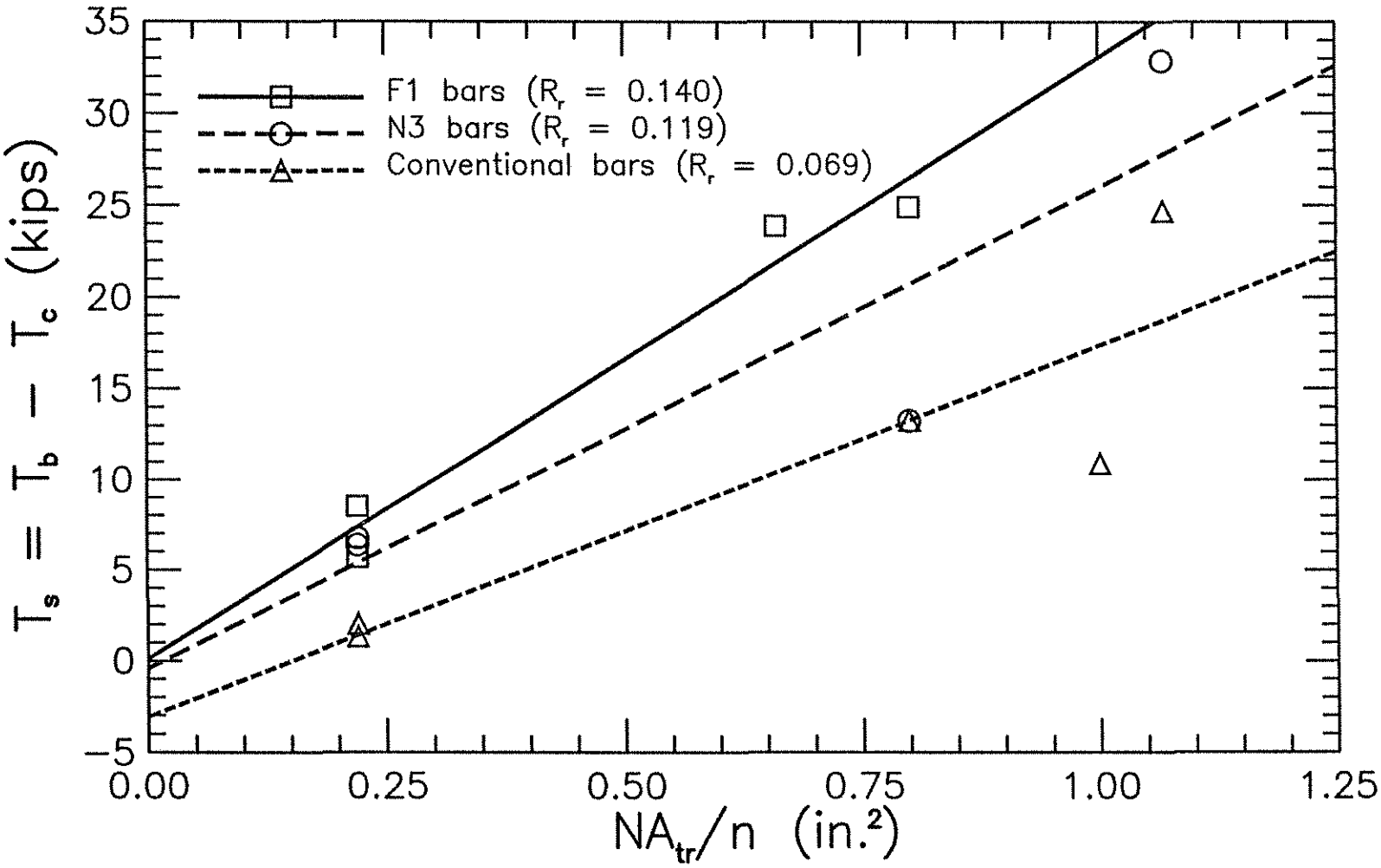

Fig. 4.4b Increase in modified bond force, T_s, versus total effective stirrup area, NA_{tr}/n, for F1, N3 and conventional bar types cast in concrete with basalt coarse aggregate

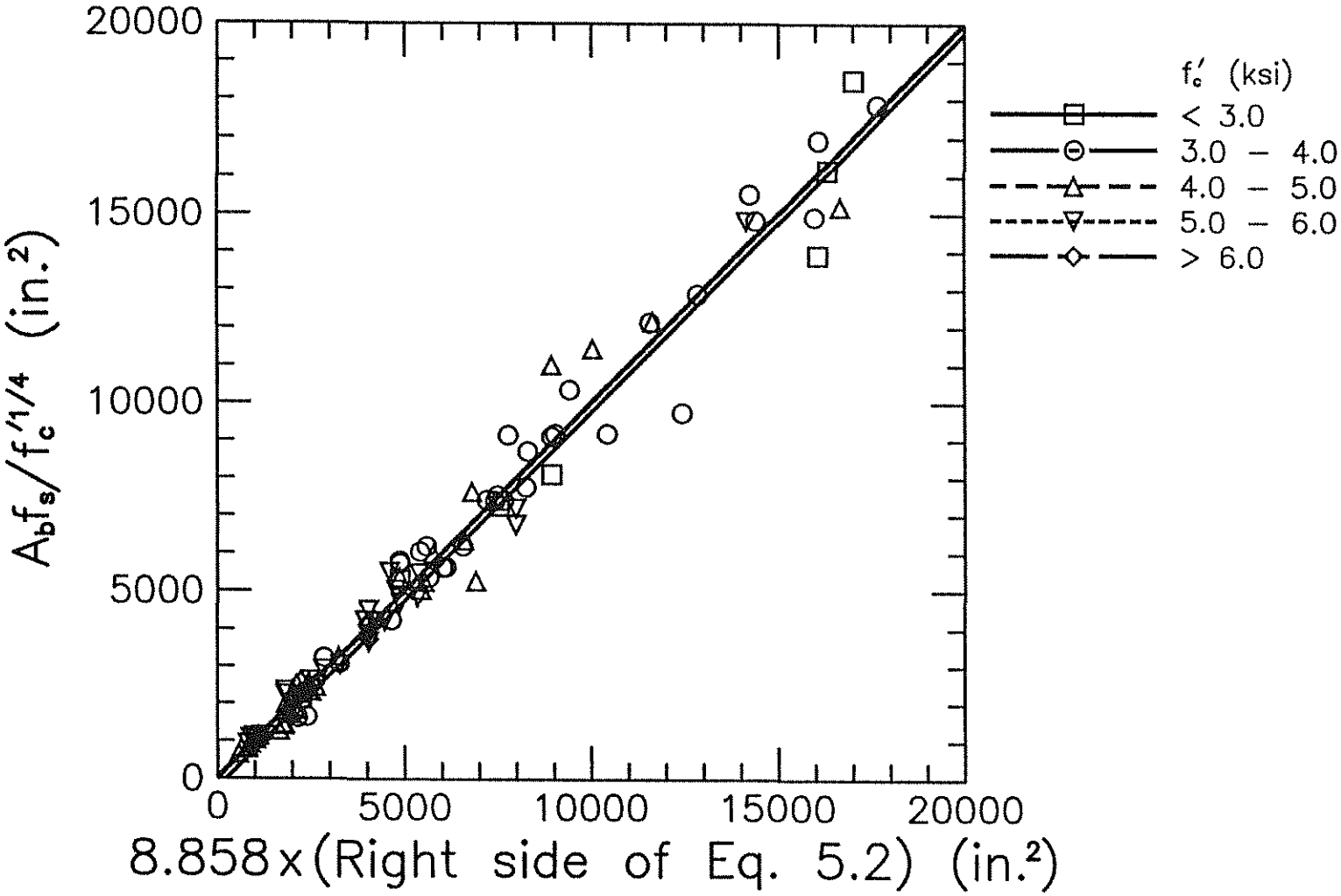

Fig. 5.1a $A_b f_s / f_c'^{1/4}$ (test) versus 8.858 x (right side of Eq. 5.2), as a function of f_c' for bars not confined by stirrups

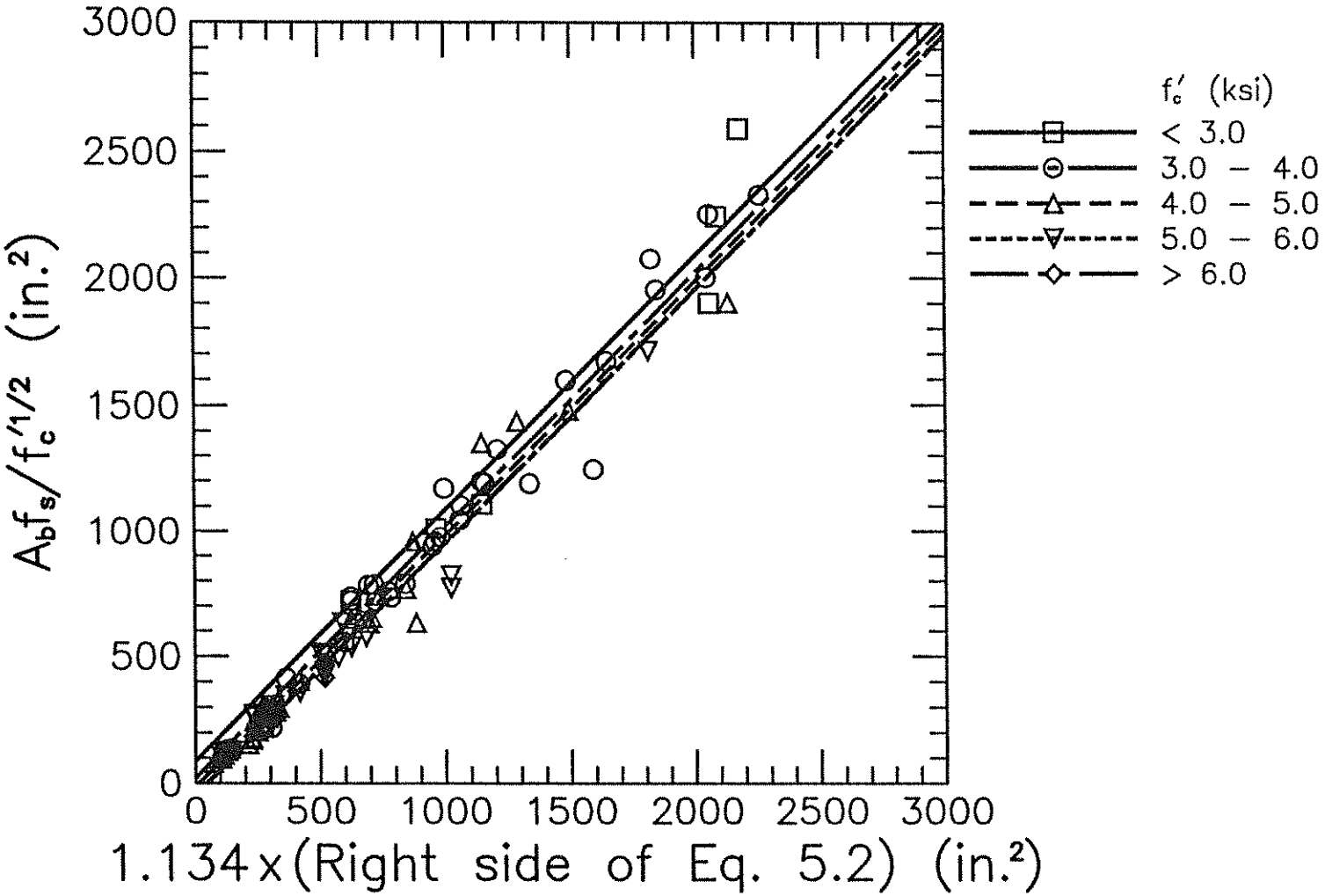

Fig. 5.1b $A_b f_s / f_c'^{1/2}$ (test) versus 1.134 x (right side of Eq. 5.2), as a function of f_c' for bars not confined by stirrups

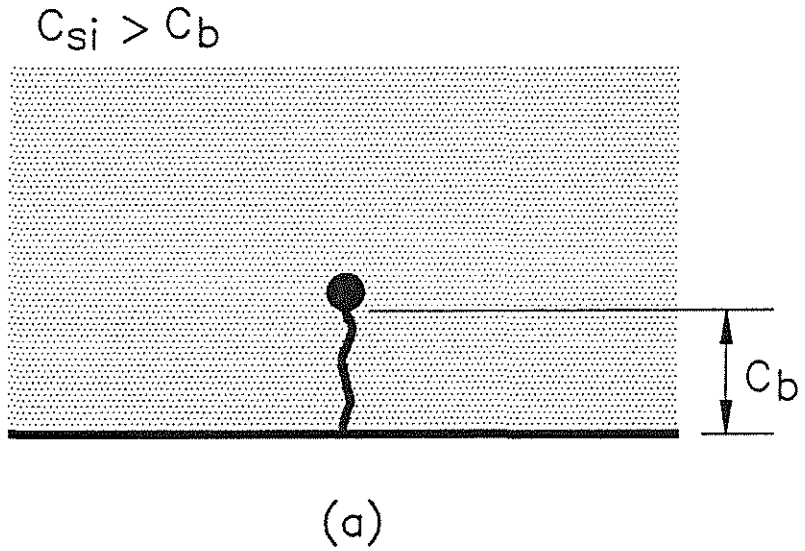

Fig. 5.2 Bond cracks: (a) $C_{si} > C_b$, (b) $C_{si} < C_b$

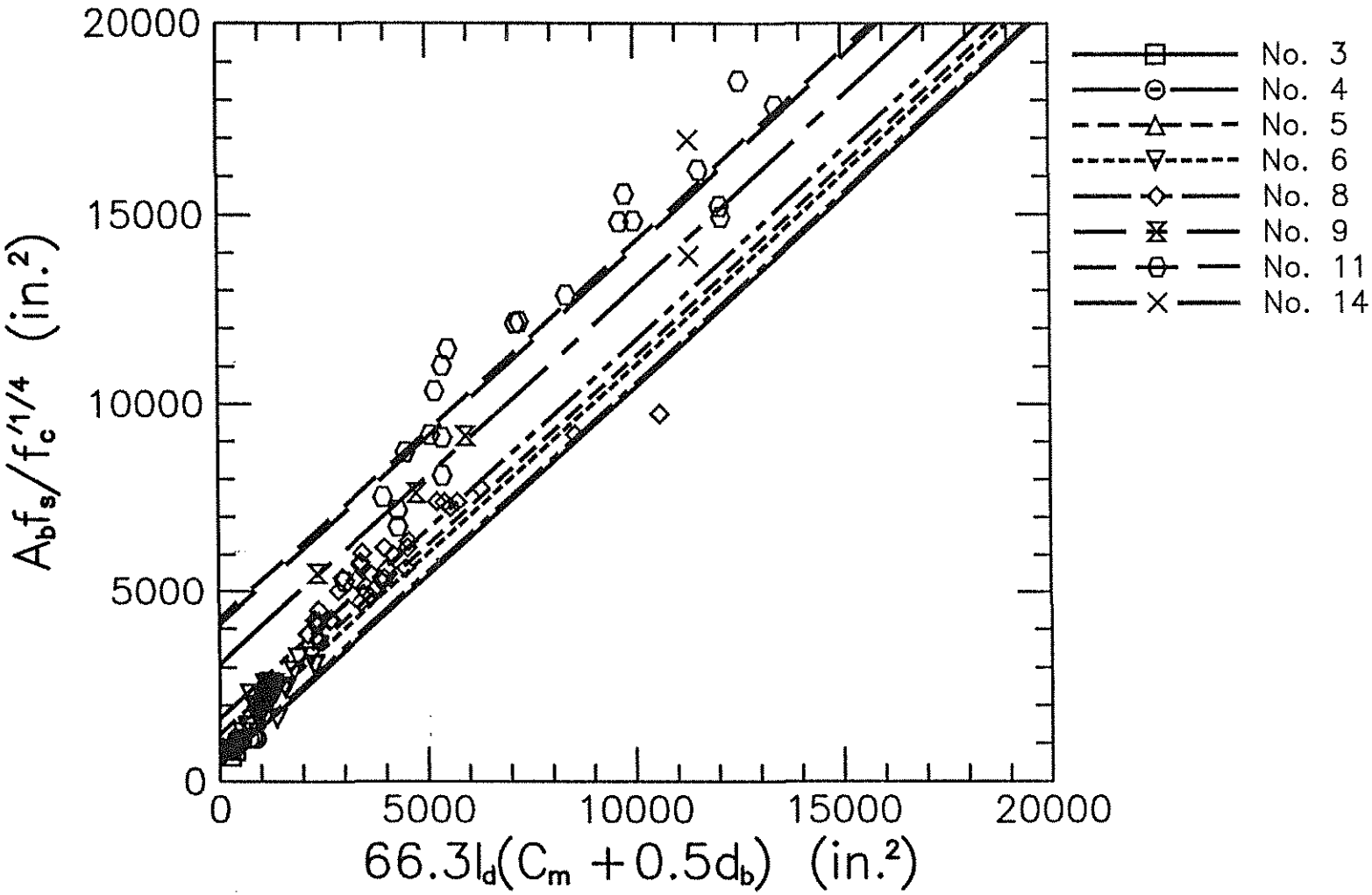

Fig. 5.3a $A_b f_s / f_c'^{1/4}$ (test) versus $66.3 l_d(C_m + 0.5 d_b)$, as a function of bar size for bars not confined by stirrups

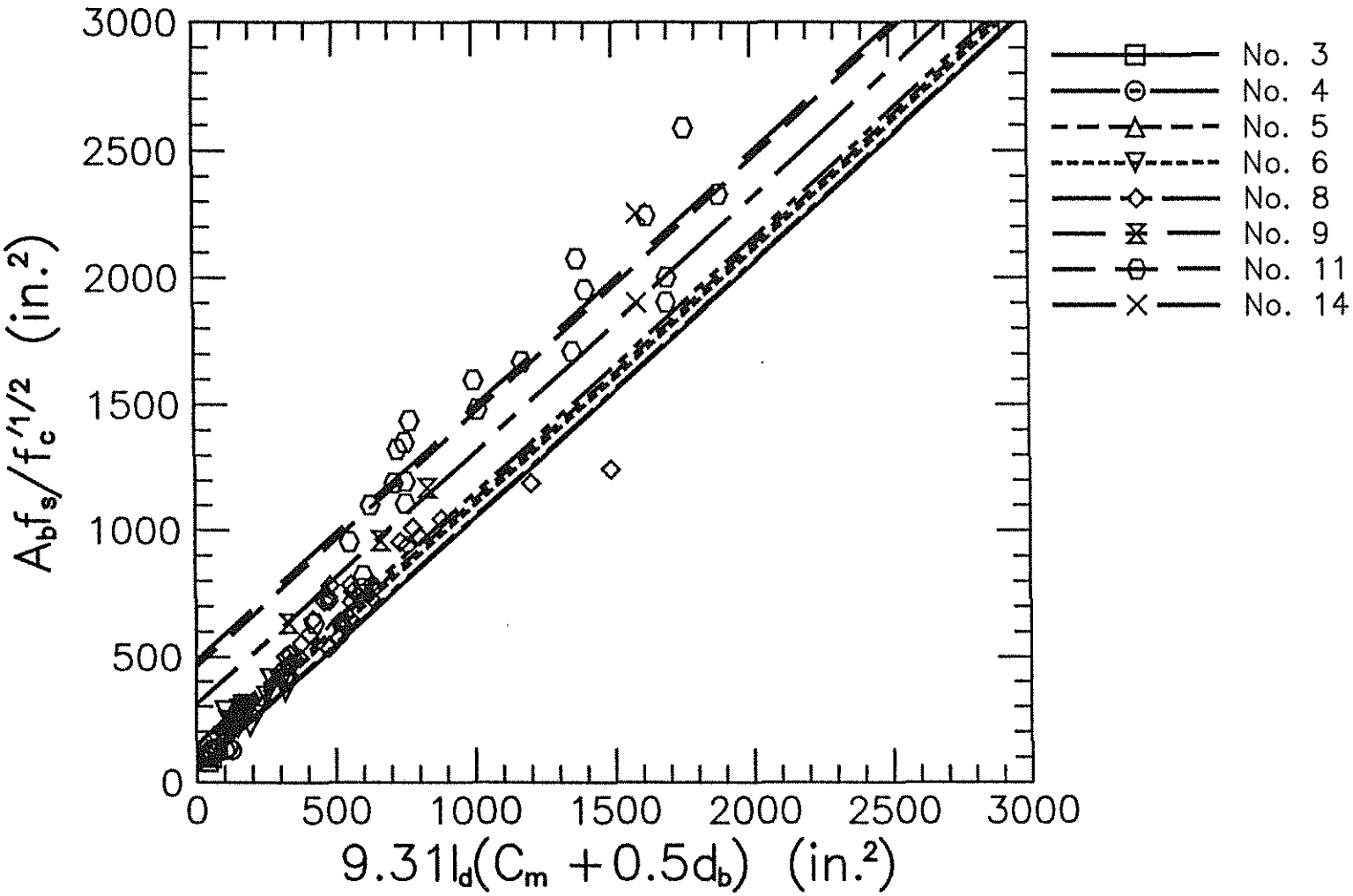

Fig. 5.3b $A_b f_s / f_c'^{1/2}$ (test) versus $9.31 l_d(C_m + 0.5d_b)$, as a function of bar size for bars not confined by stirrups

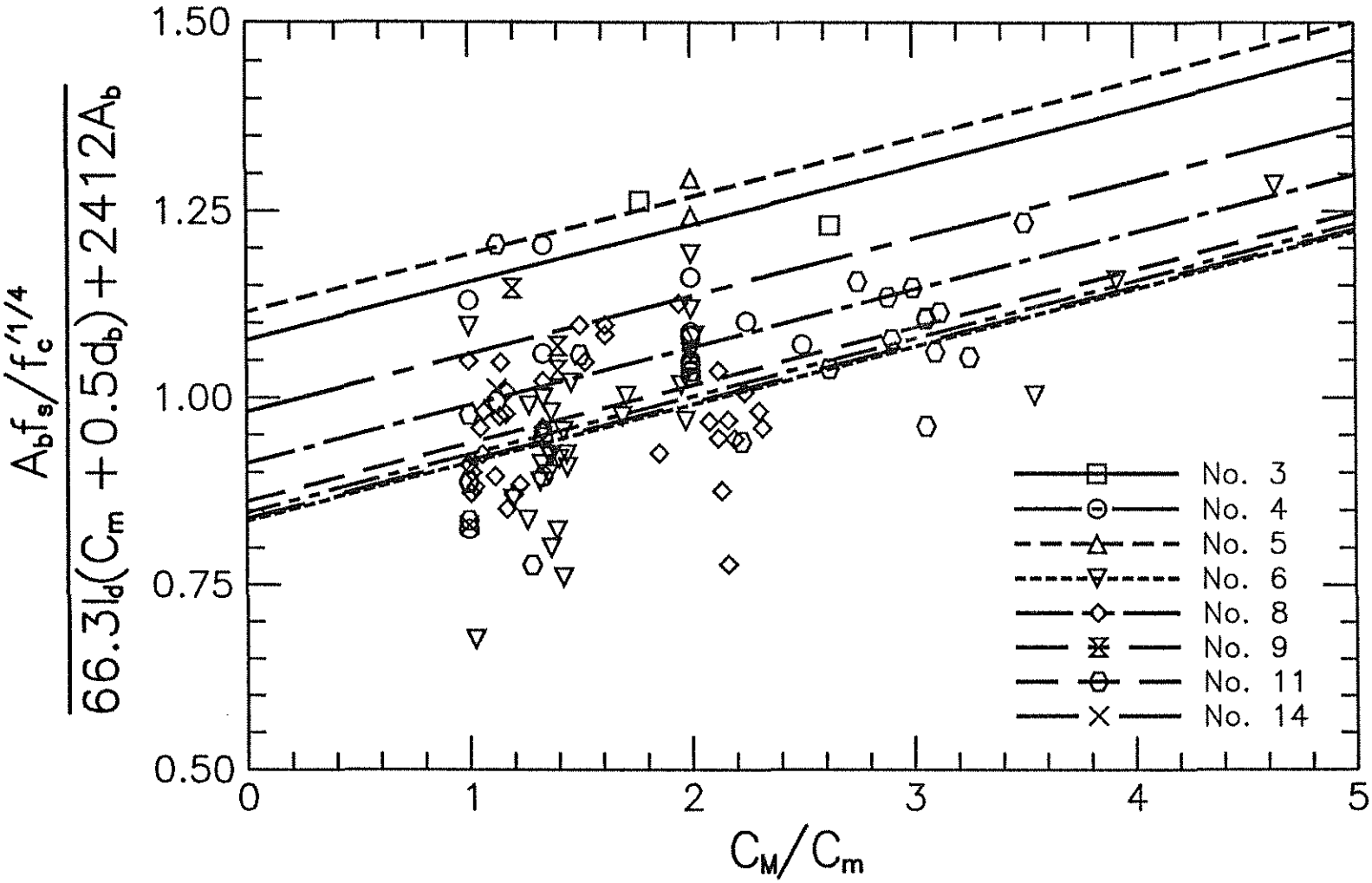

Fig. 5.4a Ratio of $A_b f_s / f_c'^{1/4}$ (test) to $66.3l_d(C_m + 0.5d_b) + 2412A_b$ versus C_M/C_m, as a function of bar size for bars without confining reinforcement

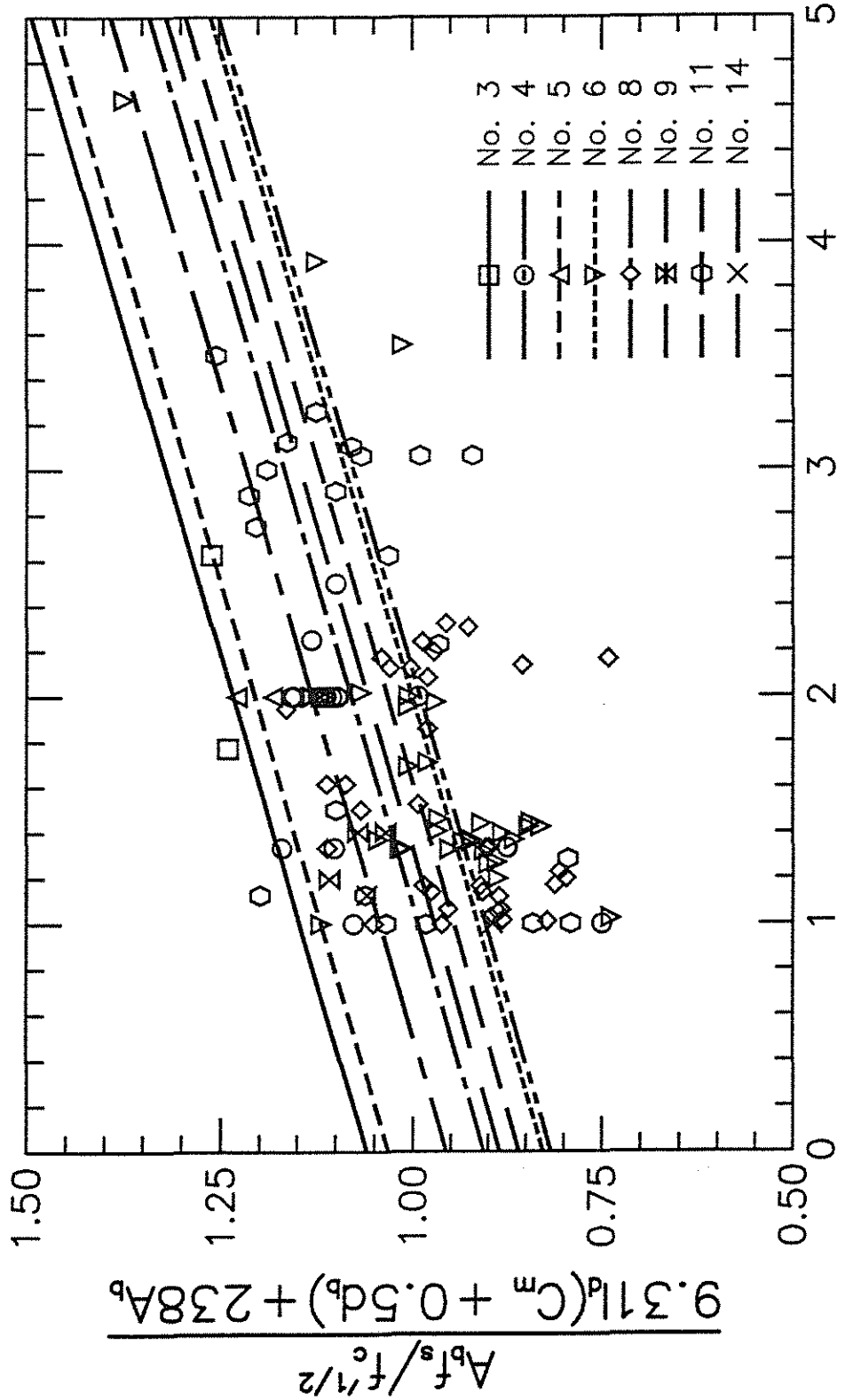

Fig. 5.4b Ratio of $A_b f_s/f_c'^{1/2}$ (test) to $9.31l_d(C_m + 0.5d_b) + 238A_b$ versus C_M/C_m, as a function of bar size for bars not confined by stirrups

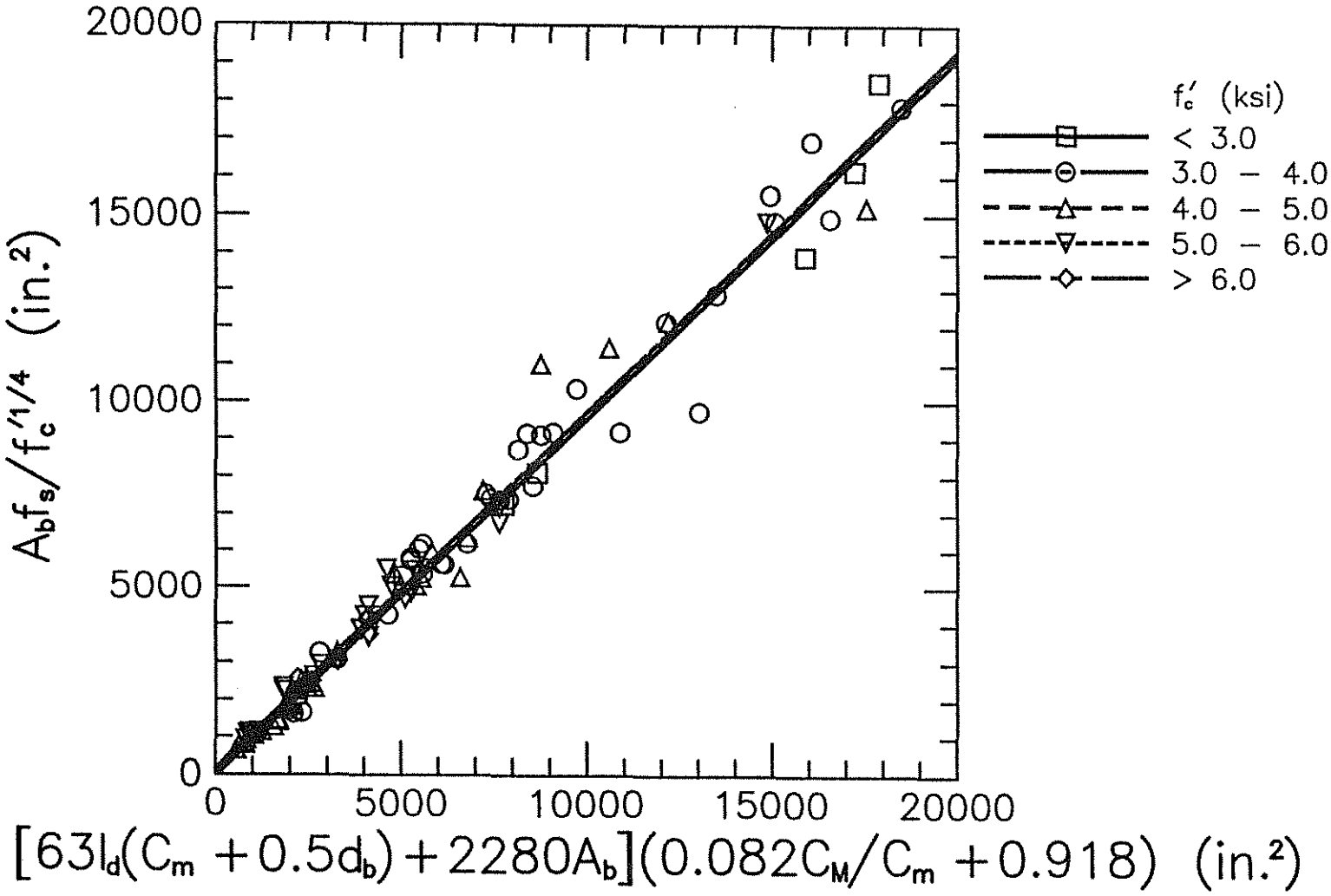

Fig. 5.5a $A_b f_s / f_c'^{1/4}$ (test) versus $A_b f_s / f_c'^{1/4}$ (prediction), as a function of f_c' for bars not confined by stirrups

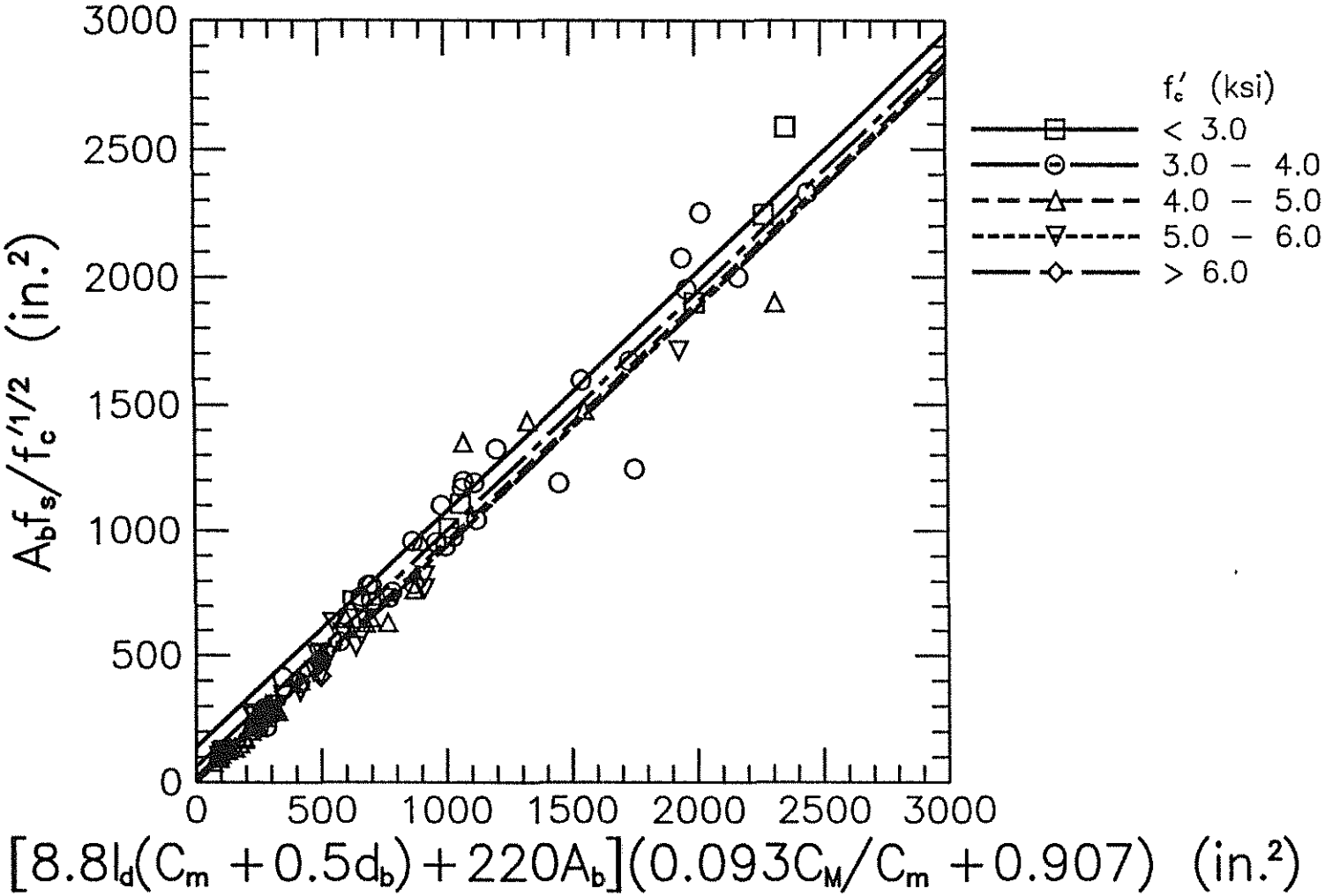

Fig. 5.5b $A_b f_s / f_c'^{1/2}$ (test) versus $A_b f_s / f_c'^{1/2}$ (prediction), as a function of f_c' for bars not confined by stirrups

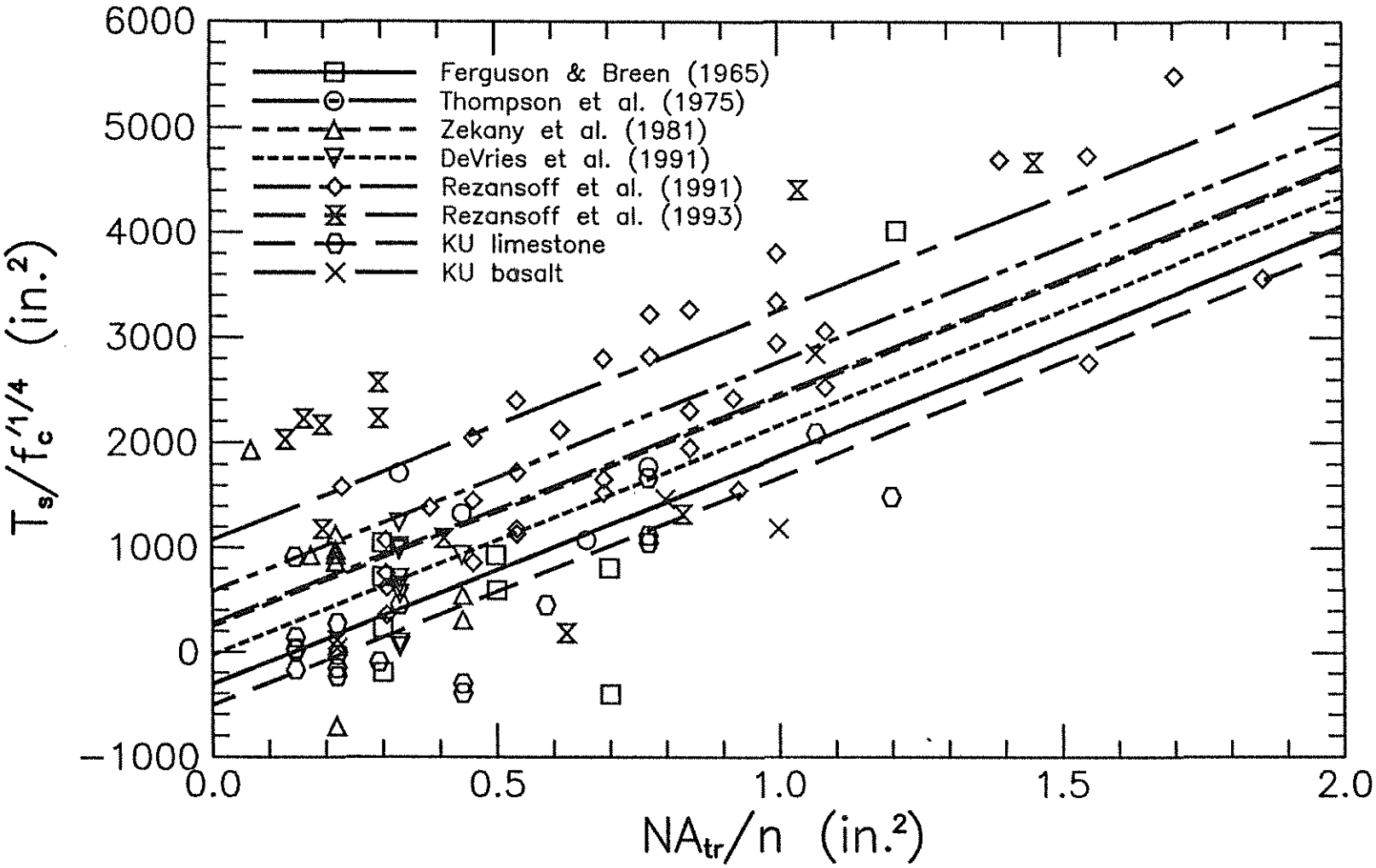

Fig. 5.6 Increase in bond strength due to stirrups, T_s, normalized with respect to $f_c'^{1/4}$, versus total effective stirrup area, NA_{tr}/n, as a function of test series for all conventional bars

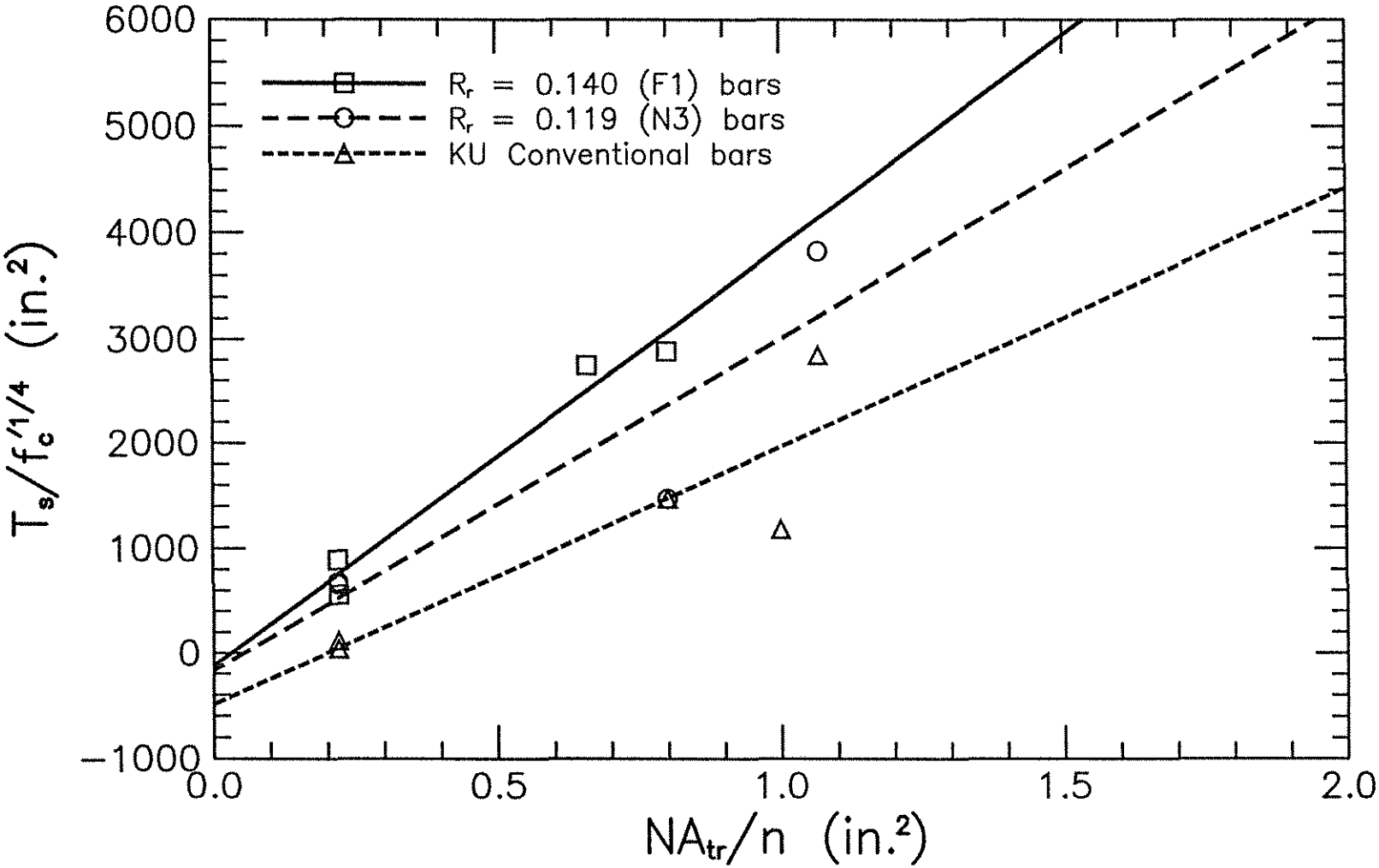

Fig. 5.7a Increase in bond strength due to stirrups, T_s, normalized with respect to $f_c'^{1/4}$, versus total effective stirrup area, NA_{tr}/n, for KU bars in concrete with basalt coarse aggregate

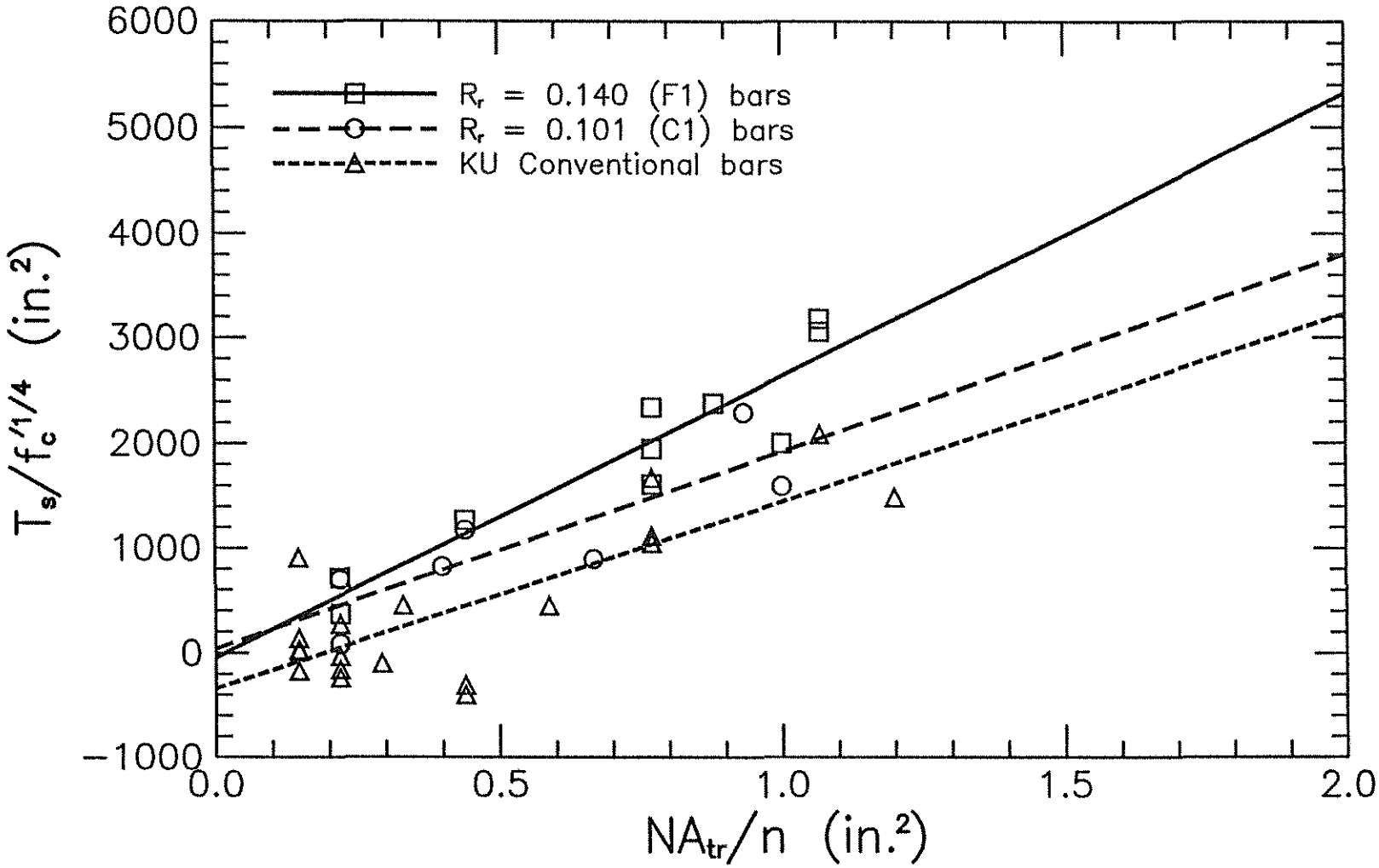

Fig. 5.7b Increase in bond strength due to stirrups, T_s, normalized with respect to $f_c'^{1/4}$, versus total effective stirrup area, NA_{tr}/n, for KU bars in concrete with limestone coarse aggregate

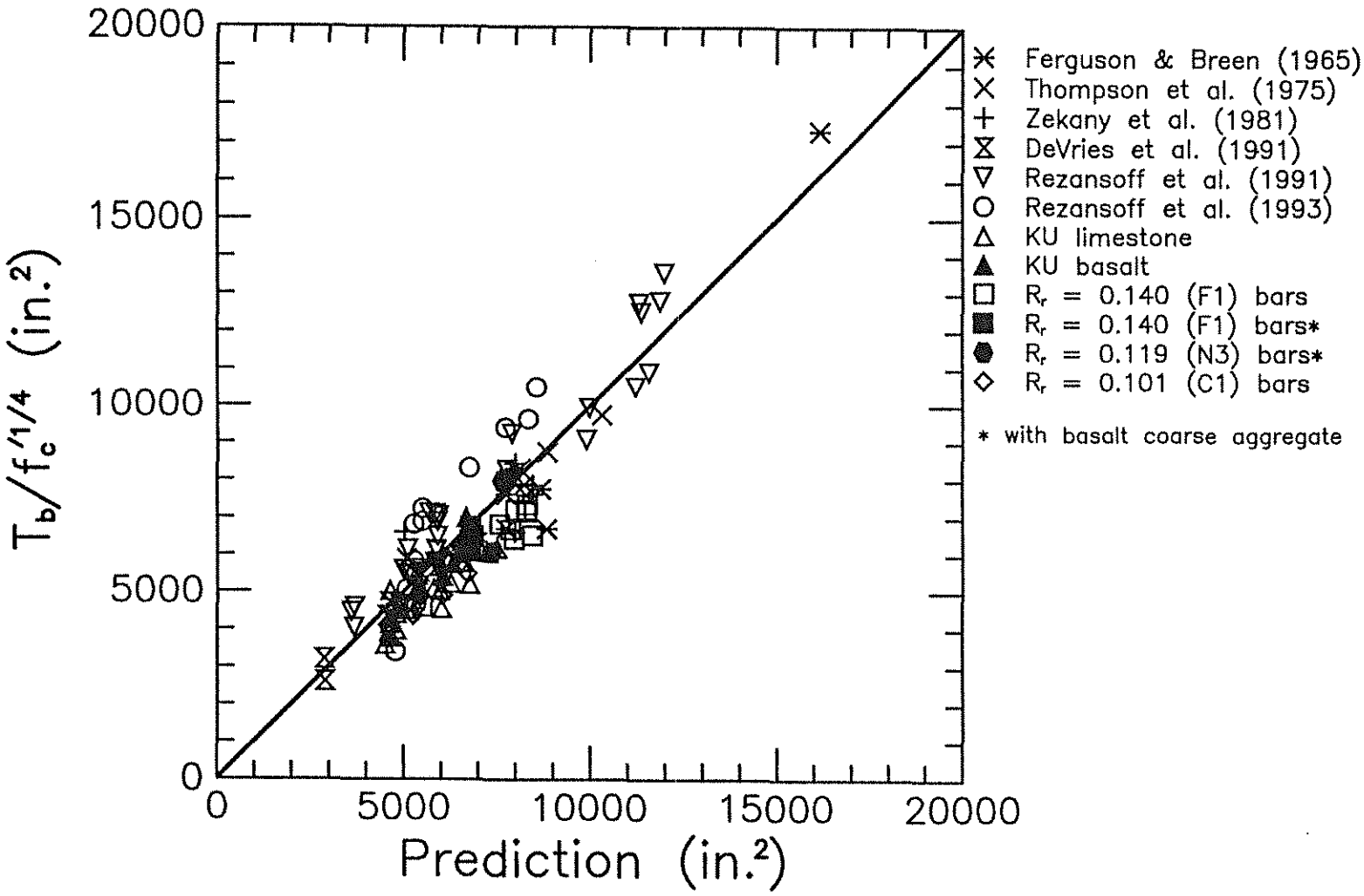

Fig. 5.8 $T_b/f_c'^{1/4}$ (test) versus $T_b/f_c'^{1/4}$ (prediction) for conventional and high R_r spliced bars confined by stirrups

APPENDIX A: PROGRAMS USED FOR MONTE CARLO SIMULATIONS

(a)

```
Program Bm;
{MONTE CARLO SIMULATION FOR BEAMS WITHOUT STIRRUPS}

Uses Crt, Dos;

{DECLARATION OF GLOBAL CONSTANTS FOR THE PROGRAM}

Const
 left = 0.0;  tol = 1.0e-6;

{DECLARATION OF GLOBAL VARIABLES FOR THE PROGRAM}

Var
 a, b, z, pz, Ls, Cb, Csi, fc, Db, Ab, Cmin, Cmax, fcm, Cbm, Cim, Lsm, Elm, R1, h, tc1, Rc1, a0,
 a1, a2, a3, a4, sd1, s1, r21, Vc, mr1, ms1, mv1, s3, result, errest, Cso, W, Cs, e1, CMm, fcR : Real;
 Nb, Ns, err : Byte;
 n, l : Integer;
 k1, i, j, k, m, m0 : Word;
 fname : String[20];
 st : String;
 fin, fout, fl : Text;

{FUNCTION EVALUATES THE EXPRESSION e^-(0.5*z^2)}

Function F(z : Real) : Real;
Begin
 f := exp(-z*z/2.0);
End;

{FUNCTION EVALUATES THE EXPRESSION FOR SIMPSON'S RULE}

Function Simpson(a,b,h : Real) : Real;
Var mid : Real;
Begin
 mid := (b+a)/2.0;
 Simpson := h/6.0*(f(a)+4.0*f(mid)+f(b));
End;

{NUMERICAL METHOD TO DETERMINE THE CURRENT IMPROVED STANDARD}
{NORMAL VALUE, z[i+1], FROM A PREVIOUS VALUE OF z[i] DURING EACH CYCLE}
{OF THE ITERATIVE PROCESS}

Procedure Adap_Quad(left,z,tol:Real; var result:Real; var errest:Real);
Var h, I1, I2, mid, result1, result2, errest1, errest2 : Real;
Begin
 m := m+1;
 h := z-left;
 I1 := Simpson(left,z,h);
 h := h/2.0;
 mid := (left+z)/2.0;
 I2 := Simpson(left,mid,h)+Simpson(mid,z,h);
 errest := abs((I2-I1)/15.0);
 if abs(errest) > tol then
  begin
   Adap_Quad(left,mid,tol/2,result1,errest1);
   Adap_Quad(mid,z,tol/2,result2,errest2);
   result := result1+result2;
   errest := errest1+errest2;
```

```
    end
   else
    result := I2-errest;
 End;

 {ITERATIVE PROCESS TO OBTAIN THE STANDARD NORMAL VALUE, z, FOR ANY}
 {RANDOMLY GENERATED CUMULATIVE PROBABILITY, pz, USING THE}
 {PROCEDURE Adap_Quad AS OPTION AS IT IS REQUIRED}

 Procedure Getz;
 Begin
  pz := Random;
  a := 0.0;  z := 2.0;  b := 4.0;  m0 := 0;
  Repeat
    m0 := m0+1;  m := 0;
    Adap_Quad(left,z,tol,result,errest);
    result := 0.5+result/sqrt(2.0*pi);
    if pz < 0.50 then
      begin
        result := 1.0-result;
        if result < pz then b := z else a := z;
      end
    else
      begin
        if result < pz then a := z else b := z;
      end;
    z := 0.5*(a+b);
    if m0 > 500 then Exit;
  Until abs(pz-result) < tol;
 End;

 {FUNCTION DETERMINES THE MINIMUM OF TWO VARIABLES}

 Function Min(a,b :Real) : Real;
 Begin
  if a < b then Min := a
  else Min := b;
 End;

 {FUNCTION DETERMINES THE MAXIMUM OF TWO VARIABLES}

 Function Max(a,b :Real) : Real;
 Begin
  if a > b then Max := a
  else Max := b;
 End;

 {FUNCTION DETERMINES BOND FORCE}

 Function Eqn : Real;
 Var Eq : Real;
 Begin
  Csi := (0.5*W-Nb*Db-Cso)/(Nb-1.0);
  Cs := Min(Cso,Csi+0.25);
  Cmin := Min(Cs,Cb);
  Cmax := Max(Cs,Cb);
  CMm := Cmax/Cmin;
  if CMm > 3.5 then CMm := 3.5;
  Eq := (63.0*Ls*(Cmin+0.5*Db)+2280.0*Ab)*(0.082*CMm+0.918);
  Eqn := Sqrt(Sqrt(fc))*Eq;
 End;

 {PROCEDURE FOR READING, FROM THE DATA FILE, AND DISPLAYING, ON THE}
```

```
{SCREEN, THE NOMINAL VALUES FOR EACH BEAM}

Procedure InputData;
Begin
 readln(fin,W,h,fc,Cb,Cso,Ls,Nb,Db,Ab);
 n := 1+n;
 writeln('       CURRENT INPUT DATA FROM FILE ',fname+'.DAT');
 writeln('       ----------------------------------------');
 writeln('       Data for beam number ..... ',n:5);
 writeln('       Beam width (ins.) ..... ',W:5:2);
 writeln('       Beam depth (ins.) ..... ',h:5:2);
 writeln('       Concrete strength (psi) ..... ',fc:4:0);
 writeln('       Concrete cover (ins.) ..... ',Cb:5:3);
 writeln('       Concrete side cover (ins.) ..... ',Cso:5:3);
 writeln('       Splice length (ins.) ..... ',Ls:5:2);
 writeln('       Number of bars spliced ..... ',Nb:2);
 writeln('       Spliced bar diameter (ins.) ..... ',Db:5:3);
 writeln('       Spliced bar area (sq. ins.) ..... ',Ab:4:2);
End;

{PROCEDURE FOR WRITING THE NOTATION AND HEADING INFORMATION FOR}
{EACH BEAM INTO THE OUTPUT FILE FOR THE BEAM}

Procedure OutData;
Begin
 writeln(fout,'    RESULTS OUTPUT FOR BEAMS W/O STIRRUPS');
 writeln(fout,'    ------------------------------------');
 writeln(fout,'    n  = Number of iterations');
 writeln(fout,'    W  = Beam width (ins.)');
 writeln(fout,'    fc = Concrete strength (psi)');
 writeln(fout,'    Cb = Concrete cover (ins.)');
 writeln(fout,'    Cso = Concrete side cover (ins.)');
 writeln(fout,'    Csi = One-half clear bar spacing (ins.)');
 writeln(fout,'    Ls = Splice length (ins.)');
 writeln(fout,'    Nb = Number of bars spliced');
 writeln(fout,'    Db = Spliced bar diameter (ins.)');
 writeln(fout,'    Ab = Spliced bar area (sq. ins.)');
 writeln(fout,' ');
 write(fout,' n   W   fc   Cb   Cso  Csi  Ls   Nb  Db   Ab  ');
 writeln(fout,' Eq1   R1   MR1   SD1   V1');
 write(fout,'-------------------------------------------------------------');
 writeln(fout,'---------------------------------');
End;

{ITERATIVE PROCESS FOR DETERMINING THE LONG-TERM IN-SITU COMPRESSIVE}
{STRENGTH OF CONCRETE}

Procedure fcstrR;
Var fc35 : Real;
Begin
 fc35 := fc;
 Repeat
  fcR := fc;
  fc := fc35*(0.89*(1.0+0.08*ln(fcR/3600)/ln(10.0)));
 until Abs(fcR-fc) < 1.0;
End;

{MAIN PROCEDURE FOR THE MONTE CARLO SIMULATIONS WHERE THE DATA FOR}
{EACH BEAM IS READ FROM THE DATA FILE; RUNS ALL THE PROCEDURES REQUIRED}
{FOR THE SIMULATIONS; COMPUTES THE MEANS, STANDARD DEVIATIONS, AND COV}
{FOR EACH BEAM; COMPUTES THE CUMULATIVE MEANS, STANDARD DEVIATIONS,}
{AND COV; AND WRITES THE RESULTS INTO FILES}
```

```
Procedure Simulate;
Begin

 {INITIALIZES VARIABLES}

 mr1 := 0.0;  ms1 := 0.0;  mv1 := 0.0;  s1 := 0.0;   k1 := 0;    s3 := 0.0;

 {ITERATION FOR READING AND PROCESSING THE DATA FOR EACH BEAM}

 While not Eof(fin) do
  begin
   Window(1,1,80,25);
   ClrScr;  InputData;  Str(n,st);
   Assign(fout,fname+'.'+st);  {$I-}Rewrite(fout);{$I+}
   Chkfile('FILE FOR OUTPUT','DISK/DRIVE');
   if err = 1 then Exit;
   OutData;

   {INITIALIZES AND EVALUATES VARIABLES}

   R1 := Eqn;
   write(fout,W:10:2,fc:6:0,Cb:7:3,Cso:7:3,Csi:7:3,Ls:7:2,Nb:3);
   writeln(fout,Db:7:3,Ab:6:2,R1:7:0);
   a0 := Ls;  a1 := Cb;  a2 := Cso;  a3 := W;  a4 := fc;
   Vc := 550.0/(fc+2.33*550.0-500.0);  Vc := sqrt(Vc*Vc+0.0084);
   Rc1 := 0.0;  sd1 := 0.0;  r21 := 0.0;  fcm := 0.0;
   Cbm := 0.0;  Cim := 0.0;  Lsm := 0.0;  E1m := 0.0;

   {ITERATION FOR PERFORMING THE MONTE CARLO SIMULATIONS k TIMES FOR}
   {EACH BEAM}

   for j := 1 to k do
    begin
     Randomize;
     Window(20,21,40,22);
     writeln('WORKING ON CYCLE ',j);
     Ls := a0;  Cb := a1;  Cso := a2;  W := a3;  fc := a4;
     fcstrR;

     {ITERATION FOR RANDOMLY GENERATING THE VARIABILITY ASSOCIATED}
     {WITH EACH OF THE VARIABLES FOR CALCULATING THE PREDICTED}
     {BOND FORCE}

     for i := 1 to 6 do
      begin
       Getz;
       if pz < 0.50 then z := -z;
       Case i of
        1 : Ls := Ls+0.6079*z;
        2 : if h > 12.0 then Cb := Cb+0.3040*z
            else Cb := Cb+0.2280*z;
        3 : if W > 12.0 then Cso := Cso+0.2551*z
            else Cso := Cso+0.1913*z;
        4 : if W > 12.0 then W := W+0.0625+0.2232*z
            else W := W+0.0625+0.1594*z;
        5 : fc := fcR*(1.0+Vc*z);
        6 : tc1 := 0.996*(1.0+0.076*z);
       end;
      end;

     {COMPUTES THE MEAN, STANDARD DEVIATION AND COV FOR EACH BEAM}
     {AND CUMULATIVE MEAN, STANDARD DEVIATION AND COV INCLUDING}
     {PRECEDING BEAMS}
```

```
        e1 := tc1*Eqn;
        Rc1 := Rc1+e1/R1;  k1 := k1+1;
        r21 := r21+e1*e1/R1/R1;
        s3 := s3+e1/R1;
        s1 := s1+e1*e1/R1/R1;
        if j > 1 then sd1 := sqrt((r21-Rc1*Rc1/j)/j);
        if k1 > 1 then ms1 := sqrt((s1-s3*s3/k1)/k1);
        fcm := fcm+fc;  Cbm := Cbm+Cb;  Cim := Cim+Csi;  Lsm := Lsm+Ls;
        E1m := E1m+e1;

        {DISPLAYS THE CURRENT RESULTS ON THE SCREEN}

        Window(10,16,70,21);
        writeln(' CURRENT RATIO = ',e1/R1:6:3);
        writeln('   MEAN RATIO  = ',Rc1/j:6:3);
        writeln(' STD DEV  = ',sd1:6:3);
        writeln('   C.O.V. 1 = ',sd1/Rc1*j:6:3);

        {WRITES THE CURRENT RESULTS INTO THE RESULT FILE FOR EACH BEAM}

        write(fout,j:3,W:7:2,fc:6:0,Cb:7:3,Cso:7:3,Csi:7:3,Ls:7:2,Nb:3,Db:7:3,Ab:6:2);
        writeln(fout,e1:7:0,e1/R1:7:3,Rc1/j:7:3,sd1:7:3,sd1/Rc1*j:7:3);
      end;
     writeln(fout,' ');
     Close(fout);

     {COMPUTES THE AVERAGE VALUES FOR ALL VARIABLES FOR EACH}
     {OF THE BEAMS}

     fc := fcm/j;  Cb := Cbm/j;  Csi := Cim/j;  Ls := Lsm/j;
     e1 := E1m/j;  mr1 := mr1+e1/R1;  mv1 := ms1/mr1*n;

     {WRITES THE CURRENT BEAM RESULTS INTO THE RESULT FILE THAT CONTAINS}
     {THE SUMMARY OF ALL THE RESULTS FOR ALL BEAMS}

     write(fl,n:3,W:7:2,fc:6:0,Cb:7:3,Cso:7:3,Csi:7:3,Ls:7:2,Nb:3,Db:7:3);
     write(fl,Ab:6:2,e1:7:0,e1/R1:7:3,sd1:7:3,sd1/Rc1*j:7:3,mr1/n:7:3);
     writeln(fl,ms1:7:3,mv1:7:3);
   end;
End;

{CHECKS TO SEE IF A SPECIFIED FILE EXISTS OR WAS OPENED SUCCESSFULLY}

Procedure Chkfile(s1,s2 : String);
Begin
 if Ioresult <> 0 then
   begin
    Window(10,10,70,15);
    ClrScr;
    writeln('     CANNOT OPEN ',s1);
    writeln;
    writeln(' PRESS ANY KEY TO END AND CHECK ',s2);
    err := 1;
    st := Readkey;
    Exit;
   end;
End;

{START OF THE MAIN PROGRAM WHERE ALL INPUT IS MADE}

BEGIN
 Window(1,1,80,25);
```

```
ClrScr;
err := 0;
n := 0;
write('    ENTER NAME OF THE DATA FILE W/O EXTENSION : ');
readln(fname);
Assign(fin,fname+'.DAT');
{$I-}Reset(fin);{$I+}
Chkfile('DATA FILE ','DATA FILE');
if err = 1 then Exit;
Assign(fl,fname+'.RST');
{$I-}Rewrite(fl);{$I+}
Chkfile('FILE FOR OUTPUT','DISK/DRIVE');
if err = 1 then Exit;
writeln;
write('    ENTER THE NUMBER OF CYCLES REQUIRED : '); readln(k);

{WRITES THE NOTATION AND HEADING INFORMATION FOR MONTE CARLO}
{SIMULATION OUTPUT RESULT FILE}

writeln(fl,'    RESULTS OUTPUT FOR BEAMS W/O STIRRUPS');
writeln(fl,'    ------------------------------------');
writeln(fl,'    W  = Beam width (ins.)');
writeln(fl,'    fc  = Concrete strength (psi)');
writeln(fl,'    Cb  = Concrete cover (ins.)');
writeln(fl,'    Cso = Concrete side cover (ins.)');
writeln(fl,'    Csi = One-half clear bar spacing (ins.)');
writeln(fl,'    Ls  = Splice length (ins.)');
writeln(fl,'    Nb  = Number of bars spliced');
writeln(fl,'    Db  = Spliced bar diameter (ins.)');
writeln(fl,'    Ab  = Spliced bar area (sq. ins.)');
writeln(fl,' ');
write(fl,'Beam  W   fc   Cb   Cso  Csi  Ls   Nb  Db   Ab  ');
writeln(fl,' E1   R1   S1   V1   MR1  MS1  MV1');
write(fl,'-------------------------------------------------------------');
writeln(fl,'-----------------------------------------');

{READS THE FIRST LINE (HEADING) FROM THE INPUT FILE}

readln(fin,st);
Simulate;
Close(fin);
Close(fl);
END.
```

(b)

```
Program Bs;
{MONTE CARLO SIMULATION FOR BEAMS WITH STIRRUPS}

Uses Crt, Dos;

{DECLARATION OF GLOBAL CONSTANTS FOR THE PROGRAM}

Const
 left = 0.0;  tol = 1.0e-6;

{DECLARATION OF GLOBAL VARIABLES FOR THE PROGRAM}

Var
 a, b, z, pz, Ls, Cb, Csi, fc, Db, Ab, Cmin, Cmax, fcm, Cbm, Cim,
  Lsm, E1m, R1, h, tc1, Rc1, a0, a1, a2, a3, a4, sd1, s1, r21,
  Vc, Av, Sv, Nv, mr1, ms1, mv1, s3, result, errest, Cso, W, Cs,
  Atr, Atm, e1, e11, e21, CMm, fcR : Real;
 Nb, Ns, err : Byte;
 n, l : Integer;
 k1, i, j, k, m, m0 : Word;
 fname : String[20];
 st : String;
 fin, fout, fl : Text;

{FUNCTION EVALUATES THE EXPRESSION e^-(0.5*z^2)}

Function F(z : Real) : Real;
Begin
 f := exp(-z*z/2.0);
End;

{FUNCTION EVALUATES THE EXPRESSION FOR SIMPSON'S RULE}

Function Simpson(a,b,h : Real) : Real;
Var mid : Real;
Begin
 mid := (b+a)/2.0;
 Simpson := h/6.0*(f(a)+4.0*f(mid)+f(b));
End;

{NUMERICAL METHOD TO DETERMINE THE CURRENT IMPROVED STANDARD}
{NORMAL VALUE, z[i+1], FROM A PREVIOUS VALUE OF z[i] DURING EACH CYCLE}
{OF THE ITERATIVE PROCESS}

Procedure Adap_Quad(left,z,tol:Real; var result:Real; var errest:Real);
Var h, I1, I2, mid, result1, result2, errest1, errest2 : Real;
Begin
 m := m+1;
 h := z-left;
 I1 := Simpson(left,z,h);
 h := h/2.0;
 mid := (left+z)/2.0;
 I2 := Simpson(left,mid,h)+Simpson(mid,z,h);
 errest := abs((I2-I1)/15.0);
```

```
  if abs(errest) > tol then
   begin
    Adap_Quad(left,mid,tol/2,result1,errest1);
    Adap_Quad(mid,z,tol/2,result2,errest2);
    result := result1+result2;
    errest := errest1+errest2;
   end
  else
   result := I2-errest;
End;

{ITERATIVE PROCESS TO OBTAIN THE STANDARD NORMAL VALUE, z, FOR ANY}
{RANDOMLY GENERATED CUMULATIVE PROBABILITY, pz, USING THE}
{PROCEDURE Adap_Quad AS OPTION AS IT IS REQUIRED}

Procedure Getz;
Begin
 pz := Random;
 a := 0.0;  z := 2.0;  b := 4.0;  m0 := 0;
 Repeat
  m0 := m0+1;  m := 0;
  Adap_Quad(left,z,tol,result,errest);
  result := 0.5+result/sqrt(2.0*pi);
  if pz < 0.50 then
   begin
    result := 1.0-result;
    if result < pz then b := z else a := z;
   end
  else
   begin
    if result < pz then a := z else b := z;
   end;
  z := 0.5*(a+b);
  if m0 > 500 then Exit;
 Until abs(pz-result) < tol;
End;

{FUNCTION DETERMINES THE MINIMUM OF TWO VARIABLES}

Function Min(a,b :Real) : Real;
Begin
 if a < b then Min := a
 else Min := b;
End;

{FUNCTION DETERMINES THE MAXIMUM OF TWO VARIABLES}

Function Max(a,b :Real) : Real;
Begin
 if a > b then Max := a
 else Max := b;
End;

{FUNCTION DETERMINES BOND FORCE}
```

```
Function Eqn : Real;
Var Eq : Real;
Begin
 Csi := (0.5*W-Nb*Db-Cso)/(Nb-1.0);
 Cs := Min(Cso,Csi+0.25);
 if Cs < Cb then Atr := 2.0*Av/Nb
 else Atr := Av;
 Cmin := Min(Cs,Cb);
 Cmax := Max(Cs,Cb);
 CMm := Cmax/Cmin;
 if CMm > 3.5 then CMm := 3.5;
 Eq := (63.0*Ls*(Cmin+0.5*Db)+2280.0*Ab)*(0.082*CMm+0.918);
 Eqn := Sqrt(Sqrt(fc))*(Eq+2187.0*Nv*Atr+202.0);
End;

{PROCEDURE FOR READING, FROM THE DATA FILE, AND DISPLAYING, ON THE}
{SCREEN, THE NOMINAL VALUES FOR EACH BEAM}

Procedure InputData;
Begin
 readln(fin,W,h,fc,Cb,Cso,Ls,Nb,Db,Ab,Av,Sv);
 n := 1+n;
 writeln('      CURRENT INPUT DATA FROM FILE ',fname+'.DAT');
 writeln('      ----------------------------------------');
 writeln('      Data for beam number ..... ',n:5);
 writeln('      Beam width (ins.) ..... ',W:5:2);
 writeln('      Beam depth (ins.) ..... ',h:5:2);
 writeln('      Concrete strength (psi) ..... ',fc:4:0);
 writeln('      Concrete cover (ins.) ..... ',Cb:5:3);
 writeln('      Concrete side cover (ins.) ..... ',Cso:5:3);
 writeln('      Splice length (ins.) ..... ',Ls:5:2);
 writeln('      Number of bars spliced ..... ',Nb:2);
 writeln('      Spliced bar diameter (ins.) ..... ',Db:5:3);
 writeln('      Spliced bar area (sq. ins.) ..... ',Ab:4:2);
 writeln('      Stirrup area (sq. ins.) ..... ',Av:4:2);
 writeln('      Stirrup spacing (ins.) ..... ',Sv:5:2);
End;

{PROCEDURE FOR WRITING THE NOTATION AND HEADING INFORMATION FOR}
{EACH BEAM INTO THE OUTPUT FILE FOR THE BEAM}

Procedure OutData;
Begin
 writeln(fout,'   RESULTS OUTPUT FOR BEAMS WITH STIRRUPS');
 writeln(fout,'   ----------------------------------------');
 writeln(fout,'   n  = Number of iterations');
 writeln(fout,'   W  = Beam width (ins.)');
 writeln(fout,'   fc  = Concrete strength (psi)');
 writeln(fout,'   Cb  = Concrete cover (ins.)');
 writeln(fout,'   Cso = Concrete side cover (ins.)');
 writeln(fout,'   Csi = One-half clear bar spacing (ins.)');
 writeln(fout,'   Ls  = Splice length (ins.)');
 writeln(fout,'   Number of bars spliced .....',Nb:7);
 writeln(fout,'   Spliced bar diameter (ins.) .....',Db:7:3);
```

```
  writeln(fout,'    Spliced bar area (sq. ins.) .....',Ab:7:2);
  writeln(fout,'    Stirrup effective area (sq. ins.) ....',Atr:7:2);
  writeln(fout,'    Stirrup spacing (ins.) .....',Sv:7:2);
  writeln(fout,' ');
  write(fout,' n   W   fc   Cb   Cso  Csi  Ls   ');
  writeln(fout,'Eq1   R1   MR1   SD1   V1');
  write(fout,'-------------------------------------------------');
  writeln(fout,'------------------------------');
End;

{ITERATIVE PROCESS FOR DETERMINING THE LONG-TERM IN-SITU COMPRESSIVE}
{STRENGTH OF CONCRETE}

Procedure fcstrR;
Var fc35 : Real;
Begin
 fc35 := fc;
 Repeat
  fcR := fc;
  fc := fc35*(0.89*(1.0+0.08*ln(fcR/3600)/ln(10.0)));
 until Abs(fcR-fc) < 1.0;
End;

{MAIN PROCEDURE FOR THE MONTE CARLO SIMULATIONS WHERE THE DATA FOR}
{EACH BEAM IS READ FROM THE DATA FILE; RUNS ALL THE PROCEDURES REQUIRED}
{FOR THE SIMULATIONS; COMPUTES THE MEANS, STANDARD DEVIATIONS, AND COV}
{FOR EACH BEAM; COMPUTES THE CUMULATIVE MEANS, STANDARD DEVIATIONS,}
{AND COV; AND WRITES THE RESULTS INTO FILES}

Procedure Simulate;
Begin

 {INITIALIZES VARIABLES}

 mr1 := 0.0; ms1 := 0.0; mv1 := 0.0;
 s1 := 0.0;  k1 := 0;  s3 := 0.0;

 {ITERATION FOR READING AND PROCESSING THE DATA FOR EACH BEAM}

 While not Eof(fin) do
  begin
   Window(1,1,80,25);
   ClrScr; InputData; Str(n,st);
   Assign(fout,fname+'.'+st); {$I-}Rewrite(fout);{$I+}
   Chkfile('FILE FOR OUTPUT','DISK/DRIVE');
   if err = 1 then Exit;

   {INITIALIZES AND EVALUATES VARIABLES}

   Nv := Ls/Sv; R1 := Eqn;
   OutData;
   writeln(fout,W:11:2,fc:6:0,Cb:7:3,Cso:7:3,Csi:7:3,Ls:7:2,R1:7:0);
   a0 := Ls; a1 := Cb; a2 := Cso; a3 := W; a4 := fc;
   Vc := 550.0/(fc+2.33*550.0-500.0); Vc := sqrt(Vc*Vc+0.0084);
   fcstrR;
   Rc1 := 0.0; sd1 := 0.0; r21 := 0.0;
```

```
fcm := 0.0;  Cbm := 0.0;  Cim := 0.0;  Lsm := 0.0;
E1m := 0.0;  Atm := 0.0;

{ITERATION FOR PERFORMING THE MONTE CARLO SIMULATIONS k TIMES FOR}
{EACH BEAM}

for j := 1 to k do
 begin
  Randomize;
  Window(20,23,40,24);
  writeln('WORKING ON CYCLE ',j);
  Ls := a0;  Cb := a1;  Cso := a2;  W := a3;  fc := a4;

  {ITERATION FOR RANDOMLY GENERATING THE VARIABILITY ASSOCIATED}
  {WITH EACH OF THE VARIABLES FOR CALCULATING THE PREDICTED}
  {BOND FORCE}

  for i := 1 to 6 do
   begin
    Getz;
    if pz < 0.50 then z := -z;
    Case i of
     1 : Ls := Ls+0.6079*z;
     2 : if h > 12.0 then Cb := Cb+0.3040*z
        else Cb := Cb+0.2280*z;
     3 : if W > 12.0 then Cso := Cso+0.2551*z
        else Cso := Cso+0.1913*z;
     4 : if W > 12.0 then W := W+0.0625+0.2232*z
        else W := W+0.0625+0.1594*z;
     5 : fc := fcR*(1.0+Vc*z);
     6 : tc1 := 0.999*(1.0+0.115*z);
    end;
   end;

  {EVALUATES THE PREDICTED BOND FORCE FOR THE TWO INTEGER VALUES}
  {FOR THE NUMBER OF STIRRUPS}

  for l := 0 to 1 do
   begin
    Nv := 1.0*(Trunc(Ls/Sv)+l);
    if l = 0 then
     begin
      e11 := tc1*Eqn*(1.0-Frac(Ls/Sv));
      e1 := tc1*Eqn;
      write(fout,j:3,'a',W:7:2,fc:6:0,Cb:7:3,Cso:7:3,Csi:7:3);
      writeln(fout,Ls:7:2,e1:7:0,e1/R1:7:3);
     end
    else
     begin
      e21 := tc1*Eqn*Frac(Ls/Sv);
      e1 := tc1*Eqn;
      write(fout,j:3,'b',W:7:2,fc:6:0,Cb:7:3,Cso:7:3,Csi:7:3);
      writeln(fout,Ls:7:2,e1:7:0,e1/R1:7:3);
      e1 := e11+e21;
     end;
```

```
        end;

        {COMPUTES THE MEAN, STANDARD DEVIATION AND COV FOR EACH BEAM}
        {AND CUMULATIVE MEAN, STANDARD DEVIATION AND COV INCLUDING}
        {PRECEDING BEAMS}

        Rc1 := Rc1+(e11+e21)/R1;  k1 := k1+1;
        r21 := r21+(e11*e11/(1.0-Frac(Ls/Sv))+e21*e21/Frac(ls/Sv))/R1/R1;
        s3 := s3+(e11+e21)/R1;
        s1 := s1+(e11*e11/(1.0-Frac(Ls/Sv))+e21*e21/Frac(ls/Sv))/R1/R1;
        if j > 1 then sd1 := sqrt((r21-Rc1*Rc1/j)/j);
        if k1 > 1 then ms1 := sqrt((s1-s3*s3/k1)/k1);
        fcm := fcm+fc;  Cbm := Cbm+Cb;  Cim := Cim+Csi;  Lsm := Lsm+Ls;
        E1m := E1m+e1;

        {DISPLAYS THE CURRENT RESULTS ON THE SCREEN}

        Window(10,18,70,23);
        writeln(' CURRENT RATIO = ',e1/R1:6:3);
        writeln('   MEAN RATIO  = ',Rc1/j:6:3);
        writeln(' STD DEV  = ',sd1:6:3);
        writeln('   C.O.V. = ',sd1/Rc1*j:6:3);

        {WRITES THE CURRENT RESULTS INTO THE RESULT FILE FOR EACH BEAM}

        write(fout,j:3,W:8:2,fc:6:0,Cb:7:3,Cso:7:3,Csi:7:3,Ls:7:2);
        writeln(fout,e1:7:0,e1/R1:7:3,Rc1/j:7:3,sd1:7:3,sd1/Rc1*j:7:3);
      end;
    writeln(fout,' ');
    Close(fout);

    {COMPUTES THE AVERAGE VALUES FOR ALL VARIABLES FOR EACH}
    {OF THE BEAMS}

    fc := fcm/j;  Cb := Cbm/j;  Csi := Cim/j;  Ls := Lsm/j;  e1 := E1m/j;
    mr1 := mr1+e1/R1;  mv1 := ms1/mr1*n;

    {WRITES THE CURRENT BEAM RESULTS INTO THE RESULT FILE THAT CONTAINS}
    {THE SUMMARY OF ALL THE RESULTS FOR ALL BEAMS}

    write(fl,n:3,W:7:2,fc:6:0,Cb:7:3,Cso:7:3,Csi:7:3,Ls:7:2,Nb:3,Db:7:3);
    write(fl,Ab:6:2,Atr:6:2,Sv:7:2,e1:7:0,e1/R1:7:3);
    writeln(fl,sd1:7:3,sd1/Rc1*j:7:3,mr1/n:7:3,ms1:7:3,mv1:7:3);
  end;
End;

{CHECKS TO SEE IF A SPECIFIED FILE EXISTS OR WAS OPENED SUCCESSFULLY}

Procedure Chkfile(s1,s2 : String);
Begin
 if Ioresult <> 0 then
  begin
    Window(10,10,70,15);
    ClrScr;
    writeln('     CANNOT OPEN ',s1);
    writeln;
    writeln('  PRESS ANY KEY TO END AND CHECK ',s2);
```

```
    err := 1;
    st := Readkey;
    Exit;
   end;
End;

{START OF THE MAIN PROGRAM WHERE ALL INPUT IS MADE}

BEGIN
 Window(1,1,80,25);
 ClrScr;
 err := 0;
 n := 0;
 write('   ENTER NAME OF THE DATA FILE W/O EXTENSION : ');
 readln(fname);
 Assign(fin,fname+'.DAT');
 {$I-}Reset(fin);{$I+}
 Chkfile('DATA FILE ','DATA FILE');
 if err = 1 then Exit;
 Assign(fl,fname+'.RST');
 {$I-}Rewrite(fl);{$I+}
 Chkfile('FILE FOR OUTPUT','DISK/DRIVE');
 if err = 1 then Exit;
 writeln;
 write('   ENTER THE NUMBER OF CYCLES REQUIRED : '); readln(k);

 {WRITES THE NOTATION AND HEADING INFORMATION FOR MONTE CARLO}
 {SIMULATION OUTPUT RESULT FILE}

 writeln(fl,'   RESULTS OUTPUT FOR BEAMS WITH STIRRUPS');
 writeln(fl,'   ------------------------------------');
 writeln(fl,'   W  = Beam width (ins.)');
 writeln(fl,'   fc  = Concrete strength (psi)');
 writeln(fl,'   Cb  = Concrete cover (ins.)');
 writeln(fl,'   Cso = Concrete side cover (ins.)');
 writeln(fl,'   Csi = One-half clear bar spacing (ins.)');
 writeln(fl,'   Ls  = Splice length (ins.)');
 writeln(fl,'   Nb  = Number of bars spliced');
 writeln(fl,'   Db  = Spliced bar diameter (ins.)');
 writeln(fl,'   Ab  = Spliced bar area (sq. ins.)');
 writeln(fl,'   Atr = Stirrup effective area (sq. ins.)');
 writeln(fl,'   Sv  = Stirrup spacing (ins.)');
 writeln(fl,' ');
 write(fl,'Beam  W   fc   Cb   Cso  Csi  Ls  Nb  Db  Ab  ');
 writeln(fl,' Atr  Sv  E1   R1   S1   V1   MR1  MS1  MV1');
 write(fl,'-------------------------------------------------------------');
 writeln(fl,'-------------------------------------------------------------');

 {READS THE FIRST LINE (HEADING) FROM THE INPUT FILE}

 readln(fin,st);
 Simulate;
 Close(fin);
 Close(fl);
END.
```